The geological relationship between Kanmantoo Cu-Au deposit mineralisation, hydrothermal metasomatism and igneous intrusives

Extended version of thesis submitted in accordance with the requirements of the University of Adelaide for an Honours Degree in Geology.

Benjamin James Kimpton

November 2018

THE GEOLOGICAL RELATIONSHIP BETWEEN KANMANTOO CU-AU DEPOSIT MINERALISATION, HYDROTHERMAL METASOMATISM AND IGNEOUS INTRUSIVES

KANMANTOO CU-AU DEPOSIT MINERALISATION

ABSTRACT

The Kanmantoo Cu-Au deposit has been in episodic operation since 1846, one decade after the capital city of Adelaide was established some 40 kilometres to the NW. Regionally and within the host stratigraphy there exists archetypal evidence of the Cambrian Delamerian Orogeny through a complex structural, metamorphic and intrusive history. Consequently, numerous theories exist within the literature regarding the syngenetic or epigenetic style of mineralisation and the debated contribution, if any, of magmatic hydrothermal fluids. This study has documented numerous felsic intrusive vein sets within the Kanmantoo Cu-Au deposit which have been utilised to constrain the role of igneous activity on mineralisation within a wider Delamerian context. Monazite U–Pb ages of felsic veins show intrusion of the system first occurred at syn-peak metamorphic, syn-orogenic conditions (495.11 ± 2.79 Ma), continuing periodically until post-peak metamorphic, extensional conditions (483.43 ± 2.52 Ma). Intrusions are coeval with mineralisation and are temporally and geochemically analogous to magmatic activity in the adjacent Monarto and Murray Bridge provinces. Analysis of monazite trace elements identifies the Kanmantoo Cu-Au deposit as a syn- to post-peak metamorphic hydrothermal anomaly, which combined with the presence of felsic veins indicate that mineralisation resulted partly from fluids generated by a pluton at depth. These findings broadly confirm the prospectivity of Delamerian affected terranes throughout large parts of South Eastern Australia where pervasive intrusive geology exists.

KEYWORDS

Kanmantoo, Delamerian Orogeny, mineralisation, hydrothermal metasomatism, igneous intrusives, U–Pb geochronology, monazite trace element, exploration tool

TABLE OF CONTENTS

LIST OF FIGURES AND TABLES

1 INTRODUCTION

Despite almost two centuries of economic and scientific investigation, the style of mineralisation defining the Kanmantoo Cu-Au deposit (Appendix A) and its subsequent place in a provincial metallogenic framework remains the subject of debate. As with other meta-sediment hosted base metal deposits, the predominant paradigms can be broadly categorised as either syngenetic or epigenetic, with the complex tectonic history of the region providing evidence for both. Importantly, the two proposed models may be used to postulate a significantly different potential for regional exploration, ranging from trough to belt scale.

Early literature arguing for a syngenetic origin theorised that base metals were deposited simultaneously to metasediments in the Kanmantoo Trough and exist today as either disseminated or remobilised ore (Lindqvist, 1969). Ensuing research principally examining sulphur isotopes, microstructures and the local metallogenic record concluded that metals were likely incorporated in the sediments through submarine exhalation and subsequently metamorphosed and remobilised (Verwoerd and Cleghorn, 1975; Seccombe, Spry, Both, Jones & Schiller, 1985; Parker, 1986; Spry, Schiller & Both, 1988; Belperio et al., 1998; Pollock et al., 2018). The importance of a structural control on mineralisation has long been recognised by researchers (Dickinson, 1942; Thomson, 1975; Parker, 1986;). This understanding has underpinned literature arguing for an epigenetic origin and was modernised through the study of oxygen and sulphur isotopes with researchers concluding that mineralisation was the result of metasomatic infiltration of fluids derived from regional metamorphism and a local crystallising magma at the peak of metamorphism (Solomon & Groves, 1994; Oliver, Dipple, Cartwright & Schiller, 1998). Research based on succeeding structural analysis, geochemistry, geochronology and geothermometry has variously opted for a syn-peak metamorphism and compressional regime (Schiller, 2000) or a post-peak metamorphism and extensional regime for mineralisation (Tedesco, 2009; Wilson, 2009;

Focke, Schmidt Mumm, Tedesco, Seifert & Bradey, 2010; Arbon, 2011; Lyons, 2012). While a magmatic component of mineralising fluids has been routinely suggested, the direct role of intrusive geology within the deposit remains poorly constrained.

With this debate in mind, the following study aims to examine the physical evidence for hydrothermal and igneous activity exposed throughout the Kanmantoo Cu-Au deposit, namely numerous vein sets and alteration types. It is theorised that veins are of a magmatically derived origin, having formed alongside the regional suite of Delamerian syn to post-deformational intrusions. By understanding the age and geochemistry of intrusive rocks within the context of the Delamerian Orogeny, a temporal and spatial connection between mineralisation and a potential source for mineralising fluids may be identified. Consequently, the prospectivity of Delamerian-affected terranes for Kanmantoo-style mineralisation can be constrained. This has been achieved by combining petrography and whole rock geochemistry with in situ U–Pb geochronology and monazite trace element analysis which provide insights into the age and formation conditions of mineralisation, intrusive veins and alteration.

2 REGIONAL GEOLOGICAL BACKGROUND

2.1 Kanmantoo Trough

The Kanmantoo Cu-Au deposit is hosted within the Kanmantoo Group, a Cambrian meta-turbidite sequence consisting of eight separate formations with a structurally enhanced thickness of 7-8km (Jago, Gum, Burtt & Haines, 2003). Three of these formations, namely the Tapanappa, Talisker and Carrickalinga Head Formations, have been linked with mineralisation (Belperio et al. 1998), with the Kanmantoo Cu-Au deposit and several other base metal deposits being hosted within the Tapanappa Formation (Fig. 1). The Kanmantoo Group was deposited in the Kanmantoo Trough, an extensional rift basin contained within the

Adelaide Rift Complex which formed along an outward margin of the simultaneously assembling supercontinent of Gondwana. Early signs of rifting are exhibited by intrusion of the Truro Volcanics into the clastic-dominated Normanville Group which underlies the Kanmantoo Group in a variably conformable fashion (Fig. 1). Dating of zircons contained within tuffs from the Normanville Group defined a lower age limit for the Kanmantoo Group of 522 ± 2 Ma (Jenkins, Cooper & Compston, 2002). Foden, Sandiford, Dougherty-Page and Williams (1999) analysed zircons in the Rathjen Gneiss, suggested to be the oldest Delamerian related intrusion to define an upper age limit for the Kanmantoo Group of 514 ± 5 Ma, suggesting that Kanmantoo Group sediments may have been deposited in less than 10 Myr. Rifting, exceptionally rapid rates of sedimentation and initiation of orogeny are indicative of an increasingly dynamic tectonic regime. This activity directly reflects global plate reconfigurations occurring throughout this time (Foden, Elburg, Dougherty-Page & Burtt, 2006), marking the start of over 100 Myr of sustained mineralisation potential throughout large parts of South Eastern Australia (Solomon & Groves, 1994).

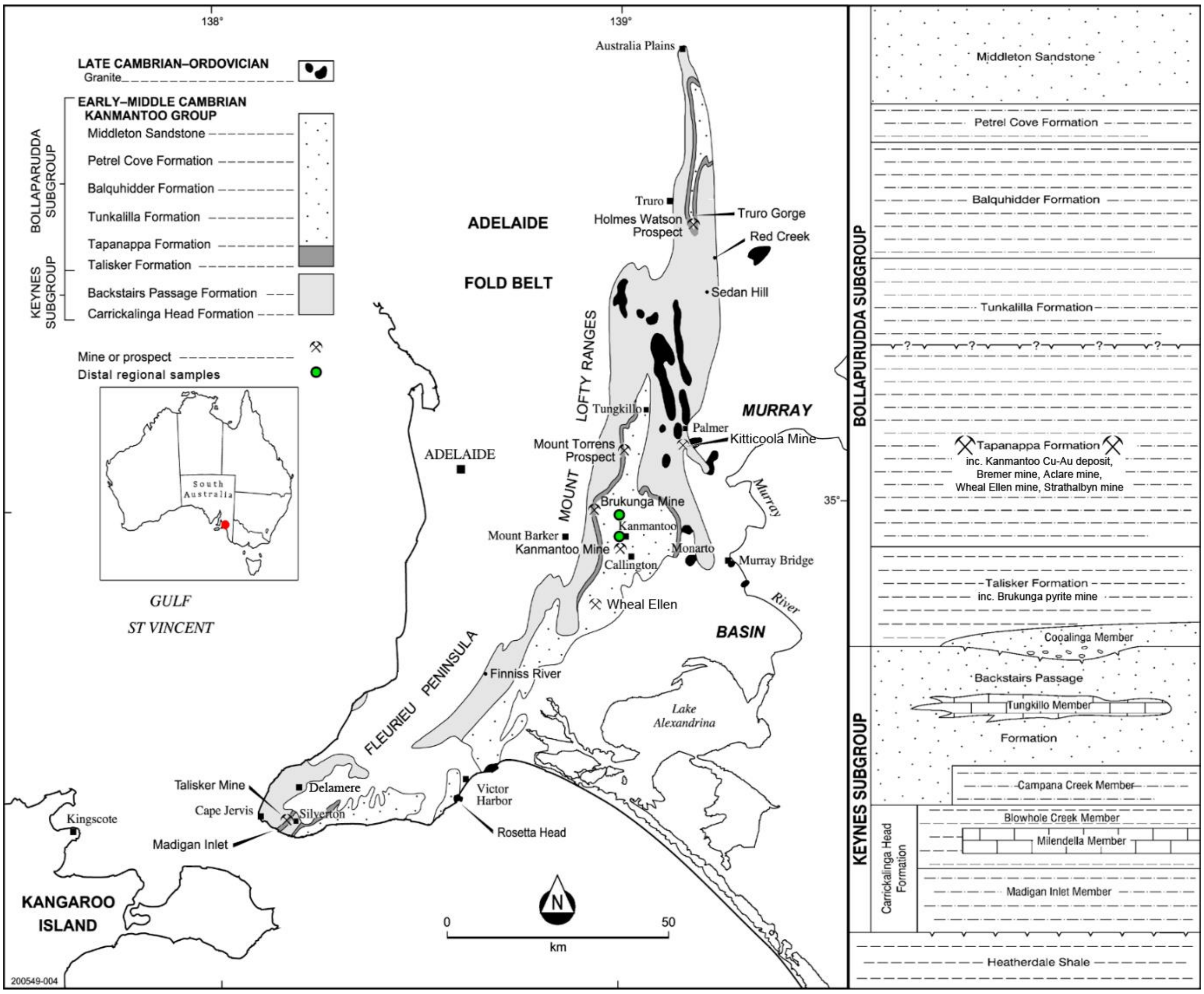

Figure 1: Geological map and stratigraphic log of the Kanmantoo Group adapted from Jago, Gum, Burtt and Haines (2003) including various associated mineral deposits and syn- to post-orogenic igneous intrusions. Green circles denote the location of regional schist samples used in this study (KMT1 = 2.64 km north of mine, BKDK1 = 9.22 km north of mine).

2.2 Delamerian Orogeny

Deposition in the Kanmantoo Trough was abruptly terminated by initiation of the Delamerian Orogeny and consequent basin inversion. Compressional deformation is interpreted to have taken place from between 514 to 490 Ma through intra-plate stress transfer (Foden et al., 2006). This deformation became archetypically observed within the Kanmantoo Trough as a series of pervasive structural, metamorphic and intrusive features described below.

2.2.1 STRUCTURAL RECORD

The Kanmantoo Trough has undergone at least three phases of deformation (D_1, D_2 and D_3) associated with the Delamerian Orogeny (Offler & Fleming, 1968; Mancktelow, 1979; Preiss, 1995; Oliver et al., 1998; Schiller, 2000). Regionally, the existence and significance of D_3 relative to proceeding phases of deformation is debated, however some authors have identified it in the vicinity of the Kanmantoo Cu-Au deposit and noted it as a structural control of ore (Oliver et al., 1998; Lyons, 2012). Relict bedding, S_0, can still be recognised within the region and the Kanmantoo Cu-Au deposit ranging from fine sedimentary laminations to metre thick beds (Schiller, 2000). Of great significance to the Kanmantoo Cu-Au deposit is the regional-scale Kanmantoo Syncline (Mancktelow, 1979), the axial plane of which is just east of the pit with a roughly N–S strike (Schiller, 2000). The syncline is but one in a series within the tightly folded Eastern Mount Lofty Ranges and Kanmantoo Group which come to form part of the Adelaide Fold Belt. A relationship between regional scale deformation structures on mineralisation including the Kanmantoo Syncline, Kanmantoo Fault and Bremer Fault has been recognised by various authors (Oliver et al., 1998; Schiller, 2000). The Kanmantoo Cu-Au deposit is situated on the western limb of the Kanmantoo Syncline, near the axial plane (Solomon & Groves, 1994; Schiller, 2000). Foden et al. (2006) suggested that slab rollback of the Pacific plate at 490 Ma caused a cessation of compressional forces with the region transitioning into an extensional regime and this appears to have reactivated peak metamorphic structures and fabrics within the deposit (Lyons, 2012).

2.2.2 METAMORPHIC RECORD

Metamorphism within the Kanmantoo Trough associated with the Delamerian Orogeny occurred exclusively at low pressure and high temperature (Offler & Fleming, 1968). Regionally, this has been described as a Barrovian metamorphic zonation, with the

Kanmantoo Cu-Au deposit being stratabound in an amphibolite facies garnet-andalusite-biotite schist (GABS) unit (Mancktelow, 1979) of anomalous chemistry rich in Fe and Mn but depleted in Na and Ca (Schiller, 2000). Evidence of peak metamorphism near the amphibolite facies andalusite–sillimanite transition (Spry, 1979) is observed within the Kanmantoo Cu-Au deposit. Estimates of peak metamorphic conditions vary slightly from pressures of 3–4 kbar and temperatures of 530–565 °C (Schiller, 2000), 3–5 kbar and 550–600 °C (Sandiford et al., 1995) and up to 3.7 kbar and 635 °C in sillimanite bearing schists (Stinear, 2017). Peak metamorphism across the orogen has been linked spatially with the intrusion of mid-crustal granitic intrusions (Sandiford et al., 1995), with age estimates of peak metamorphism generally ranging from syn-D_2 (Schiller, 2000) to post D_3 (Oliver et al., 1998).

2.2.3 INTRUSION RECORD

A diverse suite of intrusions dated from syn- to post-Delamerian Orogeny or 514 ± 4 to 478 ± 2 Ma (Foden et al., 2006) are observed within approximately 50 km of the Kanmantoo Cu-Au deposit. This suite extends outwards to other Delamerian-affected terranes throughout South Australia and South Eastern Australia (Foden et al., 1990; Preiss, 1995). Intrusions range from felsic to mafic compositions, with syntectonic I- and S- type magmatism broadly transitioning to A-type magmatism with the cessation of orogenesis (Foden et al., 2006). Significant intrusions within 50 km of the Kanmantoo Cu-Au deposit include the Monarto, Mannum, Murray Bridge and Palmer Granites. Mineralisation is known to be associated with intrusions on a limited scale, with the Palmer Granite hosting the Kitticoola Cu-Au deposit (Griessmann, 2011) and the Monarto Granite having been associated with various historical Cu-Au workings (Schiller, 2000). Past literature has alluded to a pluton at depth as a possible source of mineralising and metamorphic fluids at the Kanmantoo Cu-Au deposit, however a temporal and genetic link with known regional intrusives remains tentative.

2.3 Mineralisation

The Kanmantoo Cu-Au deposit is commonly described as a series of lenses and pods rich in chalcopyrite, pyrrhotite and magnetite with trace amounts of gold, silver, bismuthinite and molybdenite. Despite being classed as stratabound, veins of mineralisation are not stratiform but are observed to cross cut bedding throughout the deposit, running parallel or sub-parallel to various deformational fabrics (Seccombe et al., 1985; Oliver et al., 1998; Schiller, 2000).

2.3.1 SYNGENETIC MODEL

Early research on the Kanmantoo Cu-Au deposit frequently supported a syngenetic model of mineralisation, with Lindqvist (1969) and Verwoerd & Cleghorn (1975) first suggesting that sulphides were deposited concurrently with Kanmantoo Group sediments before being remobilised into their current structural and stratigraphic configurations during later orogeny. Spry (1976) concluded that Cu was present in the country rock either during sedimentation or in the earliest stages of metamorphism, with sulphur isotope ratios suggesting a hydrothermal origin and mobilisation of disseminated sulphides (Seccombe et al., 1985). Seccombe et al. (1985) further developed this concept by examining sulphur isotopes from other localities within the Kanmantoo Group to conclude that sulphur was leached from pyritic horizons (Parker, 1986) during hydrothermal circulation, with a seawater component accounting for regional isotopic variations as the result of fluid mixing. In both cases, the lack of a proximal magmatic intrusion is cited as a primary reason for discounting a partial igneous source of sulphur and consequent isotopic variation (Spry, 1976; Seccombe et al., 1985). Seccombe et al. (1985) noted the importance of a relatively constant stratigraphic level of the various base metal deposits within the Tapanappa Formation and noted that most deposits could have been stockworks, veins or disseminated zones within submarine exhalation vents. These vents are theorised to be part of 3–4 km deep circulation systems driven by convection or seismic pumping of seawater and discharged fluids. More direct evidence of sedimentary exhalative processes linked to mineralisation has been observed regionally, namely in the presence of laminated garnetiferous cherts transitioning into narrow magnetite BIFs within the wall rock surrounding Pb-Zn deposits of the Tapanappa Formation (Anderson, 1993). Laminated chert layers in proximity to the Aclare Ag Mine were observed to have a spatial relationship with disseminated sphalerite and galena (Toteff, 1994). More recently, Pollock et al. (2018) observed disseminated sulphides locally concordant with bedding in the Nugent lode, consistent with syngenetic mineralisation.

2.3.2 EPIGENETIC MODEL

The idea of an epigenetic style of mineralisation at the Kanmantoo Cu-Au deposit can be traced back to Dickinson (1942), Thomson (1975) and Parker (1986) who suggested that structural features pervasive throughout the region would have played a major role in the concentration of metals during metamorphism. However, the epigenetic case was first strongly championed by Oliver et al. (1998), who concluded that mineralisation was the result of late to post-peak metamorphic, metasomatic infiltration of fluids derived from regional metamorphism and a local crystallising magma. Subsequent research has largely supported an epigenetic model for mineralisation either through the introduction of igneous derived fluids, metamorphic fluids or some combination of both during or after peak metamorphism (Solomon & Groves, 1994; Gum, 1998; Schiller, 2000; Burtt, 2008; Tedesco, 2009; Wilson, 2009; Focke, 2010; Arbon, 2011; Lyons, 2012).

Early analytical evidence for epigenetic mineralisation included the interpretation of anomalous $\delta^{34}S$ (Oliver et al., 1998; Gum, 1998) and $\delta^{18}O$ (Oliver et al., 1998) isotope signatures from within the Kanmantoo deposit as being indicative of a magmatic fluid source. Seccombe et al. (1985) considered an igneous source for the anomalously fractionated sulphur, but because of a lack of igneous source rocks within the area, concluded that the $\delta^{34}S$ values were a result of crustal circulation of seawater. This was disputed by Oliver et al. (1998) who argued that the large amount of seawater circulation needed to replicate observed $\delta^{34}S$ levels was not realistically achievable. Oliver et al. (1998) noted an abundance of Fe-rich minerals within the system that transgressed bedding and concluded that Fe metasomatism was spatially correlated with ore. The large variety of minerals within the deposit including andalusite and staurolite in veins (Oliver et al., 1998) and the limited amount of strain exhibited in rocks within the deposit relative to the region (Oliver et al., 1998; Schiller, 2000) may indicate that fluid assisted mineralisation occurred during or after peak metamorphism. Oliver et al. (1998) suggested a change from regional, metamorphically-derived fluid flow at the peak of metamorphism to localised fluid flow derived from an igneous intrusion.

Recent research has largely supported the post-peak mineralisation model driven by the proposed intrusion of a magmatic pluton. Monazite U-Pb mineralisation ages from 469–498 Ma have been suggested by Wilson (2009) and Focke (2010) correlating approximately to known intrusions of granites within the wider region (Foden et al., 2006), but also with syn- to post-peak metamorphism (Sandiford et al., 1995). Ti in quartz thermometry has been used by various researchers (Focke, 2009; Schmidt Mumm, Tedesco & Focke, 2009; Tedesco, 2009) to establish peak mineralisation was concurrent with local shearing and quartz vein intrusion. Pervasive Fe-rich metasomatism (Oliver et al., 1998), which has a strong spatial and temporal connection with mineralisation is also proposed to be a signature of magmatic thermal processes and mantle upwelling (Tedesco, 2009; Wilson, 2009). The presence of elevated bismuth throughout the Kanmantoo Cu-Au deposit has also been linked to a granitic or magmatic source (Arbon, 2011). Lyons (2012) suggests that magmatic fluids began infiltrating the Kanmantoo Cu-Au deposit around 492 Ma after termination of the Delamerian Orogeny, with sulphur isotopes suggesting an I-type magma source.

3 METHODS

3.1 Sample collection

Thirty-two rock samples were collected from existing diamond drill core or directly from the main pit walls. Geological logging records belonging to Hillgrove Resources Ltd. were utilised to find representative drill core samples containing veins and intrusions of perceived mineralogical uniqueness. Samples were sourced from across the deposit, including the East Kavanagh, Main Kavanagh, Spitfire and Nugent lodes (Fig. 2) from ten separate diamond drill holes. Hillgrove Resources Ltd. geologists assisted in selecting veins and intrusions from the pit walls that were not well represented within existing drill core. Two Tapanappa Formation schist samples from 2.64 km and 9.22 km north of the Kanmantoo Cu-Au deposit open pit (Fig. 1) were selected from existing University of Adelaide collections to serve as comparative representations of district suites. Eighteen samples were made into 30-35µm polished thin sections by Ingham Petrographics, Queensland. Four additional samples were made into 40 µm polished thin sections by Adelaide Petrographic Laboratories, South Australia. Detailed sample information is presented in Appendix B.

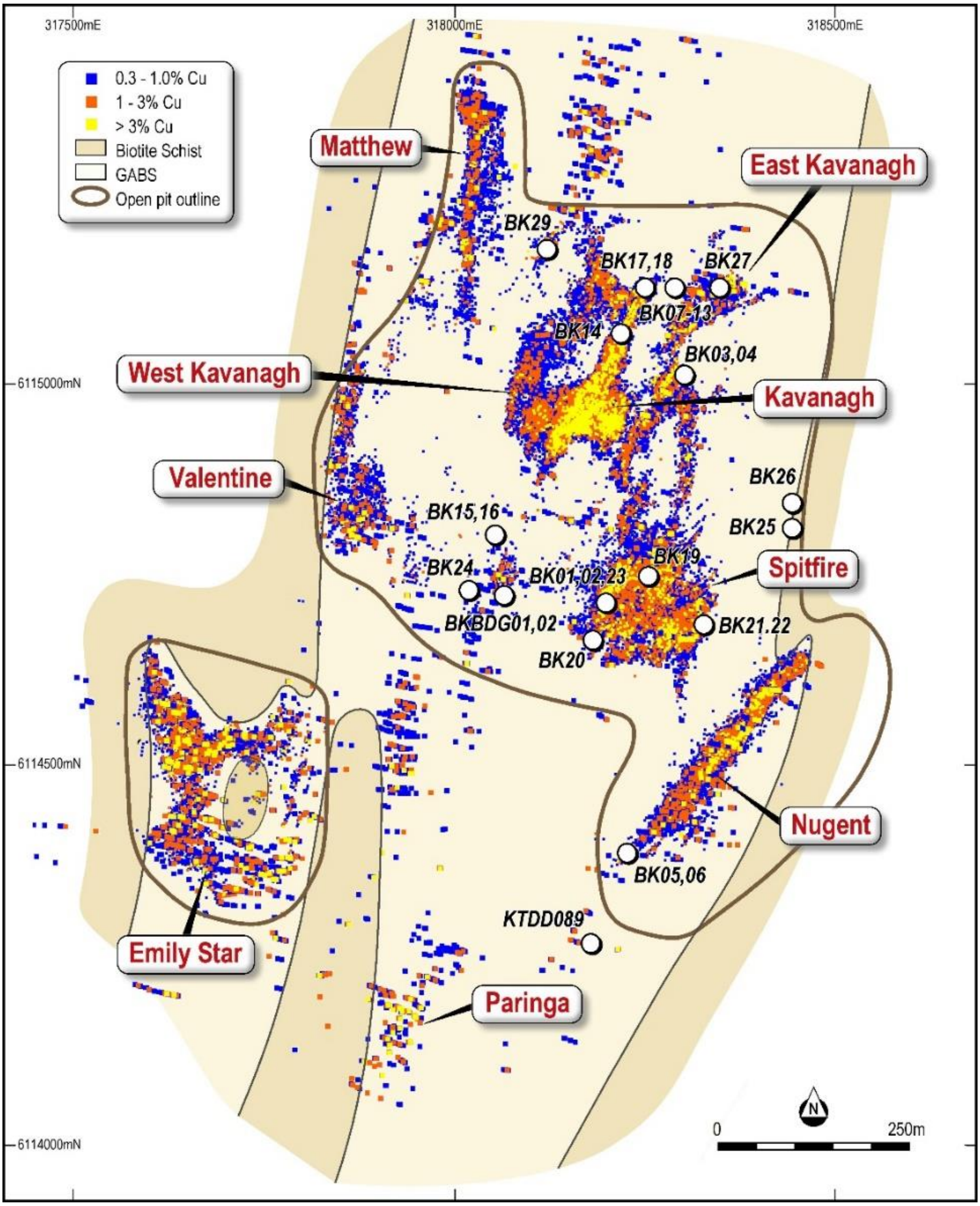

Figure 2: Locations of diamond drill hole and grab samples used in this study relative to deposit lodes and previously assayed copper concentrations adapted from Rolley and Wright (2017).

3.2 Microscopy

3.2.1 PETROGRAPHIC ANALYSIS

Petrographic analysis was conducted on an Olympus BX51 polarizing microscope at the University of Adelaide to confirm the mineralogy and paragenetic relationships of the twenty-two total thin sections.

3.2.2 SEM-MLA

The FEI Quanta 600 Scanning Electron Microscope (SEM) at Adelaide Microscopy, University of Adelaide was used to conduct Mineral Liberation Analysis (MLA) on eighteen representative samples. Electron Backscatter (EBS) images were processed to broadly identify the location of monazite, apatite, zircon and xenotime with relation to veins, alteration, sulphides and host rock. Imaging parameters are detailed in Appendix C.

3.3 Whole rock geochemistry

Twelve vein samples were cut to remove unaltered host rock and non-disseminated sulphides before being sent to ALS Limited, South Australia for whole rock and trace element geochemical analysis. Extended methods are presented in Appendix D.

3.4 LA-ICP-MS

3.4.1 U–PB GEOCHRONOLOGY

Laser Ablation Inductively Coupled Plasma Mass Spectrometry (LA-ICP-MS) was conducted using the Agilent 7900x with attached RESOlution LR 193 nm Excimer laser system at Adelaide Microscopy, University of Adelaide. A total of twelve individual samples were analysed by in situ laser ablation for monazite U–Pb (ten samples) and apatite U–Pb (seven samples) at a fluence of 2.0 J/cm^2 and 3.5 J/cm^2 respectively. Where possible, spots were taken from across the entirety of the sample including within vein sets, sulphides and adjacent altered host rock. Data processing and reduction was completed using *Iolite Software* (Paton, Hellstrom, Paul, Woodhead, & Hergt, 2011). Extended methods and data reduction techniques are presented in Appendix F.

3.4.2 MONAZITE TRACE ELEMENTS

In situ monazite grains from ten samples were analysed for trace elements concurrently to U–Pb analysis through LA-ICP-MS at Adelaide Microscopy, University of Adelaide. Data processing and reduction was completed using *Iolite Software* (Paton, Hellstrom, Paul, Woodhead, & Hergt, 2011). Extended methods and data reduction techniques are presented in Appendix I.

4 RESULTS

4.1 Petrology

Petrographic analysis was conducted on twenty-two samples (Table 1) using both optical microscopy and SEM-MLA imaging, resulting in the identification of four mineralogically distinct vein and alteration types which are described below. Extended petrographic descriptions are presented in Appendix B.

Table 1: List of thin section samples used in this study and their determined petrographic classifications.

Sample	Lode	Category	Use
BK01	Spitfire	Felsic vein	SEM-MLA, Geochem, U–Pb monazite
BK05	Nugent	Felsic vein	SEM-MLA, Geochem, U–Pb monazite
BK08	Main Kavanagh	Felsic vein	-
BK10	Main Kavanagh	Felsic vein	-
BK11	Main Kavanagh	Felsic vein	SEM-MLA, U–Pb apatite
BK12	Main Kavanagh	Felsic vein	-
BK18	Main Kavanagh	Felsic vein	SEM-MLA, U–Pb monazite, U–Pb apatite
BK20	Spitfire	Felsic vein	-
BK21	Spitfire	Felsic vein	SEM-MLA
BK23	Spitfire	Felsic vein	-
BK25A	East Haul Road	Felsic vein	SEM-MLA, Geochem, U–Pb monazite, U–Pb apatite
BK25B	East Haul Road	Felsic vein	SEM-MLA, Geochem, U–Pb monazite, U–Pb apatite
KTDD089	Nugent	Felsic vein	SEM-MLA, U–Pb monazite, U–Pb apatite
BK17	Main Kavanagh	Quartz vein	SEM-MLA, Geochem
BK27	NE Pit Wall	Quartz vein	SEM-MLA
BK06	Nugent	Chlorite alteration	SEM-MLA, U–Pb monazite
BK14	Main Kavanagh	Chlorite alteration	SEM-MLA, U–Pb monazite, U–Pb apatite
BK29	N Pit Wall	Aluminous segregation	SEM-MLA, Geochem
BKBDG1	S Pit Wall	Aluminous segregation	SEM-MLA, Geochem
BKBDG2	S Pit Wall	Aluminous segregation	SEM-MLA, Geochem, U–Pb apatite
KMT1	2.64 km N of mine: (54H 0318294 6117492)	Regional sample	SEM-MLA, U–Pb monazite
BKDK1	9.22 km N of mine: (54H 0318258 6123907)	Regional sample	SEM-MLA, U–Pb monazite

4.1.1 FELSIC VEINS

Felsic veins occur within all major lodes of the deposit as centimetre scale (1-10 cm wide), undeformed veins discordant to bedding. Veins range from parallel to deformational fabrics through to cross cutting all observable fabrics. Felsic veins are commonly quartzofeldspathic and fine grained (<2 mm) with rare feldspathic phenocrysts (up to 4 mm). Compositionally, veins contain variable proportions of albite, plagioclase, K-feldspar, quartz, biotite, tourmaline and muscovite. Albite is the dominant mineral in veins ranging from 30-60 %, with trace amounts of Ca-plagioclase. K-feldspar ranges from 15-60 %, quartz from 10-20 %

and mica being the smallest proportion of veins from 0-10 %. Chlorite alteration of mica and sericitic alteration of feldspars and chlorite is observed throughout samples, with varying levels of alteration and sample degradation. Considering the mineralogical compositions, fine grained texture and thin intrusive structure, felsic veins may be categorised as felsic aplites with a granitic to leucogranitic composition (Fig. 3b, a). They range from being devoid of sulphides to having large quantities of chalcopyrite, pyrrhotite and pyrite, while increasingly disseminated sulphides are concentrated heavily around vein contacts (Fig. 3c). Felsic veins are observed to overprint pervasive features in surrounding host rock such as schistosity and porphyroblasts, the latter replaced by feldspathic and phosphatic minerals including albite, K-feldspar, monazite, apatite and xenotime.

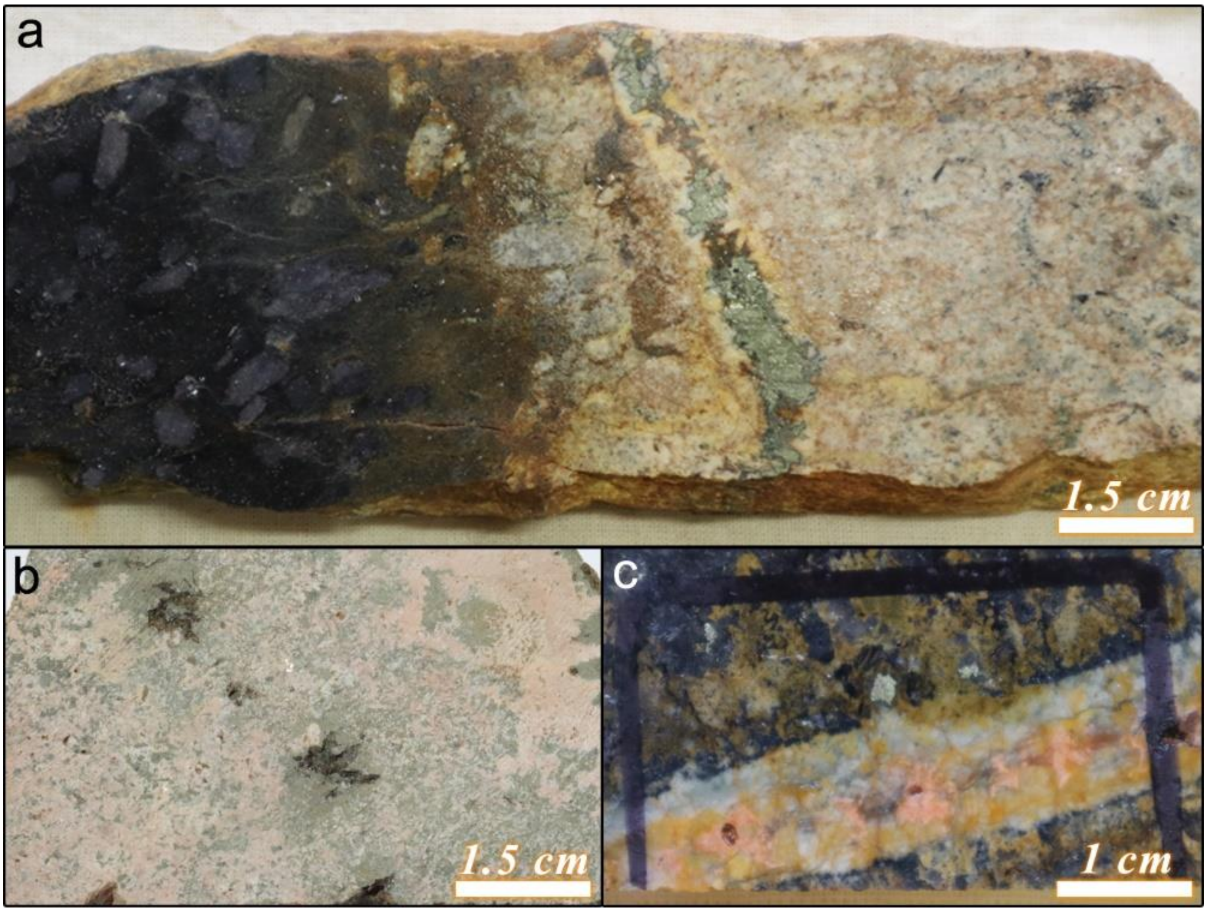

Figure 3: Representative photographs of felsic veins in hand sample. (a) BK25 - Leucogranitic vein comprised of albite and trace plagioclase (60 %), K-feldspar (20 %), tourmaline (10 %) and quartz (10 %) with sericitic and some chlorotic alteration and replacement throughout. Large (up to 3 mm) feldspar crystals have developed around sulphides (chalcopyrite, pyrrhotite and pyrite) with felsic veins fining outwards from the sulphides. Note the progressive alteration of surrounding host rock. (b) BK05 - Granitic vein comprised of altered primary and secondary K-feldspar and albite (2-4 mm), biotite, quartz, minor muscovite and limonite. Pervasive chlorite alteration throughout replacing biotite, with a later sericitic alteration of K-feldspar and chlorite shows that the sample is considerably degraded. Pre-alteration proportions are roughly estimated to be that of an alkali feldspar granite: K-feldspar (40-50 %), albite (10-15 %), quartz (15-20 %), biotite (15-20 %) with accessory ilmenite and minor tourmaline. (c) BK01 - comprised predominately of fine-moderately sized (40-200 µm) albite (60%), K-feldspar (20 %) and quartz (10 %) with chlorite replacing biotite (5 %), minor rutile and late carbonate (5 %). Sericitic alteration is seen to alter feldspars and chlorite throughout. Within hand sample, large (0.5 cm) grains of chalcopyrite are observed within the centre of veins.

4.1.2 QUARTZ VEINS

Numerous generations of quartz veins from centimetre to metre scale occur throughout the deposit. These veins are always discordant to bedding but exhibit various deformational histories ranging from undeformed to tightly folded or intensely boudinaged. The association between quartz veining and mineralisation is equally variable. Deformed quartz veins (sample BK27) are observed to have the largest range in width, but are generally monomineralic and are devoid of, or overprinted by, mineralisation. Undeformed quartz veins (sample BK17) are commonly smaller and contain staurolite, andalusite and sulphides.

4.1.3 CHLORITE ALTERATION

Chlorite occurs throughout the mine and within many samples, but particularly in samples BK14 and BK06 where it is pervasive and occurs in vein like form, characterized by centimetre wide sections of coarse (up to 1 cm), monomineralic chlorite. Both BK14 and BK06 contain or are spatially associated with disseminated sulphides in surrounding host rock. Strong Berlin blue interference colours for chlorite are common throughout samples indicating that chlorite is Fe-rich. Chlorite alteration is observed to overprint and replace all metamorphic assemblages observed within the deposit.

4.1.4 ALUMINOUS SEGREGATIONS

Aluminous segregations (samples BK29 and BKBDG) are exposed as intensely boudinaged, 1-15 cm width veins, running discordant to bedding throughout the main pit (Fig. 4b) consistent with an early orogenic formation. They are primarily composed of 65-75 % coarse pink andalusite, with the remainder being comprised of either quartz or mica.

4.1.5 REGIONAL SAMPLES

Two distal Tapanappa Formation samples (Fig. 1) were studied to compare with mine samples in terms of age and the chemistry of regional metamorphism. KMT1, collected 2.64 km due north of the mine is a strongly foliated garnet–andalusite schist. BKDK1, collected 9.22 km due north of the mine is a strongly foliated garnet–staurolite schist. Both samples are devoid of mineralisation and any alteration type associated with the Kanmantoo Cu-Au deposit.

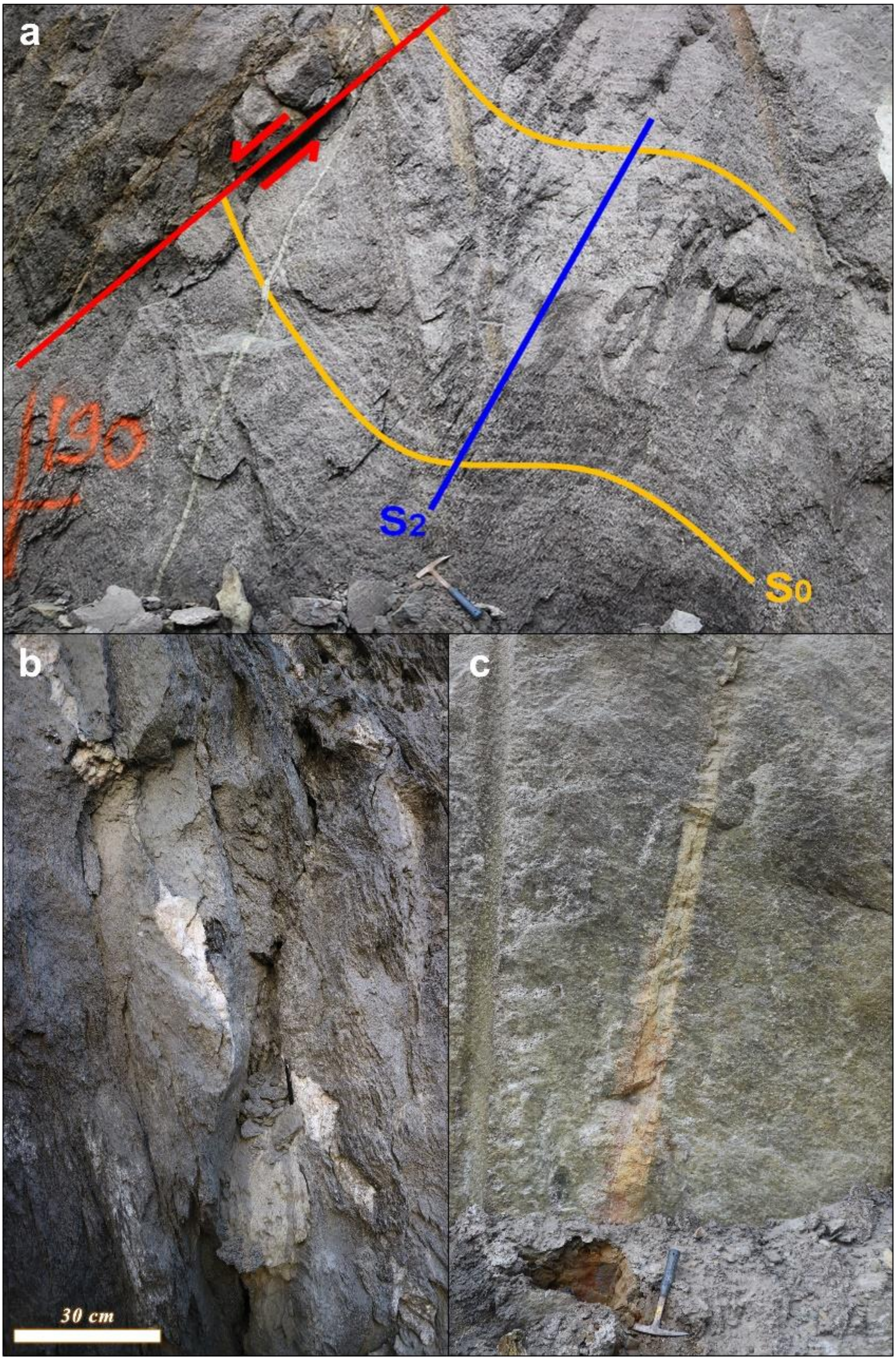

Figure 4: Characteristic field relationships between generations of veining and pervasive structural fabrics throughout the deposit. (a) Facing South Pit Wall - Relict bedding (S_0) is folded by the dominant schistosity (S_2). Note the undeformed quartz veins approximately sub-parallel to S_2 and offset by a late moderately steeply dipping normal fault. (b) Facing North Pit Wall - Segregation and boudinaging typical of post-folding, syn-S_2 veining including some quartz veins and aluminous segregations. (c) Facing East Pit Wall - Undeformed vein, observed generally as either sub-parallel to or cross cutting S_2 in joints typical of felsic veins and some quartz veins.

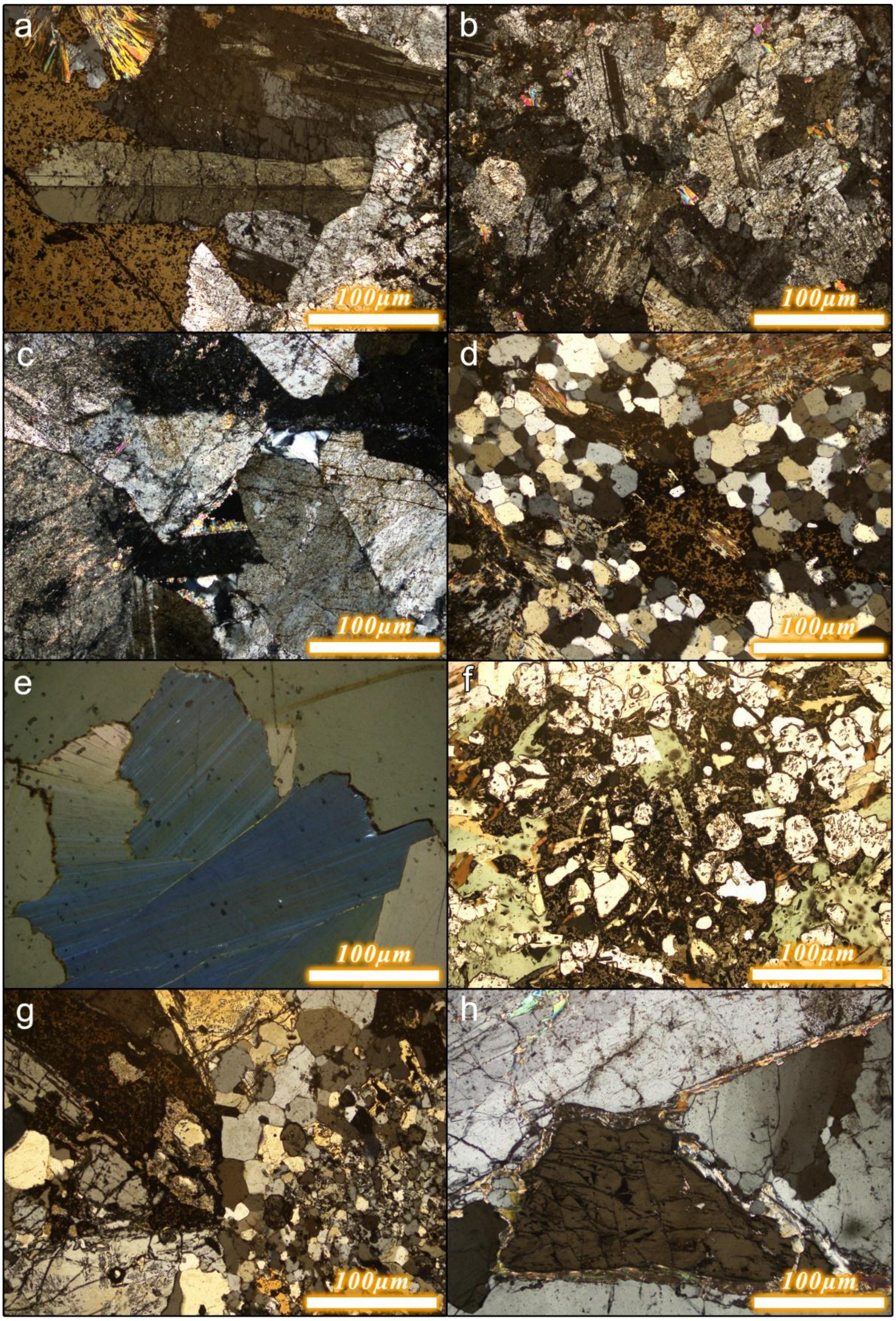

Figure 5: Representative photomicrographs showing examples of vein and alteration types. (a) BK25A - Felsic vein - K-feldspar, albite, quartz and sericite with syn to post pyrrhotite veining generating large feldspathic crystals. (b) BK25B - Felsic vein - Albite, K-feldspar, quartz with sericitic alteration. (c) BK01 - Felsic vein - Albite and K-feldspar with sericite replacing chlorite after biotite. (d) BK01 - Felsic vein - Disseminated pyrrhotite in host adjacent to vein overprinting a weak schistosity defined by biotite. (e) BK14 - Chlorite alteration - Radiating chlorite with intense Berlin (Prussian) blue interference indicative of Fe-rich hydrothermal fluids. (f) BK14 - Chlorite alteration - Pyrrhotite with late syn to post-chlorite replacing all host rock assemblages. (g) BK17 - Quartz vein - Quartz and staurolite with synchronous pyrrhotite. (h) BK29 - Aluminous segregation - Andalusite and quartz with interconnecting muscovite.

4.2 SEM-MLA

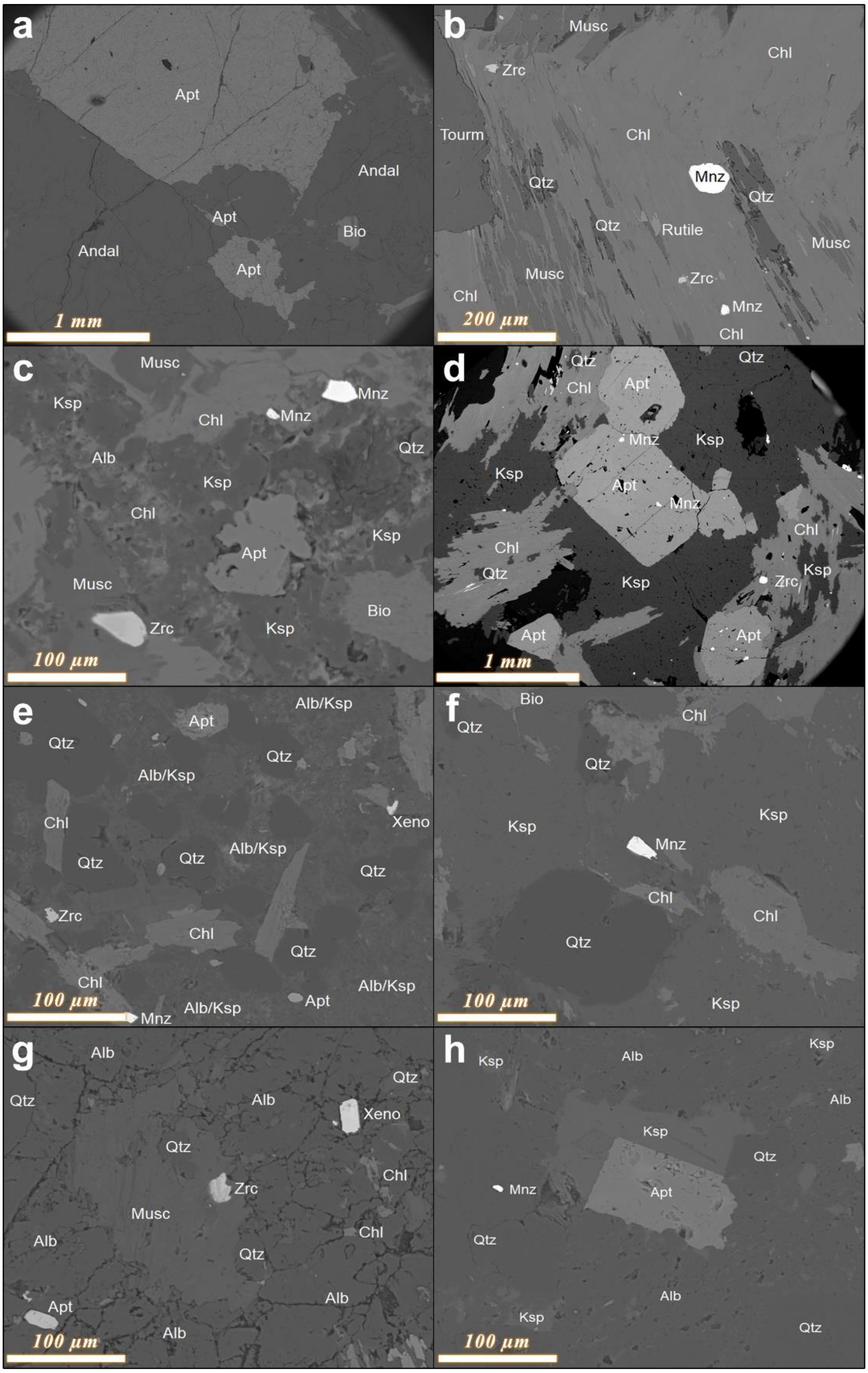

Figure 6: SEM-MLA BSE images showing relationships of datable minerals throughout representative samples. (a) BKBDG2 - Aluminous segregation - Large undeformed apatite enclosed by andalusite. (b) BK06 - Chlorite alteration - Monazite and zircon within chlorite and muscovite adjacent to tourmaline crystals. (c) BK01 - Felsic vein - Monazite, apatite and zircon in vein. (d) BK05 - Felsic vein - Monazite, apatite and zircon in vein. (e) BK21 - Felsic vein - Monazite, apatite, zircon and xenotime in vein. (f) BK21 - Felsic vein - Monazite in vein. (g) BK25A - Felsic Vein - Apatite, zircon and xenotime in vein. (h) KTDD089 - Felsic vein - Monazite and apatite in vein.

4.3 Whole rock geochemistry

Whole rock and trace element geochemical data were collected for twelve samples representing the felsic vein (5 samples), quartz vein (1 sample) and aluminous segregation (6 samples) petrographic classifications. The full geochemical dataset is presented in Appendix E. Felsic veins are plotted alongside known regional intrusive values for relative plutonic and geotectonic classifications. BK25 samples are observed to plot broadly within the quartz diorite space whereas BK01 and BK05 have varying compositions in the syenite and syenodiorite classifications respectively (Fig. 7a). Felsic veins are observed to have a peraluminous composition and except for BK01, an increasingly S-type classification relative to regional intrusive values (Fig. 7b). Trace element geotectonic classifications for felsic veins indicate a syn-collisional to within plate granite classification, with the exception of BK01 which has a marked depletion across trace elements (Fig. 8; 9). Quartz veins and aluminous segregations are depleted across the entire suite of rare earth and incompatible elements, whereas felsic veins and regional intrusives contain a near order of magnitude higher level of Sr relative to mine host rocks, quartz veins and aluminous segregations (Fig. 9).

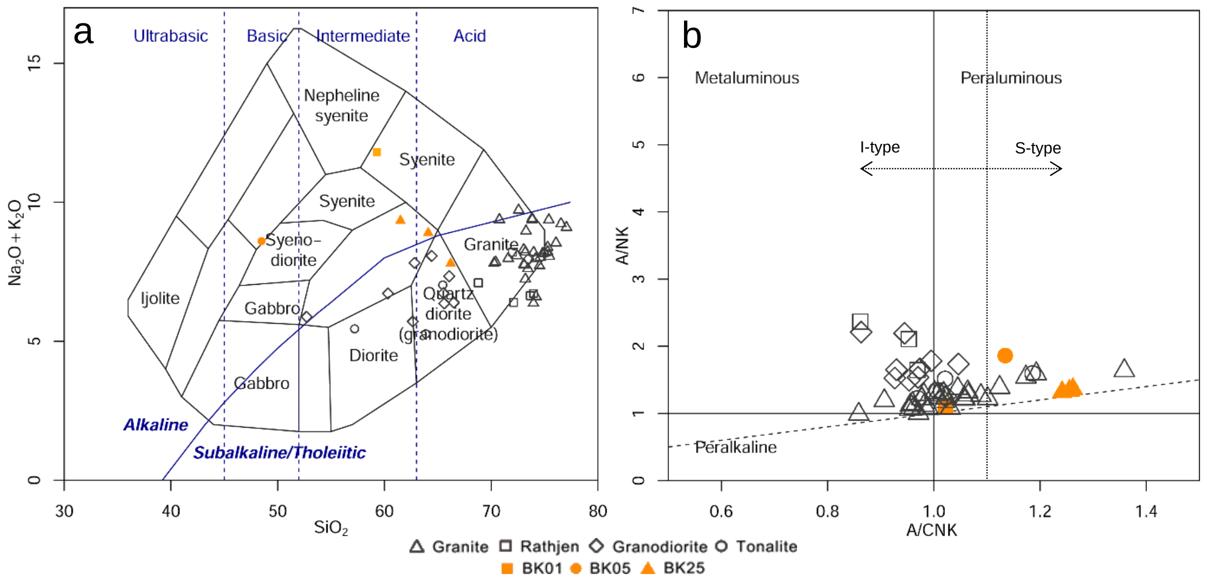

Figure 7: Selected whole rock geochemical plutonic classification diagrams. Regional Delamerian intrusives of various ages in red (Foden et al., 1990; Foden et al., 1999; Foden et al., 2002; Mancktelow, 1979) illustrate the known geochemical range of exposed felsic to felsic-intermediate bodies within 40-kilometres of the Kanmantoo open pit, not including the Black Hill suite. (a) Total alkali-silica (TAS) diagram after Cox, Bell and Pankhurst (1979) showing plutonic classification of mine and regional intrusives. (b) A/NK vs. A/CNK diagram after Shand (1943) showing distribution of mine and regional intrusive geochemistry from metaluminous to peraluminous and I to S-type.

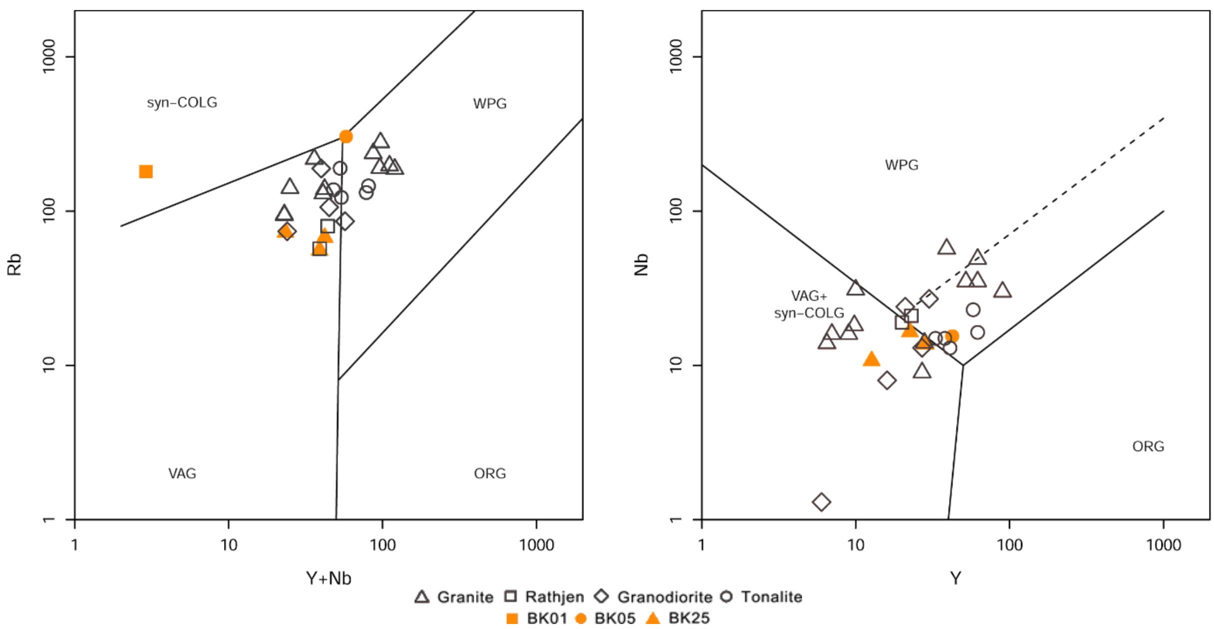

Figure 8: Selected trace element discrimination diagrams for the tectonic classification of granitic rocks after Pearce, Harris & Tindle (1984) and Foden et al., (1990). Syn-COLG = syn-collisional granite, WPG = within-plate granite, VAG = volcanic-arc granite and ORG = ocean-ridge granite. Regional Delamerian intrusives of various ages in red (Foden et al., 1990; Foden et al., 1999; Foden et al., 2002; Mancktelow, 1979) illustrate the known geochemical range of exposed felsic to felsic-intermediate bodies within 40-kilometres of the Kanmantoo open pit, not including the Black Hill suite.

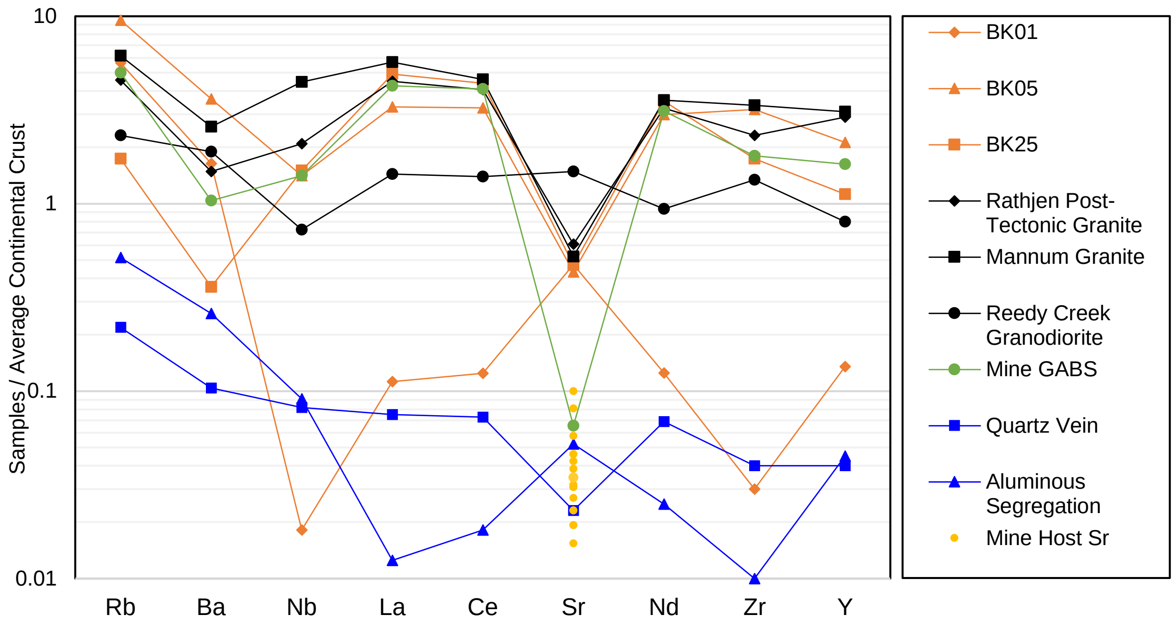

Figure 9: Average continental crust-normalised incompatible element variation diagram after Foden et al. (1990). Representative samples for the felsic vein, quartz vein and aluminous segregation petrographic classifications in contrast to regional intrusive and host rock values. Mannum granite and Reedy Creek granodiorite (Foden et al., 1990), Rathjen post-tectonic granite (Foden et al., 1999), garnet andalusite biotite schist - GABS (Tedesco, 2009), mine host rocks Sr values (Oliver et al., 1998; Schiller, 2000).

Aluminous segregations are characterised by low SiO_2 (<50 wt%) and high Al_2O_3 (> 50 wt%) relative to mine host rock (Fig. 10). Mine selvages, or host rock alteration halos surrounding ore shoots are observed to have a similar composition, marked principally by a depletion in SiO_2 (Fig. 10).

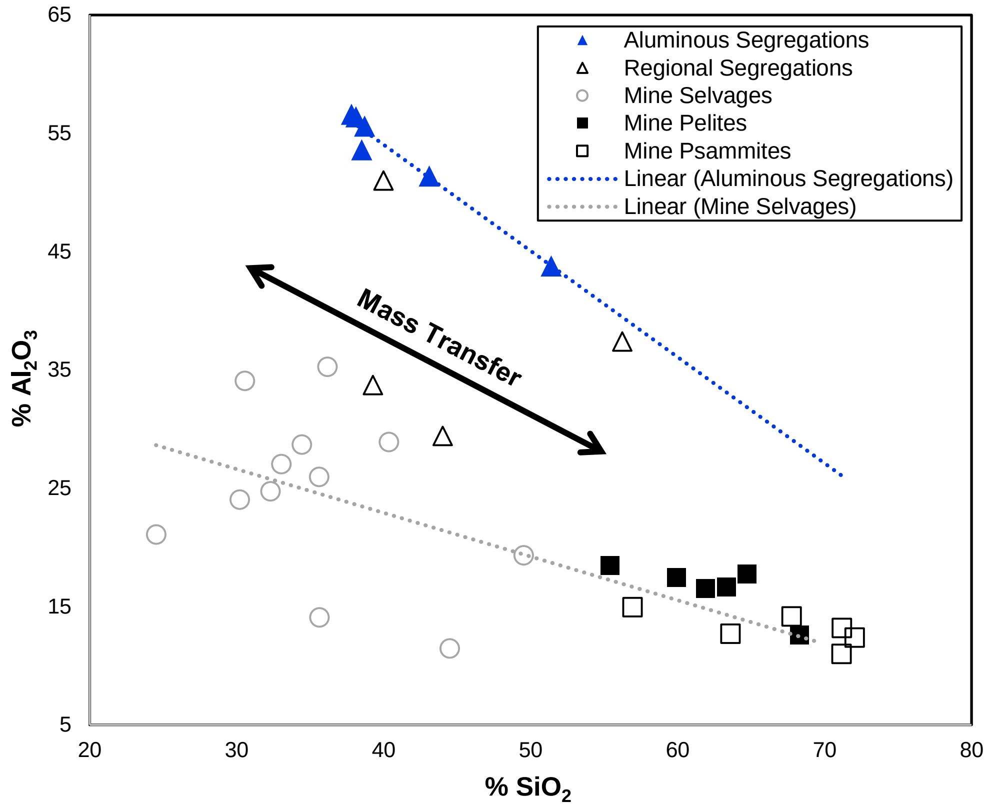

Figure 10: Harker geochemical variation diagram emphasising a mass transfer gradient from host rock to observed mineralogical segregations through selective diffusion of aluminium and silica. Aluminous segregations as described in this study (4.1.4), regional aluminous segregations (Mancktelow, 1979), mine selvages (Oliver et al., 1998; Schiller, 2000), mine pelites and psammites (Oliver et al., 1998).

4.4 LA–ICP–MS

4.4.1 MONAZITE U–PB GEOCHRONOLOGY

A total of 433 individual analyses were performed for monazite U–Pb geochronology, conducted in situ on ten separate samples representing felsic veins, chlorite alteration and regional schists. Monazite is abundant in all analysed samples, with grains ranging in size from 15–50 µm. High resolution imaging of individual grains to identify intergrowths and structural integrity was only conducted on a small number of grains. In vein samples, monazites were predominately located directly in the vein–host contact zone, whereas those in alteration and regional samples were found to be more evenly distributed. Examination of individual analyses during data processing indicated that monazite grains were sometimes intergrown with zircon, or had strong mirrored zirconium and silicon contents, and where these signatures could not be isolated, a total of 91 analyses were removed during Iolite processing. A further 14 total monazite analyses were removed for anomalous silicon contents indicative of host rock contamination. Three individual analyses returned no readable data and were not included in calculations. The full dataset of monazite U-Pb geochronology of standards and unknowns is presented in Appendix G.

Six individual felsic veins, two chlorite alteration samples and two regional schists were selected for monazite U–Pb geochronology (Table 2). Two distinct generations of felsic veins were identified, the oldest ranging from 495.11 ± 2.79 Ma to 491.06 ± 7.03 Ma (Fig. 11a, b, c, f) and the youngest at 485.35 ± 2.46 Ma and 483.43 ± 2.52 Ma (Fig. 11d, e). Chlorite alteration (Fig. 12a, b) and regional schist ages (Fig. 12c, d) include overlapping uncertainties and range from 503.44 ± 3.32 Ma to 496.98 ± 2.18 Ma.

Table 2: List of samples analysed for monazite U–Pb geochronology.

Sample	Total n	Discounted for Zr	Discounted for Si	Laser Error	Final n	Weighted mean age
BK01	37	4	1	-	32	495.11 ± 2.79 Ma
BK05	55	18	9	-	28	492.8 ± 2.94 Ma
BK18	20	7	1	-	12	491.17 ± 5.54 Ma
BK25A	50	14	-	-	36	485.35 ± 2.46 Ma
BK25B	50	12	1	-	37	483.43 ± 2.52 Ma
KTDD089	32	14	1	-	17	491.06 ± 7.03 Ma
BK06	39	7	1	1	31	501.1 ± 4.04 Ma
BK14	21	1	-	-	20	503.44 ± 3.32 Ma
KMT1	60	8	-	1	51	496.98 ± 2.18 Ma
BKDK1	69	6	-	1	62	499.09 ± 1.54 Ma

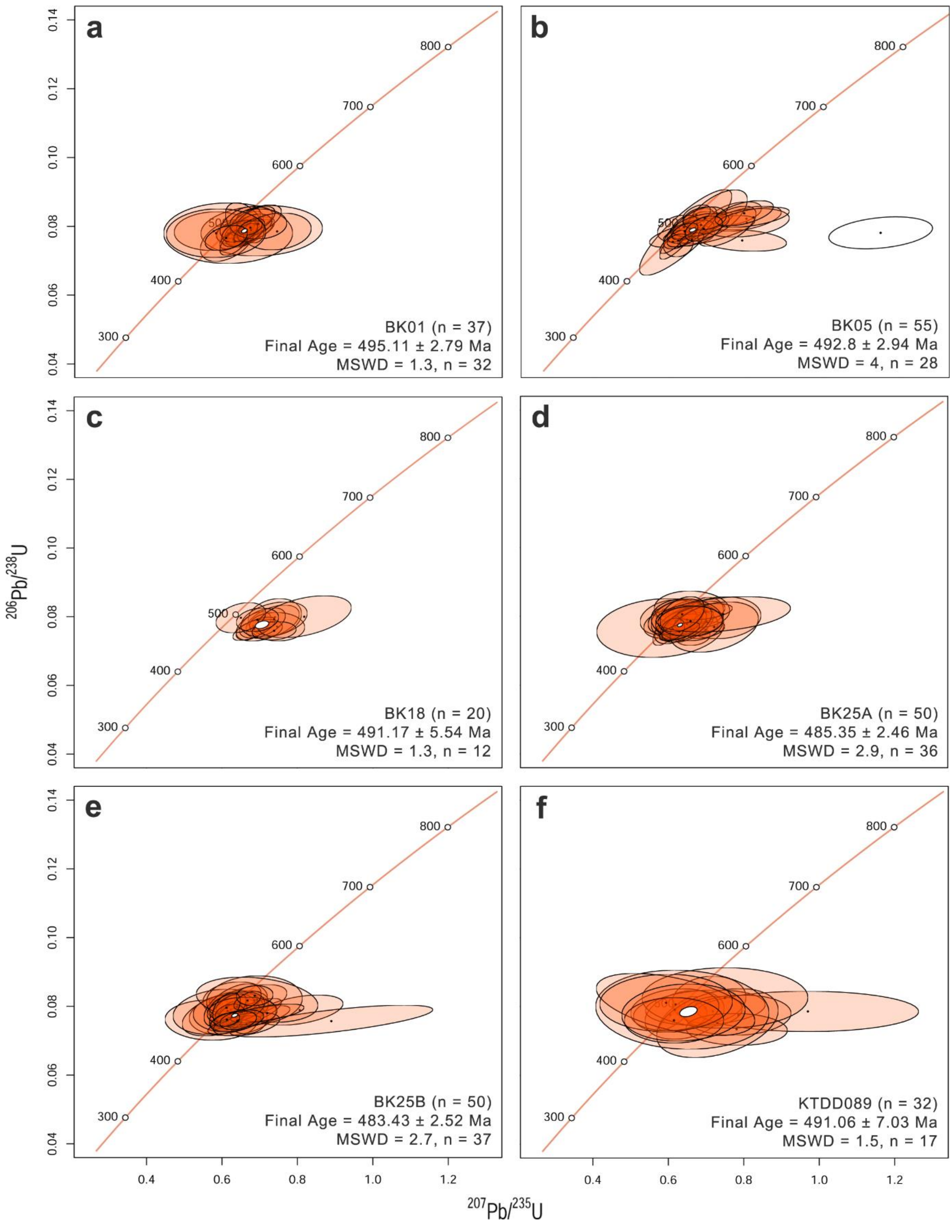

Figure 11: Wetherill concordia diagrams (Wetherill, 1956) ($^{206}Pb/^{238}U$ vs. $^{207}Pb/^{235}U$) for in situ monazite U–Pb analyses conducted on felsic vein samples. Orange ellipses used to calculate the quoted weighted mean age, discordant white ellipse in (b) removed due to Zr contamination not isolated during processing. All ellipses are presented with 2σ errors on both axes.

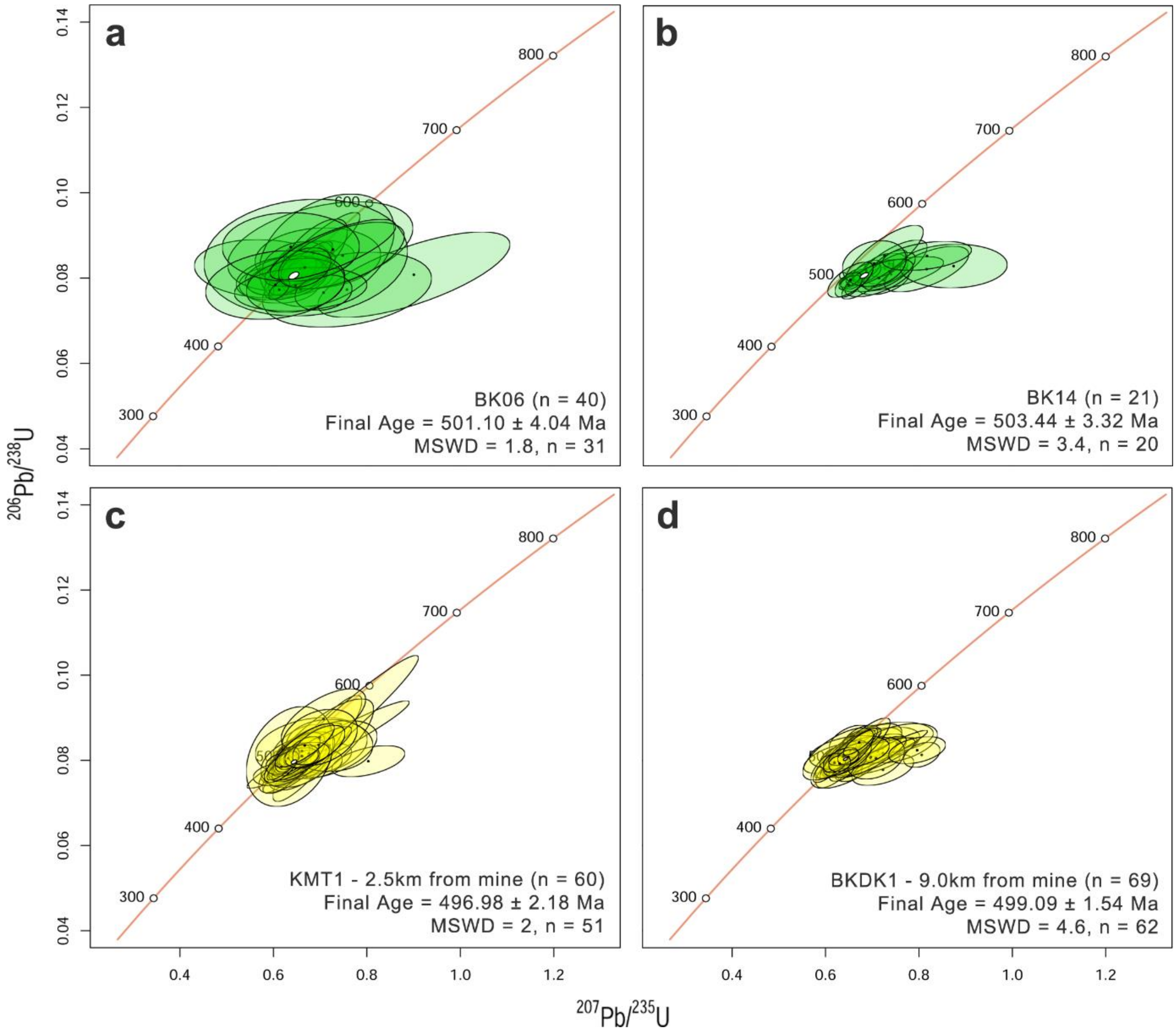

Figure 12: Wetherill concordia diagrams ($^{206}Pb/^{238}U$ vs. $^{207}Pb/^{235}U$) for in situ monazite U–Pb analyses conducted on chlorite alteration and regional samples. Green and yellow ellipses used to calculate the quoted weighted mean age, all ellipses are presented with 2σ errors on both axes. (a) BK06 - Chlorite alteration. (b) BK14 - Chlorite alteration. (c) KMT1 - 2.64 km north of mine. (d) BKDK1 - 9.22 km north of mine.

4.4.2 MONAZITE TRACE ELEMENTS

Monazite trace element data was collected concurrently to U–Pb data across a suite of elements for the felsic vein, chlorite alteration and regional schist samples. Mine samples have high values of LREE and Gd/Lu and low values of HREE, Y_2O_3 and Eu/Eu* relative to regional samples (Fig. 13). Disparities between mine and regional samples are greatest for the most distal sample, BKDK1, whereas KTM1 contains more variable proportions of elements.

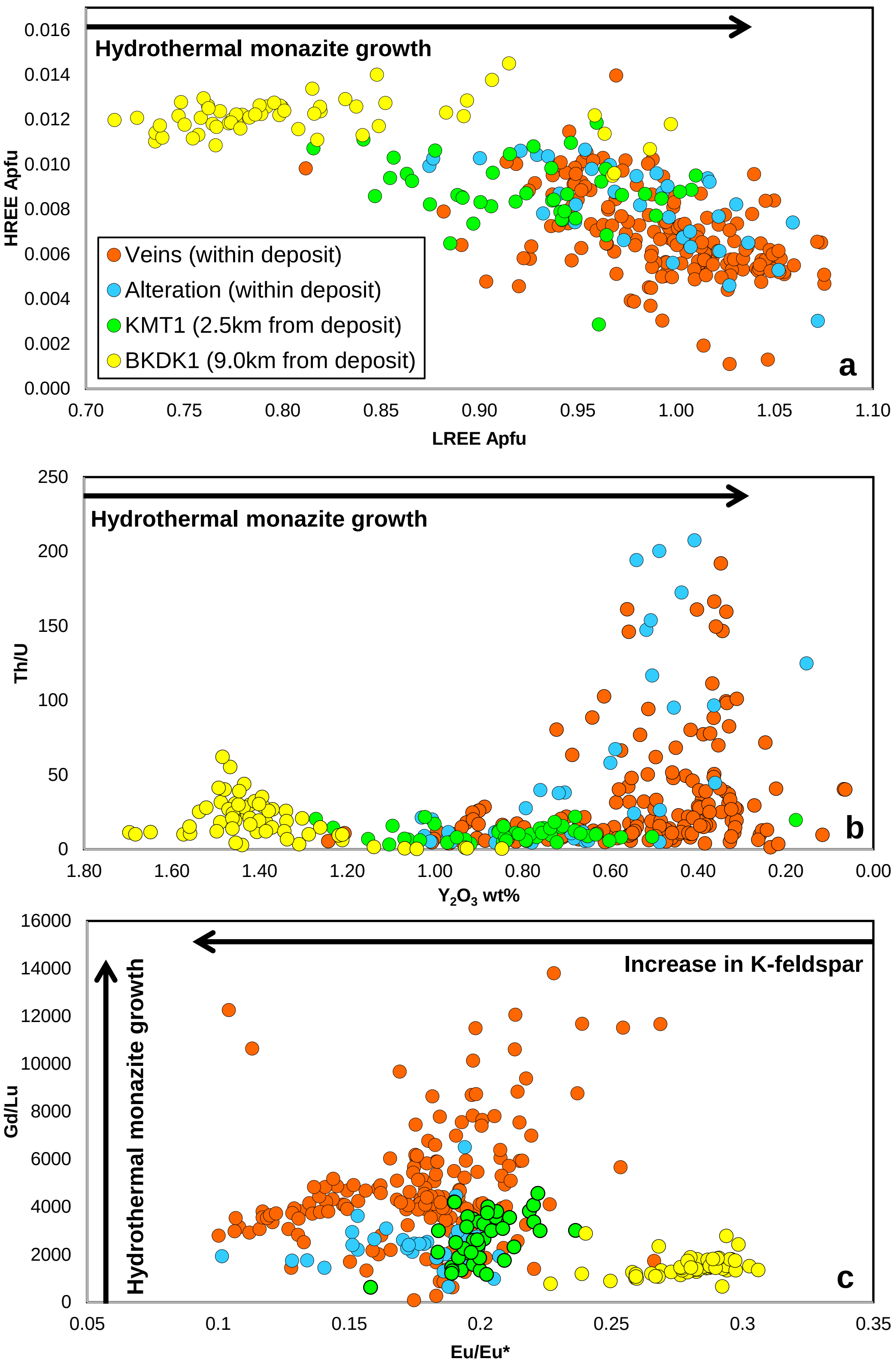

Figure 13: Selected monazite trace element and oxide discrimination diagrams across the entire monazite U–Pb sample suite including the felsic vein, chlorite alteration and regional schist samples. (a) HREE vs. LREE, highlights hydrothermal monazite as a function of LREE enrichment (Poitrasson et al., 2000) where Apfu = Atoms per formula unit. (b) Th/U vs. Y_2O_3, after Rubatto, Hermann & Buick (2006) highlights hydrothermal monazite as a function of Y depletion. (c) Gd/Lu vs. Eu/Eu* after Rubatto et al. (2006), highlights hydrothermal monazite as a function of Gd/Lu and K-feldspar as a function of Eu/Eu*, where Eu* = ((Sm + Gd)/2).

4.4.3 APATITE U–PB GEOCHRONOLOGY

A total of 317 individual analyses were performed for apatite U–Pb geochronology, conducted in situ on six separate samples representing the felsic vein, chlorite alteration and aluminous segregation classifications. From these six samples, three are presented below (Fig. 14) as interpretable data whereas three have been presented in the Appendix H due to excessive error. Apatite was found to be relatively abundant across all analysed samples, with grains generally ranging from 50 µm to 200 µm in diameter. Within vein and alteration samples, individual apatites were predominately located directly within the vein–host contact zone, with 1–5 analyses being taken per grain. The aluminous segregation, BKBDG2 (Fig. 14a), had a single large (2 mm) apatite grain which was analysed fifty-five times. Data reduction was straightforward for the samples presented in Figure 14, with only 11 individual analyses being removed during Iolite processing for host rock contamination as evidenced by anomalous silica contents. No analyses were removed for discordance. The full dataset of apatite U-Pb geochronology results and uninterpreted figures are presented in Appendix K.

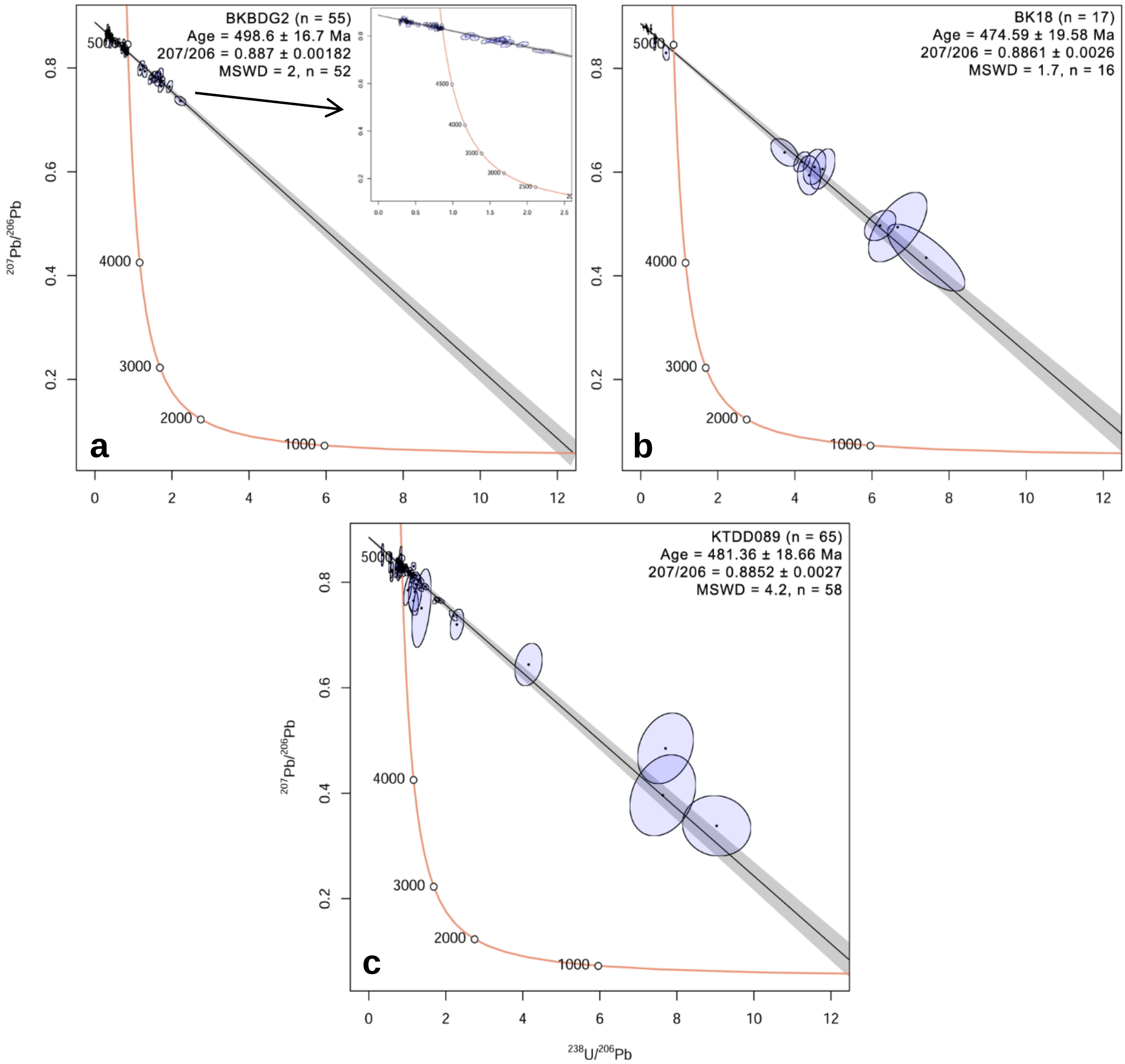

Figure 14: Terra-Wasserburg concordia diagrams ($^{207}Pb/^{206}Pb$ vs. $^{238}U/^{206}Pb$) for in situ apatite U–Pb analyses conducted on aluminous segregation and felsic vein samples. Blue ellipses used to calculate the quoted age, all ellipses are presented with 2σ errors on both axes. (a) BKBDG2 - Aluminous segregation. (b) BK18 - Felsic vein. (c) KTDD089 - Felsic vein.

5 DISCUSSION

This study has documented numerous felsic intrusive veins within the Kanmantoo Cu-Au deposit. The aim of this study is to provide a genetic and temporal constraint on felsic veins and other rock types within a regional Delamerian context to ascertain the significance of magmatic activity in relation to mineralisation.

5.1 Geochronology

5.1.1 RELATIVE AGES

The amount of structural deformation experienced by vein sets is interpreted as a proxy for their relative timing. Intensely boudinaged or tightly folded veins (Fig. 4b) represented by aluminous segregations and an early generation of quartz veining (sample BK27) are considered to have formed first. This was followed by the earliest felsic veins and a second generation of quartz veins (sample BK17) which run parallel or sub-parallel to syn-peak metamorphic fabrics (Fig. 4a) and finally a second generation of felsic veins which cut across all known fabrics (samples BK25A, B) (Fig. 4c).

5.1.2 ABSOLUTE AGES

The Delamerian Orogeny was a relatively short-lived but intense event, with peak metamorphic ages and conditions varying spatially throughout the Kanmantoo Group (Sandiford et al., 1995; Stinear, 2017). Additionally, the Kanmantoo Cu-Au deposit records several pervasive alteration events which are variably recorded in mineral geochronometers. This complexity is best observed within monazite U–Pb concordia plots (Figures 11 & 12) which display a spread of concordant data points across the entire time-frame of the Delamerian Orogeny (550-450 Ma). Monazite U–Pb was selected as the primary geochronological tool given the abundance of suitable monazites observed in samples relative to zircon and xenotime, which were numerous but commonly too small for ablation analysis. Unlike zircon, monazite reactivity allows for geochronological sensitivity in amphibolite facies rocks (Williams, Jercinovic, Harlov, Budzyń & Hetherington, 2011; Grand'Homme et al., 2016) which permits age dating for both felsic vein and metamorphic samples. Apatite was also abundant and was trialled in this study, primarily to investigate its utility by means of reconnaissance data.

5.1.3 INTERPRETATION OF MONAZITE U–PB GEOCHRONOLOGY

The existence of two generations of felsic intrusive veining is supported by both relative and absolute geochronological observations. Previous researchers had noted the possibility of two generations of fluid and mineralising activity within the Kanmantoo Cu-Au deposit, generally at peak and post-peak metamorphic conditions (Arbon, 2011; Booth, 2018) which aligns with monazite U–Pb ages of felsic veins in this study (Fig. 11). Wilson (2009) and Lyons (2012) suggested a progressive system of mineralisation beginning with Cu emplacement directly after peak metamorphism and continuing through to Au emplacement lasting until at least 485 Ma. Oliver et al. (1998) concluded that mineralisation occurred at peak metamorphism, likely continuing into post-peak metamorphic conditions. The emplacement of felsic veins throughout these periods adds weight to a progressive influx of hydrothermal fluids, with at least a proportion having magmatic origins in either the direct supply of magmatic fluids and/or partial melting of host meta-sediment. Samples which experienced the strongest chlorite alteration (samples BK06, 14) recorded the oldest ages (Fig. 12a, b). While overlapping of uncertainties with regional schist, peak metamorphic ages (Fig. 12c, d) suggests they are of the same generation, slightly older ages in chlorite samples may explained by partial U loss within monazites, shifting data further up concordia lines (Fig.

12a, b) and resulting in a significant proportion of analyses having a high Th/U ratio (Fig. 13b). Harrison et al. (2002) showed that U loss can be expected within monazites that have experienced fluid alteration of moderate temperature and chemical variability. Arbon (2011) conducted geothermometry on chlorite within the deposit and showed that temperatures of alteration ranged from roughly 300 to 400 °C, with Fe-rich chlorites associated with variable chemical compositions including those containing high-Bi forming at the lowest temperatures. Grand'Homme et al. (2016) concluded that temperatures below 400 °C may result in only partial resetting of monazites, potentially allowing for U loss. When considering data spread and accounting for U loss, chlorite alteration sample ages are likely to be altered representations of peak metamorphism within the Kanmantoo Cu-Au deposit that do not represent the later Fe-rich chlorite alteration and associated fluid influx. Monazite U-Th-Pb dating by Wilson (2009) produced an age of 492 ± 9 Ma for unmineralized sections of the deposit while Stinear (2017) dated nearby metasediments at 492.4 ± 5.3 Ma. Regional peak metamorphism likely occurred between 500 and 493 Ma regionally (Oliver et al., 1998; Lyons, 2012) and is discussed further below in section 5.4.

5.1.4 INTERPRETATION OF APATITE U–PB GEOCHRONOLOGY

Apatite U–Pb age data are not considered as reliable as monazite due to the clustering of data far from the lower intercept on Tera–Wasserburg plots (Fig. 14), which translates to relatively large uncertainties that cover much of the Delamerian Orogeny. Consequently, apatite U–Pb results have not been heavily relied upon to make interpretations in this discussion, except in relation to aluminous segregations which are included in Figure 16. Aluminous segregations do not contain monazite and were represented by BKBDG2 which contained a large (2 mm diameter) apatite grain allowing for over 50 individual analyses. This sample produced an age of 499.09 ± 16.7 Ma, loosely consistent with relative ages and the observations of Mancktelow (1979) who observed metamorphic segregations forming from the lowest metamorphic grades, but ultimately unreliable due to the large uncertainty.

5.2 Geochemistry

5.2.1 FELSIC VEINS

Standing (2006) first described the presence of copper bearing felsic veins in the Kanmantoo Cu-Au deposit as late stage 10–20 cm wide porphyry dykes with a feldspathic composition including feldspar phenocrysts. Standing (2006) also documented a sheared pegmatite containing feldspar, biotite and copper sulphide within a mineralised shear zone in a cutting behind the Wheel of Fortune prospect. Lyons (2012) completed a more in-depth study by mapping a series of abundant copper bearing veins containing K-feldspar, quartz, biotite, muscovite and sulphides ranging from 10–30 cm in width. These veins were described as relatively young and either predated or were synchronous with the emplacement of the major ore bodies and the sulphide bearing quartz veins mentioned above (Lyons, 2012). Lindqvist (1969) described near-monomineralic albite veins infilling late joint sets within the mine and suggested their formation was due to the break down and chloritisation of biotite releasing alkalis and water into circulating ground fluids. Late joint infilling veins in this study, represented by BK25 although albite rich, were observed to contain interspersed K-feldspar, vuggy quartz, hypogene copper and trace amounts of Ca-plagioclase as well as abundant zircon, monazite, apatite and xenotime, more reminiscent of the descriptions given by Standing (2006). Whole rock discrimination plots of late stage veins (Fig. 7) reflect an albitised sample with increasing partial melting of metasediment (S-type) and peraluminous composition (Shand, 1943). Felsic veins are generally observed to have rare earth and incompatible element patterns like those of regional granitic intrusions (Fig. 7; 8; 9) as described by Foden et al. (1990), and do not match known metasomatic rocks which are heavily depleted across the entire suite. However, the felsic vein sample BK01 shows a highly variable trace element composition which is hard to reconcile with other samples and may reflect sampling contamination by quartz or host rock. Most notably, all felsic veins contain elevated levels of Sr relative to Kanmantoo Group host rocks. It is possible that veins relate to felsic magmatism and not intermediate magmatism as represented by the regional granodiorite sample which varies considerably (Foden et al., 1990). Tectonic discrimination plots of felsic veins in Figure 8 closely match the regional intrusive suite across the syn-collisional, within plate and volcanic arc granite classifications. Pearce et al. (1984) noted that post-orogenic granites are hard to distinguish from volcanic arc and syn-collisional granites in this context. In combination with field observations of previous authors (Standing, 2006; Lyons, 2012), whole rock and trace element compositions of felsic veins indicate an igneous intrusive origin for the majority of samples. In either case, felsic vein forming fluids show clear geochemical signatures of the known regional intrusive suite and this would suggest that broader hydrothermal fluids have a magmatic signature as alluded to previously (Oliver et al., 1998; Focke et al., 2009; Schmidt Mumm et al., 2009; Tedesco, 2009; Wilson, 2009; Arbon, 2011; Lyons, 2012).

5.2.2 ALUMINOUS SEGREGATIONS, QUARTZ VEINS AND CHLORITE ALTERATION

Aluminous segregations were extensively sampled for whole rock and trace element geochemical analysis together with one quartz vein. Mancktelow (1979) first described metamorphic segregations regionally, including aluminous segregations within Kanmantoo Group meta-sediments comparable to those of the Kanmantoo Cu-Au deposit. Segregations were observed to outcrop as veins and pods cross-cutting bedding with a mineralogy strongly reflecting that of the host metasediment but with a coarser grain size and a strong depletion in REE (Mancktelow, 1979), a description that matches aluminous segregations in this study.

The four aluminous segregations sampled by Mancktelow (1979) are plotted alongside aluminous segregations from this study in Figure 10. As a classification, aluminous segregations contain low silica and high alumina contents, in a similar fashion to mine selvages described by various authors (Oliver et al., 1998; Schiller, 2000). Figure 9 highlights the marked depletion in rare earth and incompatible elements of aluminous segregations from this study relative to host rock. Nero (1993) and Lyons (2012) described three generations of quartz veining within the Kanmantoo Cu-Au deposit. Oliver et al. (1998) went further to describe highly aluminous selvages associated with syn-D_3 quartz veining which unlike earlier and later quartz veining, was observed to be sulphide bearing, strongly reminiscent of BK17. Lyons (2012) added that syn-D_3 sulphide bearing quartz veins commonly contained staurolite at their contacts with country rock and were of a similar generation to the K-feldspar veins discussed below. Notably, Oliver et al. (1998) described aluminous selvages surrounding syn-D_3 quartz veining within the mine as containing pink andalusite and euhedral, honey brown staurolite. Aluminous segregation samples in this study are not associated with mineralisation but are comprised primarily of pink andalusite and occur as early, strongly boudinaged veins. BK27 is an early, intensely boudinaged quartz vein which does not contain sulphides and notably contains pink andalusite, whereas BK17 is a younger, undeformed quartz vein bearing sulphides and with staurolite at its contact with host rock. While these rocks may represent a different generation and mineralogy of veining, they are considered to be the outcome of a common physical process. Oliver et al. (1998) described in detail the mechanics of metasomatic mass transfer within the Kanmantoo Cu-Au deposit, and this provides a reasonable explanation for the presence of aluminous segregations and at least some generations of quartz veining within the deposit. Ague (1991) described the prevalence of mass transfer processes during regional metamorphism of pelites resulting in quartz veining, while Mancktelow (1979) suggested a silica-aluminium mass transfer exchange for aluminous segregations (Figure 10). The changing composition of mass transfer products through metamorphism and the first observation of mineralisation at near syn-peak metamorphic conditions may indicate a changing input of fluids to the system from regional metamorphic to localised magmatic hydrothermal (Oliver et al., 1998).

Chlorite alteration samples were not submitted for whole rock or trace element geochemical analysis, however petrographic observations can be used to infer some chemical properties. Chlorite alteration encountered in this study generally exhibited Berlin blue interference colours ranging from weak to strong during cross-polarised microscopy (Figure 5e). Kranidiotis and MacLean (1987) demonstrated that increasing Berlin blue optical properties indicated chlorite contained increasing Fe/Fe+Mg levels where Fe is primarily the product of Fe-rich hydrothermal fluids. Arbon (2011) concluded that the Kanmantoo Cu-Au deposit experienced two generations of chlorite alteration, the first being synchronous to major mineralisation and the result of Fe-Mg-rich fluids, while the second post-dated mineralisation and was the result of Fe-rich fluids. Petrographic descriptions in this study (Appendix B) suggest that chlorite ranges from being synchronous to mineralisation to considerably post-dating mineralisation, approximately confirming the presence of variably Fe-rich hydrothermal fluids throughout peak to retrograde conditions (Arbon, 2011). Notably, sample BK14 contains a large sulphide content synchronous or post-dating second generation chlorite with strong Berlin blue interference. Fe-rich hydrothermal fluids are inferred to be a signature of magmatically derived fluids (Oliver et al., 1998; Tedesco, 2009; Wilson, 2009; Arbon, 2011). However, it remains unclear if host meta-sediments contained high Fe levels at the time of deposition (Lyons, 2012), or because of hydrothermal metasomatic mass-transfer driven by a pluton at depth (Oliver et al., 1998).

5.3 Monazite trace elements as hydrothermal exploration guides

Monazite trace element compositions are observed to vary significantly from regional samples through to mine alterations and felsic veins. Figure 13 shows a consistent and strong vector in the direction of the Kanmantoo Cu-Au deposit marked by LREE enrichment and Y depletion, indicative of hydrothermal monazite. Poitrasson et al. (2000) and Seydoux-Guillaume et al. (2012) demonstrate that monazite of hydrothermal origin can be discriminated from that of metamorphic origin by analysis of trace element and radiogenic distributions as displayed in Figure 13. A hydrothermal signature within veins is consistent with the principal location of monazite in vein contacts and alteration halos. Monazite within BKDK1 (9.22 km north of the mine) shows little to no evidence of hydrothermal alteration in its monazite chemistry whereas KMT1 (2.64 km north of the mine) aligns more closely to mine sample trace element compositions. Monazite of all recorded ages from within the mine show a strong hydrothermal signature (Figure 13), indicating a sustained influx of hydrothermal fluids. Cartwright, Vry and Sandiford (1995) suggested that metamorphic fluids in the Mount Lofty Ranges moved from low to high temperatures while Oliver et al. (1998) proposed a northward progression of metamorphic fluids moving through the Kanmantoo Cu-Au deposit (Fig. 15; 17) on a 20 km scale creating anomalous metasediment chemistry. The monazite trace element results appear to align with these findings. However, the possible existence of complex metamorphic subdomains within the orogen (Sandiford et al., 1995; Stinear, 2017) may affect data on a large scale. Further analysis of meta-sediment monazite trace element compositions east, south and west of the Kanmantoo Cu-Au deposit could help to constrain regional metamorphic fluid flow and elucidate whether hydrothermal alteration signatures continue to increase through and beyond the deposit or mark the deposit as a 'bullseye' along a roughly N-S strike, pointing to a vertical column of magmatic hydrothermal fluids moving upwards from depth and mixing with regional fluids as first proposed by Oliver et al. (1998). Forbes et al. (2015) and Forbes et al. (2016) proposed that IOCG deposits throughout the Gawler Craton could be identified through analysis of glacially dispersed hydrothermal monazite (displaying LREE enrichment and Y depletion) in Permian cover sequences. Within the Olympic Dam deposit, sulphide bearing basaltic dikes relating to the Delamerian Orogeny were shown to contain hydrothermal monazite (Kamenetsky et al., 2015), monazite broadly contains a notable proportion of the deposit's REE enrichment (Schmandt et al., 2017). It is suggested here that monazite trace element analysis could serve as an exploration tool for hydrothermal and/or remobilised deposits hosted in complex metamorphic terranes such as the Kanmantoo Cu-Au deposit where monazites remain in situ and could be analysed in the context of whole rock geochemistry.

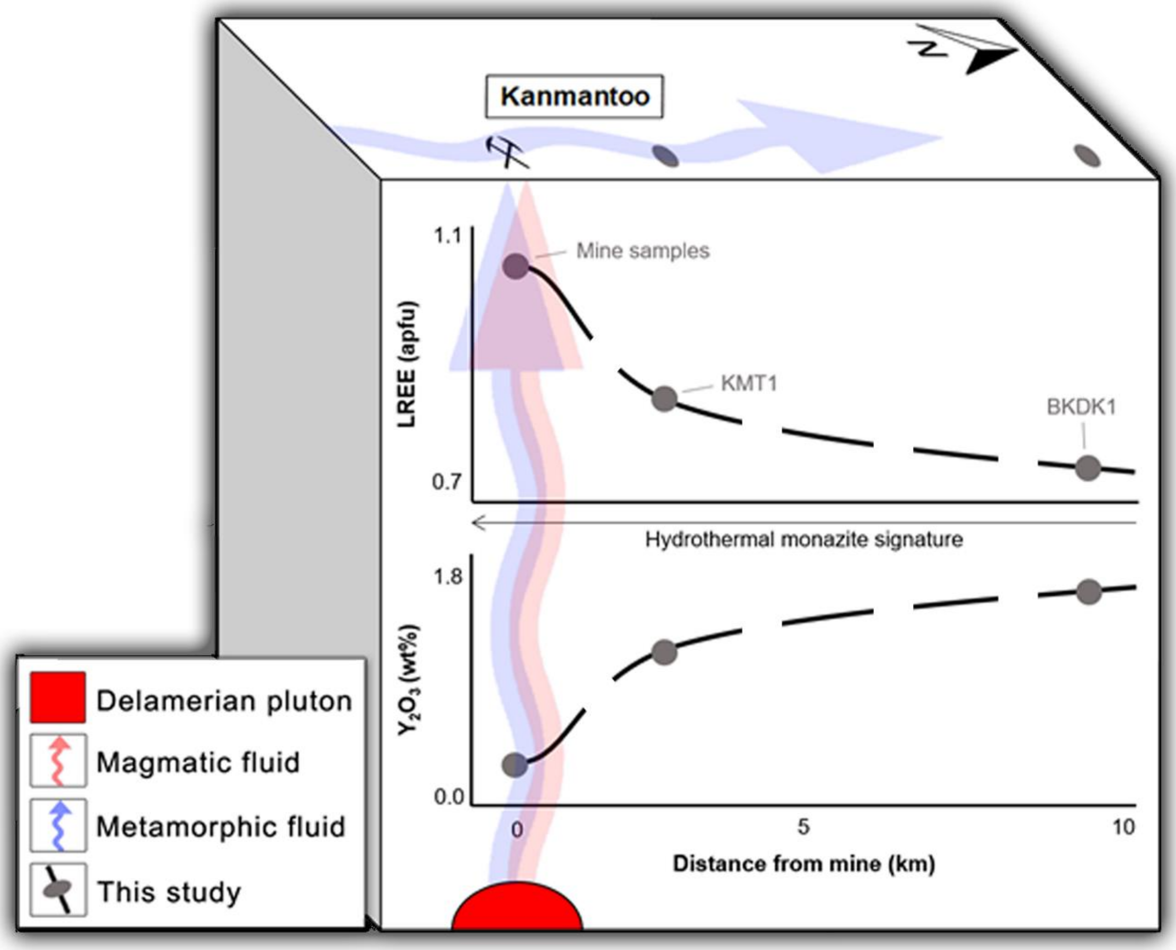

Figure 15: Block model illustrating the approximate spatial distribution of monazite trace element values (Fig. 13) from mine and regional samples. The black dashed lines represent a trend interpreted from data collected in this study (grey circles) with an apparent hydrothermal vector (increasing LREE, decreasing Y) in the direction of the Kanmantoo Cu-Au deposit. It is proposed that a pluton at depth provided a vertical column of magmatic hydrothermal fluids which mixed with regional metamorphic fluids moving laterally in a northerly direction as suggested by Oliver et al. (1998). This hypothesis could be tested by analysis of meta-sediment monazites at similar intervals south of the mine, completing the predicted bell curve and marking the deposit as a bullseye anomaly.

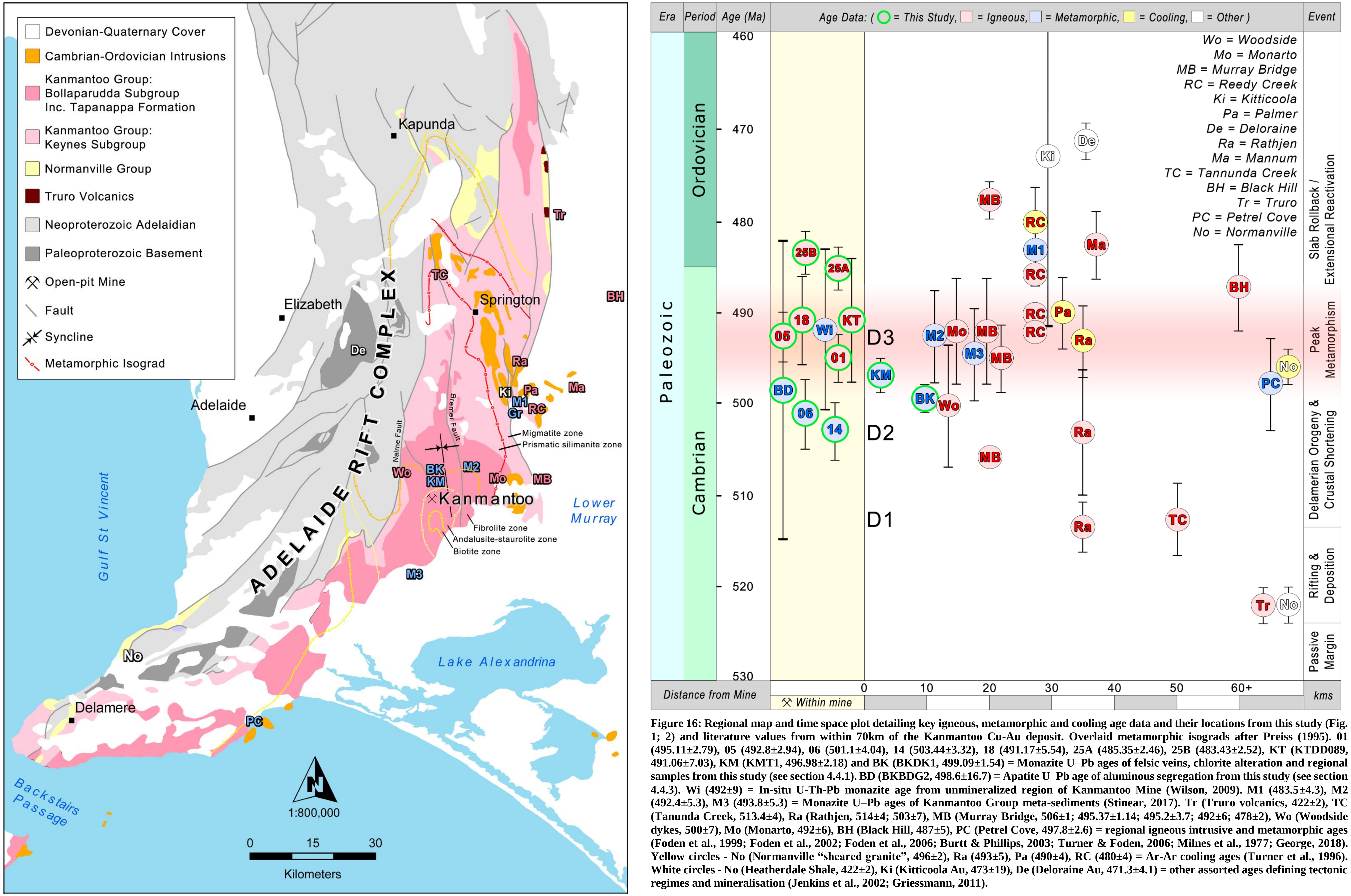

Figure 16: Regional map and time space plot detailing key igneous, metamorphic and cooling age data and their locations from this study (Fig. 1; 2) and literature values from within 70km of the Kanmantoo Cu-Au deposit. Overlaid metamorphic isograds after Preiss (1995). 01 (495.11±2.79), 05 (492.8±2.94), 06 (501.1±4.04), 14 (503.44±3.32), 18 (491.17±5.54), 25A (485.35±2.46), 25B (483.43±2.52), KT (KTDD089, 491.06±7.03), KM (KMT1, 496.98±2.18) and BK (BKDK1, 499.09±1.54) = Monazite U–Pb ages of felsic veins, chlorite alteration and regional samples from this study (see section 4.4.1). BD (BKBDG2, 498.6±16.7) = Apatite U–Pb age of aluminous segregation from this study (see section 4.4.3). Wi (492±9) = In-situ U-Th-Pb monazite age from unmineralized region of Kanmantoo Mine (Wilson, 2009). M1 (483.5±4.3), M2 (492.4±5.3), M3 (493.8±5.3) = Monazite U–Pb ages of Kanmantoo Group meta-sediments (Stinear, 2017). Tr (Truro volcanics, 422±2), TC (Tanunda Creek, 513.4±4), Ra (Rathjen, 514±4; 503±7), MB (Murray Bridge, 506±1; 495.37±1.14; 495.2±3.7; 492±6; 478±2), Wo (Woodside dykes, 500±7), Mo (Monarto, 492±6), BH (Black Hill, 487±5), PC (Petrel Cove, 497.8±2.6) = regional igneous intrusive and metamorphic ages (Foden et al., 1999; Foden et al., 2002; Foden et al., 2006; Burtt & Phillips, 2003; Turner & Foden, 2006; Milnes et al., 1977; George, 2018). Yellow circles - No (Normanville "sheared granite", 496±2), Ra (493±5), Pa (490±4), RC (480±4) = Ar-Ar cooling ages (Turner et al., 1996). White circles - No (Heatherdale Shale, 422±2), Ki (Kitticoola Au, 473±19), De (Deloraine Au, 471.3±4.1) = other assorted ages defining tectonic regimes and mineralisation (Jenkins et al., 2002; Griessmann, 2011).

5.4 Delamerian

Past research on the Kanmantoo Cu-Au deposits metallogenesis has frequently noted the importance of Delamerian related activity either via the in situ remobilisation of metals or by the direct supply of external metal bearing fluids. Figure 16 is a schematic detailing the development of the Delamerian Orogeny within 70 radial kilometres of the Kanmantoo Cu-Au deposit and incorporates all major dates from the onset of Kanmantoo Trough rifting, peak metamorphism and the progression from syn to post-tectonic magmatism. Estimates for the onset, duration and modality of peak metamorphism within the Kanmantoo Cu-Au deposit vary somewhat between authors (Lyons, 2012), but can be summarised as reaching temperatures greater than 500 °C during compression over a roughly 10 Myr period between 500 to 490 Ma (Seccombe et al., 1985; Parker, 1986; Oliver et al., 1998; Foden, 2006; Wilson, 2009; Lyons, 2012). The first appearance of felsic veins (data from this study) between 495.11 ± 2.79 Ma and 491.06 ± 7.03 Ma is consistent with these estimates, and also with large-scale magmatic activity in the adjoining provinces of Monarto and Murray Bridge between 495.2 ± 3.7 Ma and 492 ± 6 Ma (Foden et al., 2006). This, along with the identification of chemical signatures indicative of mineralisation related to magmatic fluids within the deposit (Oliver et al., 1998; Focke et al., 2009; Schmidt Mumm et al., 2009; Tedesco, 2009; Wilson, 2009; Arbon, 2011; Lyons, 2012), suggests that peak-metamorphism at the local scale was generated as a direct result of the intrusion of a pluton or plutons at depth, as is observed regionally (Sandiford et al., 1995). Within the mine, peak metamorphism is generally correlated with the generation of key structural features from late D_2 through D_3 which have served, at least partially, as fluid pathways for ore precipitation during and after peak metamorphism (Oliver et al., 1998; Wilson, 2009; Arbon, 2011; Lyons, 2012). Collectively, Figure 16 highlights a complex set of individual processes that occurred at peak metamorphism and were capable of providing the chemical, thermal and structural conditions that culminated in the generation of a hydrothermal deposit.

5.4.1 FELSIC VEIN FORMATION

Recent research has investigated the conditions under which pegmatite and aplite veins crystallised throughout different terranes globally. Hossain and Tsunogae (2008) concluded that felsic pegmatites in the Paleoproterozoic basement of Bangladesh crystallised at ~4.8 kbar and 660-670 °C, while Dill (2015) estimated temperatures of 660 °C for aplites in the Miesbrunn pegmatite-aplite swarm. Tuttle and Bowen (1958) demonstrated that wet melting and subsequently crystallisation within albite, orthoclase and quartz granite systems can occur at 660 °C. These conditions are not dissimilar to peak metamorphism within the Kanmantoo Cu-Au deposit as discussed above and are well below peak metamorphic temperatures in the intrusion-related core of the orogen which reach 790-860 °C (Stinear, 2017). Various authors have suggested the presence of a pluton at depth below the deposit at around this time (Oliver et al., 1998; Focke et al., 2009; Schmidt Mumm et al., 2009; Tedesco, 2009; Wilson, 2009; Arbon, 2011; Lyons, 2012) and this is thought to have released mineralising magmatic hydrothermal fluids. Notably, Gum (1998) observed pegmatites intruding along late shear zones 10 km to the west of the deposit and noted the pegmatite rich Monarto intrusive suite. The transition from a peak-metamorphic and compressional regime to an early post-peak metamorphic and extensional regime as described by Foden et al. (2006) could have reactivated peak-metamorphic structures and fabrics within the Kanmantoo Cu-Au deposit (Lyons, 2012). It is proposed that high temperatures, ample fluid pathways and pressure instabilities at this time would have provided the optimal conditions for fluids to travel from depth and crystallise/precipitate below and within the Kanmantoo Cu-Au deposit together with magmatic hydrothermal fluids.

5.5 Mineralisation

Central to the debate regarding the origin of the Kanmantoo Cu-Au deposit is the question as to whether metals were deposited together with Kanmantoo Trough sediments and locally remobilised or precipitated hydrothermally from external sources at a confluence of optimum temperature, redox and structural conditions. Marshall and Gilligan (1993) concluded that remobilisation of massive sulphide deposits is most effective under prograde and retrograde conditions from 350–500 °C, although recent research suggests that these conditions may not be ideal for Cu remobilisation in other terranes (Pitcairn, Craw, Olivo, Kerrich & Brewer, 2006). Regionally however, early remobilisation of massive sulphides is observed in the Wheal Ellen, South Hill and Strathalbyn deposits hosted in rocks of a similar metamorphic grade to that of the Kanmantoo Cu-Au deposit (Preiss, 1995) where major ore bearing veins are concordant with S_0 and S_1 (Seccombe et al., 1985). Sandiford et al. (1995) estimated peak metamorphic temperatures within the Kanmantoo Trough of 550-600 °C and so it is expected that prograde temperatures and chemistry, developing over some 10 Myr were enough to remobilise ore through pervasive metamorphic fluid flow (Ague, 1991; Oliver et al., 1998). Recent research suggesting the presence of non-remobilised mineralisation conformable to bedding in the Nugent lode (Pollock, 2018) is difficult to reconcile with all other structural and metamorphic literature on the deposit and warrants further investigation. The structural record within the Kanmantoo Cu-Au deposit is more complex than in surrounding deposits, with many early fabrics being replaced by a syn-peak metamorphic schistosity. However, relict bedding and multiple generations of veining are preserved. The majority of past research suggests that all mineralisation is roughly conformable to these later fabrics and structures rather than to bedding. Intensely boudinaged or tightly folded quartz veins and aluminous segregations consistent with an earlier metamorphic development are not observed to have a strong spatial and temporal relationship with ore as shown in this study and by many other researchers (Seccombe et al., 1985; Oliver et al., 1998; Lyons, 2012). The major ore bodies, shear zones and their contemporaneous selvages in association with lightly deformed sulphide bearing quartz and felsic intrusive veins first appear as near syn-peak metamorphic structures and continue to form through retrograde conditions (Oliver et al., 1998; Lyons, 2012). Mass transfer products within the deposit transition from being devoid of mineralisation in the earlier stages of the Delamerian Orogeny, to being sulphide bearing near the peak of metamorphism and thereafter, possibly reflecting a changing input of hydrothermal fluids at ~492.8 ± 2.94 Ma.

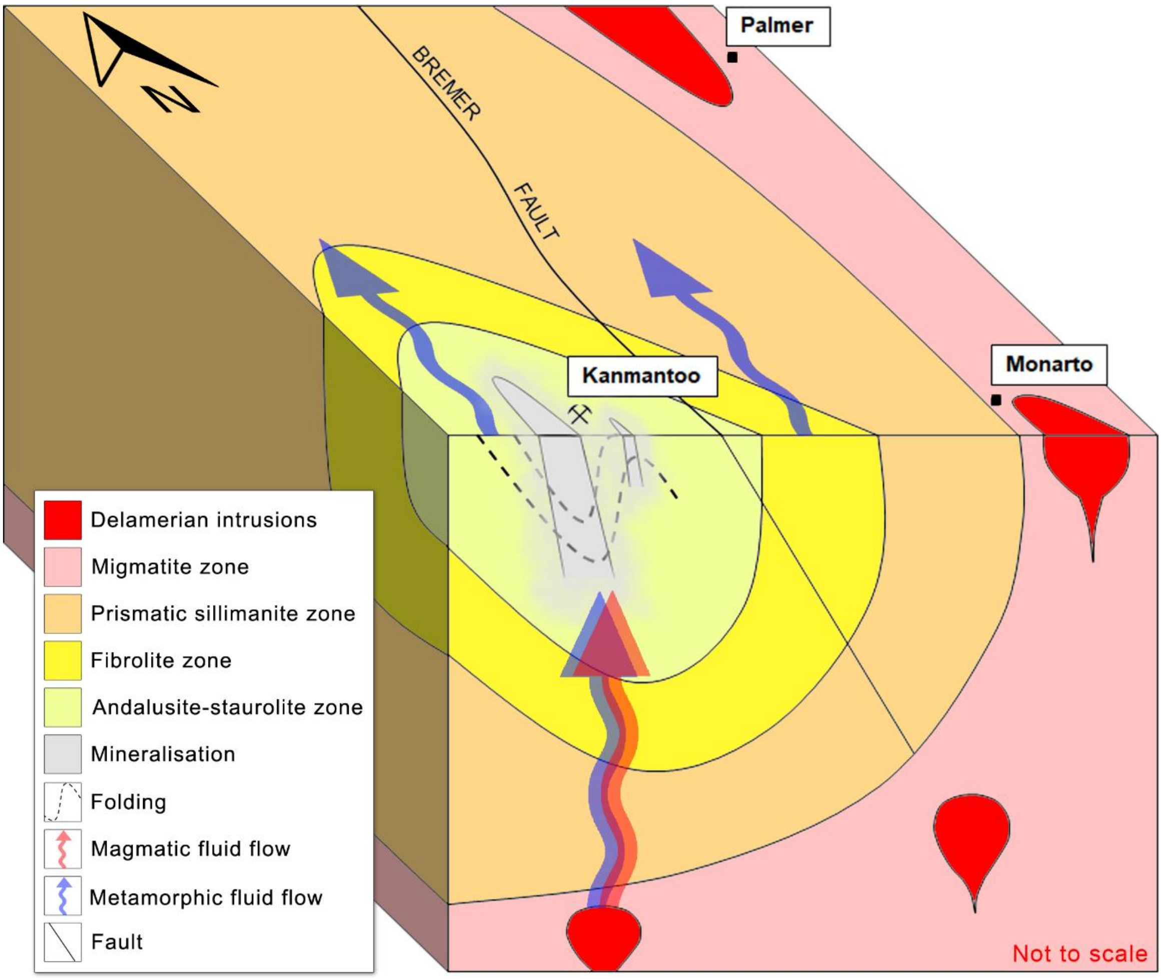

Figure 17: Block model illustrating the interpreted role of magmatic and metamorphic fluids on mineralisation within the Kanmantoo Cu-Au deposit at ~3–4 kbar (Schiller, 2000). Plutons at depth generating igneous intrusives, magmatic hydrothermal and metamorphic fluids permeating upwards, aided by pervasive and later reactivated structural features, to precipitate metals at the observed level as a series of partially structurally controlled ore bodies. Regional metamorphic fluids travelling laterally also contribute to mineralisation, with high metamorphic temperatures being partially driven by distal regional plutons. Northward direction of regional metamorphic fluids after Oliver et al. (1998).

6 CONCLUSIONS

The Kanmantoo Cu-Au deposit is a multifaceted structure that, in its final form, exists as the product of at least 45 Ma of sustained and intense geological activity. In this context, it is the product of hydrothermal fluid flow beginning at peak metamorphic conditions during the Delamerian Orogeny at ~495 Ma and continuing through post-peak conditions. The fluid flow can be identified through syn- to post-peak metamorphic, hydrothermal monazite signatures which vector toward the deposit, in contrast to regional metamorphic signatures. Mineralisation was precipitated as variable structurally-controlled ore shoots within a meta-turbidite sequence. Mineralising fluids are likely to have been a combination of both metamorphic and magmatically derived fluids with the thermal and chemical energy to transport and precipitate ore, as indicated in part by the presence of late, metalliferous quartz and felsic veins. Some of the economic metals have likely travelled upwards from depth before mixing with lateral metalliferous metamorphic fluids at a regional stratabound confluence, generating unique Kanmantoo-style mineralisation. The Delamerian Orogeny is therefore a foremost component in the genesis of the Kanmantoo Cu-Au deposit through the creation and sustained reactivation of structural controls, pervasive regional metamorphism and magmatism. This confirms the continued prospectivity of Delamerian affected terranes, particularly where both magmatism and pervasive structural controls are present.

7 FUTURE RESEARCH

1. Succeeding research could expand the monazite trace element data set acquired in this study by sampling at regular intervals on a ~10 km radial scale around the Kanmantoo Cu-Au deposit. The deposit is hypothesised to be identifiable by a hydrothermal monazite ‘bullseye’ anomaly along N-S and E-W transects (Fig. 15). Proposed title: *Hydrothermal monazite as an exploration tool in complex metamorphic terranes; Kanmantoo Cu-Au deposit case study*.

2. There remains a strong scientific and economic imperative to constrain the crustal evolution and exploration potential of Delamerian Orogeny affected terranes throughout South Eastern Australia.

8 ACKNOWLEDGEMENTS

My supervisors Dr Richard Lilly, Peter Rolley, Dr David Kelsey and colleague Maddy Booth are thanked for their invaluable assistance, scientific insights and personal guidance throughout the year. Funding, background knowledge and logistical support for this project has been provided by Hillgrove Resources Limited and its dedicated team of geologists and field staff who are all thanked including Hayden Arbon. Both the University of Adelaide and Adelaide Microscopy have provided the facilities, analytical equipment and training essential to undertaking this study, particularly Dr Sarah Gilbert. Within the Department of Earth Sciences, and in no particular order, thank you to Megan Williams, Brad Cave, Mitchell Bockmann and Prof Martin Hand for your invaluable guidance with data processing and interpretation. Furthermore, a sincere thanks is extended to Dr Anthony Milnes and Dr Wolfgang Preiss for their assistance in accessing the wealth of knowledge that already exists regarding the subject. Finally, a special thanks to the AusIMM and its EEF Scholarship Committee for providing exceptional financial, developmental and mentoring support throughout my Honours year.

8 REFERENCES

AGUE, J. J. (1991). Evidence for major mass transfer and volume strain during regional metamorphism of pelites. *Geology*, 19(8), 855-858.

ANDERSON, J. A. (1993). Kanmantoo Trough. In W. V. Preiss (Ed.), *South Australian Resources: Technical Sessions, Abstracts* (pp. 38-43). South Australia: Department of Mines and Energy.

ARBON, H. (2011). *Bismuth distribution in the Cu-Au mineralisation of the Kanmantoo deposit, South Australia* (Honours thesis). University of Adelaide, Australia.

BELPERIO, A. P., PREISS, W. V., FAIRCLOUGH, M. C., GATEHOUSE, C. G., GUM, J., HOUGH, J., & BURTT, A. (1998). Tectonic and metallogenic framework of the Cambrian Stansbury Basin - Kanmantoo Trough, South Australia. *AGSO Journal of Australian Geology & Geophysics*, 17, 183-200.

BOOTH, M. (2018). *Distribution and mineralogical association of Au at the Kanmantoo Cu-Au deposit* (Honours thesis). University of Adelaide, Australia.

BURTT, A. C., & PHILLIPS, D. (2003). Ar/Ar dating of a pegmatite, Kinchina Quarry, Murray Bridge, South Australia. *MESA Journal*, 28, 50-52.

BURTT, A. C. (2006). Chapter 8, Kanmantoo Trough. In: B. J. Cooper and M. A. McGeough (Eds.), *South Australia Mineral Explorers Guide. 2nd Edition* (pp. 1-20). Adelaide: South Australian Department of Primary Industries and Resources.

CARTWRIGHT, I., VRY, J. K., & SANDIFORD, M. (1995). Changes in the stable isotope ratios of metapelites and marbles during regional metamorphism, Mount Lofty Ranges, South Australia: implications for crustal scale fluid flow. *Contributions to Mineralogy and Petrology*, 120, 292-310.

CHEW, D., PETRUS, J., & KAMBER, B. (2014). U–Pb LA-ICPMS dating using accessory mineral standards with variable common Pb. *Chemical Geology*, 363, 185-199.

COOPER, J. A., JENKINS, R. J., COMPSTON, W., & WILLIAMS, I. S. (1992). Ion-probe zircon dating of a mid-Early Cambrian tuff in South Australia. *Journal of the Geological Society of London*, 149, 185-192.

COX, K. G., BELL, J. D., & PANKHURST, R. J. (1979). *The interpretation of igneous rocks*. London: Allen & Unwin.

DICKINSON, S. B. (1942). The structural control of ore deposition in some South Australian copper fields. *Geological Survey of South Australia, Bulletin*, 20, 79-99.

DILL, H. G. (2015). Pegmatitic rocks and their geodynamic setting in the Central European Variscides. In F. Pirajno (Ed.), *The Hagendorf-Pleystein province: the center of pegmatites in an Ensialic Orogen* (pp. 55-109). Switzerland: Springer International Publishing.

FLÖTTMANN, T., HAINES, P., JAGO, J., JAMES, P., BELPERIO, A., & GUM, J. (1998). Formation and reactivation of the Cambrian Kanmantoo Trough, SE Australia: implications for early Palaeozoic tectonics at eastern Gondwana's plate margin. *Journal of the Geological Society, London*, 155, 525-539.

FOCKE, D., SCHMIDT MUMM, A., TEDESCO, A., SEIFERT, T., & BRADY, R. (2009). Pressure, temperature and fluid composition variation of the mineralising system at the Kanmantoo Cu-Au deposit: Combining fluid inclusion analysis with Ti in quartz thermometry. *Journal of Geochemical Exploration*, 101, 35.

FODEN, J. D., TURNER, S. P., & MORRISON, R. S. (1990). Tectonic implications of Delamerian magmatism in South Australia and western Victoria. *Geological Society of Australia Special Publication*, 16, 465-482.

FODEN, J. D., SANDIFORD, M., DOUGHERTY-PAGE, J., & WILLIAMS, I. (1999). Geochemistry and geochronology of the Rathjen Gneiss: implications for the early tectonic evolution of the Delamerian Orogen. *Australian Journal of Earth Sciences*, 46, 377-389.

FODEN, J. D., ELBURG, M. A., TURNER, S. P., SANDIFORD, M., O'CALLAGHAN, J., & MITCHELL, S. (2002). Granite production in the Delamerian Orogen, South Australia. *Journal of the Geological Society, London*, 159, 557-575.

FODEN, J. D., ELBURG, M. A., DOUGHERTY-PAGE, J., & BURTT, A. (2006). The timing and duration of the Delamerian Orogeny: Correlation with the Ross Orogen and implications for Gondwana assembly. *The Journal of Geology*, 156, 10-33.

FORBES, C., GILES, D., FREEMAN, H., SAWYER, M., & NORMINGTON, V. (2015). Glacial dispersion of hydrothermal monazite in the Prominent Hill deposit: an exploration tool. *Journal of Geochemical Exploration*, 81, 18-29.

FORBES, C., GILES, D., FREEMAN, H., SAWYER, M., & NORMINGTON, V. (2016). Using REE chemistry of glacially dispersed hydrothermal monazite to target IOCG deposits in the Gawler Craton. *MESA Journal*, 81, 18-29.

GEORGE, C. (2018). *Adakitic rocks of Kinchina and their relationship to Gondwanan subduction.* (Honours thesis). University of Adelaide, Australia.

GRAND'HOMME, A., JANOTS, E., SEYDOUX-GUILLAUME, A., GUILLAUME, D., BOSSE, V., & MAGNIN, V. (2016). Partial resetting of the U-Th-Pb systems in experimentally altered monazite: Nanoscale evidence of incomplete replacement. *Geology*, 44(6), 431-434.

GRIESSMANN, M. (2011). *Gold mineralisation in the Adelaide fold belt* (Doctoral dissertation). University of Adelaide, Australia.

GUM, J. (1998). The sedimentology, sequence stratigraphy and mineralisation of the Silverton subgroup, South Australia (Doctoral dissertation). University of Adelaide, Australia.

HARRISON, T. M., CATLOS, E. J., & MONTEL, J. (2002). U-Th-Pb dating of phosphate minerals. *Reviews in Mineralogy and Geochemistry*, 48(1), 524-558.

HOSSAIN, I., & TSUNOGAE, T. (2008). Fluid inclusion study of pegmatite and pelite veins of Paleoproterozoic basement rocks in Bangladesh: Implications for magmatic fluid compositions and crystallization depth. *Journal of Mineralogical and Petrological Sciences*, 103, 121-125.

JAGO, J. B., GUM, J. C., BURTT, A. C., & HAINES, P. W. (2003). Stratigraphy of the Kanmantoo Group: a critical element of the Adelaide Fold Belt and the Palaeo-Pacific plate margin, Eastern Gondwana. *Australian Journal of Earth Sciences*, 50, 343-363.

JENKINS, R. J., COOPER, J. C., & COMPSTON, W. (2002). Age and biostratigraphy of Early Cambrian tuffs from SE Australia and southern China. *Journal of the Geological Society of London*, 159, 645-658.

JOCHUM, K. P., WEIS, U., STOLL, B., KUZMIN, D., YANG, Q., RACZEK, I., & FRICK, D. A. (2011). Determination of reference values for NIST SRM 610–617 glasses following ISO guidelines. *Geostandards and Geoanalytical Research*, 35(4), 397-429.

KAMENETSKY, V. S., EHRIG, K., MAAS, R., MEFFRE, S., KAMENETSKY, M., MCPHIE, J., APUKHTINA, O., HUANG, Q., THOMPSON, J., CIOBANU, C. L., & COOK, N. J. (2015). The supergiant Olympic Dam Cu-U-Au-Ag ore deposit: toward a new genetic model. *Proceedings of the World Class Ore Deposits: Discovery to Recovery Conference*, Hobart, TAS: Society of Economic Geologists

KRANIDIOTIS, P., & MACLEAN, W. H. (1987). Systematics of chlorite alteration at the Phelps Dodge massive sulphide deposit, Matagami, Quebec. *Economic Geology*, 82(7), 1898-1911.

LINDQVIST, W. F. (1969). *Geology and metamorphic history of the Kanmantoo Copper Deposit, South Australia* (Doctoral dissertation). University of London, United Kingdom.

LYONS, N. (2012). *Evidence for magmatic hydrothermal mineralisation at Kanmantoo copper deposit, South Australia* (Honours thesis). University of Adelaide, Australia.

MANCKTELOW, N. S. (1979). *The structure and metamorphism of the Southern Adelaide Fold Belt* (Doctoral dissertation). University of Adelaide, Australia.

MARSHALL, B., & GILLIGAN, L. B. (1993). Remobilization, syn-tectonic processes and massive sulphide deposits. *Ore Geology Reviews*, 8, 39-64.

MILNES, A. R., COMPSTON, W., & DAILY, B. (1977). Pre- to syn-tectonic emplacement of early Palaeozoic granites in south-eastern South Australia. *Journal of the Geological Society of Australia*, 24, 87-106.

NERO, L. (1993). *Structure and metamorphism of the Kanmantoo Mine and surrounding area, Kanmantoo Group, South Australia* (Honours thesis). Monash University, Australia.

OLIVER, N. H. S., DIPPLE, G. M., CARTWRIGHT, I., & SCHILLER, J. (1998). Fluid flow and metasomatism in the genesis of the amphibolite-facies, pelite-hosted Kanmantoo copper deposit, South Australia. *American Journal of Science*, 298, 181-218.

PARKER, A. J. (1986). Tectonic development and metallogeny of the Kanmantoo Trough in South Australia. *Ore Geology Reviews*, 1, 203-212.

PATON, C., HELLSTROM, J., PAUL, B., WOODHEAD, J., & HERGT, J. (2011). Iolite: Freeware for the visualisation and processing of mass spectrometric data. *Journal of Analytical Atomic Spectrometry*, 26(12), 2508-2518.

PAYNE, J. L., HAND, M., BAROVICH, K., & WADE, B. (2008). Temporal constraints on the timing of high-grade metamorphism in the northern Gawler Craton: implications for assembly of the Australian Proterozoic. *Australian Journal of Earth Sciences*, 55(5), 623-640.

PEARCE, J. A., HARRIS, N. B. W., & TINDLE, A. G. (1984). Trace element discrimination diagrams for the tectonic interpretation of granitic rocks. *Journal of Petrology*, 25(4), 956-983.

PITCAIRN, I. K., CRAW, D., OLIVO, G. R., KERRICH, R., & BREWER, T. S. (2006). Sources of metals and fluids in orogenic gold deposits: Insights from the Otago and Alpine Schists, New Zealand. *Economic Geology*, 101, 1525–1546.

POITRASSON, F., CHENERY, S., & SHEPHERD, T. J. (2000). Electron microprobe and LA-ICP-MS study of monazite hydrothermal alteration: Implications for U-Th-Pb geochronology and nuclear ceramics. *Geochimica et Cosmochimica Acta*, 64(19), 3283-3297.

POLLOCK, M. V., SPRY, P. G., TOTT, K. A., KOENIG, A., BOTH, R. A., & OGIERMAN, J. (2018). The origin of the sediment-hosted Kanmantoo Cu-Au deposit, South Australia: Mineralogical considerations. *Ore Geology Reviews*, 95, 94-117.

PREISS, W. V. (1995). Early and Middle Palaeozoic Orogenesis: Delamerian Orogeny. In J. F. Drexel & W. V. Preiss (Eds.), *The geology of South Australia. Vol. 2, The Phanerozoic* (pp. 45-57). South Australia: Geological Survey, Bulletin 54.

ROLLEY, P., & WRIGHT, M. (2017). Kanmantoo copper deposits. In N. Phillips (Ed.), *Australian Ore Deposits: Monograph 32* (pp. 667-670). Melbourne: Australasian Institute of Mining and Metallurgy.

RUBATTO, D., HERMANN, J., & BUICK, I. S. (2006). Temperature and Bulk Composition Control on the Growth of Monazite and Zircon During Low-pressure Anatexis (Mount Stafford, Central Australia). *Journal of Petrology*, 47(10), 1973-1996.

SCHMANDT, D., COOK, N. J., CIOBANU, C. L., EHRIG, K., WADE, B. P., GILBERT, S., KAMENETSKY, V. S. (2017). Rare earth element fluorocabonate minerals from the Olympic Dam Cu-U-Au-Ag deposit, South Australia. *Minerals*, 7(10), 202.

SCHOENE, B., CROWLEY, J., CONDON, D., SCHMITZ, M., & BOWRING, S. (2006). Reassessing the uranium decay constants for geochronology using ID-TIMS U–Pb data. *Geochimica et Cosmochimica Acta*, 70(2), 426-445.

SCHILLER, J. C. (2000). *Structural geology, metamorphism and the origin of the Kanmantoo copper deposit, South Australia* (Doctoral dissertation). University of Adelaide, Australia.

SCHMIDT MUMM, A. S., TEDESCO, A. S., & FOCKE, D. (2009). Application of Ti-in-quartz thermometry to Au and Cu-Au mineralising systems. *Journal of Geochemical Exploration*, 101, 93.

SECCOMBE, P. K., SPRY, P. G., BOTH, R. A., JONES, M. T., & SCHILLER, J. C. (1985). Base metal mineralization in the Kanmantoo Group, South Australia: a regional sulfur isotope study. *Economic Geology*, 80, 1824-1841.

SEYDOUX-GUILLAUME, A. M., PAQUETTE, J. L., WIEDENBECK, M., MONTEL, J. M., & HEINRICH, W. (2002). Experimental resetting of the U-Th-Pb systems in monazite. *Chemical Geology*, 191, 165-181.

SEYDOUX-GUILLAUME, A. M., MONTEL, J. M., BINGEN, B., BOSSE, V., DE PARSEVAL, P., PAQUETTE, J. L., JANOTS, E., & WIRTH, R. (2012). Low-temperature alteration of monazite: Fluid mediated coupled dissolution–precipitation, irradiation damage, and disturbance of the U–Pb and Th–Pb chronometers. *Chemical Geology*, 330-331, 140-158.

SHAND, S. J. (1943). *The Eruptive Rocks: 2nd Edition*. New York: John Wiley.

SOLOMON, M. & GROVES, D. I. G. (1994). Syndeformational, turbidite-hosted, gold deposits. In M. Solomon (Ed.), *The geology and origin of Australia's mineral deposits* (pp. 713-723). Oxford: Clarendon Press.

SPRY, P. G. (1976). *Base metal mineralisation in the Kanmantoo Group, S.A.: South Hill, Bremer and Wheal Ellen areas* (Honours thesis). University of Adelaide, Australia.

SPRY, P. G., SCHILLER, J. C., & BOTH, R. A. (1988). Structure and metamorphic setting of base metal mineralisation in the Kanmantoo Group, South Australia. *Proceedings of the Australasian Institute of Mining and Metallurgy*, 293, 57-65.

STANDING, J. (2005). *Structural controls on copper mineralisation at the Kanmantoo project, S.A.* (Independent technical report). Adelaide: Fluid Focus Pty. Ltd.

STANDING, J. (2006). *Ongoing structural investigations at the Kanmantoo Cu-Au project, South Australia.* (Independent technical report). Adelaide: Jigsaw Geoscience Pty. Ltd.

STINEAR, M. D. (2017). *Refining the physical and temporal record of metamorphism during the Delamerian Orogeny* (Honours thesis). University of Adelaide, Australia

TEDESCO, A. (2009). *Late-stage orogenic model for Cu-Au mineralisation at Kanmantoo mine: new insights from titanium in quartz geothermometry, fluid inclusions and geochemical modelling* (Honours thesis). University of Adelaide, Australia.

THOMPSON, J., MEFFRE, S., MAAS, R., KAMENETSKY, V., KAMENETSKY, M., GOEMANN, K., EHRIG, K., & DANYUSHEVSKY, L. (2016). Matrix effects in Pb/U measurements during LA-ICP-MS analysis of the mineral apatite. *Journal of Analytical Atomic Spectrometry*, 31, 1206-1215.

THOMSON, B. P. (1975). Kanmantoo Trough – regional geology and comments on mineralisation. In C. L. Knight (Ed.), *Economic geology of Australia and Papua New Guinea: Vol. 1* (pp. 555-560). Melbourne: Australasian Institute of Mining and Metallurgy.

TURNER, S., & FODEN, J. D. (1996). Petrogenesis of late-Delamerian A-type granites and granophyre, South Australia: magma mingling in the Mannum granite, South Australia. *Mineralogy and Petrology*, 56, 147-169.

TURNER, S. P., KELLEY, S. P., VANDENBERG, A. H. M., FODEN, J. D., SANDIFORD, M., & FLÖTTMANN, T. (1996). Source of the Lachlan fold belt flysch linked to convective removal of the lithospheric mantle and rapid exhumation of the Delamerian-Ross fold belt. *Geology*, 24, 941-944.

TUTTLE, O. F., & BOWEN, N. L. (1958). Origin of Granite in the light of experimental studies in the system NaAlSi3O8–KAlSi3O8–SiO2–H2O. *GSA Memoirs*, 74(1), 1-145.

TOTEFF, S. (1994). *Synsedimentary mineralisation in the Kanmantoo Trough: Field Excursion Guide, September 1994* (Report Book 95/43). South Australia: Department of Mines and Energy.

VERWOERD, P. J., & CLEGHORN, J. H. (1975). Kanmantoo Copper Orebody. In C. L. Knight (Ed.), *Economic geology of Australia and Papua New Guinea: Vol. 1* (pp. 560-565). Melbourne: Australasian Institute of Mining and Metallurgy.

WETHERILL, G. W. (1956). Discordant uranium-lead ages, I. *Transactions of the American Geophysical Union*, 37(3), 320-326.

WILLIAMS, M. L., JERCINOVIC, M. J., HARLOV, D. E., BUDZYN, B., & HETHERINGTON, C. J. (2011). Resetting monazite ages during fluid-related alteration. *Chemical Geology*, 283, 218-225.

WILSON, G. L. (2009). *Structural setting and timing of the Kanmantoo Cu-Au deposit, Callington, SA* (Honours thesis). University of Adelaide, Australia.

APPENDIX A: HISTORICAL BACKGROUND

As of writing this thesis, Kanmantoo is Australia's oldest, non-continually active, but currently operational mineral deposit. With the mine potentially approaching its end of life in coming years, it is important to reflect on the extensive history of mining in the region, as minerals will undoubtedly play a critical role in South Australia's future.

Besides coal, mining was non-existent within Australia until the early 1840s, when pioneering settlers helped drive economic development in the free province of South Australia by discovering and extracting various base and precious metal deposits. The first workings begun at Wheal Gawler, Australia's first metal mine just 5 km from the centre of Adelaide in Glen Osmond. Within a few short years several other mining operations had begun including Kanmantoo in 1846 and elsewhere throughout the Adelaide Hills and north toward Kapunda and Burra. Kanmantoo Mine was owned and operated by the South Australian Company which established the township of Kanmantoo as a miners' village and divided surrounding agricultural acreage as to avoid areas with visible mineralisation (Chilman, 1982). The name Kanmantoo was derived from 'Kungna Tuko' a local Peramangk Aboriginal people's word that described the long red hill which defined the area (Mills, 1981). In 1848 the first smelter in South Australia was built in Kanmantoo, allowing for production of a 50 % concentrate (Dickinson, 1942). Once processed, ore was exported directly to England via either Cape Horn or the Cape of Good Hope. Despite a brief exodus of labour in pursuit of the Victorian gold rush, high copper prices continued to spur production in the colony and by 1875 an estimated 24,000 tonnes of ore bearing an average grade of 8.5 % Cu had been extracted from the Kanmantoo group of mines alone (Verwoerd & Cleghorn, 1975).

"Indeed, this is so evidently a mineral district, and one, the position of which, offers so many advantages that, under circumstances of capital and labor different from those at present obtaining in the colony, I should not be surprised to see many of these old Mines tried again."

- J. B. Austin, 1863.

Little did Austin know that the Kanmantoo Mine would still be operating 155 years later with a local workforce, spurred by its proximity to Adelaide and supplying smelters in China for the production of micro-chips and electric vehicle components. This quote was actually written of the wider Bremer and Kanmantoo region, specifically with respect to smaller inactive prospects such as the Paringa Mine which had often been the subject of small-scale operations in the preceding decades. The Kanmantoo Mines themselves were still profitable enough to remain active through this time when labour was leaving the colony for the Victorian goldrush, generating high wages locally in a familiar cyclical fashion. Austin (1863) detailed the average wage of a South Australian miner at this time, ranging from 5s 6d to 9s 6d per day for men (roughly $30 to $52AUD in 2018 after adjusting for inflation and converting from GBP) depending on remoteness and merit, while boys made from 2s to 3s and 6d per day (roughly $13 to $20AUD).

By 1874 the Kanmantoo Mine had changed ownership two times and operations ceased due to low copper prices. Prospecting and minor unsuccessful production occurred throughout the early 20th century, but the mine lay mostly dormant until the 1950's when Mines Exploration Pty. Ltd. (a subsidiary of Broken Hill South Ltd.) explored the area. Diamond drilling returned positive economic results and open pit mining led by Kanmantoo Mines Ltd. begun in 1971 before closing in 1976 due to falling copper prices, by which point the open pit was approximately 100m deep. Another long dormant period was broken when Hillgrove Resources Ltd. initiated exploration and later production at the mine from 2004. 10,764t of copper and 3,812oz of gold were produced from a total 3.5 million tonnes of ore in the half year ending 30th June 2018 (Half year report - Hillgrove Resources, 23/08/2018). As of 2018, the open pit is approximately 250m deep and projected to be up to 360m deep in sections by 2020; some 300m deeper than the extent of 19th Century operations.

Historical background references:

AUSTIN, J. B. (1863). *The mines of South Australia, including also an account of the smelting works in that colony: Together with a brief description of the country, and incidents of travel in the bush*. Adelaide: C. Platts., E. S. Wigg., G. Dehane., J. Howell., W. C. Rigby., & G. Mullett.

CHILMAN, J. K. (1982). *Silver and a trace of gold: A history of the Aclare mine.* South Australia: Department of Mines and Energy, Special Publication No. 1.

DICKINSON, S. B. (1942). The structural control of ore deposition in some South Australian copper fields. *Geological Survey of South Australia, Bulletin*, 20, 79-99.

MILLS, A. R. (1981). *Kungna Tuko: A history of Kanmantoo*. Adelaide: Aldis Printing

VERWOERD, P. J., & CLEGHORN, J. H. (1975). Kanmantoo Copper Orebody. In C. L. Knight (Ed.), *Economic geology of Australia and Papua New Guinea: Vol. 1* (pp. 560-565). Melbourne: Australasian Institute of Mining and Metallurgy.

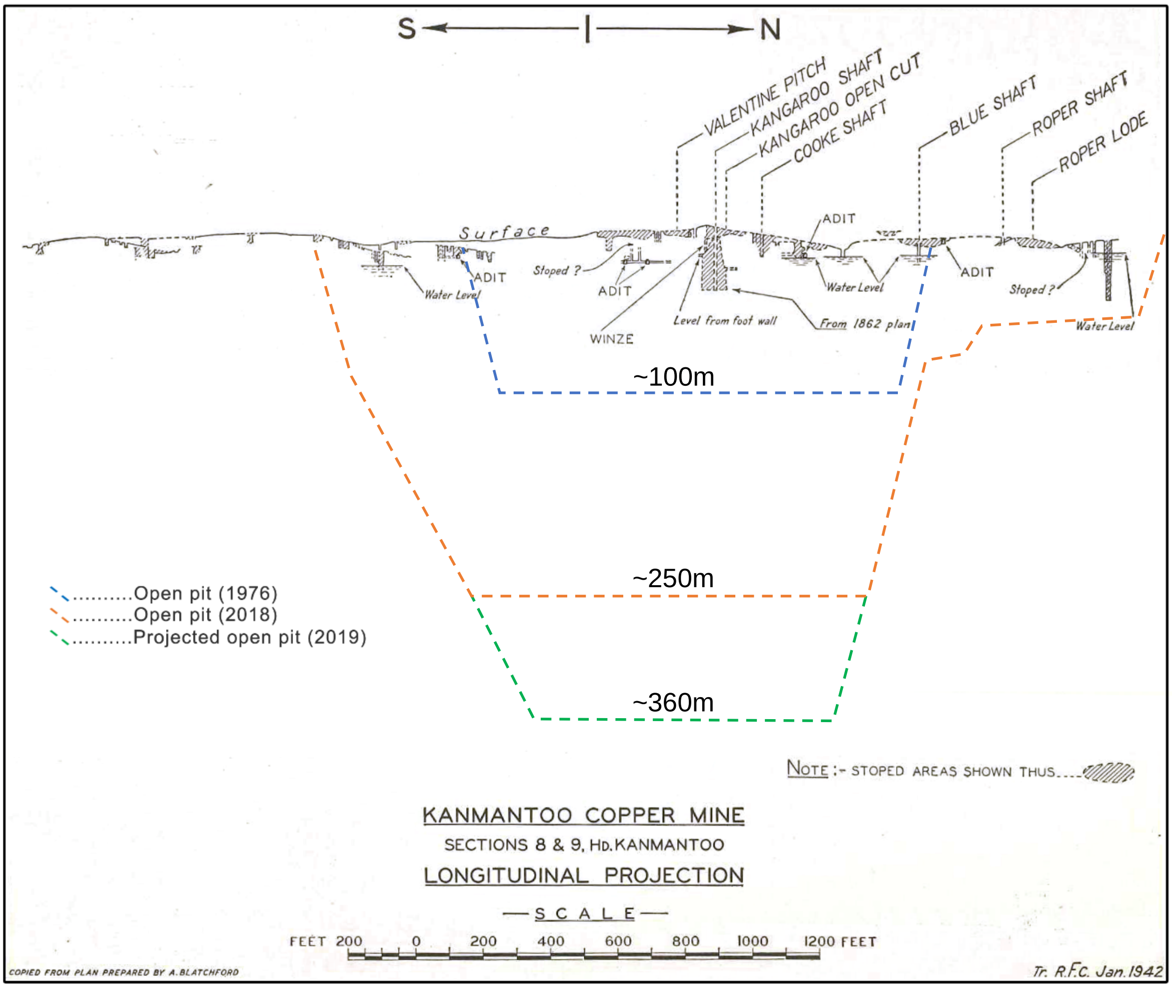

Appendix Figure 1: Approximate location and depth of the modern mine relative to historical workings, adapted from Dickinson (1942).

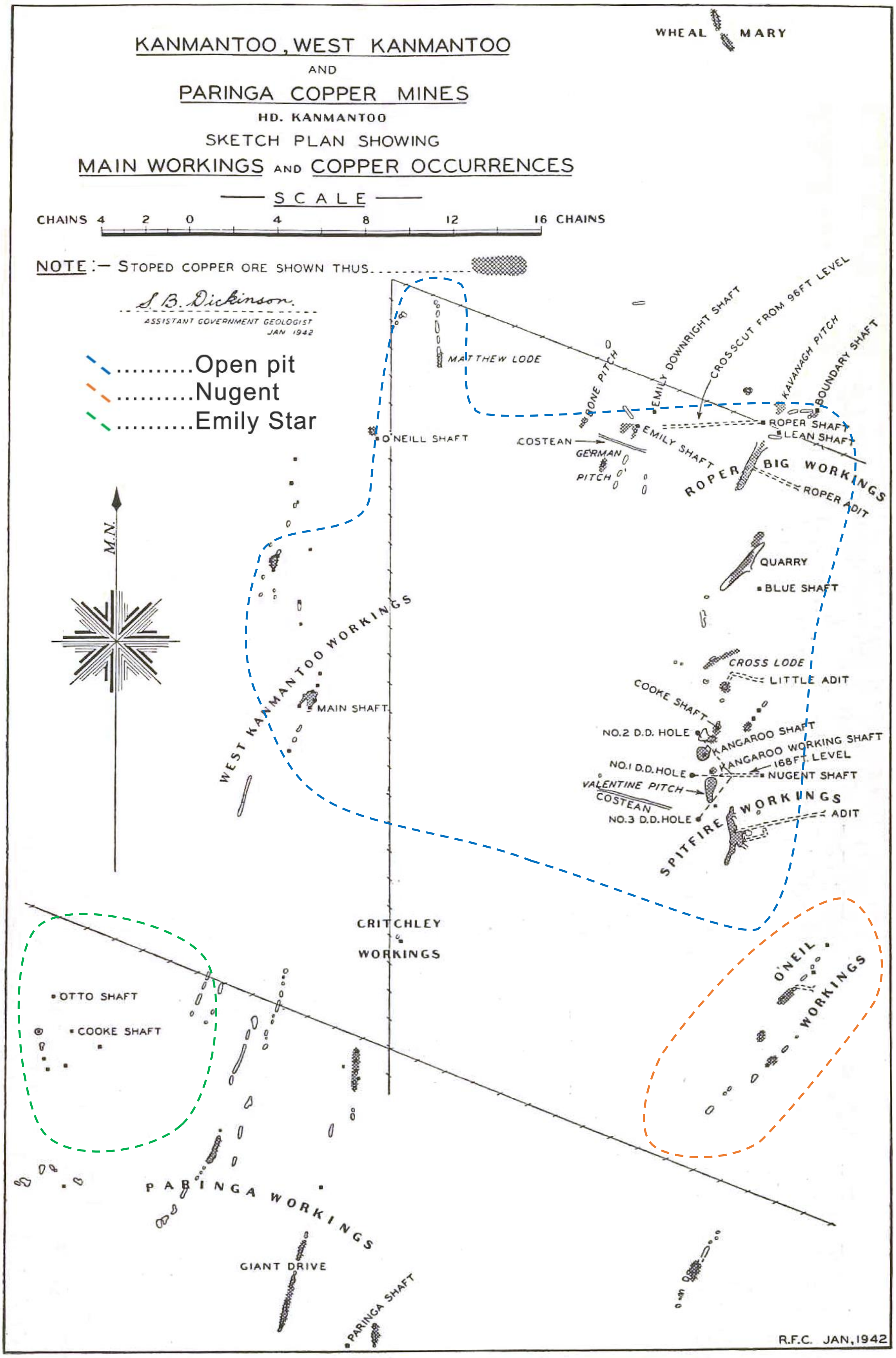

Appendix Figure 2: Approximate location of the modern mine relative to historical workings, adapted from Dickinson (1942).

Appendix Figure 1: The Kanmantoo Mine in full operation, April 2018, 172 years after the first workings. Top: East haul road, facing ESE. Bottom: Excavation and drilling operations with the morning sun rising over the pit, facing S.

APPENDIX B: EXTENDED PETROGRAPHIC DESCRIPTIONS

BK01

Drill hole: KTDD180 (318231.5E 6114755N),
60.22 - 60.38 metres, Spitfire Lode

Classification: Felsic vein

Observed in drill core as a 1cm wide vein sharply crosscutting adjacent schistosity at a near 90° angle with a diffusive alteration halo. Host is comprised of biotite (40%), quartz (30%), garnet (15%), staurolite (9%), muscovite (5%) and minor sapphirine (1%) with chlorite alteration and replacement of mica throughout. Alteration halo exhibits progressive exsolution and replacement of host with feldspathic assemblage. Disseminated sulphides including chalcopyrite and pyrrhotite are interspersed throughout the host and increasingly toward the vein contact.

Vein is comprised predominately of fine-moderately sized (40-200µm) albite (60%), K-feldspar (20%) and quartz (10%) with chlorite replacing biotite (5%), minor rutile and late carbonate (5%). Sericitic alteration is seen to alter feldspars and chlorite throughout. Within hand sample, large (0.5cm) grains of chalcopyrite are observed within the centre of veins, likely forming simultaneously.

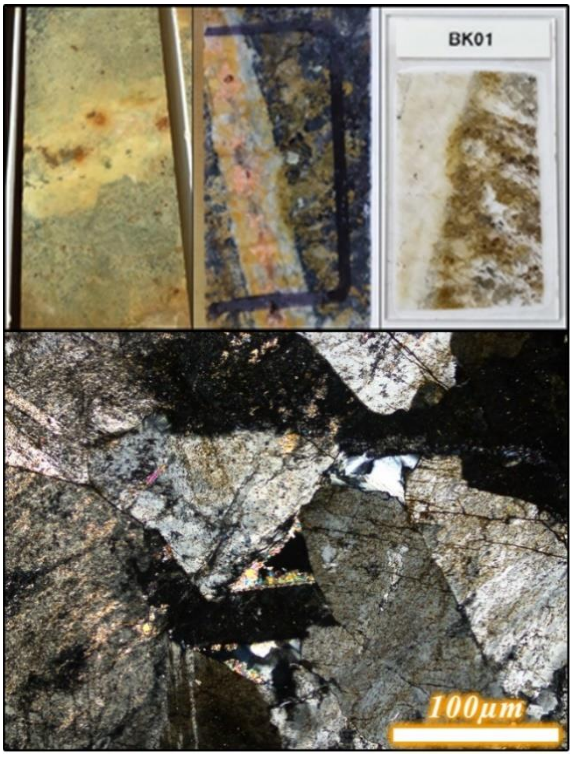

Appendix Figure 2: BK01 - Top left: NQ (47.6mm) half drill core specimen. Top centre: Quarter core thin section outline. Top right: Thin section (28x48mm, 35µm). Bottom: Photomicrographic of felsic vein with albite, k-feldspar and sericite/chlorite replacing biotite.

BK05

Drill hole: KTRCD125 (318236E 6114437N),
99.35 - 99.45 metres, Nugent Lode

Classification: Felsic vein

Observed as a highly altered section (>10cm) of drill core with a breccia like fabric comprised of beige and dark green minerals, appearing to overprint a vein/intrusion.

Rock is comprised of altered primary and secondary K-feldspar and albite (2-4mm), biotite, quartz, minor muscovite and limonite. Pervasive chlorite alteration throughout replacing biotite, with a later sericitic alteration of K-feldspar and chlorite has made the sample considerably degraded. Pre-alteration proportions are roughly estimated to be that of an alkali feldspar granite: K-feldspar (40-50%), albite (10-15%), quartz (15-20%), biotite (15-20%) with accessory ilmenite and minor tourmaline.

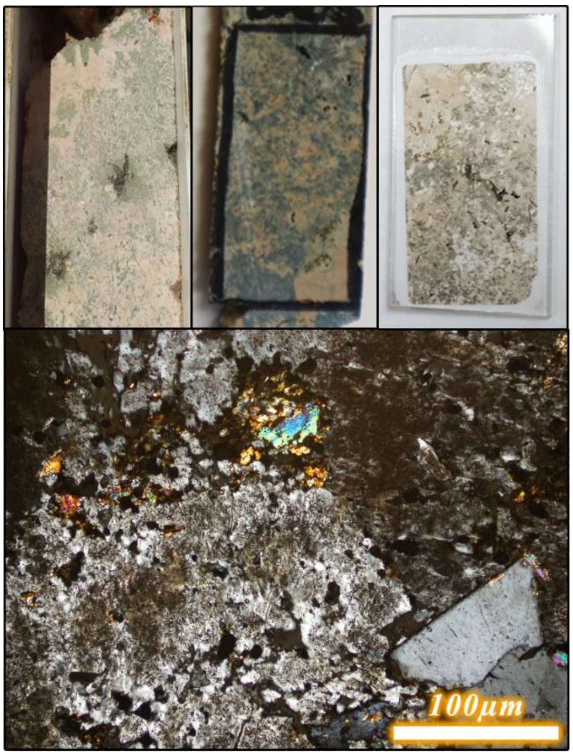

Appendix Figure 3: BK05 - Top left: NQ (47.6mm) half drill core specimen. Top centre: Quarter core thin section outline. Top right: Thin section (28x48mm, 35µm). Bottom: Felsic vein with K-feldspar, albite, quartz, biotite and sericite alteration.

BK06

Drill hole: KTRCD125 (318236E 6114437N), 99.55 - 99.65 metres, Nugent Lode

Classification: Chlorite alteration

Observed ~10cm downhole from *BK05* as a highly altered section (>20cm) of drill core. Sample contains pervasive late chlorite alteration throughout, 10cm downhole from *BK05*. Radiating chlorite makes up the entire groundmass of the sample (70%) and has been degraded/weathered. Large (up to 200µm) tourmaline crystals with intense zonation are interspersed randomly throughout with pyrrhotite and chalcopyrite (4%) and minor muscovite (1%). Pre-alteration compositions cannot be determined.

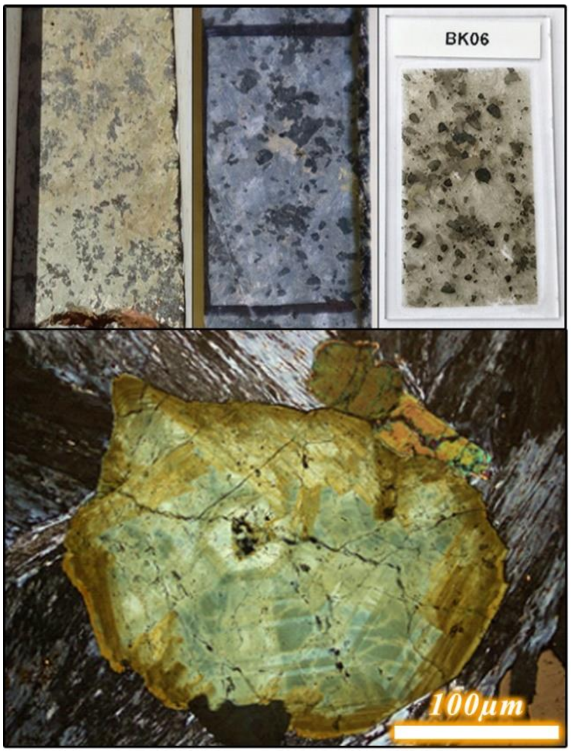

Appendix Figure 4: BK06 - Top left: NQ (47.6mm) half drill core specimen. Top centre: Quarter core thin section outline. Top right: Thin section (28x48mm, 35µm). Bottom: Zoned tourmaline crystal in radiating chlorite with disseminated chalcopyrite.

BK11

Drill hole: KTDD102 (318274.9E 6115087N), 64.9 - 65 metres, Main Kavanagh Lode

Classification: Felsic vein

Observed as a series of small millimetre scale central veins with broad (up to 3cm), diffusive alteration halos permeating into surrounding host rock. Host rock is a quartz-rich garnet andalusite biotite schist with some chlorite alteration throughout. Approaching the vein, relict andalusite porphyroblasts are exsolved with a feldspathic mineralogy which permeates into the surrounding rock destroying fabrics and obscures the central vein contact.

Veins are comprised of albite (45%), K-feldspar (15%), quartz (35%) and chlorite replacing biotite (5%) with sericitic alteration of feldspars and some chlorite throughout.

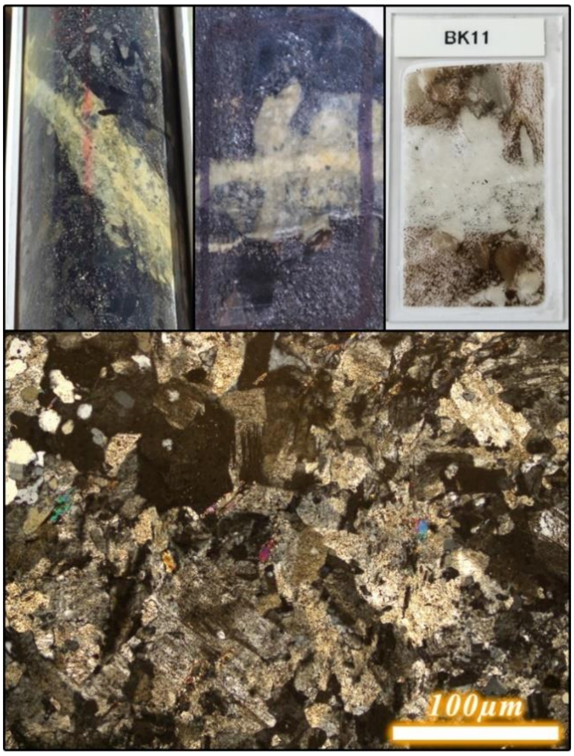

Appendix Figure 5: BK11 - Top left: NQ (47.6mm) half drill core specimen. Top centre: Quarter core thin section outline. Top right: Thin section (28x48mm, 35µm). Bottom: Tourmaline crystal in radiating chlorite with disseminated chalcopyrite.

BK14

Drill hole: KTDD105 (318203.8E 6115062N), 64.2 - 64.3 metres, Main Kavanagh Lode

Classification: Chlorite alteration

Observed in drill core as a large (20cm) monomineralic vein/segregation comprised entirely of coarse grained (up to 1.5cm), undeformed and radiating chlorite. Forms a sharp contact with adjacent host rock, however, chlorite alteration is then pervasive throughout.

Host rock is comprised of chlorite alteration (35%), staurolite (25%), biotite (15%), garnet (15%) and muscovite (10%). Sulphides including chalcopyrite and pyrrhotite are observed to be disseminated throughout, increasing toward contact with chlorite segregation. Sulphides are syn to post-chlorite, exsolving all other minerals (see Figure X).

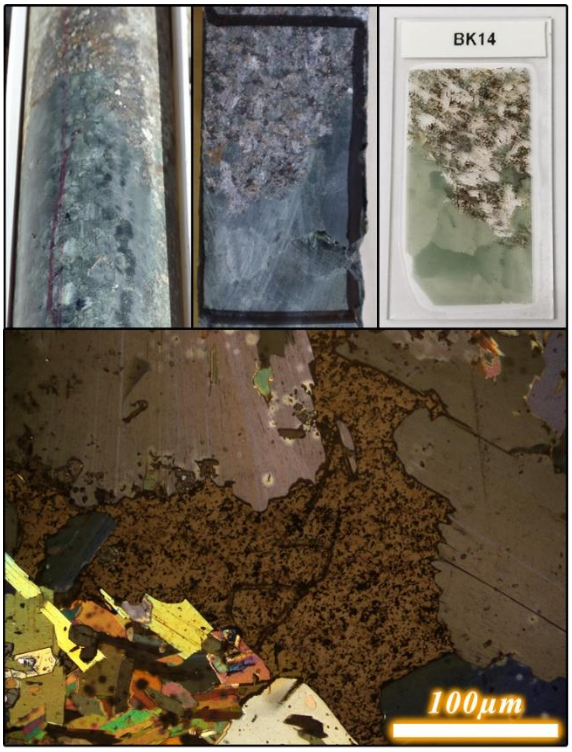

Appendix Figure 6: BK14 - Top left: NQ (47.6mm) drill core specimen. Top centre: Quarter core thin section outline. Top right: Thin section (28x48mm, 35μm). Bottom: Chlorite alteration and biotite, muscovite and staurolite host with pyrrhotite.

BK17

Drill hole: KTDD104 (318231.4E 6115093N), 28.4 - 28.5 metres, Main Kavanagh Lode.

Classification: Quartz vein

2cm wide sulphide bearing quartz vein sharply cutting through host rock. Host is comprised of fine-grained (<5μm) quartz (60%), chlorite replacing mica (20%), disseminated pyrrhotite up to 25μm (10%), garnet (5%) and staurolite (5%).

Vein is internally and externally undeformed, comprised predominantly of large (up to 200μm) quartz (75%), large (up to 0.5cm) staurolite grains (15%), minor andalusite (5%) and pyrrhotite and chalcopyrite (5%). Sulphides appear to have a late-syn to post-veining timing evidenced by vein mineral inclusions.

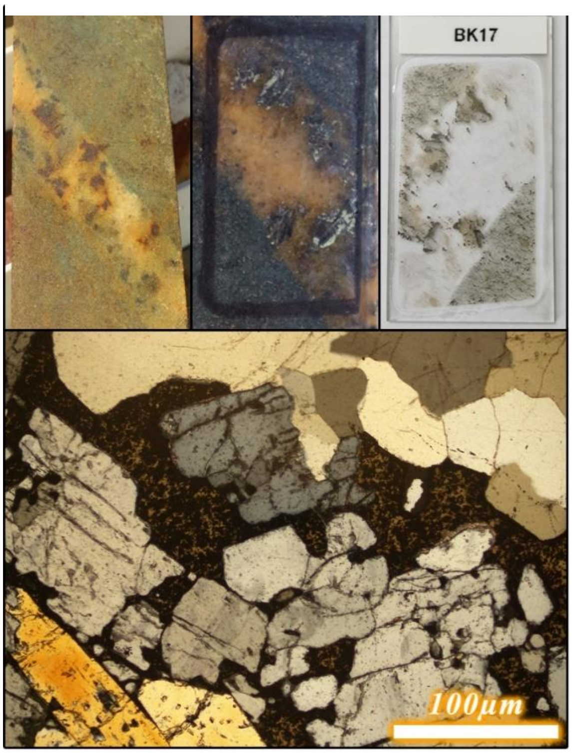

Appendix Figure 7: BK17 - Top left: NQ (47.6mm) half drill core specimen. Top centre: Quarter core thin section outline. Top right: Thin section (28x48mm, 35μm). Bottom: Quartz and staurolite vein with syn to post-vein pyrrhotite.

BK18

Drill hole: KTDD104 (318228.3E 6115093N), 34.5-34.7 metres, Main Kavanagh Lode

Classification: Felsic vein

70mm wide vein observed sharply cutting through host rock with dark alteration minerals on vein contacts. Host rock is a quartz rich (50%) schist with biotite (35%), garnets (10%) and chlorite replacing biotite throughout (5%). Vein contact is generally sharp however a diffusive alteration halo is seen to replace host with a feldspathic mineralogy in areas.

Vein is feldspar rich and highly altered with chlorite and sericite throughout. Comprised of albite (50%), K-feldspar (25%), tourmaline (20%) and quartz (5%). The vein is also observed to contain numerous large chalcopyrite and pyrrhotite grains up to 50mm. Dark alteration minerals congregating on the edges of veins are internally zoned tourmalines reminiscent of *BK06* and appear to have been introduced syn- to post-veining.

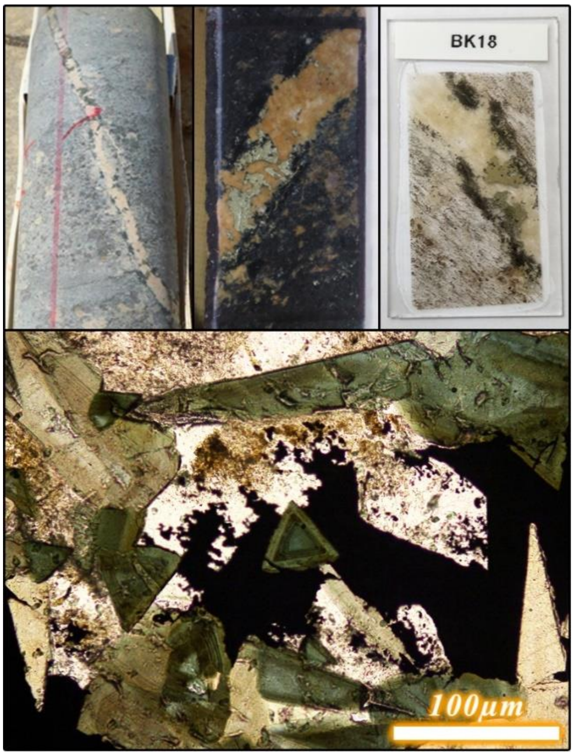

Appendix Figure 8: BK18 - Top left: NQ (47.6mm) whole drill core specimen. Top centre: Quarter core thin section outline. Top right: Thin section (28x48mm, 35µm). Bottom: Sulphide (black) replacing tourmaline, chlorite and felsic vein.

BK21

Drill hole: KTDD140 (318313.9E 6114718N), 65.2-65.7 metres, Spitfire Lode

Classification: Felsic vein

1cm wide vein observed sharply cutting through host rock with strings of sulphides permeating outwards into host. Host rock is a quartz rich (50%) garnet (5%), andalusite (15%), biotite (25%) schist with chlorite alteration and replacement of biotite, plus minor staurolite (5%). Vein contact is generally sharp however a thin alteration halo is seen to replace host with a feldspathic mineralogy in areas.

Vein is feldspar rich and highly altered with chlorite and sericite throughout entirely replacing some parts of the original composition. Comprised of albite (40%), K-feldspar (40%), chlorite after biotite (10%) and quartz (10%). The vein is also observed to contain numerous large chalcopyrite and pyrrhotite grains up to 50mm which appear coeval to early post veining.

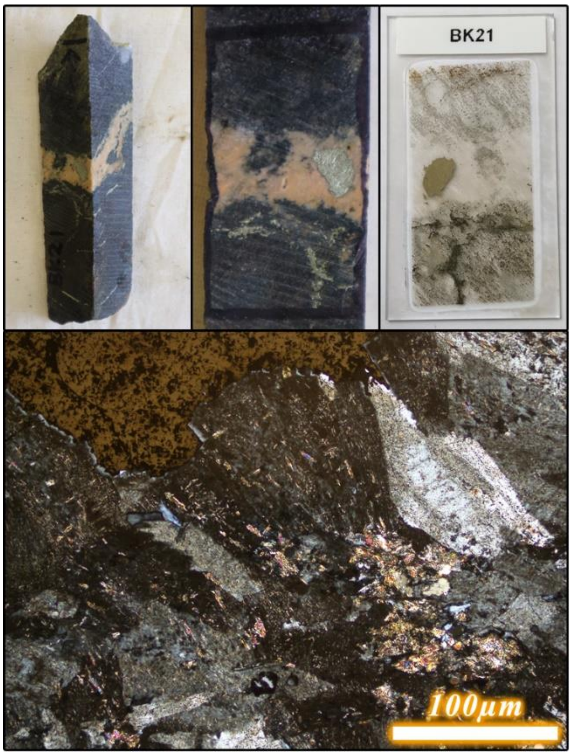

Appendix Figure 9: BK21 - Top left: NQ (47.6mm) quarter drill core specimen. Top centre: Quarter core thin section outline. Top right: Thin section (28x48mm, 35µm). Bottom: Felsic vein with sericitic and chlorite alteration and pyrrhotite

BK25A

Location: East Haul Road (318326.8E 6114809N)

Classification: Felsic vein

Observed within the pit wall as an undeformed vein (10cm wide) cross-cutting all fabrics within a late joint set (J2). Abundant sulphides including chalcopyrite, pyrrhotite and pyrite are found either disseminated throughout or as a late infilling vein/s running parallel to the length of the vein. Evidence of a very late introduction of sulphides as J2 veins are interpreted to be one of the oldest generations of veins within the deposit. Host rock is a garnet, andalusite, biotite schist which is exsolved and destroyed by the intense vein alteration halo within thin sections.

Vein is feldspar rich with albite and trace plagioclase (60%), K-feldspar (20%), tourmaline (10%) and quartz (10%) with sericitic and some chlorite alteration and replacement throughout. Large (up to 3mm) feldspar crystals have developed around sulphides which are thought to be late syn to post-veining, with felsic veins fining outwards from the sulphides.

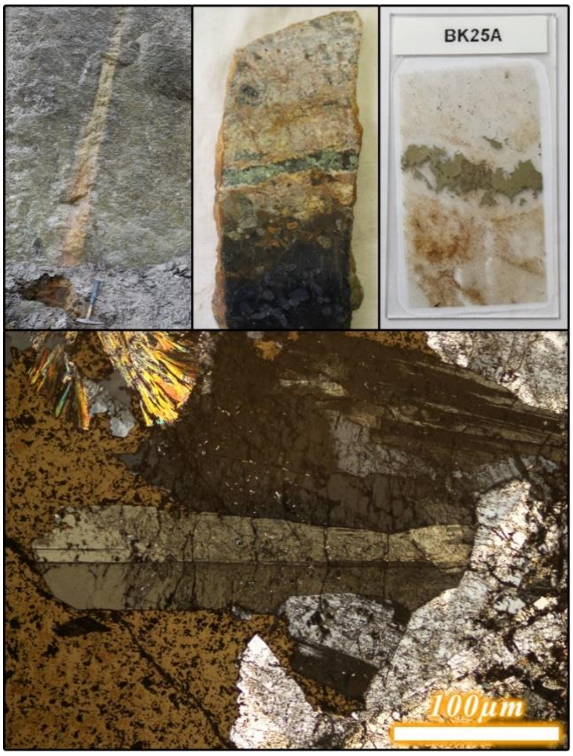

Appendix Figure 10: BK25A - Top left: Vein as observed in pit wall (facing east). Top centre: Cut grab sample (7cm wide). Top right: Thin section (28x48mm, 35µm). Bottom: Felsic vein with albite, K-feldspar, quartz, sericite and pyrrhotite.

BK25B

Location: East Haul Road (318326.8E 6114809N)

Classification: Felsic vein

As with *BK25A*, observed within the pit wall as an undeformed vein (10cm wide) cross-cutting all fabrics within a late joint set (J2). Abundant sulphides including chalcopyrite, pyrrhotite and pyrite are found either disseminated throughout or as a late infilling vein/s running parallel to the length of the vein. Evidence of a very late introduction of sulphides as J2 veins are interpreted to be one of the oldest generations of veins within the deposit. Host rock is a garnet, andalusite, biotite schist which is exsolved and destroyed by the intense vein alteration halo within thin sections.

Vein is feldspar rich with albite and trace plagioclase (60%), K-feldspar (20%), tourmaline (10%) and quartz (10%) with sericitic and some chlorite alteration and replacement throughout. Large (up to 3mm) feldspar crystals have developed around sulphides which are thought to be late syn to post-veining, with felsic veins fining outwards from the sulphides.

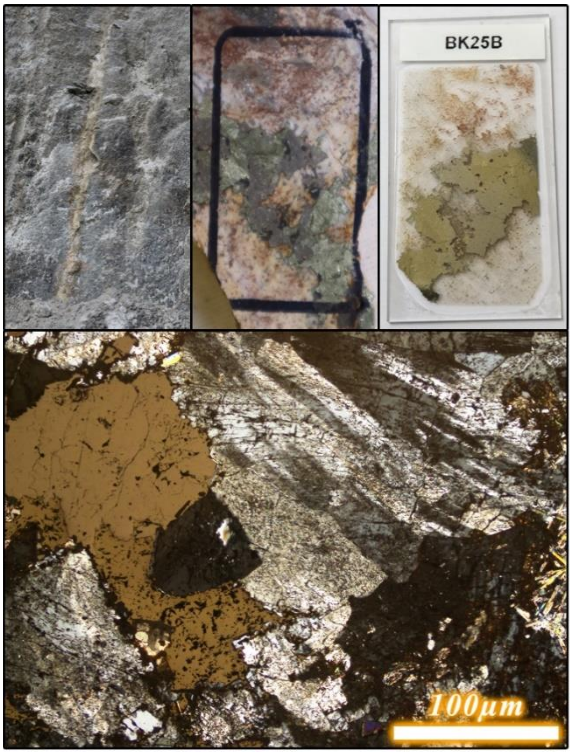

Appendix Figure 11: BK25B - Top left: Vein as observed in pit wall (facing east). Top centre: Thin section outline. Top right: Thin section (28x48mm, 35µm). Bottom: Felsic vein albite, K-feldspar, quartz, sericite, chalcopyrite and pyrrhotite.

BK27

Location: NE Pit Wall (318315E 6115087N), East Kavanagh Lode

Classification: Quartz vein

Exposed within the mine as a large metre scale, boudinaged vein. Hand sample shows predominant coarse grained (up to 2cm) quartz with minor coarse grained (1cm) muscovite on edges and rare pink andalusite.

Thin section is comprised of coarse grained (1cm) quartz (90%) with small inclusions (0.5cm) of andalusite, reminiscent of BK29/BKBDG (4%) tightly wrapped by sericite-muscovite and biotite (1%). A small (1cm) section/inclusion of host rock is comprised predominantly of biotite (70%) and garnet (30%) with minor muscovite.

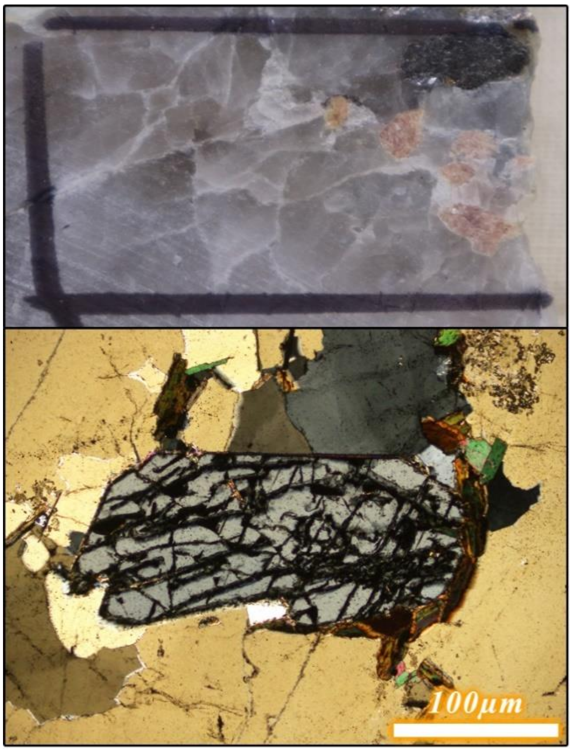

Appendix Figure 12: Top: BK27 - Thin section outline (35x20mm) with pink andalusite and small black inclusion of host rock. Bottom: Photomicrograph of andalusite grain within quartz and minor biotite and muscovite which trails back toward host inclusion.

BK29

Location: North Pit Wall (318136E 6115119N)

Classification: Aluminous segregation

Exposed as intensely boudinaged white veins with large pink andalusite porphyroblasts throughout. Sharply enclosed by a host of fine-grained biotite, garnet and honey-brown staurolite with large white andalusite porphyroblasts interspersed.

Internally, the vein exhibits large (up to 3cm) prismatic andalusite (65%) and large (up to 2cm) equant quartz (31%) with fine muscovite-sericite commonly filling the contact between the two major minerals (4%). Consistent with external strain partitioning, crystals are undeformed, with pink andalusite being distinctively non-poikiloblastic and exhibiting a clear cleavage running parallel to the length of the crystal. Devoid of opaque minerals and sulphides.

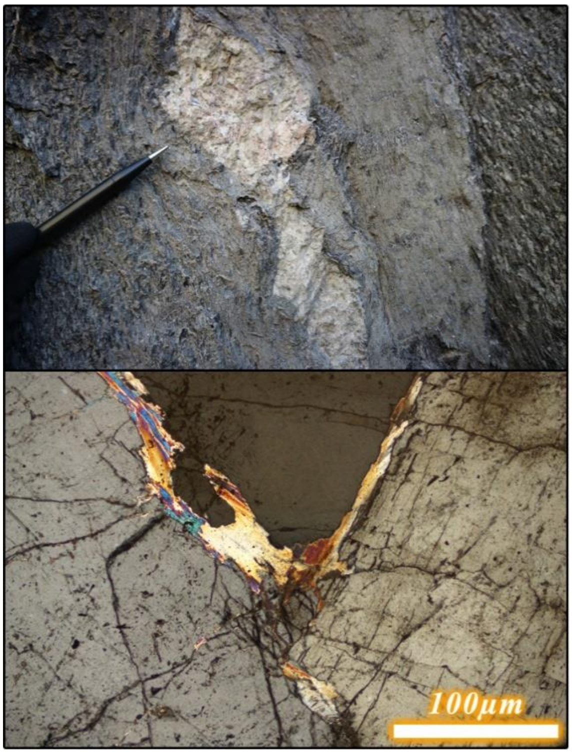

Appendix Figure 13: BK29 - Top: North Pit Wall exposure of boudinaged pink andalusite, aluminous segregation. Bottom: Representative photomicrograph of large andalusite and quartz (top middle) crystals with interjoining muscovite.

BK-BDG1/2

Location: South Pit Wall (318100E 6114847N)

Classification: Aluminous segregation

Exposed as small (up to 5cm), pink, chocolate-tablet boudins. Sharply enclosed by a host of fine-grained biotite, garnet and large white andalusite porphyroblasts.

Internally, veins are comprised of fine grained (up to 300µm) pink, equant-prismatic andalusite (65%) and coarser (up to 5mm) biotite. Biotite is observed to form linearly within the centre of tablets, with andalusite more evenly interspersed. Both minerals are observed to become increasingly fine moving outwards to the lengthwise edges of tablets. Despite having different accessory minerals, BKBDG and BK29 are both classified as aluminous segregations, reflective of their highly-aluminous composition (See Appendix E). Devoid of opaque minerals and sulphides.

Appendix Figure 14: BKBDG - Top left: Thin section billet (35x20mm). Top centre & right: Respective thin sections (28x48mm, 35µm). Bottom: Representative photomicrograph of andalusite and biotite (far left).

KTDD089

Drill hole: KTDD180 (318157.9E 6114270N), 60.22 - 60.38 metres, Nugent Lode.

Classification: Felsic vein

2cm wide vein crosscutting adjacent schistosity at a near 90° angle with a broad diffusive alteration halo. Host is comprised of fine-grained quartz (40%) and biotite (40%) with poikiloblastic-andalusite porphyroblasts (10%), garnet (5%) and minor chlorite and carbonate alteration (5%). Alteration halo exhibits progressive exsolution and replacement of host with feldspathic assemblage and thinly disseminated copper sulphides.

Vein has experienced alteration but is comprised predominately of fine grained (up to 80 µm) albite (50%) with K-feldspar (20%), quartz (20%), chlorite and carbonate alteration (5%) and ilmenite (5%). Biotite has likely been altered to chlorite, plus minor sericitic alteration of feldspars.

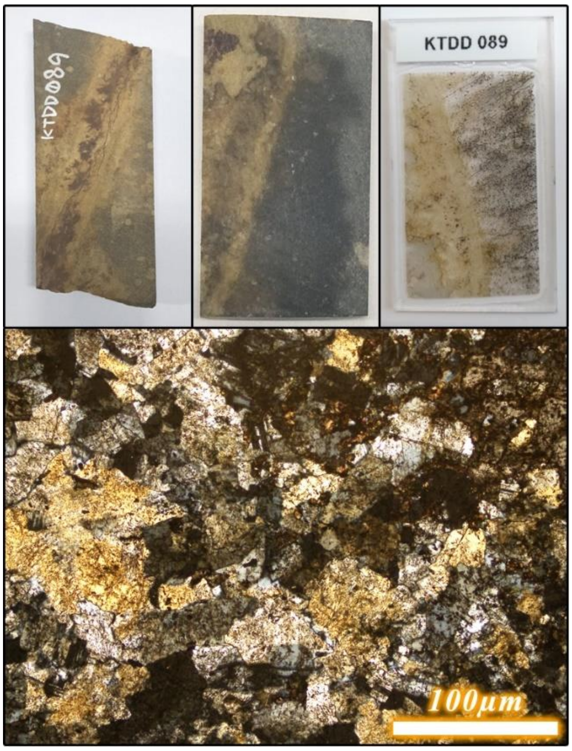

Appendix Figure 15: KTDD089 - Top left: NQ (47.6mm) half drill core specimen. Top centre: Quarter core thin section outline. Top right: Thin section (28x48mm, 35µm). Bottom: Felsic vein with albite, K-feldspar and quartz.

BKDK-1

Location: 9.22 km north of mine (54H 0318258 6123907)

Classification: Regional sample

Strongly foliated Garnet-*Staurolite* schist representing an unaltered, peak metamorphic assemblage. Biotite (40%), quartz (40%), garnet (10%), staurolite (9%) and andalusite (1%). Devoid of mineralisation.

KMT-1

Location: 2.64 km north of mine (54H 0318294 6117492)

Classification: Regional sample

Strongly foliated Garnet-*Andalusite* schist representing an unaltered, peak metamorphic assemblage. Biotite (45%), quartz (35%), garnet (8%), andalusite (8%), muscovite (3%) and staurolite (1%). Devoid of mineralisation.

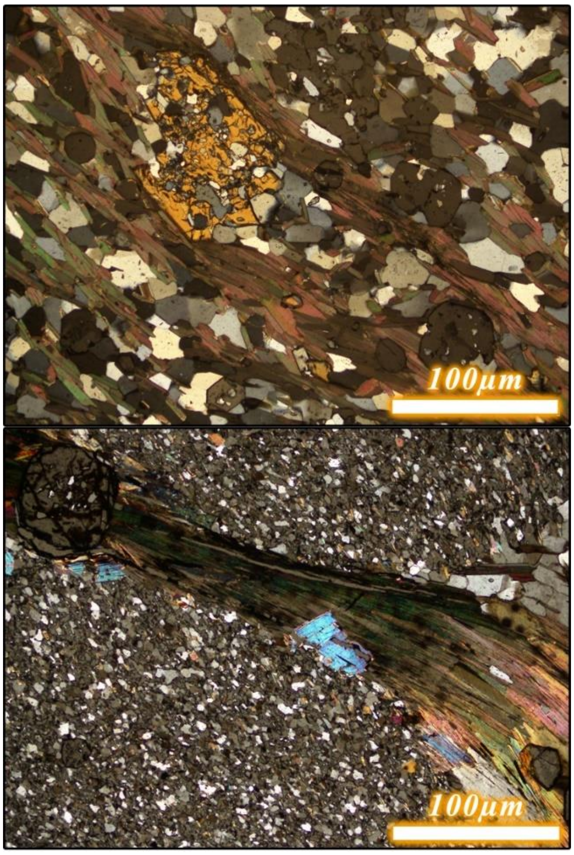

Appendix Figure 16: Top: BKDK1 - Photomicrograph showing staurolite replacing quartz with biotite wrapping around and garnet overprinting. Bottom: KMT1 - Photomicrograph showing andalusite replacing quartz with biotite wrapping around and garnet and muscovite overprinting.

Appendix Table 1: Descriptions of specimens forgone at hand sample or thin section stage

Sample	Lode	Description	Reason forgone
BK02	Spitfire	1cm thick feldspathic vein in altered GABS	Weathering
BK03	East Kav.	~0.25cm thick opaque white vein in unaltered GABS	Size
BK04	East Kav.	1.5cm thick feldspathic vein with breccia texture in altered GABS	Integrity
BK07	Main Kav.	1cm thick red-white ferruginous vein in unaltered GABS	Mineralogy
BK08	Main Kav.	Group of <1cm thick feldspathic veins in altered GABS	Weathering
BK09	Main Kav.	1.5cm thick feldspathic vein with breccia texture in altered GABS	Integrity
BK10	Main Kav.	Heavily altered 1cm thick feldspathic vein in altered GABS	Weathering
BK12	Main Kav.	Heavily altered diffusive feldspathic vein in altered GABS	Weathering
BK13	Main Kav.	~0.25cm thick feldspathic vein with thin alteration halo in GABS	Size + weathering
BK15	Main Kav.	2cm thick quartz vein in mildly altered GABSS	Weathering
BK16	Main Kav.	1cm thick feldspathic and/or ferruginous vein in GABSS	Integrity
BK19	Spitfire	1cm thick quartz vein in unaltered BGCS	Mineralogy
BK20	Spitfire	<0.25cm thick feldspathic vein in altered GABSS	Size + weathering
BK22	Spitfire	1cm thick feldspathic vein in altered BGCS	Integrity
BK23	Spitfire	<0.25cm thick feldspathic vein in altered BGCS	Size + weathering
BK24	Main Kav.	Coarse grained quartz vein	Mineralogy
BK26	East Wall	Felsic vein (see: BK25A/B)	Over represented
BK28	Main Kav.	Sulphide vein in unaltered BGCS	Mineralogy

APPENDIX C: SEM-MLA PARAMETERS

Appendix Table 2: FEI Quanta 600 Scanning Electron Microscope (SEM) Parameters

Samples	BK01, BK05, BK06, BK11, BK14, BK18, BK25A, BK25B, BK-BDG1, BK-BDG2, BKDK1, KMT1, KTDD089
Spot size	7.2
Beam energy	25 Kv
Working distance	10 mm
Minimum grain size	4 µm
Magnification	250x

APPENDIX D: EXTENDED WHOLE ROCK GEOCHEMISTRY METHODS

Geochemical analysis was conducted by ALS Limited, South Australia on twelve vein samples. Whole rock analysis (ALS code: ME-ICP06) was conducted on an acid digested, fused bead using Inductively Coupled Plasma Atomic Emission Spectroscopy (ICP-AES). Samples were processed for trace element analysis (ALS code: ME-MS81) by lithium borate fusion and acid dissolution before Inductively Coupled Plasma Mass Spectrometry (ICP-MS). Supplementary trace element data (ALS code: ME-4ACD81) was collected utilising four-acid digestion and ICP-AES.

APPENDIX E: WHOLE ROCK GEOCHEMISTRY RESULTS

Appendix Table 3: Whole rock geochemistry results (%)

Sample	SiO2	Al2O3	Fe2O3	CaO	MgO	Na2O	K2O	Cr2O3	TiO2	MnO	P2O5	SrO	BaO	Total	LOI
BK01	59.3	18.05	4.9	0.83	0.78	6	5.8	<0.002	0.01	0.03	<0.01	0.02	0.04	98.27	2.51
BK05	48.5	17.6	12.5	3.34	2.72	0.22	8.39	0.015	0.65	0.07	2.45	0.02	0.1	99.4	2.82
BK17	69.7	18.95	8.12	0.06	0.35	0.03	0.21	0.002	0.04	0.02	0.03	<0.01	<0.01	98.48	0.97
BK25-A	61.5	19.05	5.2	0.48	0.32	7.75	1.59	0.011	0.65	0.05	0.19	0.02	0.01	99.68	2.86
BK25-B	66.2	16.5	5.79	0.54	0.35	6.49	1.31	0.012	0.67	0.07	0.27	0.01	0.01	101.37	3.15
BK25-C	64.1	18.7	4.77	0.51	0.35	7.71	1.19	0.016	0.82	0.05	0.21	0.02	0.01	101.39	2.93
BK29-1	43.1	51.4	2.46	0.14	0.37	0.1	0.84	0.002	0.06	0.01	0.1	0.01	0.01	99.47	0.87
BK29-2	51.4	43.8	1.45	0.14	0.23	0.06	0.59	<0.002	0.05	0.01	0.07	<0.01	0.01	98.59	0.78
BK29-3	38.5	53.6	2.7	0.14	0.55	0.19	2.13	<0.002	0.14	0.01	0.08	0.01	0.04	99.81	1.72
BKBDG-1	38.1	56.4	2.84	0.08	0.79	0.07	0.87	0.003	0.12	0.01	<0.01	<0.01	0.01	100.02	0.73
BKBDG-2	37.8	56.6	2.64	0.13	0.73	0.05	0.79	0.002	0.11	0.01	0.03	<0.01	0.01	99.65	0.75
BKBDG-3	38.7	55.6	2.11	0.13	0.62	0.04	0.64	0.002	0.09	0.01	0.02	<0.01	0.01	98.73	0.76

Appendix Table 4: Trace element geochemistry results (ppm)

Sample	Ba	Ce	Cr	Cs	Dy	Er	Eu	Ga	Gd	Hf	Ho	La	Lu	Nb	Nd
BK01	410	4.1	10	0.57	0.64	0.31	0.14	9.5	0.52	0.2	0.1	1.8	0.03	0.2	2
BK05	905	107	110	0.76	10.3	4.01	2.2	19.7	11.95	9.3	1.6	52.6	0.42	15.5	47.8
BK17	26	2.4	10	0.06	0.18	0.08	0.05	30.4	0.2	0.2	0.03	1.2	0.01	0.9	1.1
BK25-A	107	158	80	0.42	3.39	1.29	1.6	14.9	7.03	4.5	0.49	86.1	0.2	10.7	59.6
BK25-B	87	118.5	90	0.37	5.71	2.99	1.35	13.9	7.09	5	1.02	64.1	0.41	13.7	46.2
BK25-C	90	145	110	0.38	5.17	2.36	1.52	14.9	7.56	5	0.84	78.6	0.31	16.5	56.4
BK29-1	114	1.3	10	0.31	0.24	0.1	0.06	46.9	0.17	<0.2	0.03	0.6	<0.01	1.4	0.7
BK29-2	65	0.6	10	0.29	0.21	0.07	0.05	42.4	0.17	<0.2	0.03	0.2	<0.01	1	0.4
BK29-3	351	0.7	10	0.5	0.17	0.08	0.05	54.4	0.2	<0.2	0.03	0.3	0.01	3.8	0.4
BKBDG-1	80.4	0.7	20	1.47	0.06	<0.03	<0.03	49.4	0.05	<0.2	<0.01	0.4	<0.01	2.9	0.3
BKBDG-2	73.8	0.9	20	1.29	0.05	<0.03	0.03	50	0.1	<0.2	0.01	0.5	<0.01	2.7	0.4
BKBDG-3	60.9	0.5	10	1.04	0.06	0.03	<0.03	48.4	0.08	<0.2	<0.01	0.2	<0.01	2.2	0.3

	Pr	Rb	Sm	Sn	Sr	Ta	Tb	Th	Tm	U	V	W	Y	Yb	Zr
BK01	0.47	180.5	0.58	1	123	<0.1	0.08	0.25	0.04	0.17	<5	<1	2.7	0.26	3
BK05	11.5	305	11.15	8	112.5	1.3	1.93	32.1	0.47	4.6	95	7	42.5	3	318
BK17	0.25	7	0.26	5	6	0.1	0.03	0.68	0.01	0.19	29	44	0.8	0.06	4
BK25-A	15.9	72.7	10.45	3	122	0.9	0.81	18.35	0.18	2.4	45	15	12.7	1.33	157
BK25-B	11.95	67.4	8.38	3	92	1.3	1.03	13.65	0.41	2.22	50	16	28.4	2.79	178
BK25-C	14.8	55.7	9.9	3	122	1.3	1.04	17.65	0.32	17.1	66	26	22.5	2.32	174
BK29-1	0.15	21.5	0.19	3	18.3	0.1	0.05	0.11	0.01	0.11	49	5	1.1	0.07	<2
BK29-2	0.08	16.5	0.14	2	13.6	0.1	0.04	<0.05	0.01	0.06	40	3	0.9	0.07	<2
BK29-3	0.07	51.4	0.13	8	34.7	0.2	0.03	0.08	0.01	0.07	86	12	0.9	0.07	<2
BKBDG-1	0.07	44.4	0.07	2	8.4	0.2	<0.01	0.12	<0.01	0.07	53	2	0.1	<0.03	<2
BKBDG-2	0.11	39.5	0.15	2	10	0.1	0.01	0.13	<0.01	0.08	52	1	0.2	0.04	<2
BKBDG-3	0.06	34.7	0.06	2	10.3	0.1	<0.01	0.07	<0.01	0.07	49	1	0.2	0.04	<2

Appendix Table 5: Supplementary trace element geochemistry results (ppm)

Sample	Ag	As	Cd	Co	Cu	Li	Mo	Ni	Pb	Sc	Tl	Zn	Cu
BK01	<0.5	<5	<0.5	8	695	10	<1	6	7	1	<10	12	-
BK05	<0.5	<5	<0.5	14	110	40	6	17	22	8	<10	43	-
BK17	2.1	<5	<0.5	108	>10000	20	<1	16	11	<1	<10	316	1.335
BK25-A	0.5	55	<0.5	41	1400	<10	<1	8	74	3	<10	31	-
BK25-B	<0.5	145	<0.5	100	1100	<10	<1	12	21	3	<10	20	-
BK25-C	<0.5	48	<0.5	36	1420	<10	<1	8	29	3	<10	22	-
BK29-1	<0.5	<5	<0.5	4	20	10	<1	7	12	1	<10	16	-
BK29-2	<0.5	<5	<0.5	2	3	10	<1	3	13	1	<10	15	-
BK29-3	<0.5	<5	<0.5	5	30	10	<1	9	19	4	<10	18	-
BKBDG-1	<0.5	<5	<0.5	6	2	20	<1	10	<2	1	<10	21	-
BKBDG-2	<0.5	<5	<0.5	6	7	20	<1	9	<2	1	<10	20	-
BKBDG-3	<0.5	<5	<0.5	4	8	20	<1	8	<2	1	<10	17	-

APPENDIX F: EXTENDED GEOCHRONOLOGY METHODS

LA-ICP-MS Analysis

Laser Ablation Inductively Coupled Plasma Mass Spectrometry (LA-ICP-MS) was conducted using the Agilent 7900x with attached RESOlution LR 193 nm Excimer laser system at Adelaide Microscopy, University of Adelaide. A total of twelve individual samples were analysed for monazite U–Pb (ten samples) and apatite U–Pb (seven samples) through in situ laser ablation, at a Fluence of 2.0 J/cm^2 and 3.5 J/cm^2 and spot size of 13µm and 40 µm respectively. SEM-BSE composite images were utilised to locate datable minerals of sufficient area for ablation. Where possible, spots were taken from across the entirety of the sample including within vein sets, sulphides and adjacent altered host rock.

The primary standard for monazite was MAdel which recorded weighted mean ages across two separate runs of ^{206}Pb/^{238}U = 518.4 ± 1.2 Ma (MSWD = 0.84) and ^{207}Pb/^{235}U = 512.5 ± 1.7 Ma (MSWD = 0.94); ^{206}Pb/^{238}U = 518.4 ± 1.2 Ma (MSWD = 1) and ^{207}Pb/^{235}U = 512.9 ± 1.8 Ma (MSWD = 0.87) respectively. A secondary in-house monazite standard 94-222/Bruna-NW (~ 450 Ma: Payne et al., 2008) recorded weighted mean ages across two separate runs of ^{206}Pb/^{238}U = 451.2 ± 1 Ma (MSWD = 0.58) and ^{207}Pb/^{235}U = 449.9 ± 1.5 Ma (MSWD = 0.74); ^{206}Pb/^{238}U = 446.4 ± 1.2 Ma (0.88) and ^{207}Pb/^{235}U = 448.4 ± 1.8 Ma (MSWD = 0.68) respectively. Ambat, a final secondary in-house standard recorded weighted mean ages across two separate runs of ^{206}Pb/^{238}U = 529 ± 5.6 (MSWD = 6.8) and ^{207}Pb/^{235}U = 530.3 ± 8 (MSWD = 7.2); ^{206}Pb/^{238}U = 517.7 ± 4 (MSWD = 3.6) and ^{207}Pb/^{235}U = 513.8 ± 4.7 Ma (MSWD = 2.2) respectively. Published data for these standards records a MAdel age of (updated from Payne, Hand, Barovich & Wade, 2008)

The primary standard for apatite was Madagascar (MAD) which recorded a concordant age of 473.9 ± 2.77 Ma (MSWD = 0.58). The secondary standard Mclure Mountain (401) recorded a concordant age of 532.37 ± 3.43 Ma (MSWD = 1.4). Olympic Dam (OD306) was included as a trial and recorded a discordant age of 1582.72 ± 7.04 Ma (MSWD = 1.9). Published data for these standards records a MAD age of 473.5 ± 0.7 Ma (Chew, Petrus & Kamber, 2014), 401 age of 530.3 ± 1.5 Ma and OD306 age of 1596.7 ± 7.1 Ma (Thompson et al., 2016) with Mclure Mountain being updated from Schoene et al. (2006), indicating the accuracy of apatite U–Pb data in this study.

Data Processing and Reduction

Monazite and apatite U–Pb data were processed and reduced using Iolite software (Paton et al., 2011) in conjunction with IGOR Pro software at the Department of Earth Sciences, University of Adelaide. Down-hole elemental fractionation and instrument drift were corrected for by the addition of several known standards at periodic intervals between unknowns. A polynomial fit was applied during the data reduction scheme (X_U_Pb_Geochron4 DRS) before signals were bracketed to further account for sources of error and noise. Bracketing was utilised extensively for monazite data where the intergrowth and/or contamination of zircon, indicated by the presence of mirrored zirconium and silicon peaks, was found to be common throughout analyses and samples. Where these interferences could not be isolated through bracketing, entire analyses were removed due to extremely elevated ^{207}Pb/^{235}U which tracked back toward to the age of the Earth, mimicking common

Pb contamination. To a lesser extent throughout monazite and apatite analyses, bracketing was also utilised to remove silicon spikes indicative of host rock contamination. The potential for zircon intergrowth and the structural integrity of dated grains is generally accounted for in advance of ablation by high resolution imaging of all selected grains, however, this was only done on a small number of representative grains across samples in this study, and therefore rigorous data reduction was necessary. Where obvious contamination was adequately isolated or not encountered, signals throughout both monazite and apatite analyses were found to be consistent, possibly reflective of small grain sizes without pervasive zonation.

APPENDIX G: MONAZITE U–PB RESULTS

Session #1 Standards	$^{207}Pb/^{235}U$	2σ	$^{206}Pb/^{238}U$	2σ	Rho	$^{207}Pb/^{235}U$ Age (Ma)	2σ (Ma)	$^{206}Pb/^{238}U$ Age (Ma)	2σ (Ma)	$^{207}Pb/^{206}U$ Age (Ma)	2σ (Ma)
External Standards											
M_MAdel1_1	0.649	0.012	0.08382	0.0009	0.32103	507.4	7.6	518.8	5.3	472	48
M_MAdel1_2	0.651	0.016	0.0835	0.001	0.16514	508.1	9.9	517	6.2	445	54
M_MAdel1_3	0.657	0.015	0.08393	0.00095	0.40516	512.1	9.3	519.5	5.7	486	48
M_MAdel1_4	0.661	0.016	0.08329	0.00098	0.15078	514.1	9.7	515.7	5.8	483	52
M_MAdel1_5	0.648	0.018	0.08266	0.00095	0.36105	506	11	511.9	5.7	457	60
M_MAdel1_6	0.653	0.017	0.08357	0.00084	0.2183	510	10	517.4	5	460	56
M_MAdel1_7	0.664	0.015	0.08347	0.00093	0.10268	516.2	9.1	516.7	5.5	513	50
M_MAdel1_8	0.654	0.015	0.0829	0.001	0.28475	511.8	9.9	513.6	6	491	54
M_MAdel1_9	0.665	0.018	0.084	0.001	0.24529	517	11	519.9	6.2	488	57
M_MAdel1_10	0.654	0.015	0.08427	0.00094	0.2296	510.4	8.8	521.5	5.6	451	49
M_MAdel1_11	0.659	0.014	0.0832	0.001	-0.08878	513.1	8.9	515.1	6.2	496	62
M_MAdel1_12	0.665	0.014	0.0844	0.001	0.23986	517	8.6	522.6	6.1	483	48
M_MAdel1_13	0.668	0.017	0.08337	0.00093	0.17933	520.3	9.9	516.2	5.5	527	53
M_MAdel1_14	0.642	0.017	0.0835	0.0012	0.34983	502	11	516.7	7.1	426	57
M_MAdel1_15	0.667	0.016	0.08365	0.00087	0.27157	517.9	9.6	517.9	5.2	517	49
M_MAdel1_16	0.661	0.015	0.0844	0.0011	0.32775	514.6	9.4	522.5	6.6	471	50
M_MAdel1_17	0.666	0.017	0.08342	0.00087	0.18045	518	10	516.5	5.2	520	54
M_MAdel1_18	0.639	0.015	0.08337	0.00094	0.16137	501	9.3	516.2	5.6	431	56
M_MAdel1_19	0.661	0.015	0.08397	0.00093	0.11095	514.4	9.2	519.7	5.6	481	53
M_MAdel1_20	0.651	0.018	0.08423	0.0009	0.19942	508	11	521.3	5.4	435	61
M_MAdel1_21	0.655	0.015	0.08368	0.00093	0.19909	512.6	9.8	518	5.5	473	54
M_MAdel1_22	0.673	0.015	0.0848	0.0011	0.43626	522	8.9	524.9	6.4	502	44
M_MAdel1_23	0.669	0.014	0.0848	0.001	0.36386	519.3	8.6	524.5	6	485	47
M_MAdel1_24	0.663	0.016	0.08409	0.00097	0.029471	516	10	520.5	5.8	494	57
M_MAdel1_25	0.653	0.015	0.084	0.0011	0.20332	509.2	9.2	520	6.5	449	54
M_MAdel1_26	0.668	0.016	0.0841	0.0011	0.33846	518.8	9.6	520.3	6.3	510	52
M_MAdel1_27	0.659	0.016	0.0844	0.0011	0.17653	513.4	9.6	522.6	6.3	465	55
M_MAdel1_28	0.645	0.015	0.0845	0.00088	0.17307	504.6	9.3	522.9	5.2	411	53
M_MAdel1_29	0.671	0.017	0.0845	0.001	0.10361	520	10	523	6.2	521	52
M_MAdel1_30	0.659	0.015	0.0843	0.001	0.2698	513.2	9.4	521.6	6	464	53
M_MAdel1_31	0.664	0.013	0.0846	0.001	0.21432	517.7	7.6	523.4	6.1	483	45
M_MAdel1_32	0.666	0.014	0.0831	0.0011	0.077967	517.3	8.3	514.7	6.6	524	52
M_MAdel1_33	0.653	0.014	0.0836	0.001	0.30312	509.7	8.6	517.5	6.2	469	47
M_MAdel1_34	0.647	0.017	0.0821	0.001	0.30428	506	10	508.7	6	485	56
M_MAdel1_35	0.644	0.015	0.08286	0.00087	0.36341	503.8	9.4	513.1	5.2	450	50
M_MAdel1_36	0.656	0.016	0.0839	0.0011	0.33657	511	10	519.5	6.4	466	54
M_MAdel1_37	0.659	0.016	0.0838	0.001	0.25762	513.1	9.8	518.7	6.1	484	52
M_MAdel1_38	0.64	0.017	0.08255	0.00083	0.19413	502	10	511.3	4.9	444	58

M_MAdel1_39	0.661	0.017	0.0839	0.0011	0.3557	514	10	519.1	6.4	495	55
Internal Standards											
X222_1	0.567	0.011	0.07286	0.00067	0.15889	455.6	6.8	453.3	4	453	44
X222_2	0.557	0.012	0.07245	0.0008	0.17673	448.9	7.6	450.9	4.8	428	49
X222_3	0.561	0.012	0.07279	0.00092	0.27018	451.6	7.9	452.9	5.6	454	46
X222_4	0.562	0.01	0.07327	0.00081	0.24127	452.4	6.8	455.8	4.8	426	43
X222_5	0.566	0.012	0.0732	0.00073	0.43808	454.5	8	455.4	4.4	444	43
X222_6	0.556	0.012	0.07255	0.00082	0.33169	448.1	7.6	451.5	5	421	46
X222_7	0.556	0.011	0.07293	0.00075	0.2788	448.7	7.1	453.8	4.5	415	43
X222_8	0.564	0.011	0.07245	0.00073	0.44065	453.3	7	450.9	4.4	458	39
X222_9	0.557	0.01	0.07205	0.00075	0.27241	449.3	6.5	448.5	4.5	447	41
X222_10	0.564	0.012	0.0722	0.00075	0.33195	454.6	7.9	449.3	4.5	481	43
X222_11	0.56	0.011	0.07267	0.0008	0.35878	451.2	7.1	452.2	4.8	439	42
X222_12	0.5577	0.0099	0.07237	0.00071	0.40396	449.6	6.5	450.4	4.3	440	37
X222_13	0.56	0.011	0.07272	0.00074	0.24434	450.8	7.4	452.5	4.5	435	45
X222_14	0.559	0.01	0.07239	0.00077	0.38278	450.7	6.7	450.5	4.6	447	39
X222_15	0.5466	0.0099	0.07189	0.00065	0.34731	442.4	6.5	447.5	3.9	411	38
X222_16	0.565	0.011	0.07226	0.00067	0.22006	454.4	6.9	449.7	4	480	40
X222_17	0.556	0.01	0.07218	0.00074	0.01756	448.2	6.8	449.3	4.5	437	48
X222_18	0.5496	0.0091	0.07145	0.00073	0.091651	444.4	6	444.8	4.4	438	42
X222_19	0.5599	0.0098	0.07283	0.00077	0.29273	451.1	6.4	454	4.9	433	39
X222_20	0.562	0.011	0.07221	0.00087	0.45966	452.1	6.9	449.4	5.2	462	39
X222_21	0.56	0.011	0.07236	0.00085	0.20472	450.8	7	450.3	5.1	459	42
X222_22	0.5519	0.0085	0.0721	0.00075	0.35275	445.9	5.6	448.7	4.5	430	34
X222_23	0.549	0.01	0.07291	0.00071	0.35795	443.9	6.5	453.6	4.3	402	40
X222_24	0.563	0.01	0.07254	0.00079	0.42884	453.4	6.6	451.4	4.8	469	41
X222_25	0.564	0.011	0.07312	0.00066	0.15272	453.8	7	454.9	3.9	437	46
X222_26	0.548	0.011	0.07239	0.0007	0.27644	443.1	6.9	450.5	4.2	405	43
Ambat_1	0.68	0.013	0.08496	0.00092	0.34817	526.2	7.7	525.6	5.5	520	40
Ambat_2	1.168	0.029	0.08947	0.00091	0.64108	784	13	552.4	5.4	1518	40
Ambat_3	0.662	0.013	0.08434	0.00081	0.33313	515.3	8.2	522	4.8	488	41
Ambat_4	0.66	0.014	0.08463	0.00084	0.47202	513.7	8.5	523.7	5	466	41
Ambat_5	0.667	0.011	0.0841	0.001	0.31218	518.2	7	520.8	6.1	502	39
Ambat_6	1.011	0.051	0.0881	0.0011	0.32636	703	26	544	6.6	1210	100
Ambat_7	0.655	0.013	0.08572	0.00084	0.20406	510.8	8	530.1	5	418	45
Ambat_8	0.666	0.011	0.08463	0.00087	0.27734	517.9	7	523.6	5.2	480	42
Ambat_9	1.031	0.057	0.08816	0.00088	0.42184	711	29	544.6	5.2	1230	110
Ambat_10	0.659	0.013	0.08441	0.00098	0.27216	513.6	7.9	522.4	5.8	471	43
Ambat_11	0.662	0.013	0.08498	0.00087	0.31468	515.2	7.9	525.7	5.2	464	43
Ambat_12	0.669	0.013	0.08528	0.00089	0.37096	519.2	8.2	527.5	5.3	479	41
Ambat_13	0.645	0.012	0.08372	0.00097	0.45952	505	7.4	518.2	5.8	439	38

Session #2 Standards	207Pb/235U	2σ	206Pb/238U	2σ	Rho	$^{207}Pb/^{235}U$ Age (Ma)	2σ (Ma)	$^{206}Pb/^{238}U$ Age (Ma)	2σ (Ma)	$^{207}Pb/^{206}U$ Age (Ma)	2σ (Ma)
External Standards											
M_MAdel1_1	0.658	0.012	0.08248	0.00084	0.36855	513.2	7.1	510.9	5	518	37
M_MAdel1_2	0.658	0.011	0.08391	0.00073	0.3351	513	6.7	519.4	4.3	479	37
M_MAdel1_3	0.65	0.012	0.084	0.00091	0.23526	507.8	7.2	519.9	5.4	447	42
M_MAdel1_4	0.653	0.012	0.0831	0.0008	0.37224	509.8	7.2	514.6	4.7	482	37
M_MAdel1_5	0.644	0.012	0.08336	0.00069	0.25092	504.1	7.2	516.1	4.1	436	38
M_MAdel1_6	0.652	0.01	0.08359	0.00077	0.36117	509.5	6.4	517.5	4.6	487	33
M_MAdel1_7	0.654	0.011	0.0839	0.00088	0.3511	510.4	6.8	519.3	5.2	466	37
M_MAdel1_8	0.666	0.013	0.0827	0.00076	0.40633	517.9	7.9	512.2	4.5	536	39
M_MAdel1_9	0.657	0.012	0.08325	0.00079	0.3512	512.5	7.2	515.4	4.7	497	39
M_MAdel1_10	0.67	0.012	0.08399	0.00066	0.14839	521.7	7.4	519.9	3.9	522	40
M_MAdel1_11	0.668	0.011	0.08506	0.00085	0.28266	518.8	6.6	526.2	5	481	36
M_MAdel1_12	0.667	0.011	0.08459	0.00066	0.34695	518.4	7	523.4	3.9	494	35
M_MAdel1_13	0.657	0.011	0.0836	0.00078	0.31712	512.3	6.9	517.5	4.6	486	39
M_MAdel1_14	0.655	0.011	0.08437	0.00085	0.35251	511.3	6.6	522.1	5	457	35
M_MAdel1_15	0.663	0.011	0.08408	0.00073	0.20362	516.1	6.7	520.4	4.3	498	37
M_MAdel1_16	0.645	0.011	0.08417	0.00076	0.49658	505	7.1	520.9	4.5	423	34
M_MAdel1_17	0.66	0.011	0.08393	0.00088	0.25178	515.5	7.4	519.5	5.2	492	40
M_MAdel1_18	0.657	0.013	0.08419	0.00095	0.34449	512.4	7.7	521	5.7	467	42
M_MAdel1_19	0.662	0.013	0.08392	0.00087	0.32391	515.1	7.7	519.5	5.2	495	39
M_MAdel1_20	0.662	0.012	0.08412	0.00083	0.38111	515.4	7	520.6	4.9	492	34
M_MAdel1_21	0.663	0.011	0.08403	0.00075	0.19433	516.1	6.6	520.1	4.5	492	37
M_MAdel1_22	0.659	0.011	0.08416	0.00086	0.1516	513.7	6.5	520.8	5.1	470	37
M_MAdel1_23	0.661	0.01	0.08378	0.00081	0.31096	514.6	6.4	518.6	4.8	492	36
M_MAdel1_24	0.649	0.011	0.08337	0.00087	0.39437	508.4	6.9	516.2	5.2	468	32
M_MAdel1_25	0.652	0.012	0.08327	0.00075	0.22476	509.4	7.3	515.6	4.5	478	42
M_MAdel1_26	0.651	0.011	0.08295	0.00081	0.28219	508.5	6.8	513.6	4.8	479	38
M_MAdel1_27	0.653	0.012	0.08261	0.00074	0.21342	509.9	7.3	511.7	4.4	494	40
M_MAdel1_28	0.656	0.011	0.08329	0.00089	0.3236	511.6	6.5	515.7	5.3	494	37
M_MAdel1_29	0.681	0.012	0.08438	0.00082	0.26437	527	7.3	522.2	4.9	563	39
M_MAdel1_30	0.755	0.062	0.0856	0.0011	0.70615	568	33	529.4	6.4	680	120
M_MAdel1_31	0.6606	0.0095	0.08366	0.00062	0.16324	514.6	5.8	517.9	3.7	487	34
M_MAdel1_32	0.668	0.012	0.08396	0.00077	0.32845	518.9	7.3	519.7	4.6	508	38
M_MAdel1_33	0.654	0.011	0.08386	0.0007	0.25757	511.6	6.8	519.1	4.1	470	36
M_MAdel1_34	0.649	0.011	0.08312	0.00072	0.3203	507.6	6.7	514.7	4.3	469	37
M_MAdel1_35	0.649	0.011	0.08364	0.00077	0.37007	507.7	6.6	517.8	4.6	467	33
M_MAdel1_36	0.657	0.011	0.08382	0.00096	0.39824	512	7	518.8	5.7	471	37
M_MAdel1_37	0.655	0.011	0.08404	0.00082	0.11031	511.3	7	520.1	4.9	464	43
M_MAdel1_38	0.657	0.011	0.08306	0.00085	0.36143	512.2	6.5	514.3	5	497	35
Internal Standards											
X222_1	0.555	0.011	0.07164	0.0008	0.371	447.7	7.1	446	4.8	449	41
X222_2	0.545	0.011	0.07133	0.00086	0.32341	441.4	7.2	444.1	5.2	419	44

X222_3	0.547	0.011	0.07113	0.00079	0.17858	442.7	7.3	443	4.8	433	48
X222_4	0.543	0.011	0.07126	0.00083	0.30387	440.2	7.1	443.7	5	415	44
X222_5	0.553	0.011	0.07156	0.00082	0.21712	446.7	6.9	445.5	5	446	46
X222_6	0.55	0.012	0.07105	0.00081	0.26153	444.1	7.8	442.4	4.9	438	49
X222_7	0.553	0.011	0.07187	0.00076	0.14587	446.6	7.5	447.4	4.6	434	48
X222_8	0.553	0.011	0.07193	0.00079	0.30663	446.3	7.5	447.8	4.8	431	47
X222_9	0.556	0.01	0.0724	0.00084	0.25199	448.7	6.9	450.5	5.1	432	45
X222_10	0.555	0.011	0.07147	0.00081	0.35773	447.9	7.4	445	4.9	455	42
X222_11	0.556	0.011	0.07223	0.00085	0.22036	448.1	7.4	449.5	5.1	432	48
X222_12	0.567	0.012	0.07179	0.00086	0.39955	455.2	8.1	446.9	5.2	488	45
X222_13	0.55	0.011	0.07183	0.00087	0.21356	444.6	7.3	447.1	5.2	423	46
X222_14	0.565	0.012	0.07192	0.00086	0.43606	454	8	447.7	5.2	472	45
X222_15	0.558	0.01	0.07088	0.00069	0.00030208	449.7	6.6	441.5	4.2	479	46
X222_16	0.563	0.013	0.07158	0.00075	0.26086	452.9	8.4	445.7	4.5	478	52
X222_17	0.564	0.013	0.0714	0.00081	0.12212	453.5	8.4	444.6	4.9	487	55
X222_18	0.57	0.012	0.07202	0.0009	0.20726	457.2	7.8	448.3	5.4	493	49
X222_19	0.56	0.013	0.07275	0.00084	0.36376	451	8.5	452.6	5	432	50
X222_20	0.565	0.012	0.07204	0.00072	0.31343	454.1	7.7	448.4	4.3	474	46
X222_21	0.564	0.012	0.07284	0.00084	0.18969	453.2	7.9	453.2	5	451	52
X222_22	0.56	0.011	0.07262	0.00084	0.25753	450.8	7.2	451.9	5.1	432	46
X222_23	0.562	0.012	0.07166	0.00086	0.40291	452	8.1	446.1	5.2	481	49
X222_24	0.551	0.0097	0.07093	0.00067	0.21607	445.2	6.3	441.7	4.1	455	42
X222_25	0.5447	0.0099	0.07145	0.00069	0.25241	441.1	6.5	444.9	4.2	425	40
X222_26	0.558	0.013	0.07149	0.00082	0.38937	449.5	8.7	445.1	4.9	455	50
Ambat_1	0.663	0.011	0.08299	0.00082	0.31562	516.3	6.8	513.9	4.9	528	36
Ambat_2	0.651	0.012	0.08253	0.00089	0.47409	508.7	7.2	511.1	5.3	495	34
Ambat_3	0.654	0.011	0.08362	0.0009	0.27687	510.2	6.8	517.6	5.4	471	39
Ambat_4	0.658	0.012	0.08303	0.0009	0.28459	514.1	6.9	514.1	5.3	497	41
Ambat_5	0.647	0.012	0.0838	0.001	0.44166	507.2	7.2	518.6	6	443	38
Ambat_6	0.659	0.012	0.08382	0.00084	0.2888	513.3	7.2	518.9	5	482	39
Ambat_7	0.657	0.012	0.08331	0.00095	0.29186	512	7.1	515.8	5.7	495	37
Ambat_8	0.637	0.012	0.0827	0.001	0.23904	499.6	7.7	512.2	5.9	433	44
Ambat_9	0.663	0.012	0.08337	0.00098	0.39602	515.7	7.5	516.2	5.8	507	38
Ambat_10	0.709	0.025	0.0904	0.0021	0.73126	543	15	558	12	478	53
Ambat_11	0.658	0.01	0.08424	0.00087	0.26414	512.8	6.3	521.4	5.2	469	35
Ambat_12	0.661	0.011	0.08389	0.00077	0.25833	514.6	6.5	519.3	4.6	484	36
Ambat_13	0.685	0.013	0.0842	0.001	0.39391	529.1	7.6	521	6.2	559	39
Session #1 Unknowns	**207Pb/235U**	**2σ**	**206Pb/238U**	**2σ**	**Rho**	**^{207}Pb/^{235}U Age (Ma)**	**2σ (Ma)**	**^{206}Pb/^{238}U Age (Ma)**	**2σ (Ma)**	**^{207}Pb/^{206}U Age (Ma)**	**2σ (Ma)**
BK01_1	0.704	0.066	0.0787	0.003	0.1043	529	40	488	18	620	210
BK01_2	0.612	0.029	0.0759	0.0025	0.42432	482	18	471	15	584	74
BK01_3	0.672	0.013	0.0778	0.0012	0.37796	521.9	8	482.7	7.1	695	44
BK01_4	0.636	0.021	0.0783	0.0014	0.2955	499	13	485.6	8.1	540	73

BK01_5	0.676	0.024	0.0781	0.0016	0.71166	524	15	484.6	9.5	701	58
BK01_6	0.64	0.012	0.0775	0.0012	0.63748	501.6	7.5	481.4	7	606	31
BK01_7	0.659	0.015	0.0795	0.0013	0.34891	513.6	9.1	493.2	7.6	600	49
BK01_8	0.668	0.013	0.07979	0.00095	0.05726	518.7	8	494.9	5.7	619	48
BK01_9	0.682	0.023	0.0791	0.0015	0.55831	527	14	490.7	9	679	61
BK01_10	0.639	0.023	0.0777	0.0013	0.07621	500	14	482.6	7.6	562	84
BK01_11	0.662	0.019	0.0793	0.0021	0.6007	515	11	492	12	622	50
BK01_12	0.577	0.043	0.0786	0.0023	0.060143	457	28	488	14	310	170
BK01_13	0.615	0.07	0.078	0.0036	0.004626	479	42	484	22	410	240
BK01_14	0.645	0.015	0.0769	0.0011	0.28717	504.7	9	477.8	6.3	626	47
BK01_15	0.645	0.016	0.0773	0.0014	0.17623	505.1	9.8	480.2	8.3	615	61
BK01_16	0.684	0.02	0.0824	0.0013	0.3159	528	12	510.3	7.7	598	63
BK01_17	0.659	0.021	0.081	0.0024	-0.42272	513	13	502	14	570	110
BK01_18	0.688	0.028	0.0816	0.0019	0.57423	531	17	505	11	644	70
BK01_19	0.647	0.022	0.0811	0.0019	0.53653	506	13	502	11	522	61
BK01_20	0.684	0.019	0.0804	0.0013	0.33294	529	12	498.3	7.9	656	59
BK01_21	0.629	0.015	0.0761	0.0011	0.5226	494.7	9.5	472.6	6.3	594	44
BK01_22	0.632	0.016	0.0755	0.0016	0.60381	497	10	469	9.5	614	36
BK01_23	0.636	0.016	0.0777	0.0015	0.36707	499.3	9.6	482.2	8.8	592	44
BK01_24	0.688	0.021	0.0819	0.0016	0.5483	531	12	507.4	9.8	627	53
BK01_25	0.646	0.019	0.0786	0.0013	0.46434	504	12	487.7	8	564	60
BK01_26	0.745	0.037	0.0785	0.0022	0.16186	563	22	487	13	870	110
BK01_27	0.676	0.015	0.0789	0.0014	0.45724	523.8	9.2	489.4	8.5	684	48
BK01_28	0.662	0.013	0.0782	0.0011	0.58498	515.3	7.9	485.2	6.5	657	32
BK01_29	0.695	0.031	0.0807	0.0018	0.050495	535	19	500	11	680	110
BK01_30	0.674	0.013	0.07961	0.00087	0.40088	522.7	7.9	493.8	5.2	652	43
BK01_31	0.583	0.054	0.078	0.0029	0.055363	460	35	484	17	320	210
BK01_32	0.61	0.023	0.0766	0.0015	0.35724	483	14	475.9	9.1	503	77
BK06_1	0.693	0.033	0.0847	0.0017	0.19578	532	20	524	10	540	110
BK06_2	0.581	0.061	0.0822	0.0028	-0.095072	452	39	509	17	180	230
BK06_3	0.613	0.035	0.0785	0.0018	0.032279	482	22	487	10	420	130
BK06_4	0.701	0.081	0.0874	0.0043	0.40835	529	49	540	25	430	230
BK06_5	0.696	0.055	0.0847	0.0029	0.11719	539	36	524	17	550	180
BK06_6	0.901	0.084	0.0808	0.0041	0.7056	647	44	500	24	1140	120
BK06_7	0.758	0.074	0.0773	0.0036	0.297	563	41	480	21	870	200
BK06_8	0.614	0.028	0.0799	0.0016	0.35875	484	17	495.2	9.3	418	88
BK06_9	0.645	0.012	0.0805	0.001	0.48111	504.9	7.2	499.3	6	528	36
BK06_10	0.698	0.036	0.0871	0.0034	0.87869	534	20	538	20	534	50
BK06_11	0.659	0.028	0.0835	0.0021	0.54376	512	17	517	12	532	64
BK06_12	0.715	0.059	0.0865	0.0054	0.35721	544	34	534	32	580	180
BK06_13	0.623	0.017	0.0797	0.0019	0.58516	491	10	494	11	478	54
BK06_14	0.648	0.029	0.0834	0.0021	0.29477	506	18	517	12	449	89
BK06_15	0.628	0.036	0.0805	0.0019	0.28603	492	22	499	12	420	120
BK06_16	0.686	0.03	0.0858	0.0033	0.66276	528	18	530	19	535	68

BK06_17	0.663	0.018	0.0806	0.0017	0.39999	516	11	500	10	584	59
BK06_18	0.664	0.026	0.0822	0.0026	0.83886	516	15	509	16	567	51
BK06_19	0.642	0.021	0.0806	0.0019	0.61509	503	13	500	11	511	55
BK06_20	0.619	0.04	0.08	0.0021	0.27776	492	28	496	13	440	140
BK06_21	0.67	0.089	0.0848	0.0056	0.11065	514	54	525	33	430	290
BK06_22	0.658	0.031	0.0822	0.0017	0.55047	512	19	509	10	553	90
BK06_23	0.659	0.058	0.0774	0.0021	0.19492	507	36	480	13	550	180
BK06_24	0.749	0.054	0.0853	0.0032	0.57809	564	30	528	19	690	110
BK06_25	0.708	0.025	0.0766	0.0017	0.20997	542	15	475	10	818	76
BK06_26	0.6133	0.0092	0.07729	0.00094	0.6097	485.3	5.8	479.9	5.7	512	27
BK06_27	0.648	0.043	0.0783	0.0026	0.20969	503	26	486	15	550	140
BK06_28	no value	NAN	no value	NAN	NaN	no value	NAN	no value	NAN	no value	NAN
BK06_29	0.638	0.06	0.0873	0.0033	0.016329	496	38	539	20	260	220
BK06_30	0.668	0.023	0.0825	0.0019	0.33347	518	14	511	11	533	73
BK06_31	0.605	0.061	0.0784	0.0033	0.21083	469	40	486	20	360	210
BK06_32	0.728	0.055	0.0867	0.0029	0.77002	553	31	536	17	610	120
BK14_1	0.726	0.02	0.0823	0.0015	0.34892	553	12	509.9	9	733	45
BK14_2	0.722	0.023	0.0796	0.0014	0.43812	551	14	493.7	8.4	786	60
BK14_3	0.656	0.012	0.07953	0.00085	0.74387	513.5	7.6	493.3	5.1	604	29
BK14_4	0.739	0.046	0.081	0.0017	0.65605	559	26	502	10	812	90
BK14_5	0.743	0.03	0.0834	0.0023	0.70669	564	17	516	14	764	60
BK14_6	0.815	0.037	0.0822	0.0022	0.63878	604	21	509	13	992	70
BK14_7	0.735	0.016	0.0835	0.0013	0.6756	558.6	9.6	516.9	8	731	33
BK14_8	0.689	0.023	0.0798	0.0019	0.80877	531	14	495	11	685	40
BK14_9	0.659	0.011	0.0798	0.001	0.53104	513.3	6.9	495	6	596	32
BK14_10	0.686	0.012	0.08192	0.00099	0.63397	530.1	7.1	507.5	5.9	628	31
BK14_11	0.686	0.013	0.08136	0.00095	0.48873	529.9	7.5	504.2	5.6	633	31
BK14_12	0.873	0.047	0.0829	0.0021	0.057146	635	25	513	13	1090	110
BK14_13	0.735	0.023	0.0817	0.0018	0.67881	559	14	506	11	780	49
BK14_14	0.725	0.034	0.0854	0.0029	0.78581	552	20	528	17	652	65
BK14_15	0.713	0.03	0.0801	0.0018	0.62212	545	17	496	11	753	65
BK14_16	0.651	0.0088	0.07933	0.00059	0.65696	508.8	5.4	492.1	3.5	585	23
BK14_17	0.816	0.039	0.0853	0.0014	0.40346	604	21	527.4	8.4	889	84
BK14_18	0.703	0.028	0.0835	0.0022	0.21295	540	17	517	13	638	93
BK14_19	0.648	0.012	0.0785	0.0012	0.50971	507.2	7.2	487	7.3	599	36
BK14_20	0.652	0.02	0.0797	0.0017	0.66817	509	12	494	10	578	49
BK18_1	0.769	0.025	0.0806	0.0013	0.51149	579	15	499.5	7.9	888	63
BK18_2	0.693	0.018	0.0786	0.0015	0.44355	534	11	487.8	8.7	731	47
BK18_3	0.737	0.027	0.079	0.0019	0.038826	560	16	490	11	853	88
BK18_4	0.842	0.058	0.0796	0.0018	0.55701	617	31	494	11	1090	120
BK18_5	0.793	0.04	0.07744	0.00088	0.39521	589	21	480.8	5.3	1002	82
BK18_6	0.739	0.027	0.079	0.0017	0.29645	561	16	490	10	860	76
BK18_7	0.715	0.02	0.0785	0.0014	0.72638	547	12	487.4	8.3	796	42

BK18_8	0.833	0.035	0.0788	0.0012	0.55795	612	19	488.8	7.4	1079	69
BK18_9	0.839	0.021	0.0802	0.0013	0.29411	618	12	497.2	7.6	1088	51
BK18_10	0.767	0.022	0.077	0.0013	0.20179	577	13	478	7.6	974	60
BK18_11	0.662	0.025	0.0792	0.0016	0.11842	515	16	491	9.7	613	89
BK18_12	0.696	0.021	0.079	0.0013	0.17904	539	11	490.2	7.7	752	58
BK25A_1	0.618	0.012	0.077	0.001	0.33883	488.3	7.8	478.4	6.1	536	42
BK25A_2	0.664	0.012	0.0767	0.00092	0.38756	516.7	7.6	476.3	5.5	692	38
BK25A_3	0.741	0.043	0.0796	0.0025	0.10992	562	25	494	15	850	120
BK25A_4	0.703	0.018	0.0816	0.0016	0.06744	540	10	505.4	9.3	690	69
BK25A_5	0.601	0.031	0.0797	0.0021	0.25726	474	20	494	12	350	110
BK25A_6	0.6093	0.0076	0.07785	0.00078	0.53226	482.9	4.8	483.3	4.7	477	25
BK25A_7	0.591	0.013	0.0752	0.0015	0.57142	472.5	8.6	467.2	9	494	44
BK25A_8	0.665	0.019	0.0742	0.0011	0.14999	517	11	461.1	6.3	750	64
BK25A_9	0.642	0.021	0.0799	0.0018	0.26681	503	13	496	11	547	69
BK25A_10	0.6155	0.0089	0.07589	0.00089	0.36585	486.8	5.6	471.5	5.4	554	35
BK25A_11	0.606	0.029	0.078	0.0018	0.29256	480	18	484	11	450	110
BK25A_12	0.661	0.029	0.0781	0.0016	-0.02845	514	18	484.5	9.8	630	110
BK25A_13	0.685	0.027	0.0813	0.0013	0.35289	529	16	503.8	8	633	82
BK25A_14	0.619	0.011	0.0768	0.0011	0.54838	488.6	6.8	476.9	6.7	540	33
BK25A_15	0.579	0.069	0.0766	0.0035	0.12919	467	49	476	21	370	260
BK25A_16	0.647	0.03	0.0778	0.0022	0.4429	505	18	483	13	594	96
BK25A_17	0.607	0.01	0.07496	0.00076	0.44961	481.4	6.5	465.9	4.6	546	34
BK25A_18	0.699	0.021	0.076	0.001	0.4395	537	12	472.1	6.2	809	55
BK25A_19	0.628	0.03	0.0791	0.0023	0.25237	494	19	491	13	500	120
BK25A_20	0.642	0.02	0.0779	0.0014	0.55164	503	12	483.4	8.3	578	59
BK25A_21	0.663	0.041	0.082	0.0022	-0.057076	515	25	508	13	540	150
BK25A_22	0.622	0.024	0.0769	0.002	0.48125	491	15	477	12	544	74
BK25A_23	0.62	0.03	0.0799	0.0021	0.4341	489	19	495	13	448	98
BK25A_24	0.703	0.018	0.0783	0.0013	0.36661	540	11	485.8	7.6	766	52
BK25A_25	0.62	0.022	0.0787	0.0016	0.4302	489	14	488.1	9.6	486	67
BK25A_26	0.653	0.015	0.0783	0.001	0.29866	509.6	9.1	485.7	6.3	609	55
BK25A_27	0.634	0.028	0.0788	0.0018	0.2193	497	18	489	10	530	100
BK25A_28	0.697	0.03	0.08137	0.00097	0.418	535	18	504.3	5.8	660	86
BK25A_29	0.65	0.039	0.079	0.0025	-0.048374	518	31	490	15	560	120
BK25A_30	0.65	0.027	0.0778	0.0021	0.55996	507	16	483	12	610	76
BK25A_31	0.722	0.048	0.0769	0.003	0.33429	550	28	477	18	850	130
BK25A_32	0.612	0.013	0.0763	0.0013	0.26564	484	8.4	473.6	7.7	526	52
BK25A_33	0.63	0.022	0.0756	0.0011	0.62082	495	13	469.7	6.4	631	65
BK25A_34	0.746	0.073	0.0806	0.0021	0.34375	574	47	500	12	830	190
BK25A_35	0.637	0.024	0.0806	0.0021	0.39427	500	15	500	12	501	76
BK25A_36	0.659	0.035	0.0786	0.0018	0.084344	513	21	488	11	610	120
BK25B_1	0.684	0.016	0.0788	0.0011	0.47962	528.5	9.6	489.1	6.4	685	42
BK25B_2	0.628	0.047	0.0776	0.0025	0.17195	487	29	481	15	460	160

BK25B_3	0.571	0.05	0.076	0.0024	-0.032044	449	32	472	14	300	180
BK25B_4	0.623	0.012	0.0779	0.0013	0.33356	491.3	7.5	483.6	7.6	509	35
BK25B_5	0.667	0.043	0.0812	0.0021	0.51855	517	26	503	12	550	120
BK25B_6	0.635	0.035	0.082	0.0021	0.13186	500	23	508	12	450	120
BK25B_7	0.609	0.047	0.078	0.0027	0.4801	479	29	484	16	420	150
BK25B_8	0.635	0.011	0.0786	0.001	0.44268	499	6.9	487.6	6.2	552	35
BK25B_9	0.806	0.047	0.0789	0.0018	0.43001	597	25	489	11	1014	99
BK25B_10	0.614	0.037	0.0779	0.0022	0.045345	488	26	484	13	480	150
BK25B_11	0.59	0.049	0.0784	0.0027	0.19176	465	31	486	16	320	170
BK25B_12	0.613	0.015	0.0765	0.0012	0.24856	484.7	9.2	475.3	7.3	510	56
BK25B_13	0.628	0.031	0.0802	0.0026	0.54037	493	19	497	15	463	87
BK25B_14	0.89	0.11	0.0757	0.0019	0.71716	621	51	470	11	1120	170
BK25B_15	0.606	0.016	0.07645	0.00093	0.24598	480	10	474.9	5.6	492	58
BK25B_16	0.636	0.021	0.0799	0.0015	0.228	498	13	495.4	9.1	487	74
BK25B_17	0.666	0.022	0.0764	0.0018	0.050145	517	13	475	11	682	64
BK25B_18	0.707	0.03	0.0773	0.0012	0.64015	541	18	480	7.3	781	70
BK25B_19	0.623	0.012	0.079	0.001	0.46939	491.1	7.7	490.2	6	479	41
BK25B_20	0.687	0.029	0.0784	0.0016	0.70896	530	17	486.4	9.6	709	61
BK25B_21	0.686	0.052	0.0818	0.0029	0.075439	527	32	507	17	590	170
BK25B_22	0.612	0.017	0.0754	0.00097	0.28574	484	11	468.6	5.8	551	62
BK25B_23	0.693	0.066	0.0819	0.0027	-0.24608	528	40	507	16	570	230
BK25B_24	0.628	0.016	0.0776	0.0014	0.44618	494	10	481.6	8.2	535	59
BK25B_25	0.615	0.02	0.0786	0.0021	0.61714	486	12	488	12	489	57
BK25B_26	0.64	0.03	0.0798	0.0018	0.29047	502	20	495	11	510	100
BK25B_27	0.633	0.029	0.0746	0.0011	0.65366	489	13	463.8	6.5	617	75
BK25B_28	0.621	0.016	0.0777	0.0012	0.21909	489	10	482.4	7.1	509	60
BK25B_29	0.665	0.036	0.0748	0.0014	0.42197	513	21	465	8.3	714	98
BK25B_30	0.653	0.038	0.0783	0.0018	0.11567	505	23	486	11	560	130
BK25B_31	0.72	0.04	0.078	0.0011	0.61815	549	23	484.3	6.6	794	93
BK25B_32	0.668	0.015	0.0817	0.0011	0.56892	519.1	8.9	506.4	6.4	570	37
BK25B_33	0.612	0.015	0.0796	0.0018	0.44635	484.2	9.3	494	11	438	54
BK25B_34	0.64	0.029	0.0758	0.0013	0.43856	501	18	471.1	7.9	662	94
BK25B_35	0.643	0.02	0.0759	0.0011	0.3091	503	12	471.7	6.7	630	65
BK25B_36	0.613	0.014	0.07611	0.0008	0.33084	484.5	8.9	472.8	4.8	524	49
BK25B_37	0.687	0.02	0.0831	0.0012	0.092902	530	12	514.3	7	587	66
KTDD089_1	0.708	0.04	0.082	0.0028	0.11553	542	23	508	16	680	120
KTDD089_2	0.626	0.021	0.0781	0.002	0.82242	493	13	485	12	525	49
KTDD089_3	0.643	0.043	0.0776	0.0029	0.26463	501	26	481	18	540	150
KTDD089_4	0.605	0.04	0.0776	0.0021	0.095507	474	25	481	13	400	140
KTDD089_5	0.698	0.065	0.0797	0.0021	0.17429	539	36	494	12	660	190
KTDD089_6	0.97	0.12	0.0786	0.0024	-0.0078251	684	67	487	15	1220	260
KTDD089_7	0.718	0.032	0.0786	0.0018	0.19131	547	19	488	11	790	97
KTDD089_8	0.786	0.057	0.0775	0.0024	0.090921	587	31	481	14	970	160
KTDD089_9	0.781	0.055	0.0734	0.0019	-0.067947	581	31	457	12	1060	160

KTDD089_10	0.73	0.066	0.0752	0.0041	0.37193	552	38	467	24	900	170
KTDD089_11	0.75	0.09	0.0825	0.0036	0.014018	578	63	510	21	740	280
KTDD089_12	0.617	0.048	0.0791	0.0025	0.17752	480	30	491	15	380	160
KTDD089_13	0.637	0.094	0.0791	0.0047	-0.080825	485	54	490	28	430	300
KTDD089_14	0.619	0.086	0.0806	0.0037	-0.51624	481	55	499	22	370	340
KTDD089_15	0.594	0.072	0.0811	0.0034	0.039606	462	45	502	20	220	230
KTDD089_16	0.615	0.054	0.076	0.0027	0.003425	486	38	472	16	500	220
KTDD089_17	0.64	0.067	0.0783	0.0034	0.09965	493	44	485	20	440	220

Session #2 Unknowns	**207Pb/235U**	**2σ**	**206Pb/238U**	**2σ**	**Rho**	**^{207}Pb/^{235}U Age (Ma)**	**2σ (Ma)**	**^{206}Pb/^{238}U Age (Ma)**	**2σ (Ma)**	**^{207}Pb/^{206}U Age (Ma)**	**2σ (Ma)**
BKDK1_1	0.623	0.013	0.0793	0.001	0.27177	491.4	8.1	493.2	6.3	479	46
BKDK1_2	0.617	0.011	0.07966	0.00092	0.26394	487.4	6.6	494	5.5	458	41
BKDK1_3	0.644	0.018	0.0811	0.0012	0.36476	504	11	502.9	7	521	57
BKDK1_4	0.645	0.013	0.0793	0.001	0.43432	504.8	7.7	492.2	6.1	565	38
BKDK1_5	0.6244	0.0095	0.07921	0.00079	0.32607	492.3	5.9	491.4	4.7	492	33
BKDK1_6	0.654	0.019	0.0846	0.0015	0.45809	511	11	523.7	8.7	478	59
BKDK1_7	0.616	0.01	0.0789	0.00074	0.28804	487.2	6.5	489.5	4.4	470	37
BKDK1_8	0.616	0.01	0.07791	0.00077	0.40748	486.7	6.4	483.6	4.6	495	35
BKDK1_9	0.612	0.024	0.0804	0.0014	0.5918	484	15	498.7	8.4	434	67
BKDK1_10	0.653	0.011	0.0774	0.001	0.47074	510.3	6.6	480.4	6.2	647	33
BKDK1_11	0.659	0.016	0.0782	0.0013	0.50706	513	10	485.4	7.8	646	44
BKDK1_12	0.661	0.014	0.0831	0.0015	0.38803	514.9	8.5	514.3	8.6	522	47
BKDK1_13	0.689	0.029	0.0793	0.0011	0.54556	530	17	492.1	6.6	686	74
BKDK1_14	0.6009	0.0098	0.07806	0.00096	0.59552	477.4	6.2	484.5	5.8	454	28
BKDK1_15	0.6167	0.0095	0.07842	0.00092	0.47477	487.5	5.9	486.6	5.5	489	31
BKDK1_16	0.618	0.016	0.0775	0.0016	0.65278	488	10	481.2	9.5	520	45
BKDK1_17	0.6382	0.0094	0.082	0.0014	0.66684	501	5.9	507.8	8.3	477	28
BKDK1_18	0.721	0.033	0.0839	0.0016	0.41915	550	19	519.4	9.4	693	84
BKDK1_19	0.648	0.013	0.07877	0.00097	0.15806	506.8	8.2	488.8	5.8	583	38
BKDK1_20	0.72	0.018	0.0845	0.0013	0.38836	549	10	523.1	7.6	660	48
BKDK1_21	0.666	0.016	0.0835	0.0013	0.49586	517.6	9.4	516.7	7.7	527	43
BKDK1_22	0.663	0.014	0.07987	0.00083	0.46533	515.6	8.5	495.3	5	602	42
BKDK1_23	0.738	0.038	0.0853	0.0015	0.28987	559	22	527.8	9.2	690	100
BKDK1_24	0.722	0.021	0.0828	0.0014	0.49027	551	13	512.9	8.3	707	53
BKDK1_25	0.608	0.012	0.07805	0.00096	0.42062	481.5	7.7	484.4	5.8	467	42
BKDK1_26	0.617	0.012	0.0805	0.0011	0.46634	487.4	7.5	498.8	6.4	428	38
BKDK1_27	0.718	0.032	0.083	0.001	0.69374	546	17	513.7	6.1	663	61
BKDK1_28	0.666	0.04	0.081	0.0031	0.72185	519	22	501	19	633	67
BKDK1_29	0.676	0.016	0.0851	0.0013	0.52541	523.7	9.6	526.5	7.5	532	37
BKDK1_30	0.723	0.027	0.0778	0.0015	0.49385	551	16	483.1	8.9	848	60
BKDK1_31	0.712	0.016	0.0822	0.0013	0.56395	545.6	9.3	509.4	7.8	702	42
BKDK1_32	0.622	0.011	0.07923	0.00081	0.40898	491	6.9	491.5	4.8	481	36
BKDK1_33	0.661	0.026	0.0807	0.0016	0.92636	517	17	500	9.6	584	50
BKDK1_34	0.754	0.035	0.084	0.0019	0.45012	569	20	520	11	764	82

BKDK1_35	0.723	0.039	0.0817	0.0022	0.95807	549	21	506	13	746	59
BKDK1_36	0.696	0.039	0.0806	0.0019	0.80547	533	22	500	11	689	87
BKDK1_37	0.686	0.021	0.0835	0.00087	0.47462	529	13	516.9	5.2	575	59
BKDK1_38	0.697	0.031	0.0808	0.002	0.83078	536	19	501	12	738	71
BKDK1_39	0.648	0.012	0.0814	0.001	0.42713	507.9	7.7	504.2	6	518	38
BKDK1_40	0.637	0.012	0.078	0.0012	0.57192	499.8	7.7	484.3	7.5	572	35
BKDK1_41	0.644	0.018	0.0799	0.001	0.31251	504	11	495.4	6.2	534	53
BKDK1_42	0.657	0.016	0.08221	0.0008	0.74256	512.2	9.5	509.3	4.8	524	47
BKDK1_43	0.708	0.025	0.0805	0.002	0.34908	543	15	499	12	753	79
BKDK1_44	0.67	0.028	0.0831	0.0028	0.85268	520	17	515	17	562	45
BKDK1_45	0.673	0.019	0.0842	0.0014	0.79753	522	11	521.2	8.5	524	42
BKDK1_46	0.643	0.014	0.0823	0.0011	0.70454	503.6	8.4	509.8	6.4	474	32
BKDK1_47	0.627	0.016	0.08	0.0018	0.86048	495	11	496	10	480	29
BKDK1_48	0.651	0.035	0.0819	0.0016	0.36545	508	21	507.5	9.5	510	110
BKDK1_49	0.61	0.015	0.0787	0.0016	0.78315	483.2	9.1	488.4	9.3	473	30
BKDK1_50	0.644	0.013	0.08052	0.00077	0.34509	504.3	8	499.2	4.6	525	44
BKDK1_51	0.806	0.016	0.0813	0.0012	0.36985	600	9.1	503.9	6.9	984	38
BKDK1_52	0.658	0.013	0.08258	0.00086	0.4195	512.6	7.7	511.5	5.1	511	38
BKDK1_53	0.619	0.013	0.0797	0.00078	0.2366	488.3	8.1	494.3	4.6	451	46
BKDK1_54	no value	NAN	no value	NAN	NaN	no value	NAN	no value	NAN	no value	NAN
BKDK1_55	0.647	0.021	0.0803	0.0016	0.68001	505	13	498	9.7	543	50
BKDK1_56	0.653	0.024	0.0824	0.0021	0.88074	510	14	510	13	529	36
BKDK1_57	0.627	0.031	0.0815	0.0025	0.68801	497	17	505	15	417	83
BKDK1_58	0.619	0.01	0.07942	0.00094	0.2949	488.8	6.4	492.6	5.6	465	37
BKDK1_59	0.638	0.013	0.08091	0.00086	0.48051	500.5	8.1	501.5	5.2	492	38
BKDK1_60	0.6491	0.0095	0.08081	0.00073	0.32708	507.6	5.8	500.9	4.4	534	31
BKDK1_61	0.672	0.014	0.0842	0.0012	0.81797	521.3	8.3	521	7.2	534	38
BKDK1_62	0.6302	0.0097	0.07927	0.00078	0.19601	495.9	6.1	491.7	4.6	508	38
BKDK1_63	0.796	0.025	0.0824	0.0013	0.39136	594	14	510.2	7.9	944	52
BK05_1	0.766	0.027	0.0837	0.0014	0.43319	577	15	518	8.2	830	67
BK05_2	0.635	0.049	0.0782	0.0051	0.85057	493	30	484	30	532	86
BK05_3	0.682	0.02	0.0814	0.0012	0.25438	527	12	504.5	6.9	631	60
BK05_4	0.659	0.021	0.0776	0.0011	0.17239	513	12	481.8	6.5	640	59
BK05_5	0.668	0.017	0.082	0.0013	0.43675	518	11	508.2	7.8	562	50
BK05_6	0.619	0.021	0.0765	0.0025	0.84259	488	14	475	15	550	39
BK05_7	0.782	0.047	0.0759	0.0013	-0.25889	588	27	471.7	7.7	1040	120
BK05_8	0.618	0.023	0.0794	0.0016	0.32247	488	15	492.2	9.5	476	85
BK05_9	0.793	0.037	0.0822	0.0015	0.51973	591	20	509.2	9.1	930	81
BK05_10	1.141	0.055	0.0781	0.0019	0.29393	778	26	485	12	1733	85
BK05_11	0.678	0.056	0.0785	0.0019	0.68407	522	30	487	11	680	110
BK05_12	0.667	0.037	0.0797	0.0018	0.82751	517	21	494	11	599	64
BK05_13	0.717	0.032	0.0835	0.0029	0.59541	548	19	517	17	698	80
BK05_14	0.794	0.045	0.081	0.0017	0.32468	591	26	502	9.9	950	110
BK05_15	0.616	0.016	0.075	0.0016	0.12205	487	10	466.1	9.6	592	66

BK05_16	0.663	0.015	0.0833	0.0012	0.47535	515.9	9.4	515.8	7	528	41
BK05_17	0.647	0.028	0.0795	0.0025	0.73385	506	17	493	15	585	60
BK05_18	0.648	0.025	0.0784	0.0014	0.48214	506	15	486.6	8.5	590	75
BK05_19	0.742	0.031	0.08	0.0024	0.61754	563	18	496	14	857	55
BK05_20	0.631	0.014	0.0798	0.0014	0.49574	496.5	8.8	494.6	8.5	527	51
BK05_21	0.675	0.03	0.0804	0.0014	0.50108	523	18	498.6	8.1	632	76
BK05_22	0.602	0.014	0.0755	0.0014	0.76454	478.3	8.7	469.2	8.3	525	32
BK05_23	0.811	0.038	0.0826	0.0012	0.57478	601	20	511.5	6.9	954	76
BK05_24	0.685	0.023	0.0823	0.0014	0.24711	529	14	510	8.3	611	77
BK05_25	0.633	0.014	0.0785	0.001	0.52396	497.3	8.9	487.2	6.2	544	42
BK05_26	0.616	0.012	0.0759	0.00077	0.34872	487.1	7.7	471.6	4.6	553	42
BK05_27	0.787	0.031	0.0838	0.0015	0.52559	592	19	518.4	9.2	881	73
BK05_28	0.651	0.013	0.07617	0.00081	0.47923	508.8	7.9	473.2	4.8	660	40
BK05_29	0.682	0.02	0.0793	0.0015	0.43863	527	12	491.9	9	663	59
KMT1_1	0.655	0.023	0.084	0.0018	0.60703	511	14	520	10	459	60
KMT1_2	0.646	0.014	0.0789	0.001	0.013044	505.5	8.6	489.4	6	580	53
KMT1_3	0.69	0.022	0.0813	0.0019	0.56777	531	14	503	11	641	57
KMT1_4	0.681	0.049	0.0832	0.0028	0.24667	523	29	515	17	610	140
KMT1_5	0.716	0.021	0.0805	0.0014	0.44441	547	12	499.1	8.5	762	55
KMT1_6	0.654	0.013	0.07837	0.0009	0.24581	510.6	7.7	486.4	5.4	620	43
KMT1_7	0.694	0.039	0.0828	0.0051	0.89312	532	22	512	30	663	74
KMT1_8	0.717	0.071	0.0837	0.0042	0.96264	543	37	518	25	608	67
KMT1_9	0.744	0.068	0.0885	0.0066	0.96573	568	41	545	39	677	72
KMT1_10	0.63	0.018	0.0778	0.0016	0.42888	496	11	482.8	9.6	572	56
KMT1_11	0.656	0.027	0.0818	0.0025	0.84239	511	16	507	15	557	49
KMT1_12	0.634	0.017	0.078	0.0017	0.72176	500	11	484	10	566	42
KMT1_13	0.702	0.046	0.0837	0.0044	0.77135	538	26	518	26	680	100
KMT1_14	0.634	0.015	0.0794	0.0013	0.45195	497.7	9.3	492.3	7.9	521	48
KMT1_15	0.67	0.019	0.0825	0.0017	0.30938	520	11	511	10	559	53
KMT1_16	0.653	0.022	0.0784	0.0012	0.26294	509	13	486.6	7.4	609	58
KMT1_17	0.803	0.032	0.0798	0.0015	0.48607	596	18	494.7	9.1	985	70
KMT1_18	0.662	0.035	0.0805	0.0034	0.83343	519	22	499	20	599	51
KMT1_19	0.634	0.015	0.079	0.0012	0.35081	497.9	9.1	490.4	7.4	535	50
KMT1_20	0.701	0.019	0.0792	0.0013	0.32457	538	12	491.3	7.6	750	57
KMT1_21	0.639	0.015	0.0805	0.0016	0.19853	501.1	9.5	499.3	9.5	538	47
KMT1_22	0.639	0.011	0.0786	0.0011	0.53974	501.2	7.1	487.5	6.4	564	35
KMT1_23	0.712	0.045	0.0825	0.0028	0.46231	543	26	511	17	680	110
KMT1_24	0.72	0.038	0.0835	0.0025	0.011826	548	23	516	15	650	130
KMT1_25	0.612	0.016	0.0768	0.00096	0.28867	485	10	477	5.7	520	57
KMT1_26	0.663	0.028	0.0811	0.0023	0.54474	520	19	503	13	611	54
KMT1_27	0.61	0.017	0.076	0.0015	0.50095	483	11	472.2	8.8	546	56
KMT1_28	0.649	0.031	0.0795	0.0024	0.32477	506	19	493	14	571	92
KMT1_29	no value	NAN	no value	NAN	NaN	no value	NAN	no value	NAN	no value	NAN
KMT1_30	0.608	0.021	0.0767	0.0011	0.25608	480	13	476.5	6.7	480	74

KMT1_31	0.634	0.019	0.0788	0.0014	0.29155	498	11	489.1	8.4	538	67
KMT1_32	0.654	0.023	0.0814	0.0021	0.58103	510	14	504	12	546	65
KMT1_33	0.631	0.017	0.0779	0.0012	0.42667	496	10	483.4	7.4	555	48
KMT1_34	0.635	0.038	0.0809	0.0048	0.2948	498	24	501	28	510	160
KMT1_35	0.682	0.035	0.0816	0.0026	0.87864	526	20	505	15	632	59
KMT1_36	0.707	0.037	0.0897	0.0029	0.64613	542	21	553	17	501	82
KMT1_37	0.633	0.015	0.0787	0.001	0.58617	497.5	9	488.3	6.1	535	40
KMT1_38	0.642	0.017	0.0805	0.0015	0.61519	503	10	498.9	8.6	527	49
KMT1_39	0.699	0.033	0.0854	0.0027	0.29994	537	20	528	16	578	90
KMT1_40	0.668	0.013	0.08028	0.00091	0.4297	518.9	8	497.7	5.4	613	37
KMT1_41	0.623	0.015	0.0788	0.0014	0.82174	491.5	9.6	489.1	8.5	519	46
KMT1_42	0.644	0.014	0.0811	0.0011	0.53199	503.9	8.7	502.8	6.6	508	41
KMT1_43	0.613	0.012	0.0791	0.001	0.22584	484.9	7.4	490.5	6.1	463	43
KMT1_44	0.654	0.017	0.08059	0.00098	0.32224	510	10	499.6	5.8	557	55
KMT1_45	0.6263	0.0094	0.0799	0.0011	0.35186	493.6	5.9	495.7	6.8	490	34
KMT1_46	0.676	0.018	0.0816	0.0011	0.24881	524	11	505.7	6.4	592	59
KMT1_47	0.661	0.016	0.0822	0.0014	0.62711	514.6	9.8	509.2	8.5	539	39
KMT1_48	0.6317	0.0099	0.0805	0.0011	0.35792	496.9	6.2	499.3	6.7	504	39
KMT1_49	0.617	0.015	0.0785	0.0015	0.65361	487.5	9.7	487.3	9.3	499	42
KMT1_50	0.661	0.015	0.081	0.0011	0.24595	514.7	8.8	502	6.4	573	49
KMT1_51	0.697	0.023	0.0836	0.0019	0.5879	536	14	518	11	601	58
KMT1_52	0.667	0.026	0.0835	0.0021	0.80844	517	15	517	13	525	47

APPENDIX H: APATITE U–PB RESULTS

Three apatite U–Pb data sets for the samples BK14, BK25B and BK11 were entirely discounted from interpretations and discussion for perceived unreliability. Samples were noted to have undergone sustained alteration events which may have resulted in some apatite grains existing within an open system, incorporating various sources of common-Pb or developing zonation with grains being too small to discriminate between rims and cores. The logistics of analysing dozens of small apatite grains (generally <200µm) throughout a sample, commonly being limited to a maximum of 4 analyses per grain or less, likely adds significant variability which results in some but not all data sets being unreliable. Samples are observed to contain multiple common-Pb trends and an inadequate spread of data along the fitted line resulting in large uncertainties and anomalously old dates that do not strongly align with known Delamerian Orogeny chronology within the Kanmantoo Cu-Au deposit region.

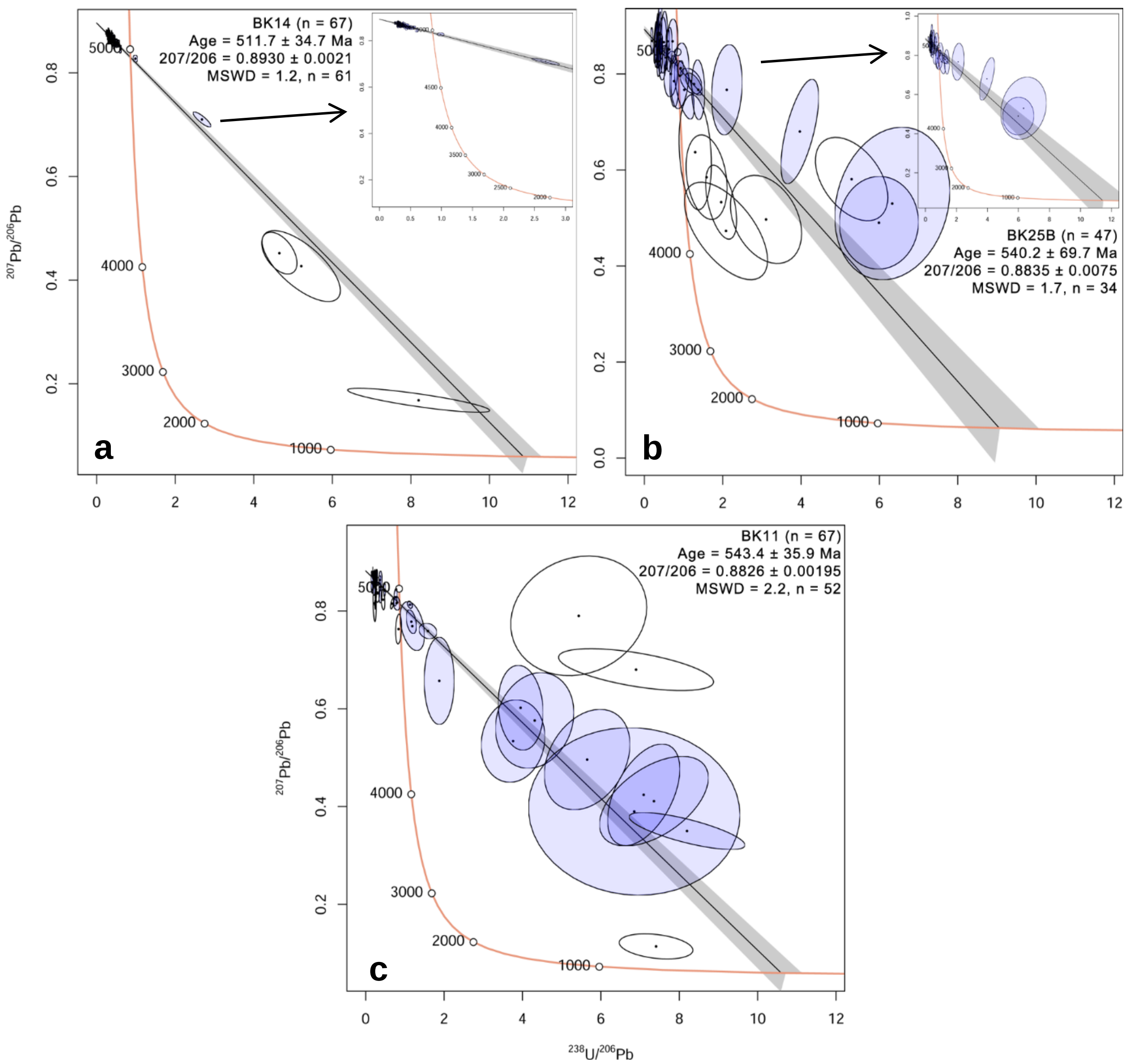

Appendix Figure 17: Terra-Wasserburg concordia diagrams ($^{207}Pb/^{206}Pb$ vs. $^{238}U/^{206}Pb$) for in situ apatite U–Pb analyses conducted on chlorite alteration and felsic vein samples. Not considered in interpretations and discussion due to perceived data unreliability. Blue ellipses used to calculate the quoted age, white ellipses removed from calculations due to excessive discordance or sample contamination, all elipses are presented with 2σ errors on both axes. (a) BK14 - Chlorite alteration. (b) BK25B - Felsic vein. (c) BK11 - Felsic vein.

	^{238}Pb/^{206}U	2σ	^{207}Pb/^{206}Pb	2σ	Rho	207Pb Age (Ma)	2σ (Ma)
Standards:							
A_MAD_1	13.15789	0.5020776	0.0565	0.0046	0.14425	-	-
A_MAD_2	12.82051	0.4930966	0.0554	0.0045	0.054868	-	-
A_MAD_3	13.33333	0.4977778	0.0563	0.0058	0.1216	-	-
A_MAD_4	12.8866	0.4981932	0.0556	0.0051	0.35388	-	-
A_MAD_5	13.29787	0.4951335	0.0588	0.0054	0.33424	-	-
A_MAD_6	13.22751	0.4899079	0.0563	0.0048	0.13843	-	-
A_MAD_7	12.95337	0.5201482	0.0577	0.0057	0.2597	-	-
A_MAD_8	13.38688	0.501784	0.057	0.0058	0.2675	-	-
A_MAD_9	12.57862	0.5537756	0.0609	0.0066	0.0053487	-	-
A_MAD_10	12.8866	0.4815868	0.0587	0.0052	0.29836	-	-
A_MAD_11	13.22751	0.4899079	0.0567	0.0046	0.2883	-	-
A_MAD_12	12.95337	0.4698113	0.0556	0.0057	0.033353	-	-
A_MAD_13	13.35113	0.4991078	0.0591	0.0049	0.43277	-	-
A_MAD_14	13.29787	0.5128169	0.0569	0.0065	0.45293	-	-
A_MAD_15	13.1406	0.5180265	0.056	0.0054	0.23063	-	-
A_MAD_16	12.8041	0.4754402	0.0592	0.0039	0.34022	-	-
A_MAD_17	13.17523	0.5034014	0.0591	0.0049	0.19749	-	-
A_MAD_18	13.02083	0.4916721	0.0583	0.0049	0.14107	-	-
A_MAD_19	13.36898	0.5183162	0.0572	0.0054	0.3234	-	-
A_MAD_20	13.42282	0.522499	0.0542	0.0055	0.45672	-	-
A_MAD_21	13.1406	0.5007589	0.0587	0.0058	0.29338	-	-
A_MAD_22	12.93661	0.4853321	0.0584	0.0061	0.29457	-	-
A_MAD_23	12.95337	0.4865902	0.057	0.005	0.17769	-	-
A_MAD_24	12.83697	0.4778847	0.0578	0.0054	0.15132	-	-
A_MAD_25	13.2626	0.5101	0.0557	0.0053	0.4408	-	-
A_MAD_26	13.31558	0.5141835	0.0579	0.0058	0.40598	-	-
A_MAD_27	13.17523	0.5034014	0.0572	0.0057	0.23079	-	-
A_MAD_28	13.31558	0.496453	0.0566	0.005	0.32109	-	-
A_MAD_29	12.93661	0.4685965	0.0565	0.0047	0.28438	-	-
A_MAD_30	13.0039	0.5073043	0.0558	0.0047	0.31263	-	-
A_MAD_31	13.38688	0.501784	0.0564	0.0052	0.28711	-	-
A_MAD_32	13.38688	0.5197049	0.06	0.0062	0.45954	-	-
A_MAD_33	12.98701	0.5059875	0.0553	0.0052	0.16255	-	-
A_MAD_34	12.97017	0.4878533	0.0577	0.0057	0.18245	-	-
A_McClure_1	11.73709	0.4821574	0.0668	0.0045	0.0087534	522	12
A_McClure_2	11.7096	0.4661902	0.0686	0.0055	0.313	523	12
A_McClure_3	11.60093	0.4979517	0.0623	0.0057	0.066517	529	14
A_McClure_4	11.75088	0.4970996	0.0661	0.0052	-0.048829	520	13

A_McClure_5	11.69591	0.4787798	0.0769	0.005	0.16919	518	13
A_McClure_6	11.96172	0.4721733	0.0668	0.0058	0.15522	510	11
A_McClure_7	12.0048	0.5044034	0.073	0.006	0.23941	505	12
A_McClure_8	11.75088	0.4556746	0.0673	0.0046	0.19899	521	11
A_McClure_9	11.44165	0.4843718	0.0651	0.0053	0.27123	535	15
A_McClure_10	11.73709	0.4683815	0.062	0.005	0.11832	528	11
A_McClure_11	11.89061	0.4807142	0.0621	0.0053	-0.13444	516	12
A_McClure_12	12.07729	0.4813415	0.0658	0.0056	0.36216	512	12
A_McClure_13	12.0048	0.4899919	0.0645	0.0055	0.10342	507	12
A_McClure_14	11.99041	0.4888176	0.0606	0.0052	0.31985	513	14
A_McClure_15	11.8624	0.4925076	0.0671	0.0059	0.1527	511	12
A_McClure_16	12.37624	0.5054652	0.0648	0.0055	0.067994	498	12
A_McClure_17	11.79245	0.4728106	0.0687	0.0063	0.12786	519	12
A_McClure_18	11.77856	0.4855709	0.061	0.0056	0.11623	524	12
A_McClure_19	11.94743	0.5281421	0.0625	0.0053	0.21361	515	15
A_McClure_20	11.66861	0.4629321	0.0674	0.0053	0.38286	524	12
A_McClure_21	11.76471	0.4844291	0.0611	0.0057	0.38097	523	14
A_McClure_22	11.83432	0.4901789	0.0645	0.0047	0.17614	516	13
A_McClure_23	11.94743	0.4995939	0.0642	0.0054	-0.012606	513	13
A_McClure_24	11.90476	0.5102041	0.0692	0.0052	0.28673	517	15
A_McClure_25	11.77856	0.4855709	0.0645	0.006	0.17367	521	13
A_McClure_26	11.69591	0.4651004	0.0717	0.0053	0.40914	515	12
A_McClure_27	11.75088	0.4694829	0.0675	0.0053	0.31872	521	12
A_McClure_28	11.60093	0.5114098	0.066	0.0052	0.2373	523	15
A_McClure_29	11.37656	0.478877	0.0679	0.0058	0.29894	536	15
A_McClure_30	11.73709	0.4821574	0.0636	0.0048	0.24354	519	14
A_McClure_31	11.52074	0.4778186	0.0698	0.0062	0.092498	529	14
A_McClure_32	11.96172	0.5007898	0.0707	0.005	0.26374	508	13
A_McClure_33	11.69591	0.4787798	0.0712	0.0063	0.13227	520	14
A_McClure_34	11.44165	0.4581895	0.0671	0.0064	0.32186	536	13
A_OD306_1	3.688676	0.1347027	0.0995	0.0042	0.40772	1552	25
A_OD306_2	3.687316	0.135963	0.1043	0.0037	0.30591	1536	29
A_OD306_3	3.694126	0.1364657	0.1036	0.0033	0.18794	1529	23
A_OD306_4	3.713331	0.1378883	0.1015	0.0029	0.2771	1528	26
A_OD306_5	3.759398	0.1399175	0.1025	0.0038	0.27274	1513	26
A_OD306_6	3.698225	0.1367687	0.1043	0.0036	0.12566	1532	24
A_OD306_7	3.779289	0.1428303	0.104	0.0035	0.3027	1497	32
A_OD306_8	3.606203	0.130047	0.1037	0.0034	0.19602	1567	26
A_OD306_9	2.725538	0.1039998	0.2095	0.0059	-0.35688	1806	30
A_OD306_10	0.8561644	0.04398105	0.4282	0.0051	-0.56151	3060	230
A_OD306_11	3.706449	0.1373777	0.0984	0.0035	0.35497	1537	26

A_OD306_12	3.667033	0.1344713	0.1007	0.0036	0.14945	1544	27
A_OD306_13	3.724395	0.1387112	0.104	0.0031	0.17615	1523	26
A_OD306_14	3.721623	0.1385047	0.1017	0.0037	0.33048	1521	26
A_OD306_15	3.667033	0.1344713	0.1047	0.0043	0.24213	1541	28
A_OD306_16	3.642987	0.1327136	0.1056	0.0034	0.40546	1550	25
A_OD306_17	3.71471	0.1379907	0.1031	0.0034	0.17699	1525	24
A_OD306_18	3.144654	0.1186662	0.1681	0.0063	-0.38134	1660	30
A_OD306_19	0.9478673	0.04402417	0.4169	0.0048	-0.55264	3350	170
A_OD306_20	1.908397	0.1129013	0.29	0.011	-0.83225	2294	90
A_OD306_21	3.536068	0.1625491	0.1283	0.0093	-0.85846	1559	33
A_OD306_22	3.652301	0.1320591	0.1023	0.0036	0.24614	1557	22
A_OD306_23	3.676471	0.1324611	0.1031	0.0032	0.074335	1535	20
A_OD306_24	3.735525	0.138146	0.1038	0.0033	0.090209	1515	24
A_OD306_25	3.709199	0.1348299	0.1105	0.0034	0.40457	1510	22
A_OD306_26	3.741115	0.1357606	0.102	0.0033	0.1571	1517	22
A_OD306_27	3.284072	0.1186364	0.1469	0.0057	-0.16831	1633	24
A_OD306_28	1.173709	0.07990037	0.3746	0.007	-0.76174	2939	73
A_OD306_29	2.913753	0.1273493	0.195	0.011	-0.52763	1727	40
A_OD306_30	3.615329	0.130706	0.1031	0.0037	0.23084	1564	25
A_OD306_31	3.588088	0.1287437	0.1019	0.0037	0.38137	1570	30
A_OD306_32	2.344666	0.08795933	0.2468	0.0052	0.018265	1990	35
A_OD306_33	3.606203	0.130047	0.1052	0.004	0.27228	1560	26
A_OD306_34	3.616637	0.1308006	0.1015	0.0025	0.11306	1571	25
	$^{238}Pb/^{206}U$	**2σ**	**$^{207}Pb/^{206}Pb$**	**2σ**	**Rho**	**207Pb Age (Ma)**	**2σ (Ma)**
Unknowns:							
BKBDG2_1	0.3660322	0.01607755	0.8663	0.0052	-0.026286	590	95
BKBDG2_2	0.5434783	0.02126654	0.8465	0.0069	0.32532	588	83
BKBDG2_3	0.4970179	0.0239616	0.8527	0.0051	-0.063442	536	63
BKBDG2_4	0.6297229	0.0226034	0.849	0.0072	0.17033	484	79
BKBDG2_5	0.2896871	0.0125878	0.8526	0.0077	0.21352	920	160
BKBDG2_6	0.3453039	0.01311582	0.8687	0.0052	0.21174	600	100
BKBDG2_7	0.4472272	0.01780108	0.857	0.0058	0.20277	562	80
BKBDG2_8	0.4327131	0.01760062	0.8558	0.0059	-0.14272	669	93
BKBDG2_9	0.3759398	0.01370908	0.8725	0.0062	0.39797	520	110
BKBDG2_10	0.4040404	0.01452913	0.8609	0.0049	0.049593	554	80
BKBDG2_11	0.3762227	0.01698522	0.8586	0.0062	-0.19651	684	98
BKBDG2_12	0.4578755	0.01719129	0.8577	0.0068	0.10229	605	96
BKBDG2_13	0.3508772	0.01354263	0.864	0.0058	-0.040688	552	91
BKBDG2_14	0.3134796	0.01179234	0.8655	0.005	-0.01444	657	98
BKBDG2_15	0.3863988	0.01418388	0.8599	0.0051	0.063071	604	93
BKBDG2_16	0.2960332	0.01226899	0.8632	0.0085	0.36953	900	160

BKBDG2_17	0.2857143	0.0155102	0.866	0.006	-0.028866	800	140
BKBDG2_18	0.3627131	0.01315608	0.8651	0.0054	-0.014792	591	81
BKBDG2_19	0.3214401	0.01136561	0.8731	0.0054	0.090454	550	110
BKBDG2_20	1.936108	0.06747328	0.764	0.0098	0.47277	487	40
BKBDG2_21	1.445087	0.05429517	0.7786	0.0088	0.53539	559	50
BKBDG2_22	0.7072136	0.0255077	0.8357	0.007	0.19101	547	70
BKBDG2_23	0.3909304	0.01421287	0.8576	0.007	0.12627	650	100
BKBDG2_24	1.293661	0.05355389	0.7936	0.0099	0.040683	553	56
BKBDG2_25	1.522533	0.0556346	0.7823	0.0095	0.31094	512	48
BKBDG2_26	2.217295	0.1229099	0.7366	0.0076	-0.38829	507	25
BKBDG2_27	1.699813	0.06356601	0.788	0.01	0.32254	439	47
BKBDG2_28	1.633987	0.07742749	0.778	0.011	0.048218	508	50
BKBDG2_29	1.172333	0.05222585	0.7965	0.0097	0.23983	581	62
BKBDG2_30	0.8305648	0.02966303	0.8322	0.0053	0.091188	497	47
BKBDG2_31	0.8149959	0.02988983	0.8377	0.0055	0.12698	481	45
BKBDG2_32	1.55521	0.06046695	0.7832	0.009	0.0079102	512	44
BKBDG2_33	1.745201	0.06700596	0.7749	0.0077	-0.037833	473	32
BKBDG2_34	1.641767	0.05929874	0.7836	0.0094	0.18688	486	48
BKBDG2_35	1.72117	0.06517341	0.765	0.01	0.51692	532	47
BKBDG2_36	0.4308488	0.01577861	0.8613	0.0058	0.15889	592	78
BKBDG2_37	0.8438819	0.03062187	0.8313	0.0053	0.35524	503	48
BKBDG2_38	0.7751938	0.02884442	0.8402	0.0076	0.6646	508	67
BKBDG2_39	0.3790751	0.0135076	0.8604	0.0063	0.11616	670	100
BKBDG2_40	0.7745933	0.02699977	0.842	0.0044	0.40845	442	46
BKBDG2_41	0.7462687	0.02673201	0.8399	0.0065	0.25015	470	64
BKBDG2_42	0.8216927	0.02903269	0.8341	0.0055	0.43408	488	51
BKBDG2_43	0.8077544	0.02936103	0.8322	0.0063	0.32887	526	58
BKBDG2_44	1.230012	0.05597842	0.8052	0.0076	0.1099	511	56
BKBDG2_45	0.6887052	0.02466437	0.8422	0.0068	0.3578	515	61
BKBDG2_46	0.3892565	0.01454598	0.8623	0.0065	0.23038	659	90
BKBDG2_47	0.8503401	0.03036929	0.8323	0.007	0.2418	486	61
BKBDG2_48	0.3344482	0.02125256	0.87	0.012	0.014221	750	200
BKBDG2_49	0.7898894	0.03618767	0.8297	0.0079	0.15344	541	75
BKBDG2_50	0.8312552	0.03178532	0.8319	0.0072	0.69559	508	70
BKBDG2_51	0.7541478	0.02729947	0.8477	0.007	0.0035326	432	65
BKBDG2_52	0.4032258	0.02764048	0.851	0.011	0.19095	880	150
BK11_1	0.2298851	0.01004096	0.87	0.0082	0.12937	900	240
BK11_2	1.128668	0.05095567	0.8127	0.006	-0.3514	461	34
BK11_3	0.2666667	0.01635556	0.869	0.012	0.047796	980	180
BK11_4	0.2531646	0.01153661	0.8622	0.0083	0.020882	1000	190
BK11_5	7.407407	0.7681756	0.114	0.021	-0.30373	730	67

BK11_6	0.2724796	0.01484902	0.872	0.011	0.2108	970	180
BK11_7	0.2403846	0.01271265	0.861	0.012	0.33709	1160	260
BK11_8	1.587302	0.1864449	0.759	0.013	-0.18228	565	70
BK11_9	0.1754386	0.007386888	0.8736	0.0071	0.20652	870	250
BK11_10	0.2118644	0.01122163	0.871	0.01	0.59476	1240	310
BK11_11	0.2295684	0.008959281	0.8637	0.0075	0.10812	910	170
BK11_12	0.2300437	0.008996418	0.8621	0.0068	0.14835	1020	190
BK11_13	0.228833	0.009425614	0.8646	0.0072	0.060628	790	190
BK11_14	0.2890173	0.01921214	0.868	0.014	-0.14752	890	230
BK11_15	0.3649635	0.02131174	0.8633	0.0077	-0.1158	610	120
BK11_16	0.1831502	0.008050558	0.878	0.01	0.006859	1190	280
BK11_17	0.2114165	0.01028029	0.87	0.01	0.083659	1110	270
BK11_18	0.243309	0.01183985	0.8628	0.0071	0.11117	870	180
BK11_19	0.2375297	0.01354089	0.8529	0.0093	-0.59255	1160	210
BK11_20	0.2409639	0.01103208	0.8128	0.0077	-0.26804	1770	210
BK11_21	0.2020202	0.01061116	0.865	0.011	-0.13476	1060	230
BK11_22	0.2155172	0.01161192	0.863	0.012	-0.16507	1340	320
BK11_23	1.164144	0.1070633	0.778	0.02	-0.38121	710	110
BK11_24	0.2570694	0.01586032	0.836	0.012	0.31891	1270	250
BK11_25	0.7874016	0.07440015	0.816	0.012	-0.24576	590	90
BK11_26	0.2298851	0.03170828	0.816	0.031	-0.15963	1710	440
BK11_27	0.1964637	0.008877533	0.8705	0.0078	0.48244	1070	250
BK11_28	0.2475248	0.01592981	0.851	0.011	0.25805	1000	290
BK11_29	0.1869159	0.008035636	0.8753	0.0063	0.30349	950	200
BK11_30	0.2702703	0.01241782	0.86	0.012	0.31099	940	210
BK11_31	0.3039514	0.04249776	0.836	0.015	0.069417	1290	230
BK11_32	0.210084	0.01103383	0.866	0.013	0.33967	890	210
BK11_33	5.649718	0.8937406	0.496	0.084	0.30202	566	91
BK11_34	0.4833253	0.02195871	0.843	0.011	0.23252	790	160
BK11_35	0.2842524	0.01211992	0.8708	0.0057	0.24525	630	120
BK11_36	0.4405286	0.0388131	0.823	0.017	-0.31664	1110	190
BK11_37	0.838223	0.06183036	0.763	0.025	0.1772	1170	180
BK11_38	7.352941	1.135381	0.411	0.075	0.5191	485	70
BK11_39	3.952569	0.4686841	0.602	0.071	-0.10534	570	110
BK11_40	5.434783	1.417769	0.79	0.1	0.14224	285	80
BK11_41	6.849315	2.204916	0.39	0.14	-0.045001	563	86
BK11_42	1.190476	0.255102	0.769	0.041	-0.37187	750	190
BK11_43	0.2132196	0.02591368	0.852	0.017	0.12091	1190	330
BK11_44	0.2630887	0.01038235	0.844	0.0082	0.22575	1100	160
BK11_45	0.6775068	0.03442616	0.8149	0.0088	0.57273	710	110
BK11_46	8.196721	1.209352	0.35	0.031	-0.76143	451	48
BK11_47	6.896552	1.617122	0.68	0.035	-0.58508	190	39

BK11_48	0.3773585	0.03987184	0.849	0.027	0.078395	1110	300
BK11_49	1.876173	0.3132821	0.657	0.073	-0.005046	910	170
BK11_50	7.092199	0.7544892	0.424	0.085	0.50297	594	92
BK11_51	0.7633588	0.03612843	0.828	0.015	0.34055	660	120
BK11_52	4.310345	0.8174792	0.576	0.08	0.16444	590	120
BK11_53	3.759398	0.6642546	0.534	0.069	0.10018	690	150
BK11_54	0.2475248	0.01286639	0.858	0.012	-0.21745	1110	270
BK11_55	0.2277904	0.01400989	0.864	0.01	0.039697	1110	220
BK11_56	0.1926782	0.007796229	0.8671	0.0063	-0.055872	1020	190
BK11_57			no value	NAN	NaN	no value	NAN
BK11_58	0.2849003	0.01298691	0.8632	0.0056	0.2233	680	130
BK11_59	0.22119	0.008806503	0.8664	0.0056	0.29702	840	150
BK11_60	0.2868617	0.01234345	0.8679	0.009	0.043853	710	150
BK11_61	0.2848191	0.01135707	0.8634	0.0063	0.19422	690	120
BK11_62	0.2380952	0.01247166	0.8628	0.0073	0.42312	950	200
BK11_63	0.1650165	0.02505201	0.859	0.019	-0.18811	1100	310
BK11_64	0.2332634	0.009250005	0.8763	0.0074	0.0088769	720	190
BK14_1	0.3030303	0.01836547	0.872	0.011	0.52762	840	220
BK14_2	0.3039514	0.01662956	0.867	0.01	0.25598	990	220
BK14_3			no value	NAN	NaN	no value	NAN
BK14_4	0.2933412	0.01204686	0.8708	0.007	0.24946	720	140
BK14_5	4.651163	0.3677664	0.452	0.033	-0.48084	652	51
BK14_6	0.3449465	0.01427857	0.8703	0.006	0.41115	600	100
BK14_7	0.3083565	0.01141004	0.8776	0.0066	-0.29778	610	130
BK14_8	0.3404835	0.01275219	0.8644	0.0077	0.21095	800	150
BK14_9	0.3881988	0.01461773	0.8677	0.0057	0.040816	577	89
BK14_10	0.4145937	0.01632935	0.8592	0.0072	0.47226	700	100
BK14_11	0.456621	0.01688872	0.8647	0.0064	0.080597	565	96
BK14_12	0.25	0.009375	0.8754	0.0048	0.32103	650	120
BK14_13	0.3637686	0.01455604	0.8683	0.0083	0.073533	780	140
BK14_14	0.6056935	0.02237874	0.8455	0.0066	0.20919	612	79
BK14_15	0.4132231	0.01485554	0.8643	0.0061	0.18234	620	100
BK14_16	0.3303601	0.01200516	0.8761	0.0057	0.42366	630	110
BK14_17	2.680965	0.1868769	0.71	0.012	-0.85878	505	16
BK14_18	0.29036	0.01096016	0.8652	0.0055	0.20978	790	120
BK14_19	0.4793864	0.01746566	0.8582	0.0054	0.042928	575	84
BK14_20	0.2909514	0.01100485	0.8724	0.006	0.15522	750	130
BK14_21	0.3277614	0.01396558	0.8667	0.0084	0.32907	810	180
BK14_22	0.9861933	0.04765628	0.8274	0.0058	-0.085767	505	45
BK14_23	0.3521127	0.01363817	0.8705	0.0062	0.39423	640	120
BK14_24	0.4068348	0.01506183	0.8706	0.0057	0.4193	552	95

BK14_25	0.4683841	0.01908638	0.8568	0.0065	0.20979	630	95
BK14_26	0.3376097	0.01253784	0.8688	0.0067	0.14789	760	100
BK14_27	0.3331113	0.01331557	0.8726	0.0068	0.33497	690	120
BK14_28	0.328084	0.01399308	0.8728	0.0083	0.16221	730	150
BK14_29	0.3619254	0.0144089	0.8651	0.0071	0.31878	780	130
BK14_30	0.3710575	0.01376837	0.8674	0.0071	0.12145	710	120
BK14_31	0.297885	0.01153561	0.8763	0.0068	0.098328	700	130
BK14_32	8.196721	1.478097	0.168	0.019	-0.84428	638	85
BK14_33	5.208333	0.8138021	0.427	0.056	-0.69062	635	96
BK14_34	0.3022061	0.01095942	0.8722	0.0051	0.0020478	640	110
BK14_35	0.2738226	0.01049703	0.8757	0.0064	-0.034198	840	140
BK14_36	0.2983294	0.01157005	0.8701	0.0066	0.3286	870	140
BK14_37	0.2936858	0.01121267	0.8677	0.0068	0.31032	910	140
BK14_38	0.4163197	0.01733221	0.8628	0.0056	0.12588	569	93
BK14_39	0.3256268	0.01272394	0.8721	0.0073	0.3832	780	150
BK14_40	0.2924832	0.01026557	0.8758	0.0081	0.27776	900	160
BK14_41	0.3119152	0.01167493	0.8659	0.0058	0.10196	770	120
BK14_42	0.3167564	0.01204016	0.874	0.007	0.23388	740	140
BK14_43	0.3865481	0.01464311	0.8709	0.0069	0.14563	620	110
BK14_44	0.4409171	0.01788553	0.8667	0.0062	0.059545	582	95
BK14_45	0.3773585	0.01367035	0.8735	0.0072	0.33083	650	120
BK14_46	0.3042288	0.01110662	0.873	0.0061	0.012714	790	120
BK14_47	0.391696	0.0148823	0.8642	0.0053	0.30026	638	94
BK14_48	0.5621135	0.02053816	0.8561	0.0059	0.31772	552	69
BK14_49	0.4761905	0.01746032	0.8601	0.0052	0.2238	589	74
BK14_50	0.5050505	0.0181104	0.8567	0.0071	0.30494	608	90
BK14_51	0.3780718	0.01415089	0.8656	0.0068	0.19076	690	120
BK14_52	0.5344735	0.01942501	0.8564	0.0066	0.27934	561	83
BK14_53	0.4016064	0.01499976	0.8649	0.006	0.22689	640	100
BK14_54	0.3709199	0.01375816	0.8641	0.0054	0.36458	651	92
BK14_55	0.4985045	0.01814099	0.8587	0.0063	0.32945	593	81
BK14_56	0.5530973	0.01988458	0.8574	0.0051	0.2819	520	66
BK14_57	0.4366812	0.016018	0.8541	0.007	0.31949	760	110
BK14_58	0.335233	0.01236193	0.8649	0.0066	0.226	780	110
BK14_59	0.4496403	0.01657846	0.8583	0.0058	0.23586	642	89
BK14_60	0.2972652	0.01148765	0.8801	0.0059	0.21156	610	110
BK14_61	0.24667	0.00912691	0.8784	0.0044	0.32149	690	110
BK14_62	0.2780868	0.01005319	0.876	0.0049	0.073791	650	110
BK14_63	0.3741115	0.01385598	0.8684	0.0061	0.3872	640	110
BK14_64	0.3926188	0.01449005	0.8642	0.0068	0.27309	750	110
BK14_65	0.3163556	0.0120097	0.8699	0.0063	0.23518	760	120

BK18_1	4.719207	0.267251	0.606	0.032	0.44998	469	55
BK18_2	7.407407	0.8230453	0.435	0.053	-0.7564	391	30
BK18_3	6.666667	0.6222222	0.494	0.055	0.60844	509	80
BK18_4	0.1388889	0.007137346	0.8816	0.0044	-0.045493	680	180
BK18_5	0.3636364	0.02644628	0.849	0.012	0.17719	980	220
BK18_6	0.07412898	0.003132211	0.8795	0.0058	0.22179	1210	390
BK18_7	0.1968504	0.009687519	0.8719	0.0058	0.16779	910	160
BK18_8	4.508566	0.243926	0.61	0.028	0.29008	452	50
BK18_9	4.18235	0.1749206	0.62	0.016	0.42058	485	37
BK18_10	4.366812	0.2478976	0.594	0.031	-0.0080473	483	55
BK18_11	0.2666667	0.01564444	0.8758	0.0078	-0.098074	640	170
BK18_12	0.1631321	0.01303993	0.8769	0.0061	-0.4647	1080	230
BK18_13	3.731343	0.2923814	0.638	0.022	-0.43727	454	45
BK18_14	6.21118	0.3356352	0.497	0.024	0.38113	466	42
BK18_15	0.3816794	0.03350621	0.8582	0.0078	-0.56424	620	120
BK18_16	0.6578947	0.07358033	0.83	0.012	-0.16463	640	110
BK25B_1	0.4314064	0.02233338	0.8626	0.0096	-0.059929	580	160
BK25B_2	0.4462294	0.02190327	0.846	0.013	0.10257	760	140
BK25B_3	0.3773585	0.0256319	0.844	0.016	-0.099027	950	230
BK25B_4	0.3401361	0.02545236	0.876	0.023	0.021446	1280	320
BK25B_5	5.291005	0.7558579	0.581	0.071	-0.44084	427	68
BK25B_6	0.3717472	0.04007684	0.882	0.039	0.7325	1510	300
BK25B_7	1.020408	0.2082466	0.767	0.05	-0.60552	660	140
BK25B_8	1.190476	0.2267574	0.785	0.022	-0.39236	518	94
BK25B_9	0.6756757	0.1415267	0.8	0.039	0.14925	1030	230
BK25B_10	0.3952569	0.05155525	0.885	0.06	0.36769	1360	510
BK25B_11	0.7575758	0.09756657	0.785	0.044	-0.11501	1110	220
BK25B_12	1.298701	0.337325	0.637	0.098	-0.20449	680	140
BK25B_13	1.960784	0.3229527	0.533	0.063	-0.49848	970	150
BK25B_14	5.988024	0.8246979	0.49	0.079	0.014618	518	92
BK25B_15	0.9090909	0.1900826	0.796	0.056	0.19944	1090	300
BK25B_16	0.462963	0.09430727	0.853	0.054	0.079313	930	400
BK25B_17	3.10559	0.7426411	0.497	0.075	-0.31831	709	94
BK25B_18	2.083333	0.8680556	0.473	0.083	-0.59756	650	130
BK25B_19	0.3773585	0.04556782	0.848	0.027	0.14971	1140	330
BK25B_20	0.4975124	0.07673077	0.866	0.053	0.26694	1500	320
BK25B_21	3.968254	0.393676	0.68	0.089	0.65152	710	120
BK25B_22	6.329114	1.20173	0.53	0.13	0.1698	525	99
BK25B_23	0.5938242	0.03878899	0.868	0.021	0.25934	870	220
BK25B_24	0.9276438	0.06023661	0.812	0.013	0.10741	589	99
BK25B_25	0.7194245	0.1138657	0.868	0.038	0.10386	1070	230

BK25B_26	0.2808989	0.03629592	0.858	0.03	0.24997	1320	380
BK25B_27	0.6369427	0.0608544	0.851	0.038	0.1665	1260	300
BK25B_28	0.3389831	0.03447285	0.884	0.029	0.44291	980	320
BK25B_29	2.105263	0.3191136	0.767	0.077	0.16211	880	190
BK25B_30	1.265823	0.1762538	0.779	0.019	-0.63168	516	57
BK25B_31	1.587302	0.4283195	0.585	0.072	-0.25135	840	190
BK25B_32	0.1930502	0.02608786	0.869	0.023	-0.18201	1270	270
BK25B_33	0.5494505	0.04226543	0.834	0.023	0.23314	1150	230
BK25B_34	1.375516	0.1381192	0.767	0.051	-0.1041	930	200
BK25B_35	0.3095975	0.03546473	0.861	0.039	0.2199	1500	460
BK25B_36	0.3378378	0.03424032	0.88	0.038	0.30453	1600	420
BK25B_37	0.3021148	0.04198574	0.867	0.035	0.19828	1320	340
BK25B_38	0.4201681	0.04236989	0.842	0.034	0.26254	1370	330
BK25B_39	0.3412969	0.03145057	0.85	0.032	0.35185	1490	370
BK25B_40	0.3597122	0.03364215	0.826	0.026	0.02992	1560	330
KTDD089_1	2.28833	0.1466207	0.72	0.024	0.30651	524	78
KTDD089_2	1.369863	0.2064177	0.751	0.061	0.45855	700	170
KTDD089_3	1.046025	0.04704925	0.8179	0.0047	-0.38435	474	29
KTDD089_4	0.727802	0.03072236	0.8371	0.0061	0.096964	499	59
KTDD089_5	1.113586	0.04216249	0.8083	0.0078	0.11201	510	53
KTDD089_6	1.214772	0.04279443	0.8137	0.0052	0.28053	429	33
KTDD089_7	0.9635768	0.03342529	0.8298	0.0048	0.22416	423	38
KTDD089_8	0.9775171	0.03535497	0.8277	0.005	-0.24073	437	38
KTDD089_9	0.81103	0.05393711	0.829	0.018	0.23391	690	150
KTDD089_10	0.3558719	0.02786186	0.852	0.018	0.18774	1380	230
KTDD089_11	0.7604563	0.02717981	0.8367	0.0048	0.15179	463	46
KTDD089_12	0.8136697	0.0317788	0.8334	0.0043	-0.1795	470	37
KTDD089_13	0.8169935	0.03137148	0.8237	0.0056	0.12006	547	53
KTDD089_14	0.8183306	0.03214392	0.8411	0.0047	0.23641	397	45
KTDD089_15	0.5824112	0.02272659	0.8482	0.0063	0.31602	473	81
KTDD089_16	0.7627765	0.03025506	0.8302	0.0053	0.088424	521	53
KTDD089_17	1.126126	0.0507264	0.81	0.011	-0.10094	497	62
KTDD089_18	0.7836991	0.04790637	0.8286	0.0053	0.10725	521	56
KTDD089_19	0.8389262	0.03659745	0.8319	0.0044	0.010262	456	36
KTDD089_20	0.990099	0.04607391	0.8204	0.0072	-0.022374	477	60
KTDD089_21	7.70416	0.5935409	0.485	0.055	0.25193	426	58
KTDD089_22	0.7347539	0.02537357	0.843	0.0032	0.20646	426	35
KTDD089_23	0.8103728	0.02889498	0.835	0.0047	0.1242	482	38
KTDD089_24	0.8920607	0.03103512	0.8242	0.0039	0.34924	498	35
KTDD089_25	2.193945	0.08664108	0.7366	0.0084	-0.60739	504	25
KTDD089_26	0.7132668	0.02899872	0.8263	0.0086	0.31599	662	93

KTDD089_27	0.838223	0.02950995	0.8359	0.0041	0.22434	422	35
KTDD089_28	1.74216	0.07587806	0.7651	0.0052	0.59744	513	37
KTDD089_29	1.166861	0.0503779	0.8305	0.0061	-0.032428	346	40
KTDD089_30	9.033424	0.7262644	0.338	0.047	-0.07081	463	40
KTDD089_31	4.149378	0.2926947	0.644	0.033	0.23661	464	59
KTDD089_32	0.8688097	0.03094804	0.8334	0.004	0.056066	446	36
KTDD089_33	7.633588	0.6992599	0.396	0.063	0.26069	449	71
KTDD089_34	1.322751	0.08398421	0.7891	0.0057	-0.68252	506	21
KTDD089_35	0.792393	0.02888279	0.8375	0.0044	0.042846	450	39
KTDD089_36	0.7861635	0.02719434	0.8322	0.0035	0.22756	497	34
KTDD089_37	1.158749	0.1101013	0.765	0.023	-0.26639	734	96
KTDD089_38	0.78125	0.03479004	0.825	0.011	-0.26682	562	80
KTDD089_39	1.219512	0.05353956	0.7966	0.0087	0.45419	536	63
KTDD089_40	0.5473454	0.02965911	0.837	0.016	0.2944	740	130
KTDD089_41	0.7824726	0.04408296	0.8278	0.0082	-0.13201	556	75
KTDD089_42	0.8058018	0.03051788	0.831	0.0074	0.29151	534	63
KTDD089_43	1.068376	0.0376671	0.8216	0.006	0.26502	439	44
KTDD089_44	1.112966	0.0383995	0.8171	0.0053	0.39828	453	37
KTDD089_45	1.472754	0.07591516	0.7919	0.0054	-0.4569	458	21
KTDD089_46	0.9041591	0.03351765	0.8295	0.005	0.22067	458	41
KTDD089_47	1.014199	0.09051673	0.785	0.024	0.60356	820	150
KTDD089_48	0.5955926	0.03440886	0.823	0.013	0.47993	810	190
KTDD089_49	1.831502	0.117404	0.766	0.0053	-0.71304	468	18
KTDD089_50	0.7722008	0.0399517	0.822	0.016	0.19804	610	110
KTDD089_51	0.5988024	0.03944207	0.82	0.016	0.22237	860	210
KTDD089_52	0.911577	0.03157696	0.8192	0.0074	0.32467	534	57
KTDD089_53	0.7656968	0.0275557	0.8354	0.007	0.042014	507	62
KTDD089_54	1.329787	0.09018504	0.8048	0.0072	-0.65153	420	27
KTDD089_55	0.8291874	0.03162738	0.853	0.013	0.44652	425	71
KTDD089_56	0.8764242	0.03226101	0.8275	0.0073	0.12895	471	56
KTDD089_57	0.7102273	0.03430075	0.824	0.013	0.41157	650	130
KTDD089_58	1.197605	0.1434257	0.782	0.031	0.15358	790	160

APPENDIX I: EXTENDED LA-ICP-MS TRACE ELEMENTS METHODS

Laser Ablation Inductively Coupled Plasma Mass Spectrometry (LA-ICP-MS) was conducted using the Agilent 7900x with attached RESOlution LR 193 nm Excimer laser system at Adelaide Microscopy, University of Adelaide. A total of twelve individual samples were analysed for monazite trace elements (ten samples) and apatite trace elements (seven samples) through in situ laser ablation simultaneously to U–Pb geochronology data collection. Analyses were taken at a fluence of 2.0 J/cm^2 and 3.5 J/cm^2 and spot size of 13µm and 40 µm respectively for monazite and apatite. SEM-BSE composite images were utilised to locate datable minerals of sufficient area for ablation. Where possible, spots were taken from across the entirety of the sample including within vein sets, sulphides and adjacent altered host rock. Data reduction for trace elements followed the same method as used for U–Pb analyses (Appendix F) with the X_Trace_Elements_IS DRS used in place of the X_U_Pb_Geochron4 DRS.

External standard NIST SRM610 was used to correct for elemental fractionation and mass bias across all analyses: P = 413 ± 46 ppm, La = 440 ± 10 ppm and Lu = 439 ± 8 ppm (Jochum et al. 2011).

APPENDIX J: MONAZITE TRACE ELEMENTS RESULTS

	Y (ppm)	2σ	La (ppm)	2σ	Pr (ppm)	2σ	Nd (ppm)	2σ	Sm (ppm)	2σ	Eu (ppm)	2σ	Gd (ppm)	2σ
Session #1 Standard:														
NIST610 - 1	203000	1300	203000	1300	193600	1200	198000	1200	190400	1300	199100	1900	197340	960
NIST610 - 2	204800	1200	204800	1200	194700	1000	197660	920	189200	1400	200800	1700	197400	1000
NIST610 - 3	204100	1200	204100	1200	194800	1000	198390	930	190600	1400	200600	1500	197900	1200
NIST610 - 4	203700	1100	203700	1100	193600	1100	196500	1200	188900	1600	199100	1500	196700	1200
NIST610 - 5	203200	1300	203200	1300	193840	970	198000	1100	190200	1700	199700	1600	197500	1100
NIST610 - 6	204700	1200	204700	1200	194700	1000	197970	990	189700	1300	201300	1700	197200	1100
NIST610 - 7	203700	1100	203700	1100	194100	1000	197810	830	190400	1400	200500	1700	197900	1000
NIST610 - 8	204300	1200	204300	1200	194500	1100	197300	1200	189200	1300	198500	1500	196700	1100
NIST610 - 9	204400	1000	204400	1000	194670	950	198700	1100	191200	1400	201000	1600	198200	1100
NIST610 - 10	203600	1000	203600	1000	193800	1000	197100	1100	188700	1400	200100	1500	196600	1100
NIST610 - 11	203500	1200	203500	1200	193500	1100	197300	1200	190000	1400	200600	1700	198100	1000
NIST610 - 12	204500	1300	204500	1300	194800	1000	198200	1100	189500	1700	199100	1800	196670	960
NIST610 - 13	203700	1200	203700	1200	193700	1100	197420	870	189500	1200	200300	1600	197300	1100
NIST610 - 14	204000	1100	204000	1100	194700	1000	198300	1100	190200	1400	199400	1700	197500	1100
NIST610 - 15	203800	1300	203800	1300	194200	1100	198300	1100	191100	1400	200400	1700	197300	1100
NIST610 - 16	204240	960	204240	960	194300	1000	197510	910	189100	1100	200100	1500	197380	860
NIST610 - 17	203000	1000	203000	1000	193810	990	197300	1200	189500	1200	199100	1200	197490	920
NIST610 - 18	204780	980	204780	980	194800	900	198110	960	190000	1200	200600	1500	197200	900
NIST610 - 19	204200	1200	204200	1200	194150	850	198500	1100	190400	1500	200100	1800	198090	920
NIST610 - 20	203800	1100	203800	1100	194370	880	197370	920	189300	1700	200400	1700	196500	1000
NIST610 - 21	204000	1100	204000	1100	194780	950	198010	870	189800	1400	199800	1700	197610	880
NIST610 - 22	203800	1200	203800	1200	193600	1100	197400	1000	189800	1700	199600	1500	197080	920
NIST610 - 23	204600	1100	204600	1100	194900	1200	197880	910	189500	1600	200800	1300	197620	970
NIST610 - 24	203400	1200	203400	1200	193500	1300	197800	1200	190300	1700	200200	1800	197100	1200
NIST610 - 25	204300	1200	204300	1200	194440	950	197780	900	189500	1500	199500	1800	197610	830
NIST610 - 26	203800	1000	203800	1000	194100	930	197770	970	190200	1500	199700	1600	197010	980

	Tb (ppm)	2σ	Dy (ppm)	2σ	Ho (ppm)	2σ	Er (ppm)	2σ	Tm (ppm)	2σ	Yb (ppm)	2σ	Lu (ppm)	2σ
NIST610 - 1	193020	960	193200	1200	198500	1000	201200	1100	192400	1100	199500	1500	194200	1100
NIST610 - 2	192860	830	192780	940	198050	840	200600	1000	191700	1000	198100	1200	193500	1000

NIST610 - 3	193500	1100	193800	1300	198700	1100	202500	1300	192800	1200	199500	1300	194800	1100
NIST610 - 4	192300	1200	192100	1300	197800	1000	199700	1100	191500	1100	197700	1300	192600	1200
NIST610 - 5	193160	910	193400	1300	198300	1000	201500	1300	192310	990	199100	1100	194300	1100
NIST610 - 6	192690	960	192600	1100	198100	1200	200400	1200	191700	1100	198200	1200	193300	1200
NIST610 - 7	193550	930	193200	1000	198740	910	201300	1000	192410	890	199400	1200	194300	1000
NIST610 - 8	192240	980	192600	1200	197690	920	200200	1100	191400	1100	198000	1100	193360	930
NIST610 - 9	193810	970	194000	1100	199050	880	201400	1100	193000	1100	199400	1100	194410	960
NIST610 - 10	192320	880	192100	1000	197000	1100	200400	1100	191360	950	197500	1300	193200	1000
NIST610 - 11	193000	1000	193300	1100	199000	1100	200900	1200	192400	1100	198200	1100	194300	1200
NIST610 - 12	192940	850	192600	1100	197670	990	200900	1100	191700	1100	199100	1100	193480	950
NIST610 - 13	192900	1100	193300	1200	198200	1000	200860	920	192260	830	198600	1100	194260	920
NIST610 - 14	192920	950	192660	990	198300	1000	200900	1100	191770	960	198800	1300	193500	920
NIST610 - 15	193700	1100	193500	1100	198100	1100	201100	1100	192200	1100	199100	1200	194000	1200
NIST610 - 16	192420	890	192510	960	198320	890	200600	1300	191960	820	198300	1000	193700	1000
NIST610 - 17	192980	960	193300	1100	198050	950	200900	1100	191910	820	198700	1100	193700	1100
NIST610 - 18	192900	890	192600	1100	198400	1000	200900	1100	192200	1000	198700	1300	193910	800
NIST610 - 19	193500	1000	193500	1200	198200	990	201300	1200	192330	970	198680	960	194050	790
NIST610 - 20	192580	810	192400	1100	198300	1200	200400	1300	191800	1000	198600	1200	193400	1100
NIST610 - 21	193400	870	193500	1000	198670	870	201300	1100	192440	970	199100	1100	194290	900
NIST610 - 22	192400	1000	192300	1100	197500	1100	200200	1300	191500	1000	198300	1100	193100	1100
NIST610 - 23	193050	870	193100	1200	198580	900	201200	1000	192680	940	199200	1100	194000	1000
NIST610 - 24	192820	890	192850	920	197800	1100	200400	1200	191200	1100	198200	1100	193700	1000
NIST610 - 25	193080	850	193100	1200	198400	1000	201260	980	192390	790	198800	1100	194020	890
NIST610 - 26	192770	960	192800	1000	198100	1000	200400	1100	191550	980	198500	1100	193600	960

	Th (ppm)	**2σ**	**U (ppm)**	**2σ**
NIST610 - 1	202500	1200	204200	1100
NIST610 - 2	201500	1100	203300	1100
NIST610 - 3	202900	1200	204800	1100
NIST610 - 4	201000	1100	202900	1100
NIST610 - 5	202300	1200	204130	910
NIST610 - 6	201500	1200	203100	1200
NIST610 - 7	202200	1100	204350	930
NIST610 - 8	201200	1400	202900	1100
NIST610 - 9	202900	1300	204500	1100

NIST610 - 10	200700	1300	203000	1100
NIST610 - 11	202300	1200	204100	1200
NIST610 - 12	201500	1200	203400	1200
NIST610 - 13	201800	1100	204100	1200
NIST610 - 14	201900	1200	203300	1200
NIST610 - 15	202000	1400	204200	1300
NIST610 - 16	201800	1100	203530	950
NIST610 - 17	201900	1000	203840	970
NIST610 - 18	201800	1000	203700	1000
NIST610 - 19	202200	1100	204210	930
NIST610 - 20	201400	1000	203500	1100
NIST610 - 21	202100	1100	204100	990
NIST610 - 22	201500	1300	203200	1200
NIST610 - 23	202200	1200	204200	1100
NIST610 - 24	201600	1100	203400	1100
NIST610 - 25	202200	1000	204000	1100
NIST610 - 26	201500	1100	203500	1100

	Y (ppm)	**2σ**	**La (ppm)**	**2σ**	**Pr (ppm)**	**2σ**	**Nd (ppm)**	**2σ**	**Sm (ppm)**	**2σ**	**Eu (ppm)**	**2σ**	**Gd (ppm)**	**2σ**
Session #2 Standard:														
NIST610 - 1	203500	1100	194500	1100	197600	1100	190900	1400	199100	1700	197700	980	198700	1700
NIST610 - 2	204700	1100	194570	980	198290	970	189700	1400	200700	1600	197490	960	198800	1500
NIST610 - 3	203800	1100	194200	1000	197550	980	189800	1300	200800	1700	197250	870	198200	1600
NIST610 - 4	204200	1000	193940	930	197510	990	190400	1400	199500	1400	197060	840	198000	1500
NIST610 - 5	202900	1100	193700	1100	197400	1100	189400	1300	200500	1500	196800	1200	196400	1600
NIST610 - 6	203500	1300	194700	1300	198200	1100	189300	1500	200000	1500	197400	1100	197900	1600
NIST610 - 7	204800	1200	194400	1100	198390	920	189600	1500	200000	1500	197200	1100	198800	1900
NIST610 - 8	204800	1100	194850	860	198200	930	190800	1600	201000	1700	197700	960	197000	1600
NIST610 - 9	203400	1100	194300	900	198600	1100	190400	1400	200400	1500	197680	930	198600	1900
NIST610 - 10	204400	1100	193800	1000	197230	930	189100	1100	199700	1700	196850	870	198700	1500
NIST610 - 11	203900	1100	194900	1100	197700	1000	189700	1300	199600	1800	197670	980	198500	1300
NIST610 - 12	203800	1000	193580	990	197220	900	189600	1400	199300	1400	197370	870	199200	1100
NIST610 - 13	204000	1100	193460	900	197300	1000	189000	1500	199400	1600	197110	980	197600	1500
NIST610 - 14	203900	1100	194100	1000	197680	850	190000	1400	199500	1700	197030	970	197600	1500

NIST610 - 15	203800	1100	194600	1100	198300	1100	190600	1700	200300	1500	197970	960	198600	1600
NIST610 - 16	204000	1000	194800	1100	197200	1000	189800	1400	200200	1600	197340	910	198300	1500
NIST610 - 17	203800	1100	193900	1100	197400	1100	189500	1500	199500	1600	197900	1100	199200	1800
NIST610 - 18	204500	1100	194300	1000	198600	1000	190200	1600	199800	1400	197190	980	198900	1700
NIST610 - 19	204200	1100	194490	900	197890	980	190500	1400	200800	1600	197750	830	198900	1600
NIST610 - 20	203600	1200	194100	1100	197300	1000	188900	1500	199100	1500	197030	990	197300	1600
NIST610 - 21	204500	1000	193810	990	197730	880	189600	1300	200500	1600	197990	890	198400	1400
NIST610 - 22	203200	1000	194400	1000	197620	950	188900	1200	199400	1400	196580	910	198200	1600
NIST610 - 23	204600	1100	194400	1000	197960	970	190200	1300	200800	1600	196850	870	198600	1400
NIST610 - 24	203800	1300	195330	940	198060	950	190700	1500	200200	1600	197400	1100	197000	1600
NIST610 - 25	203300	1200	193900	1100	197420	910	190100	1500	200100	1400	197200	1100	197700	1500
NIST610 - 26	204400	1300	193930	940	198380	970	190300	1500	200300	1500	197700	1100	198400	1700
	Tb (ppm)	**2σ**	**Dy (ppm)**	**2σ**	**Ho (ppm)**	**2σ**	**Er (ppm)**	**2σ**	**Tm (ppm)**	**2σ**	**Yb (ppm)**	**2σ**	**Lu (ppm)**	**2σ**
NIST610 - 1	192900	1000	193400	1200	198320	940	201000	1000	192370	990	199200	1100	194600	1100
NIST610 - 2	193400	900	193050	960	198210	980	201100	1000	192020	870	198700	1200	193840	920
NIST610 - 3	192760	810	193100	1000	198340	920	200900	1000	192340	890	198500	1000	193900	840
NIST610 - 4	192260	910	192200	1100	198090	850	200300	1000	191400	890	198600	1100	193340	830
NIST610 - 5	192300	1000	191700	1100	197300	1100	200400	1200	191690	980	198300	1200	193100	1100
NIST610 - 6	193200	1000	193800	1200	198790	950	201500	1000	192400	1100	198700	1200	193900	1000
NIST610 - 7	193190	940	192600	1100	198400	1100	200600	1100	192200	1000	198000	1200	193500	1100
NIST610 - 8	193500	860	193000	1000	198130	820	201000	1000	192270	880	198600	1100	193970	960
NIST610 - 9	193490	880	193300	1100	198700	950	201190	950	192330	850	198700	1300	194080	980
NIST610 - 10	192680	780	193100	1200	197600	1000	200540	940	191300	1000	198600	1300	193400	1100
NIST610 - 11	193500	870	193600	1000	198580	910	201200	1100	192650	830	199430	950	194910	910
NIST610 - 12	192440	810	193200	1100	198430	810	201030	880	191980	800	199300	1100	193630	830
NIST610 - 13	192840	870	192910	990	198090	830	201200	1000	192030	920	198200	1100	194100	870
NIST610 - 14	192380	970	192700	1000	197450	870	200090	990	191420	770	198000	1100	193190	930
NIST610 - 15	193750	870	193180	960	199130	880	202000	1100	192710	850	199000	1200	194100	1000
NIST610 - 16	192950	840	192800	1100	198070	980	200300	1100	191870	870	198200	1100	194000	940
NIST610 - 17	192500	1100	192900	1200	198000	1100	200800	1200	191960	960	199500	1200	193600	1000
NIST610 - 18	192770	990	192700	990	198240	830	200600	1000	192200	800	198500	1100	193420	870
NIST610 - 19	192520	900	193200	1100	198580	820	201560	970	192340	930	198600	1200	194100	1000
NIST610 - 20	192670	980	192800	1100	197400	1000	200200	1200	191490	950	198600	1200	193280	990
NIST610 - 21	193220	870	192460	990	198590	840	201400	1000	192570	930	199900	1300	194100	1000

NIST610 - 22	192650	930	192600	1100	197760	900	200200	970	191660	800	197700	1000	193930	940
NIST610 - 23	193060	910	193800	1000	198480	950	201000	1100	192490	910	198600	1100	194110	930
NIST610 - 24	192980	910	192200	1100	198300	1000	200500	1100	191600	1100	198600	1200	193300	1000
NIST610 - 25	192780	980	192900	1100	198000	1000	201200	1100	191810	870	198400	1100	193470	980
NIST610 - 26	193270	970	193300	1100	198300	980	200900	1200	192400	1000	199300	1100	194240	930
	Th (ppm)	**2σ**	**U (ppm)**	**2σ**										
NIST610 - 1	202400	1100	203400	1100										
NIST610 - 2	201300	1100	204200	1100										
NIST610 - 3	202000	1200	203940	940										
NIST610 - 4	201700	1100	203500	1000										
NIST610 - 5	201600	1400	203400	1200										
NIST610 - 6	202200	1400	204200	1100										
NIST610 - 7	201600	1100	203800	1100										
NIST610 - 8	202100	1100	203700	940										
NIST610 - 9	202800	1200	204600	1100										
NIST610 - 10	200900	1100	203000	1000										
NIST610 - 11	202400	1100	204500	1100										
NIST610 - 12	201300	1200	203320	870										
NIST610 - 13	202200	1100	203990	970										
NIST610 - 14	201400	1100	203500	1000										
NIST610 - 15	202400	1400	204500	1000										
NIST610 - 16	201500	1200	203120	970										
NIST610 - 17	201600	1200	203700	1100										
NIST610 - 18	202100	1200	203800	1000										
NIST610 - 19	202200	1200	204400	1000										
NIST610 - 20	201500	1000	203210	910										
NIST610 - 21	202500	1200	204300	1100										
NIST610 - 22	201300	1100	203330	960										
NIST610 - 23	202800	1200	204200	1100										
NIST610 - 24	200700	1400	203400	1000										
NIST610 - 25	201500	1200	203800	1100										
NIST610 - 26	202200	1200	203700	1200										
	Y (ppm)	**2σ**	**La (ppm)**	**2σ**	**Pr (ppm)**	**2σ**	**Nd (ppm)**	**2σ**	**Sm (ppm)**	**2σ**	**Eu (ppm)**	**2σ**	**Gd (ppm)**	**2σ**

Session #1 Unknowns:														
BK01_1	2708	44	107900	1700	22090	350	77900	1200	12840	210	1901	31	6890	130
BK01_2	2738	62	110800	2400	22420	480	82300	1100	13430	260	1881	41	6870	130
BK01_3	3570	140	110200	1400	22090	340	79700	1100	13290	230	2073	62	8300	320
BK01_4	6980	370	102200	1800	22200	320	81900	1400	14350	270	2175	38	10190	270
BK01_5	5990	250	106700	1400	22380	290	83700	1100	15170	310	2408	53	11320	220
BK01_6	7090	190	103900	1200	22040	340	80000	1400	14190	220	2185	32	10350	170
BK01_7	7080	120	105100	1600	22260	290	79800	1000	13780	170	2094	22	10050	150
BK01_8	7200	120	104400	1600	22440	310	80700	1100	14120	200	2120	23	10140	160
BK01_9	4400	120	106400	1600	22200	280	78900	1200	13170	180	1814	21	7950	130
BK01_10	2868	51	115400	1400	21300	280	73060	940	12080	170	1865	24	6670	100
BK01_11	2894	57	109700	2000	22130	370	77900	1300	12380	290	1762	34	6780	130
BK01_12	6400	190	106500	1600	22300	320	81500	1200	14310	210	2236	31	10190	160
BK01_13	6800	150	105400	1900	21930	320	79900	1600	13960	310	2061	34	9670	200
BK01_14	7310	160	103100	1400	22410	280	80800	1100	14110	210	2191	28	10280	200
BK01_15	7190	110	106000	1600	22290	320	81400	1100	14160	220	2176	30	10150	170
BK01_16	5510	290	104800	2300	22460	510	84400	1900	14770	360	2188	58	9720	270
BK01_17	5030	430	107800	2200	21880	360	80000	1400	13710	310	1971	28	9070	180
BK01_18	7570	160	105400	1900	22180	370	80200	1400	14080	190	2184	37	10290	180
BK01_19	7390	120	105500	1600	22120	290	79500	1200	13770	190	2084	33	9820	150
BK01_20	6730	130	105300	1700	22280	370	79500	1300	13940	200	2120	35	10000	170
BK01_21	8340	220	104600	2400	22440	400	83100	1600	15040	270	2521	61	12580	350
BK01_22	7120	320	107700	1900	22160	360	82800	1500	14110	340	2158	35	10370	210
BK01_23	7830	140	106400	1800	22250	400	82100	1400	14430	290	2201	34	10530	210
BK01_24	5610	360	103700	1400	22440	300	83300	1100	14530	180	2061	39	9360	300
BK01_25	7090	350	107200	1500	22590	390	82500	1800	14450	370	2271	38	10340	210
BK01_26	4380	140	102200	1400	22660	320	85400	1100	15880	230	2425	39	10610	200
BK01_27	6270	150	105700	2200	22900	420	83300	1300	14680	240	2297	35	10200	190
BK01_28	4530	380	103000	1400	22400	280	82200	1000	15280	200	2473	60	10350	320
BK01_29	5280	120	105200	1400	22190	270	79300	1200	14050	230	2336	38	9630	170
BK01_30	2860	58	111400	2300	22060	420	80400	1400	13360	270	2038	52	7200	190
BK01_31	3890	170	107400	1000	22250	300	79900	1100	13430	170	1984	23	8190	200
BK06_1	5540	140	109600	1900	21890	340	79300	1500	14360	270	1198	30	9240	210

BK06_2	3210	170	121300	1500	20380	280	66100	1300	10540	270	1421	42	6120	230
BK06_3	4722	72	117200	1300	21380	280	73300	1000	12760	170	1366	19	7630	140
BK06_4	3841	67	119400	1400	21360	220	73820	950	12730	210	1684	22	7790	140
BK06_5	4254	77	117700	1600	22210	400	84900	1400	14500	240	1862	29	10130	220
BK06_6	2840	510	102800	2000	21880	330	78100	1200	10980	420	1130	100	5100	440
BK06_7	5650	140	108900	1900	22370	380	83500	1800	14970	370	1938	36	10320	250
BK06_8	7920	140	96100	1700	23440	360	85600	1300	15370	220	2262	34	10500	190
BK06_9	7630	170	100900	2300	22720	490	82900	1700	14830	380	2331	63	10220	330
BK06_10	6790	490	105500	3000	22650	660	84200	2500	14880	470	2216	98	10570	600
BK06_11	4630	110	112200	2500	21410	490	80600	1800	14210	470	1869	26	9200	300
BK06_12	6240	130	108700	2000	22110	330	78400	1800	13640	280	1453	91	9020	160
BK06_13	8110	150	97040	940	23540	340	86400	1400	15490	220	2252	34	10680	180
BK06_14	7630	390	99000	2100	22810	560	85000	2800	15440	480	2366	92	10880	450
BK06_15	5220	320	108100	2600	22130	410	80400	2000	13860	430	2177	38	8970	400
BK06_16	4075	98	120300	1900	21110	250	75100	1700	12190	300	1757	39	7480	240
BK06_17	3994	57	124300	1600	19680	300	63390	840	10060	140	1476	17	5764	85
BK06_18	3830	120	111500	1700	21450	250	73800	1100	12170	230	1868	29	6940	150
BK06_19	8060	120	97900	1400	23180	280	86300	1300	15670	240	2477	32	11350	170
BK06_20	1200	140	101600	2100	22930	540	82200	1800	12450	410	1165	69	6000	350
BK06_21	3970	140	121200	3000	21280	620	76000	1400	12800	350	1553	50	7740	170
BK06_22	2860	120	118600	2000	20720	360	69100	1100	10450	180	1570	35	5770	150
BK06_23	5980	460	106800	1900	21950	380	78200	1900	13640	440	1957	49	8490	440
BK06_24	3443	79	117400	1700	20300	300	69100	1000	11050	180	1506	17	6390	130
BK06_25	3580	140	115300	1600	21990	310	83200	1200	14550	250	1831	34	9350	200
BK14_1	5180	310	106600	1500	22720	380	83300	1600	14200	260	2470	37	9640	180
BK14_2	5370	250	102000	2100	22620	510	84800	2100	15200	370	2493	69	10930	380
BK14_3	7570	320	103000	3100	22410	530	85500	2800	15430	460	2753	85	12180	290
BK14_4	3838	98	102200	1400	22590	330	82300	1300	14820	210	2468	29	10610	170
BK14_5	4297	87	103500	1500	22570	320	82900	1100	15090	230	2336	32	9770	200
BK14_6	5120	110	102500	1600	22370	480	82900	1400	14420	260	2461	40	10360	220
BK14_7	5420	230	102200	1900	23030	450	83300	1800	15180	250	2418	55	10070	240
BK14_8	7950	110	103000	1400	22810	260	83900	1100	14650	230	2555	28	10250	160
BK14_9	6780	350	103200	1800	22760	340	85000	1600	15740	340	2688	37	11500	240
BK14_10	6130	150	103800	2000	22990	610	87200	1900	15510	430	2551	63	10760	400

BK18_1	5320	140	107100	1700	22720	370	85100	1800	15040	410	2739	70	11110	390
BK18_2	3980	150	122900	2000	20890	400	71300	2100	12190	360	1965	48	7530	310
BK18_3	5580	230	118000	3000	20700	640	71700	1700	12370	330	1902	41	8400	320
BK18_4	3769	85	102400	1300	22280	310	80100	1100	13350	210	2131	35	8180	160
BK18_5	3630	140	105000	1300	22220	360	80000	1200	13840	190	2274	37	8920	190
BK18_6	4660	110	103800	1200	22260	290	82200	1200	14390	240	2218	31	9120	160
BK18_7	4770	130	114500	2000	21670	410	75600	1500	13750	330	2181	46	9340	180
BK25A_1	2500	110	112400	1800	21860	360	77400	1700	13210	350	2020	160	7970	370
BK25A_2	2859	40	122600	1700	20250	250	67430	940	11090	180	926	28	6040	120
BK25A_3	2453	94	109300	1400	21720	270	77200	1100	13080	170	1518	51	7260	120
BK25A_4	3371	53	120300	1500	21100	230	72500	1000	12240	160	953	12	6780	110
BK25A_5	1847	42	105800	1200	22090	270	79700	1300	14020	200	3045	79	8640	200
BK25A_6	3990	90	113000	1800	21650	400	78100	1300	13110	270	1742	54	8530	180
BK25A_7	3001	42	110900	1600	21980	260	78500	1100	13080	220	1339	71	7300	150
BK25A_8	3293	82	107600	1500	21810	330	78800	1200	13210	200	2100	100	8380	180
BK25A_9	2484	47	112900	1700	21460	290	75800	1200	12050	170	1382	64	6670	150
BK25A_10	2866	65	114000	1900	21380	240	73100	1100	12200	200	1115	54	6860	120
BK25A_11	2040	130	105400	1500	22060	340	79700	1300	13910	250	2379	82	8300	160
BK25A_12	2782	55	115400	1700	21140	260	73500	1000	12110	180	1345	28	6602	97
BK25A_13	2603	39	112600	1900	21520	360	76500	1300	12920	230	1524	21	7180	120
BK25A_14	2579	99	108600	1500	21820	270	78200	1100	13290	180	2230	63	8180	120
BK25A_15	2980	130	112300	1700	21900	360	78300	1100	13020	260	1314	97	7350	150
BK25A_16	3499	80	111400	2700	21760	330	76700	1300	13050	250	1780	77	8110	170
BK25A_17	2657	88	116200	2000	21300	320	72400	1200	11890	210	1113	31	6550	160
BK25A_18	3326	53	110900	1300	21320	310	75000	1100	12590	180	1272	63	7240	130
BK25A_19	3247	68	110900	1700	21630	290	78570	990	13330	200	1159	27	7380	110
BK25A_20	2000	44	107800	1400	21630	300	77600	1100	12610	210	1761	72	6990	150
BK25A_21	2543	45	108700	1700	22160	330	80400	1200	13410	250	1547	27	7450	150
BK25A_22	2599	45	110900	1600	21680	350	77300	1100	12740	210	1432	22	6960	130
BK25A_23	3079	82	111300	1700	21730	320	78400	1200	12890	260	1440	110	7500	260
BK25A_24	3000	170	108200	2100	22040	520	81900	1600	13560	330	2186	55	8610	230
BK25A_25	2730	110	110500	1900	22170	400	79800	1400	13230	220	1582	60	7380	200
BK25A_26	3150	120	110700	1400	22050	270	78800	1300	12880	210	1514	75	7400	140

BK25A_27	2460	220	106200	1200	22360	310	81000	1200	13620	220	2182	72	8390	230
BK25A_28	2071	67	106400	1500	22590	400	82500	1500	13860	210	2879	64	8760	190
BK25A_29	3400	370	102500	1400	22490	300	82300	1300	13980	230	2696	40	9660	320
BK25B_1	3054	53	112700	1500	21510	310	74900	1200	13030	270	1740	190	7650	280
BK25B_2	2644	59	116500	1300	21190	330	73000	1200	11650	210	1221	19	6310	150
BK25B_3	2629	42	116800	1400	21200	280	73790	940	11960	150	1201	16	6410	100
BK25B_4	2140	67	106200	1700	22060	320	79400	1100	13450	180	3002	81	8730	200
BK25B_5	3592	85	110700	2100	21530	420	78300	1500	12700	280	1265	36	7250	220
BK25B_6	2753	52	112400	1400	21400	290	74400	1100	11680	160	1266	20	6290	110
BK25B_7	3125	76	108500	1200	21690	260	78100	1000	12930	280	1176	60	7170	210
BK25B_8	2641	46	117700	1500	21150	330	73200	1300	11740	190	1315	39	6530	120
BK25B_9	4420	170	102600	1500	22540	290	81600	1200	14320	220	2939	47	10280	210
BK25B_10	2962	54	113100	1800	21220	350	73600	1200	12400	230	1309	41	7020	140
BK25B_11	3170	110	118200	1400	21000	300	72500	1100	11300	230	1211	20	6180	120
BK25B_12	2932	66	112200	2200	21280	360	75600	1200	12130	210	1077	38	6470	130
BK25B_13	4120	390	108700	2200	22100	450	77800	1700	13730	340	2300	180	9170	440
BK25B_14	3930	220	115300	1600	20910	300	72000	1400	12330	270	1198	80	7660	320
BK25B_15	2452	57	116800	3600	21090	390	73200	1700	11250	340	911	20	5890	130
BK25B_16	3129	88	111800	1500	21440	410	75500	1300	12490	230	1366	41	7180	130
BK25B_17	4380	170	102100	1400	22720	320	80400	1300	13990	270	2613	39	10040	200
BK25B_18	3010	110	111100	1200	21380	250	75740	910	12820	200	1580	36	7400	160
BK25B_19	3660	210	108300	1600	22130	300	79600	870	13760	200	2060	150	8670	360
BK25B_20	3822	84	106600	2000	22290	390	80800	1600	14580	180	2621	98	9790	270
BK25B_21	2574	46	107600	1500	22300	300	79700	1200	13650	210	2809	54	9020	170
BK25B_22	4360	240	107800	2700	21860	370	79800	1700	13850	280	2210	100	9410	370
BK25B_23	3240	120	114400	3900	21550	590	76100	1700	13300	360	1219	55	7240	240
BK25B_24	5290	370	106300	1900	22200	400	80700	1900	14220	290	2417	62	10350	380
BK25B_25	2485	61	119700	2800	21010	450	73100	1000	11600	350	943	25	6070	180
BK25B_26	3680	210	110500	1300	21460	370	75800	1300	12850	280	1690	130	8010	370
BK25B_27	3285	71	112000	1700	21420	320	75300	1400	12870	220	1670	150	7750	260
BK25B_28	4242	69	115600	1300	21240	300	73910	890	12810	160	1669	78	7890	130
BK25B_29	3720	220	111500	1500	21580	300	74600	1200	12760	190	1907	37	8400	220
BK25B_30	4250	300	109200	1300	22100	290	77500	1100	13550	190	2254	63	9170	280
BK25B_31	3470	140	111100	1400	21740	320	76700	880	13000	210	1924	77	8050	220

BK25B_32	2942	54	116300	1800	21340	280	73700	1100	12220	210	1354	22	6842	99
BK25B_33	3720	110	106800	2600	22150	390	78000	1800	13410	300	2369	61	8810	200
BK25B_34	3840	120	102700	2100	22050	480	80400	1700	13890	260	3082	91	9250	190
BK25B_35	4030	160	104900	1600	22120	370	81500	1500	14210	280	2860	110	9910	230
BK25B_36	3281	56	112400	1900	20950	410	73000	1500	12530	280	1770	130	7670	220
BK25B_37	3026	69	111300	2700	21970	520	81100	1500	13710	250	1363	22	7170	120
BK25B_38	2940	290	102100	1600	22530	360	81600	1300	14100	210	2919	36	9190	240
BK25B_39	2550	130	106100	1400	22130	290	78300	1100	13540	220	1771	69	7840	130
BK25B_40	1710	140	108600	1700	21720	300	75900	1100	12880	180	2147	77	7240	120
KTDD089_1	4040	110	127100	2000	19240	240	59900	1000	9850	230	1566	29	6340	240
KTDD089_2	9790	460	112000	1800	21170	310	74900	1200	13900	380	2286	66	11580	470
KTDD089_3	5050	260	124200	1700	19720	250	62770	860	10020	190	1717	27	6006	91
KTDD089_4	4864	80	130700	1700	19010	290	59670	960	10600	180	1894	26	7020	100
KTDD089_5	4190	130	130300	1800	19450	230	60970	950	9850	170	1486	28	5910	130
KTDD089_6	3613	95	134500	1900	18630	370	57200	1000	9470	160	1511	35	5570	100
KTDD089_7	5690	260	119300	1800	20240	310	66300	1700	11250	370	1732	50	7210	330
KTDD089_8	4620	120	126500	1600	19450	230	61000	1000	10610	150	1832	41	6750	140
KTDD089_9	5190	160	127100	1800	19390	270	60910	840	10870	220	1855	53	6950	210
KTDD089_10	2592	45	138100	1900	18190	230	53020	650	8180	110	1280	17	4586	83
KTDD089_11	4052	72	135400	2000	18490	280	55300	1000	8480	140	1423	21	5005	71
KTDD089_12	3910	140	127500	1600	19040	290	58470	860	9390	150	1400	35	5600	110
KTDD089_13	2830	160	127400	2000	19050	350	60200	940	9380	190	1532	24	5327	91
KTDD089_14	4834	96	126300	1600	19610	250	59900	1100	9550	160	1587	24	5646	95
KTDD089_15	3550	250	134300	2000	18320	240	53260	930	8080	260	1336	48	4650	180
KTDD089_16	5410	140	124900	1400	19350	300	59860	810	9860	140	1744	22	6178	93
KTDD089_17	3280	190	134900	2600	18530	290	54140	880	8450	170	1294	30	4830	110
KTDD089_18	2708	44	107900	1700	22090	350	77900	1200	12840	210	1901	31	6890	130

	Tb (ppm)	2σ	Dy (ppm)	2σ	Ho (ppm)	2σ	Er (ppm)	2σ	Tm (ppm)	2σ	Yb (ppm)	2σ	Lu (ppm)	2σ
BK01_1	562	10	1635	25	139	2	167	4	10	0	27	2	2	0
BK01_2	570	10	1662	37	141	4	167	5	9	1	30	2	2	0
BK01_3	722	30	2046	71	165	5	188	6	10	1	25	2	2	0
BK01_4	1044	41	3450	160	301	15	337	17	16	1	42	3	2	0
BK01_5	1099	16	3220	99	259	10	258	10	11	1	26	2	1	0
BK01_6	1051	20	3486	74	300	8	320	10	15	1	35	2	2	0
BK01_7	1041	14	3479	47	295	5	307	6	14	1	30	2	2	0
BK01_8	1067	14	3575	51	305	5	317	5	15	1	32	2	2	0
BK01_9	732	12	2299	49	198	4	228	5	11	0	28	1	2	0
BK01_10	567	8	1708	26	149	3	169	4	9	0	24	1	1	0
BK01_11	558	12	1643	30	144	3	170	5	10	1	29	2	2	0
BK01_12	996	21	3244	82	274	7	291	7	14	1	34	2	2	0
BK01_13	994	16	3372	61	277	7	280	6	13	1	29	2	2	0
BK01_14	1047	16	3469	57	307	7	338	10	17	1	38	2	2	0
BK01_15	1030	13	3493	46	302	4	323	6	16	1	36	2	2	0
BK01_16	906	34	2870	130	242	12	269	12	14	1	37	3	2	0
BK01_17	846	24	2570	130	218	16	237	20	11	1	32	2	2	0
BK01_18	1075	18	3615	55	327	6	359	9	17	1	44	3	3	0
BK01_19	1032	15	3576	54	313	5	336	7	16	1	39	2	2	0
BK01_20	975	18	3277	68	290	5	318	7	16	0	36	2	2	0
BK01_21	1271	38	4040	110	355	10	388	17	19	1	51	3	3	0
BK01_22	1036	23	3523	93	301	9	314	12	14	1	33	2	2	0
BK01_23	1098	17	3699	55	333	7	358	9	17	1	45	3	3	0
BK01_24	899	38	2880	150	252	13	275	13	14	1	34	2	2	0
BK01_25	1038	24	3440	130	297	15	317	19	15	1	35	3	2	0
BK01_26	894	19	2529	68	204	5	223	6	12	0	32	2	2	0
BK01_27	1003	17	3138	46	250	5	243	6	10	1	22	1	1	0
BK01_28	896	41	2550	150	202	13	212	11	11	1	27	2	1	0
BK01_29	931	18	2794	50	212	4	194	5	8	0	17	1	1	0
BK01_30	600	11	1790	41	150	4	173	5	10	1	30	2	2	0
BK01_31	744	24	2220	78	176	6	181	4	9	0	23	1	1	0
BK06_1	904	20	2990	61	279	7	359	8	23	1	71	3	5	0
BK06_2	549	21	1778	81	164	8	212	10	13	1	38	2	2	0

BK06_3	720	10	2467	32	238	4	319	6	20	1	62	2	4	0
BK06_4	690	8	2189	36	197	3	241	5	14	0	40	2	3	0
BK06_5	829	14	2511	41	220	5	269	6	16	1	49	2	3	0
BK06_6	413	57	1390	250	134	26	183	38	11	2	37	8	4	1
BK06_7	908	18	2981	70	276	5	350	8	21	1	64	3	5	0
BK06_8	1067	18	3729	65	353	7	439	9	25	1	67	3	4	0
BK06_9	1031	29	3587	67	351	6	483	10	32	1	105	5	8	0
BK06_10	990	55	3410	190	313	20	403	23	24	2	72	4	5	1
BK06_11	823	24	2609	57	231	6	295	7	17	1	53	3	3	0
BK06_12	902	16	3139	50	304	6	384	7	24	1	76	4	5	0
BK06_13	1048	19	3714	56	361	7	455	10	26	1	70	3	5	0
BK06_14	1105	42	3670	160	334	15	390	16	23	1	60	4	4	1
BK06_15	846	38	2700	130	248	13	305	15	17	1	52	3	3	0
BK06_16	687	15	2282	40	208	5	267	7	16	1	45	2	3	0
BK06_17	565	10	2001	32	193	3	252	5	15	1	43	2	3	0
BK06_18	625	17	1995	67	187	7	230	8	13	1	39	2	3	0
BK06_19	1129	17	3796	61	362	5	467	9	28	1	88	3	6	0
BK06_20	401	31	869	84	56	6	45	6	2	0	4	1	0	0
BK06_21	708	18	2309	70	210	7	259	11	15	1	44	4	3	0
BK06_22	507	14	1584	54	147	6	185	8	11	1	32	2	2	0
BK06_23	841	49	2940	190	285	20	349	27	21	2	57	4	3	0
BK06_24	576	11	1905	40	179	4	226	5	14	1	42	2	3	0
BK06_25	749	16	2253	71	195	8	236	10	13	1	41	3	3	0
BK14_1	918	14	2790	110	244	17	314	29	20	2	69	8	5	1
BK14_2	1017	37	3060	110	246	9	269	17	14	1	37	3	2	0
BK14_3	1177	33	3590	93	325	10	410	18	25	1	83	5	5	0
BK14_4	976	14	2545	41	173	5	173	6	9	0	24	2	2	0
BK14_5	902	15	2651	44	216	3	280	7	23	1	112	5	15	1
BK14_6	976	24	2837	57	231	5	279	7	17	1	53	2	4	0
BK14_7	944	30	2970	100	257	10	298	14	17	1	48	4	3	0
BK14_8	1031	13	3671	42	377	6	538	10	38	1	132	3	10	1
BK14_9	1099	21	3322	80	292	13	364	22	23	2	76	7	5	1
BK14_10	1022	28	3141	83	285	8	356	10	25	2	84	5	6	1

BK18_1	979	23	2969	92	245	7	270	10	13	1	38	3	2	0
BK18_2	709	30	2357	83	205	6	257	8	15	1	47	2	3	0
BK18_3	839	22	3020	130	281	15	352	25	22	2	72	7	5	1
BK18_4	736	13	2138	38	179	4	208	7	11	1	33	2	2	0
BK18_5	795	21	2165	54	170	6	188	10	11	1	31	4	2	0
BK18_6	836	13	2643	46	232	4	268	8	15	1	43	2	3	0
BK18_7	895	12	2816	61	241	7	284	10	18	1	60	3	4	0
BK25A_1	630	22	1618	41	119	6	128	10	7	1	18	2	1	0
BK25A_2	545	9	1737	23	156	3	191	3	11	0	29	2	2	0
BK25A_3	593	8	1637	41	128	5	149	6	9	1	24	2	2	0
BK25A_4	624	8	2008	25	184	3	233	4	14	1	39	2	2	0
BK25A_5	704	17	1646	32	101	3	91	4	4	0	11	1	1	0
BK25A_6	770	20	2306	56	182	3	199	5	10	0	27	2	2	0
BK25A_7	617	10	1800	24	153	3	179	4	10	0	30	2	2	0
BK25A_8	728	17	1952	42	145	4	146	7	7	0	22	2	1	0
BK25A_9	546	12	1544	21	125	3	143	4	8	0	25	2	2	0
BK25A_10	586	9	1776	32	154	4	183	7	10	1	29	2	2	0
BK25A_11	635	9	1423	51	93	8	96	11	6	1	15	2	1	0
BK25A_12	548	8	1628	24	142	3	172	4	9	0	25	2	2	0
BK25A_13	569	8	1612	19	133	3	155	4	9	0	24	2	1	0
BK25A_14	644	8	1640	42	123	6	136	8	8	0	21	2	1	0
BK25A_15	611	11	1759	41	148	7	179	12	11	1	30	3	2	0
BK25A_16	722	18	2070	48	166	4	185	5	10	0	27	2	2	0
BK25A_17	543	16	1643	56	140	5	173	6	10	1	32	2	2	0
BK25A_18	618	14	1852	34	162	3	193	4	11	0	29	2	2	0
BK25A_19	619	10	1901	30	166	3	203	5	13	1	36	2	3	0
BK25A_20	544	11	1336	24	97	2	109	3	6	0	17	1	1	0
BK25A_21	583	8	1622	27	129	2	153	4	9	0	27	2	2	0
BK25A_22	552	9	1554	29	131	2	156	4	9	0	26	2	1	0
BK25A_23	632	21	1799	43	153	4	176	6	10	1	29	2	2	0
BK25A_24	735	17	1845	76	121	9	118	12	6	1	15	2	1	0
BK25A_25	623	21	1683	62	131	5	155	6	8	0	28	2	2	0
BK25A_26	613	8	1795	45	153	7	189	11	10	1	31	2	2	0
BK25A_27	676	29	1610	110	102	9	98	11	5	1	13	2	1	0

BK25A_28	663	14	1433	37	85	3	78	4	4	0	11	1	1	0
BK25A_29	831	43	2020	170	128	15	114	15	5	1	11	2	1	0
BK25B_1	669	27	1918	37	150	3	169	8	9	1	27	2	2	0
BK25B_2	514	12	1545	36	138	3	160	4	9	0	24	2	2	0
BK25B_3	526	8	1553	22	133	2	159	4	9	0	26	1	2	0
BK25B_4	741	16	1770	41	100	4	78	6	3	0	9	2	0	0
BK25B_5	620	17	1875	46	172	4	211	4	13	1	38	2	2	0
BK25B_6	521	8	1568	24	140	2	168	4	9	0	22	1	1	0
BK25B_7	602	20	1786	55	155	4	191	4	11	0	35	2	2	0
BK25B_8	531	8	1611	24	138	3	162	4	9	0	22	1	1	0
BK25B_9	953	18	2525	62	171	5	145	6	7	0	16	1	1	0
BK25B_10	584	11	1762	20	152	3	178	4	10	0	26	2	2	0
BK25B_11	510	13	1642	47	154	6	197	7	11	1	30	2	1	0
BK25B_12	536	11	1655	40	147	4	179	4	11	1	33	2	2	0
BK25B_13	834	53	2380	170	176	13	173	14	9	1	20	3	1	0
BK25B_14	704	36	2270	110	197	8	227	7	13	0	33	1	2	0
BK25B_15	461	9	1374	32	122	3	152	4	9	0	30	3	2	0
BK25B_16	596	9	1797	46	161	5	193	8	11	1	31	2	2	0
BK25B_17	951	21	2533	78	173	7	150	6	6	0	17	2	1	0
BK25B_18	633	18	1819	58	148	6	166	7	9	1	24	2	2	0
BK25B_19	764	42	2120	110	160	6	175	5	9	0	25	1	1	0
BK25B_20	891	20	2345	40	157	3	157	6	8	1	24	2	2	0
BK25B_21	761	12	1826	28	108	2	91	3	4	0	10	1	1	0
BK25B_22	878	41	2450	110	181	7	194	6	10	1	27	2	2	0
BK25B_23	632	13	1981	45	173	7	197	8	11	1	32	3	2	0
BK25B_24	1014	48	2920	170	213	14	204	15	9	1	23	2	1	0
BK25B_25	511	11	1511	44	131	3	160	6	10	0	29	2	2	0
BK25B_26	732	42	2130	120	170	6	184	4	9	0	28	2	2	0
BK25B_27	685	25	1928	49	156	4	170	9	9	1	25	3	2	0
BK25B_28	756	12	2414	33	217	4	264	6	16	1	48	3	4	0
BK25B_29	773	28	2196	99	163	8	162	8	8	1	20	2	1	0
BK25B_30	877	37	2470	130	175	10	166	10	8	1	21	2	1	0
BK25B_31	717	26	2031	70	157	4	162	3	8	0	21	1	1	0
BK25B_32	575	8	1748	25	151	3	183	4	10	0	27	1	2	0

BK25B_33	815	18	2186	59	148	5	130	5	6	0	14	2	1	0
BK25B_34	835	20	2337	61	176	5	195	11	12	1	47	5	5	1
BK25B_35	911	29	2405	79	160	7	148	9	7	1	18	2	1	0
BK25B_36	685	15	2006	26	157	5	168	9	9	1	21	2	1	0
BK25B_37	607	14	1855	41	163	3	197	5	11	1	31	2	3	0
BK25B_38	803	36	1970	130	113	11	90	11	4	1	8	1	0	0
BK25B_39	635	18	1668	68	128	8	140	10	8	1	22	3	1	0
BK25B_40	544	10	1249	64	84	8	86	10	4	1	11	2	1	0
KTDD089_1	605	19	2080	53	195	4	228	5	12	0	30	1	2	0
KTDD089_2	1332	66	4760	220	447	19	549	24	32	2	92	5	6	0
KTDD089_3	621	14	2297	71	238	9	290	14	17	1	40	3	2	0
KTDD089_4	736	11	2652	36	248	3	274	6	13	1	24	2	1	0
KTDD089_5	585	16	2067	57	204	6	247	9	14	1	35	2	2	0
KTDD089_6	563	14	2007	57	188	6	214	6	11	0	27	2	1	0
KTDD089_7	724	34	2630	110	268	12	350	19	22	2	67	8	5	1
KTDD089_8	685	15	2458	58	234	5	265	7	13	0	28	2	1	0
KTDD089_9	719	24	2630	100	254	8	295	8	14	1	31	1	1	0
KTDD089_10	437	7	1481	26	136	2	152	4	8	0	17	1	1	0
KTDD089_11	513	8	1890	32	190	3	231	5	13	1	29	1	1	0
KTDD089_12	552	14	1944	58	189	6	233	8	12	1	30	1	2	0
KTDD089_13	490	9	1565	43	144	6	174	9	10	1	25	2	1	0
KTDD089_14	595	10	2197	38	221	4	285	6	16	1	40	2	2	0
KTDD089_15	474	23	1686	99	167	11	206	15	11	1	23	2	1	0
KTDD089_16	640	12	2438	44	248	5	304	8	16	1	37	2	2	0
KTDD089_17	459	14	1608	62	152	7	186	11	9	1	23	2	1	0
KTDD089_18	562	10	1635	25	139	2	167	4	10	0	27	2	2	0
	Th (ppm)	**2σ**	**U (ppm)**	**2σ**										

BK01_1	16610	390	113	3
BK01_2	22530	500	117	4
BK01_3	25080	860	4200	890
BK01_4	42000	1400	1480	160
BK01_5	42500	1400	4290	310
BK01_6	50600	2000	1956	63
BK01_7	39860	750	1537	19
BK01_8	39260	960	1595	26
BK01_9	28370	860	673	53
BK01_10	12490	490	142	4
BK01_11	20760	350	187	10
BK01_12	35600	490	2080	130
BK01_13	14800	650	2162	73
BK01_14	40900	1600	2280	130
BK01_15	42600	1100	2140	110
BK01_16	36600	1300	1680	220
BK01_17	28500	1200	2290	190
BK01_18	30350	940	2970	140
BK01_19	24000	2400	1627	36
BK01_20	33150	890	3520	290
BK01_21	27700	2100	11500	1200
BK01_22	24510	640	3280	550
BK01_23	37500	1300	3170	270
BK01_24	29360	790	1450	220
BK01_25	50600	2900	3020	430
BK01_26	41100	970	2390	230
BK01_27	45600	1700	3109	69
BK01_28	45700	2800	690	100
BK01_29	38800	1300	2210	120
BK01_30	24140	550	145	5
BK01_31	20080	410	859	88
BK06_1	18330	990	482	27
BK06_2	19130	390	92	2
BK06_3	18170	340	314	7

BK06_4	22080	560	110	5
BK06_5	28720	450	148	11
BK06_6	21800	3300	490	110
BK06_7	32310	960	858	39
BK06_8	60500	1700	3040	140
BK06_9	48800	1600	5070	770
BK06_10	43200	4700	3790	640
BK06_11	29300	1000	436	57
BK06_12	29700	2400	1080	170
BK06_13	60300	1200	2838	87
BK06_14	52400	4000	4630	850
BK06_15	36200	2600	3120	460
BK06_16	23920	550	162	9
BK06_17	12500	230	81	4
BK06_18	17630	700	675	68
BK06_19	64500	2300	7350	220
BK06_20	11600	1500	93	30
BK06_21	19230	550	165	20
BK06_22	12540	690	130	12
BK06_23	39700	3900	1000	160
BK06_24	17550	370	102	5
BK06_25	26100	1500	275	55
BK14_1	30330	680	5610	160
BK14_2	29300	2000	4150	340
BK14_3	37810	780	7740	260
BK14_4	26130	710	5450	150
BK14_5	44900	1800	1880	160
BK14_6	28940	600	5130	340
BK14_7	23400	1900	2210	280
BK14_8	35120	620	6978	94
BK14_9	31450	750	7150	220
BK14_10	36100	1100	8190	370
BK18_1	34750	900	3450	170

BK18_2	17040	810	1350	110
BK18_3	11300	1600	1430	200
BK18_4	19260	460	2330	120
BK18_5	21400	1100	2900	170
BK18_6	16110	930	1083	65
BK18_7	18290	440	2258	94
BK25A_1	27700	2800	2500	150
BK25A_2	15000	380	297	83
BK25A_3	19300	270	718	52
BK25A_4	11220	180	228	3
BK25A_5	9070	300	6410	270
BK25A_6	33640	930	1790	140
BK25A_7	17710	800	870	140
BK25A_8	26960	540	2780	220
BK25A_9	18610	640	673	88
BK25A_10	19120	310	395	71
BK25A_11	30900	1700	3200	210
BK25A_12	19830	270	284	44
BK25A_13	20220	360	656	25
BK25A_14	24060	410	4800	330
BK25A_15	16560	850	640	130
BK25A_16	28140	810	1240	150
BK25A_17	16330	590	424	29
BK25A_18	20300	1600	930	170
BK25A_19	16730	570	364	36
BK25A_20	18290	310	1453	85
BK25A_21	15940	330	833	22
BK25A_22	18780	340	511	31
BK25A_23	24900	2500	750	150
BK25A_24	43800	1100	1546	50
BK25A_25	22300	1500	895	82
BK25A_26	18080	590	630	100
BK25A_27	35500	2600	1840	160
BK25A_28	33700	1200	5310	110

BK25A_29	49400	1800	3240	210
BK25B_1	17030	710	2950	660
BK25B_2	21410	330	133	2
BK25B_3	20910	340	130	3
BK25B_4	14600	1200	4220	190
BK25B_5	14230	670	509	81
BK25B_6	6040	350	223	5
BK25B_7	20840	800	710	180
BK25B_8	19730	400	499	47
BK25B_9	45100	1600	4360	220
BK25B_10	17740	570	588	54
BK25B_11	16110	460	207	6
BK25B_12	16630	580	169	7
BK25B_13	31100	2300	2040	260
BK25B_14	22500	2000	550	110
BK25B_15	17510	670	227	19
BK25B_16	18180	380	568	79
BK25B_17	31500	1100	2030	100
BK25B_18	22770	760	715	84
BK25B_19	30400	2800	2590	410
BK25B_20	26790	610	5160	310
BK25B_21	13080	330	3327	95
BK25B_22	27600	2800	3430	270
BK25B_23	19110	510	399	67
BK25B_24	34700	2600	1781	50
BK25B_25	16480	540	166	11
BK25B_26	23400	1500	1230	180
BK25B_27	22400	1800	1620	280
BK25B_28	21230	750	548	25
BK25B_29	26000	1300	1298	41
BK25B_30	26300	2200	1993	82
BK25B_31	20390	510	1390	140
BK25B_32	20410	270	202	10
BK25B_33	20240	650	1912	83

BK25B_34	30300	1300	3590	230
BK25B_35	28000	1200	4590	250
BK25B_36	28480	990	1350	180
BK25B_37	24600	1100	154	6
BK25B_38	46300	2100	2906	89
BK25B_39	40300	3100	1210	130
BK25B_40	38900	1600	1558	76
KTDD089_1	18000	1200	191	24
KTDD089_2	17030	780	3110	300
KTDD089_3	14850	630	168	14
KTDD089_4	1970	200	170	4
KTDD089_5	12160	260	158	5
KTDD089_6	7410	630	144	8
KTDD089_7	38600	5300	481	66
KTDD089_8	5210	180	165	5
KTDD089_9	4540	480	213	7
KTDD089_10	4634	84	56	2
KTDD089_11	4730	160	94	3
KTDD089_12	8190	990	132	5
KTDD089_13	10010	300	67	4
KTDD089_14	12740	450	124	4
KTDD089_15	4970	470	73	8
KTDD089_16	8850	440	140	3
KTDD089_17	5600	340	70	6
KTDD089_18	16610	390	113	3

	Y (ppm)	**2σ**	**La (ppm)**	**2σ**	**Pr (ppm)**	**2σ**	**Nd (ppm)**	**2σ**	**Sm (ppm)**	**2σ**	**Eu (ppm)**	**2σ**	**Gd (ppm)**	**2σ**
Session #2 Unknowns:														

BKDK1_1	11720	190	97100	1200	23570	330	89000	1200	16540	230	4173	67	13010	190
BKDK1_2	11550	190	96700	1400	23030	280	89200	1300	15410	240	3412	66	11920	200
BKDK1_3	11650	190	95700	1400	23130	310	89200	1100	16160	250	3710	68	12470	200
BKDK1_4	11320	220	98000	1900	23750	470	90400	1700	16770	340	4147	76	12990	260
BKDK1_5	10550	160	97100	1500	23170	350	86000	1200	16100	250	4030	61	12060	180
BKDK1_6	13360	480	95600	1900	23010	330	89400	1700	16690	510	4090	250	15010	840
BKDK1_7	7330	170	96100	1300	22730	360	82800	1300	14890	240	2856	42	9030	160
BKDK1_8	8420	200	97700	1400	23100	310	83700	1300	15170	230	3411	66	10190	230
BKDK1_9	8200	130	98600	1400	22220	290	78800	1200	14070	200	3307	39	8560	130
BKDK1_10	6670	550	94600	1700	22930	500	83100	1600	14590	320	3010	170	10470	420
BKDK1_11	8970	170	96700	1700	23200	420	85300	1900	16160	330	3712	62	10700	240
BKDK1_12	10910	270	96600	2100	23390	480	87300	1900	16280	370	4212	78	12370	250
BKDK1_13	11460	270	96300	1700	23390	480	88400	1800	16000	320	3730	120	12760	280
BKDK1_14	11070	230	97500	2000	23440	460	87800	1700	16460	310	4413	96	12700	340
BKDK1_15	11340	300	96600	2300	23130	510	87700	1800	16010	340	4199	99	12550	340
BKDK1_16	9540	180	97100	1500	23010	330	85800	1300	15690	230	3971	54	11320	190
BKDK1_17	10310	140	96400	1500	22950	300	84800	1200	15770	250	3898	46	11370	180
BKDK1_18	9930	200	97300	2000	22850	450	86800	1500	15900	330	3975	74	11680	220
BKDK1_19	9600	220	96100	1600	23100	410	85600	1500	16040	280	4150	68	12020	230
BKDK1_20	12110	260	96600	2000	23420	510	89600	1900	16960	440	4000	100	13200	340
BKDK1_21	11200	200	96500	1400	23190	330	87500	1300	16440	290	4055	66	12450	230
BKDK1_22	10260	250	96600	1400	22790	330	87100	1100	15590	230	4030	100	11950	300
BKDK1_23	11480	250	97200	1800	23220	450	86700	1400	16300	330	4121	84	12860	370
BKDK1_24	10790	210	95200	1400	23150	350	86300	1200	16080	230	4115	58	11920	200
BKDK1_25	11730	400	95800	3300	22960	770	88400	2700	16940	590	4410	150	13670	470
BKDK1_26	11980	370	99870	2600	23580	560	88600	2100	15550	370	3696	84	12910	370
BKDK1_27	10960	180	96000	1300	23010	330	87500	1300	16260	210	4044	54	12410	220
BKDK1_28	11310	190	96800	1200	23530	340	88700	1300	16530	230	4135	49	12650	180
BKDK1_29	11450	210	96600	1600	23130	460	86800	1700	16130	270	4037	74	12170	250
BKDK1_30	7300	510	107300	2100	22260	340	81800	1600	13290	380	3170	170	10360	490
BKDK1_31	11580	160	95700	1600	22890	370	87400	1200	16290	270	4070	67	12680	220
BKDK1_32	11790	380	95800	2700	23140	560	87500	2000	17120	500	4580	120	14350	600
BKDK1_33	11200	240	96700	1600	23230	460	85900	1700	15860	320	4209	86	11650	220
BKDK1_34	11030	240	97600	1500	23200	330	87800	1400	16410	300	4053	54	12580	230
BKDK1_35	10800	270	97200	1400	23150	320	86200	1300	15940	300	4086	77	11530	290

BKDK1_36	11500	290	97200	1900	23740	510	90200	1800	16650	340	4020	120	12820	250
BKDK1_37	10140	240	97600	1900	23360	490	88000	1800	15980	320	4121	74	11940	330
BKDK1_38	11110	170	97000	1400	23540	340	88600	1200	16110	270	3689	55	12330	200
BKDK1_39	12390	390	96800	2900	23330	650	89600	1700	17790	530	4570	120	14540	470
BKDK1_40	11400	210	95400	1400	23090	330	87000	1300	16450	280	4028	48	12410	260
BKDK1_41	11190	200	96300	1400	23160	420	87500	1600	16630	290	4373	72	12790	260
BKDK1_42	10980	220	95700	1500	23290	430	87800	1600	16200	250	3930	71	12160	230
BKDK1_43	11300	190	97600	1700	23390	370	88500	1300	16220	300	3678	55	12140	230
BKDK1_44	12270	530	95700	2100	23090	640	86800	2400	16880	520	4410	130	14600	700
BKDK1_45	11460	180	95100	1400	23410	430	87900	1300	17100	380	4339	65	13160	250
BKDK1_46	11510	180	96500	1400	22890	350	87700	1400	16490	280	4240	62	12960	230
BKDK1_47	12980	480	97900	1900	23680	450	89800	1700	17140	360	4440	150	14930	680
BKDK1_48	13250	230	96300	1600	23430	450	87600	1800	17020	320	4390	120	14750	420
BKDK1_49	11390	240	98200	1800	23770	500	89500	1700	16380	310	3862	63	12440	240
BKDK1_50	10540	160	96800	1300	23010	350	87300	1400	16140	230	4068	66	12150	170
BKDK1_51	11690	180	98500	1500	22970	340	87900	1200	14960	230	3002	41	11510	170
BKDK1_52	10580	210	95100	1500	22970	340	86100	1400	16480	310	4170	110	13400	430
BKDK1_53	10530	560	94700	2300	22840	610	90000	2100	17570	490	4860	140	15500	370
BKDK1_54	9540	600	95900	2700	23380	520	89300	2100	16920	550	4550	170	13570	630
BKDK1_55	11760	160	95500	1300	23640	380	88600	1300	16460	270	3862	48	12490	200
BKDK1_56	10860	190	96700	1400	22870	300	85800	1000	16180	250	4105	56	12150	210
BKDK1_57	11510	270	96300	1500	23260	350	87000	1300	17050	270	4460	83	13650	360
BKDK1_58	10910	290	94900	2100	23030	410	87400	1800	16330	320	4207	75	12810	320
BKDK1_59	11030	160	96600	1400	23230	340	87600	1400	16230	260	4044	53	12400	200
BKDK1_60	12280	350	95800	1900	23490	590	88800	2200	16760	400	4330	130	14130	450
BK05_1	6800	260	100600	2500	22520	620	83600	2000	14240	410	2181	59	9070	200
BK05_2	7270	220	101100	1500	22600	550	84400	1900	13880	320	2114	55	9020	250
BK05_3	3900	150	107600	2800	22250	450	79700	2100	13510	360	1614	36	7970	230
BK05_4	3010	260	103400	1900	22620	420	83100	1400	13240	280	2009	54	7000	160
BK05_5	6580	330	101800	1500	22410	290	82800	1400	14300	220	2120	31	9380	200
BK05_6	4600	170	102600	1300	22710	350	84100	1100	14510	210	2482	38	9400	200
BK05_7	4400	290	98600	3000	22220	770	82100	2200	13340	480	2050	110	7790	210
BK05_8	5670	500	100200	1300	22630	270	84300	1200	14610	240	2111	68	9460	320
BK05_9	5850	390	98900	1600	22740	350	85800	1500	15580	270	2422	44	10350	210

BK05_10	4290	260	102000	2000	22420	380	80700	1400	13010	310	1579	43	7150	320
BK05_11	7400	230	99740	1400	22530	320	82600	1200	14440	210	2330	41	9560	150
BK05_12	4820	280	101900	1800	22530	370	83300	1300	14050	250	1862	41	8400	150
BK05_13	3450	460	101900	1600	22650	450	83800	1500	14280	230	1929	51	8510	240
BK05_14	4380	290	107700	1500	21810	320	79400	1200	13760	230	2053	33	8360	250
BK05_15	3320	160	98200	2700	22350	730	80000	2600	12270	380	1693	63	6420	230
BK05_16	7950	300	103600	3300	23500	910	83800	3200	15340	560	2053	63	9970	200
BK05_17	3050	240	99550	2700	23040	750	85800	2100	15070	580	1940	81	9340	290
BK05_18	532	22	98100	1800	22150	480	79700	1400	10270	220	713	19	3431	83
BK05_19	506	70	98900	3700	21210	640	77300	2900	8860	280	723	25	2980	140
BK05_20	4344	83	108400	1600	21540	300	75400	1100	13010	180	1928	38	7350	120
BK05_21	4570	220	109100	1700	21440	450	72900	1400	12730	290	1860	36	7260	180
BK05_22	5500	240	103800	2100	22550	460	83300	1900	14320	360	2030	99	9600	360
BK05_23	6660	240	105700	2100	22200	400	81200	1900	14370	300	1610	100	9900	240
BK05_24	4340	600	103700	2200	22530	470	82400	2100	13970	270	2870	110	8670	340
BK05_25	5610	450	107500	2600	21820	450	79400	1900	13370	370	2087	42	8430	310
BK05_26	4850	220	106100	2200	22520	450	82500	1700	14180	360	2134	40	8770	340
BK05_27	7620	260	100300	1900	22870	370	84800	1500	14450	250	2276	28	9290	190
BK05_28	1940	110	104700	3400	22110	790	77600	2600	11540	490	1158	55	5410	290
BK05_29	9500	4200	99920	1700	22520	460	82100	1700	12570	390	1710	100	7000	760
BK05_30	3260	250	102700	2000	22710	400	83700	1900	14100	290	2355	68	8150	190
BK05_31	912	51	100200	1700	22130	400	79200	1500	10600	190	814	24	3800	100
BK05_32	4970	440	104000	1400	22730	370	83900	1400	14720	300	2572	38	9090	240
BK05_33	5560	350	99730	1700	22430	430	83800	1800	13370	380	1923	79	8490	410
BK05_34	1910	190	96900	1500	22720	280	79700	1100	10520	170	951	36	4350	160
BK05_35	4330	200	103100	2000	22780	610	80800	1400	13760	400	2407	64	8070	180
BK05_36	2550	200	104300	2300	21960	610	80400	2400	13520	360	2110	40	7360	280
BK05_37	1750	120	108400	2000	21670	660	77900	2300	13050	420	2293	50	7190	200
BK05_38	6420	300	105300	1700	22590	350	85920	980	15440	210	2270	51	10910	210
BK05_39	6420	230	99200	1500	22360	330	82200	1600	14000	270	2196	44	8850	130
BK05_40	3110	350	104500	1400	22230	270	81000	1000	14350	210	2496	30	8390	190
BK05_41	3910	270	98000	3500	21990	720	80500	2100	12120	640	1640	110	5780	320
BK05_42	6570	260	100500	1600	22450	350	82800	1300	14160	270	2151	34	9240	200
BK05_43	6970	280	99510	2200	22610	550	83500	1900	13860	430	2094	45	8910	230
BK05_44	7890	130	99740	1300	22590	310	81900	1400	14300	220	2160	30	9540	140

BK05_45	7930	310	100500	1800	22860	360	84000	1700	14800	320	2320	60	10290	200
BK05_46	5290	230	100200	2200	22680	430	83500	1700	13790	240	2021	52	8700	270
BK05_47	6620	260	101200	1500	22690	340	83200	1200	14380	250	2347	48	9440	230
BK05_48	3620	280	106000	1800	22470	430	81800	1500	14140	260	2287	42	8120	180
KMT1_1	5920	190	102300	2400	22770	460	86600	1900	14980	400	2423	60	9860	320
KMT1_2	6230	180	101400	2200	22650	420	83900	1200	14920	240	2408	37	10070	170
KMT1_3	5605	80	103100	1400	22760	350	84100	1300	14580	240	2338	36	9120	160
KMT1_4	6730	200	105200	2900	22820	600	86400	2200	15090	360	2377	56	10060	320
KMT1_5	6730	200	101500	2400	23020	580	86800	1900	15610	360	2587	59	10610	220
KMT1_6	5580	240	104300	2800	22440	780	84400	2500	14820	530	2266	69	9120	400
KMT1_7	6040	360	102500	2500	22790	690	86400	3400	15500	860	2719	93	11100	440
KMT1_8	7880	240	102900	3000	22690	720	88900	3200	16080	470	2531	79	11430	380
KMT1_9	5130	340	104300	3800	22760	970	89300	4200	16050	730	2630	110	10620	380
KMT1_10	6160	200	103500	3800	23470	710	89400	2500	16080	470	2602	71	11310	400
KMT1_11	4530	150	101200	2400	23190	460	86500	1900	15520	360	2563	70	10180	270
KMT1_12	3970	100	102800	1700	22740	360	85700	1700	15190	270	2560	66	9680	310
KMT1_13	5360	190	101000	1800	22450	390	83800	1600	15060	370	2502	47	9780	230
KMT1_14	6420	140	101900	2400	22430	480	85900	2100	15250	370	2474	61	10570	360
KMT1_15	5990	100	101000	1600	22570	350	84400	1300	14830	250	2409	38	9260	180
KMT1_16	6650	140	102900	2400	22610	410	83700	1700	14770	330	2572	54	10170	220
KMT1_17	5260	110	102600	1900	22790	350	85600	1400	14840	240	2433	36	9210	150
KMT1_18	5790	390	103400	3400	23100	800	86100	2700	15650	660	2532	81	10980	240
KMT1_19	4980	120	100600	1500	22560	340	84600	1200	15040	240	2660	43	10150	190
KMT1_20	1390	160	109200	2600	21520	450	77500	2000	10340	260	312	45	4970	150
KMT1_21	6610	170	101900	3100	23040	670	87100	2300	15700	410	2635	51	11300	340
KMT1_22	7230	210	102400	2200	22610	520	85900	2600	15270	380	2632	61	10880	290
KMT1_23	7650	220	103200	2200	23270	590	86000	2300	15370	390	2758	68	11640	280
KMT1_24	5950	160	98200	1300	22480	340	81600	1200	15070	200	1899	77	8940	150
KMT1_25	8050	260	102600	2400	23340	470	86200	1900	16060	350	2490	51	11030	250
KMT1_26	7330	160	101000	2100	22560	420	83700	1400	14970	280	2468	41	10500	190
KMT1_27	5680	110	103100	1900	22890	430	85500	1700	15010	320	2541	56	10490	270
KMT1_28	7480	260	102300	2800	22820	840	83400	1900	15170	450	2685	98	11300	280
KMT1_29	5800	280	101300	1300	22630	310	84000	1200	14910	250	2456	57	9680	270
KMT1_30	6590	160	102700	1700	22640	340	84500	1400	14940	230	2507	43	10280	200

KMT1_31	4740	150	103900	2000	22960	370	85200	1500	14920	300	2521	38	9950	190
KMT1_32	5720	380	102700	1700	23050	390	86000	1600	15380	270	2622	57	9690	280
KMT1_33	8690	430	101700	2000	22820	430	85800	1500	16280	300	3073	65	12600	320
KMT1_34	6240	850	87900	4700	20800	830	72900	4700	13600	1000	2670	140	9000	1000
KMT1_35	10010	210	100700	2100	22970	490	85700	1500	15780	280	3027	46	11900	200
KMT1_36	8350	350	100600	1700	23110	390	86400	1500	15910	330	3086	50	12110	270
KMT1_37	8630	230	100400	2000	22750	450	85800	1800	15240	330	2475	86	10730	210
KMT1_38	8140	230	101400	2300	22440	440	83200	1500	15270	370	2984	48	11610	270
KMT1_39	6640	130	101200	1500	22660	400	85300	1400	15090	250	2366	37	9940	200
KMT1_40	6370	340	101500	1900	22520	510	84000	1600	14980	370	2453	46	10200	270
KMT1_41	9700	240	99600	2100	23270	410	87600	1700	16340	330	3006	73	12490	310
KMT1_42	8420	420	99560	2800	22510	540	82900	2200	15870	390	3062	89	11910	390
KMT1_43	5350	130	102500	1800	22780	460	86700	1800	15390	330	2450	70	9540	240
KMT1_44	9070	200	101000	2100	22270	560	83600	1500	15160	280	2947	52	11290	300

	Tb (ppm)	**2σ**	**Dy (ppm)**	**2σ**	**Ho (ppm)**	**2σ**	**Er (ppm)**	**2σ**	**Tm (ppm)**	**2σ**	**Yb (ppm)**	**2σ**	**Lu (ppm)**	**2σ**
BKDK1_1	1404	17	5336	70	544	9	718	17	46	2	142	7	10	1
BKDK1_2	1231	17	4812	68	532	7	770	13	53	1	175	5	13	1
BKDK1_3	1322	21	5028	75	532	7	743	14	49	2	161	6	12	1
BKDK1_4	1404	24	5227	91	521	11	684	20	42	2	137	6	9	1
BKDK1_5	1315	20	4990	84	498	8	636	12	39	1	124	5	8	0
BKDK1_6	1564	89	5470	200	544	9	735	23	48	3	165	12	12	1
BKDK1_7	934	19	3408	66	356	7	495	12	33	1	102	4	8	0
BKDK1_8	1071	23	3767	63	373	5	514	12	34	1	111	6	8	1
BKDK1_9	940	13	3625	54	396	6	614	11	47	1	166	5	13	1
BKDK1_10	1030	59	3150	190	266	17	303	24	17	2	52	5	4	0
BKDK1_11	1133	19	4095	73	405	9	565	17	38	2	123	6	9	1
BKDK1_12	1353	28	5102	99	502	11	639	16	37	1	116	5	8	1
BKDK1_13	1329	29	5060	110	522	14	722	22	49	2	158	8	12	1
BKDK1_14	1378	29	4982	88	488	14	613	18	38	2	119	5	8	1
BKDK1_15	1357	32	4986	92	499	12	654	17	41	1	136	6	9	0
BKDK1_16	1207	14	4496	68	442	8	548	12	33	1	103	4	7	0
BKDK1_17	1234	16	4704	59	472	7	616	10	38	1	119	4	8	0
BKDK1_18	1231	18	4448	83	446	10	559	14	35	1	111	5	8	1
BKDK1_19	1253	20	4421	97	415	12	525	21	32	1	98	5	7	0

BKDK1_20	1403	35	5210	130	541	12	733	18	46	2	154	6	11	0
BKDK1_21	1321	20	5113	74	516	10	674	15	42	1	133	5	9	1
BKDK1_22	1275	24	4677	74	475	14	616	27	38	2	119	9	8	1
BKDK1_23	1380	31	5187	98	522	12	673	16	42	2	131	5	9	1
BKDK1_24	1325	18	5048	79	509	11	637	14	39	1	119	5	8	0
BKDK1_25	1477	47	5490	140	537	14	652	18	41	2	126	5	8	1
BKDK1_26	1344	33	5070	130	528	13	735	19	50	2	169	7	13	1
BKDK1_27	1355	18	5111	79	512	9	667	13	42	1	132	5	9	1
BKDK1_28	1378	20	5242	70	536	7	685	13	43	1	136	5	9	0
BKDK1_29	1383	27	5253	91	523	12	654	12	40	1	126	5	8	1
BKDK1_30	1037	56	3270	180	280	15	324	18	19	1	57	5	4	1
BKDK1_31	1390	20	5220	72	537	8	695	12	44	1	136	5	9	1
BKDK1_32	1504	63	5360	150	498	10	609	18	38	2	114	7	8	1
BKDK1_33	1281	24	4994	98	508	9	662	14	40	1	129	5	9	1
BKDK1_34	1365	21	5075	98	501	13	647	17	40	1	133	5	9	0
BKDK1_35	1268	30	4940	110	500	12	639	15	40	1	127	5	9	0
BKDK1_36	1368	25	5110	110	524	15	690	27	44	2	140	9	10	1
BKDK1_37	1258	27	4650	88	450	11	558	18	34	1	105	4	7	0
BKDK1_38	1296	19	4882	63	506	7	689	11	47	1	151	5	10	1
BKDK1_39	1583	46	5450	120	512	12	630	22	39	2	116	7	8	1
BKDK1_40	1352	22	5163	74	527	9	694	17	44	2	140	6	10	1
BKDK1_41	1399	27	5236	82	512	9	634	11	39	1	113	4	7	0
BKDK1_42	1313	21	5014	89	513	9	682	16	43	2	138	5	9	1
BKDK1_43	1298	22	4967	78	524	9	730	12	47	1	154	4	11	0
BKDK1_44	1565	50	5500	160	517	16	639	24	38	3	121	10	8	1
BKDK1_45	1470	23	5529	87	539	10	652	13	39	1	118	4	7	1
BKDK1_46	1432	21	5302	87	524	8	673	14	42	1	127	5	9	0
BKDK1_47	1618	74	5680	170	556	11	707	15	45	2	137	5	10	1
BKDK1_48	1597	37	5645	91	541	11	709	21	45	2	141	9	10	1
BKDK1_49	1320	21	5057	94	525	10	716	19	47	2	156	7	12	1
BKDK1_50	1319	20	4978	70	492	7	628	10	39	1	118	4	8	1
BKDK1_51	1191	16	4684	61	531	9	798	15	58	2	200	6	15	1
BKDK1_52	1397	35	4884	83	466	16	594	27	36	2	111	8	8	1
BKDK1_53	1569	44	4730	170	382	19	430	32	27	3	84	9	6	1
BKDK1_54	1358	34	4630	230	415	39	496	65	27	4	84	13	6	1

BKDK1_55	1354	17	5198	76	544	7	744	13	48	1	155	5	11	0
BKDK1_56	1343	21	5105	83	511	8	652	12	41	1	126	4	8	0
BKDK1_57	1494	32	5504	96	522	9	641	14	37	1	115	3	7	0
BKDK1_58	1400	28	5184	99	490	12	596	17	35	2	102	5	7	1
BKDK1_59	1337	19	5155	81	518	8	678	13	42	1	129	4	9	1
BKDK1_60	1526	50	5530	110	531	11	681	21	44	2	138	7	10	1
BK05_1	877	21	3008	79	274	9	331	14	21	1	72	5	7	1
BK05_2	888	28	3170	130	286	10	334	24	19	4	81	32	10	5
BK05_3	695	15	2179	50	190	6	232	9	15	1	47	4	5	1
BK05_4	555	14	1591	73	129	9	143	14	9	2	38	14	4	2
BK05_5	938	34	3140	130	271	11	293	9	15	1	38	3	2	0
BK05_6	837	22	2429	66	191	6	188	6	9	1	21	1	1	0
BK05_7	675	24	2180	100	189	11	201	10	9	1	23	2	1	0
BK05_8	883	47	2790	200	228	19	232	21	10	1	21	2	1	0
BK05_9	955	30	2950	140	249	13	271	14	14	1	37	3	3	0
BK05_10	632	38	2100	150	190	14	231	17	16	2	60	8	5	1
BK05_11	958	20	3330	94	298	8	348	12	21	2	70	9	8	2
BK05_12	740	22	2350	100	202	11	220	12	12	1	38	5	4	1
BK05_13	697	41	1960	180	150	17	146	19	7	1	13	2	1	0
BK05_14	745	33	2330	130	196	11	219	11	12	1	31	2	2	0
BK05_15	552	15	1681	52	142	5	148	7	8	1	25	3	2	0
BK05_16	1009	30	3730	120	356	14	399	20	20	1	57	3	4	1
BK05_17	747	18	1984	63	156	10	185	21	14	3	55	17	4	2
BK05_18	174	4	368	11	23	1	22	2	1	0	2	1	0	0
BK05_19	144	6	303	16	23	3	27	6	2	1	8	4	1	0
BK05_20	684	10	2231	32	219	4	355	7	32	1	134	4	12	1
BK05_21	695	23	2295	81	228	11	355	23	29	2	105	8	8	1
BK05_22	896	32	2840	100	239	8	261	7	14	1	38	4	2	0
BK05_23	983	26	3318	98	303	9	361	8	20	1	56	3	4	0
BK05_24	744	59	2250	240	186	24	201	24	10	1	23	3	2	0
BK05_25	834	42	2750	180	242	18	261	19	13	1	32	2	2	0
BK05_26	792	31	2480	110	214	10	234	10	13	1	33	2	2	0
BK05_27	947	23	3413	94	316	10	342	13	17	1	38	3	2	0
BK05_28	417	25	1176	72	94	8	105	8	6	1	18	3	1	0

BK05_29	670	150	2900	1000	420	190	1010	470	99	49	820	410	88	45
BK05_30	635	16	1798	69	149	9	159	13	8	1	23	3	2	0
BK05_31	234	10	578	33	42	3	43	4	2	0	6	1	0	0
BK05_32	824	39	2530	170	212	16	223	16	11	1	26	2	2	0
BK05_33	815	46	2690	150	223	13	226	13	10	1	23	2	1	0
BK05_34	307	20	937	75	81	8	89	9	7	2	41	18	3	1
BK05_35	696	23	2145	76	187	8	223	15	14	2	54	10	6	2
BK05_36	559	32	1570	110	123	9	150	10	10	1	37	2	4	1
BK05_37	506	18	1222	65	91	6	108	10	7	1	23	4	2	0
BK05_38	1003	28	3170	110	276	9	328	9	18	1	49	3	3	0
BK05_39	877	20	3000	84	261	10	267	8	13	1	30	2	2	0
BK05_40	679	36	1840	140	140	13	143	13	7	1	19	2	1	0
BK05_41	464	29	1525	86	169	9	286	25	32	2	171	12	21	3
BK05_42	910	24	3075	98	271	9	288	11	14	1	32	2	2	0
BK05_43	891	25	3193	97	268	10	289	14	15	2	47	8	5	1
BK05_44	1001	14	3543	56	315	5	333	6	15	1	36	2	2	0
BK05_45	1046	27	3590	130	315	11	343	11	16	1	41	2	2	0
BK05_46	816	28	2610	110	215	7	231	10	11	1	29	4	2	0
BK05_47	918	20	3061	86	273	8	310	9	16	1	43	3	3	0
BK05_48	679	26	1970	110	156	10	159	11	7	1	17	2	1	0
KMT1_1	899	33	2872	79	270	8	342	10	22	1	71	4	5	0
KMT1_2	935	17	2988	57	281	7	379	10	26	1	90	4	7	0
KMT1_3	838	12	2718	37	262	4	356	7	25	1	78	2	6	0
KMT1_4	975	29	3127	90	288	8	368	13	25	1	82	6	7	1
KMT1_5	1023	23	3221	68	271	8	319	11	18	1	54	3	4	0
KMT1_6	816	38	2610	120	246	11	340	14	23	2	86	5	7	1
KMT1_7	1016	40	3010	130	228	18	235	19	13	2	35	4	3	0
KMT1_8	1129	35	3700	120	322	10	381	16	19	1	55	6	4	1
KMT1_9	938	26	2660	110	201	13	233	23	13	2	38	7	3	1
KMT1_10	1024	32	3027	85	251	9	283	13	16	2	43	5	3	0
KMT1_11	875	21	2364	72	184	8	207	11	13	1	40	3	3	0
KMT1_12	830	26	2339	62	173	5	183	7	10	1	31	2	3	0
KMT1_13	874	24	2716	86	238	9	280	14	17	1	56	4	4	0
KMT1_14	987	25	3047	73	265	7	333	16	21	1	74	8	6	1

KMT1_15	842	13	2780	39	274	5	376	9	26	1	89	3	7	0
KMT1_16	969	19	3032	55	259	5	284	9	15	1	42	2	3	0
KMT1_17	806	12	2504	43	241	5	341	9	25	1	91	3	8	0
KMT1_18	1004	32	2980	140	238	19	258	24	14	2	40	5	3	0
KMT1_19	910	15	2593	46	207	6	235	10	14	1	39	3	3	0
KMT1_20	348	14	927	56	76	7	83	10	5	1	14	2	1	0
KMT1_21	1066	27	3120	87	248	7	277	7	16	1	46	4	3	0
KMT1_22	1070	18	3378	79	281	8	317	14	17	1	49	4	3	1
KMT1_23	1114	18	3549	80	306	8	342	11	17	1	52	4	4	0
KMT1_24	905	15	3143	57	302	7	449	14	38	2	159	10	14	1
KMT1_25	1063	31	3700	110	346	9	415	14	24	2	75	6	5	1
KMT1_26	1023	15	3433	57	314	6	391	7	22	1	63	3	5	0
KMT1_27	980	28	2958	61	241	5	274	8	17	1	56	3	4	0
KMT1_28	1105	25	3590	99	296	9	316	15	16	1	41	6	3	0
KMT1_29	879	29	2840	120	266	11	337	13	20	1	66	4	5	1
KMT1_30	987	22	3154	68	276	5	324	8	19	1	56	3	4	0
KMT1_31	891	17	2559	58	203	7	225	12	13	1	39	4	3	0
KMT1_32	877	32	2820	140	271	19	356	31	23	2	73	8	6	1
KMT1_33	1308	45	4010	160	337	17	388	22	22	2	69	5	5	1
KMT1_34	930	110	2980	370	237	34	242	40	14	2	39	7	3	1
KMT1_35	1300	26	4490	110	389	11	416	13	21	1	50	3	3	0
KMT1_36	1242	27	3920	130	321	15	345	15	17	1	46	3	3	0
KMT1_37	1105	23	3797	76	347	7	403	12	22	1	62	5	4	1
KMT1_38	1216	27	3890	110	319	10	324	10	15	1	38	2	3	0
KMT1_39	925	17	3044	51	293	5	401	8	28	1	97	4	8	0
KMT1_40	961	28	3030	150	261	15	298	14	17	1	50	3	3	0
KMT1_41	1319	28	4450	100	385	10	427	13	22	1	59	4	4	0
KMT1_42	1232	45	4020	150	332	17	359	21	19	1	47	4	4	0
KMT1_43	855	21	2725	63	247	6	316	11	20	1	63	3	5	0
KMT1_44	1226	24	4127	84	361	8	400	10	20	1	49	3	4	0
	Th (ppm)	**2σ**	**U (ppm)**	**2σ**										
BKDK1_1	109000	4200	3440	120										
BKDK1_2	140800	3600	2549	47										
BKDK1_3	121600	3100	3027	97										

BKDK1_4	102500	3400	4060	260
BKDK1_5	80700	1900	3136	76
BKDK1_6	134600	6800	11900	2200
BKDK1_7	3160	150	3058	49
BKDK1_8	4190	490	7090	700
BKDK1_9	668	20	3459	71
BKDK1_10	6060	330	14010	800
BKDK1_11	10200	1000	7010	660
BKDK1_12	78400	1800	4250	190
BKDK1_13	127800	4500	4170	430
BKDK1_14	79500	3700	6770	940
BKDK1_15	29100	2800	10120	500
BKDK1_16	37100	1600	6120	250
BKDK1_17	22100	1100	6640	200
BKDK1_18	68000	1900	4670	220
BKDK1_19	71800	3200	7700	640
BKDK1_20	122300	3000	4880	180
BKDK1_21	107900	3700	3630	190
BKDK1_22	86400	6300	4180	650
BKDK1_23	100600	2400	4560	620
BKDK1_24	92500	3000	3445	57
BKDK1_25	113900	4400	6310	730
BKDK1_26	135800	4600	4870	490
BKDK1_27	96300	3100	3345	82
BKDK1_28	96600	1700	3421	55
BKDK1_29	28600	1300	6640	180
BKDK1_30	6310	710	11600	1400
BKDK1_31	113000	2800	4230	150
BKDK1_32	101400	2400	8400	1000
BKDK1_33	86000	3000	4100	100
BKDK1_34	104700	2500	5460	360
BKDK1_35	69200	6900	4720	240
BKDK1_36	108900	7400	4520	560
BKDK1_37	50600	2300	5080	710
BKDK1_38	118000	2300	3670	250

BKDK1_39	94800	5500	9520	830
BKDK1_40	108400	5500	3625	91
BKDK1_41	87000	1800	5240	180
BKDK1_42	110100	4200	3135	71
BKDK1_43	129000	2500	2951	68
BKDK1_44	102800	5000	9700	1700
BKDK1_45	83300	2600	4340	280
BKDK1_46	96000	1800	4620	330
BKDK1_47	115200	2600	10000	2000
BKDK1_48	119100	5600	11930	520
BKDK1_49	120700	4700	3101	62
BKDK1_50	75300	4000	3990	160
BKDK1_51	137300	2700	2211	46
BKDK1_52	98200	2900	8100	1500
BKDK1_53	100000	10000	15000	1200
BKDK1_54	87300	4400	8900	2000
BKDK1_55	132200	2300	3205	43
BKDK1_56	84700	1700	3300	170
BKDK1_57	95000	3800	6860	550
BKDK1_58	70600	3100	5880	730
BKDK1_59	97200	2000	3201	55
BKDK1_60	111300	4200	7300	1000
BK05_1	13350	400	2498	79
BK05_2	14200	1700	4040	900
BK05_3	22000	580	667	81
BK05_4	16200	1300	990	130
BK05_5	19780	440	2470	150
BK05_6	22360	750	3050	180
BK05_7	12420	420	1336	55
BK05_8	17800	1600	1810	220
BK05_9	23700	1100	3690	260
BK05_10	14600	1700	1190	100
BK05_11	15710	590	2922	99
BK05_12	9020	410	1890	190

BK05_13	9020	910	780	180
BK05_14	16990	380	1830	240
BK05_15	11670	500	1076	52
BK05_16	16190	620	2790	110
BK05_17	18600	1000	1240	150
BK05_18	2300	54	57	24
BK05_19	4200	360	105	46
BK05_20	13010	290	272	5
BK05_21	12400	1700	310	22
BK05_22	24370	930	2460	270
BK05_23	28950	610	1770	220
BK05_24	17000	1900	1670	310
BK05_25	20100	1200	1390	170
BK05_26	19600	1800	1540	160
BK05_27	11360	470	2860	160
BK05_28	9590	840	134	34
BK05_29	104000	47000	9700	4100
BK05_30	12340	510	1190	140
BK05_31	5460	290	570	170
BK05_32	18100	1200	1760	210
BK05_33	17500	1000	1920	190
BK05_34	5190	410	401	49
BK05_35	16600	2100	1510	150
BK05_36	15050	920	561	83
BK05_37	8100	530	199	39
BK05_38	30400	1100	4210	430
BK05_39	13450	580	2615	64
BK05_40	18100	1300	1140	220
BK05_41	14030	510	1625	68
BK05_42	17400	1100	2444	79
BK05_43	14200	1200	2480	160
BK05_44	18450	540	2659	56
BK05_45	20700	1000	4420	250
BK05_46	19400	1200	2910	230
BK05_47	20600	1400	4280	260

BK05_48	10910	340	1000	120
KMT1_1	26400	1700	1870	450
KMT1_2	8400	180	1553	34
KMT1_3	10350	190	709	49
KMT1_4	29700	2300	2450	220
KMT1_5	40900	1100	3570	120
KMT1_6	25400	3500	1650	210
KMT1_7	39200	3000	4830	230
KMT1_8	42600	2400	2530	140
KMT1_9	39000	2000	4570	290
KMT1_10	45100	2400	4540	160
KMT1_11	32650	960	4150	220
KMT1_12	21580	890	2620	300
KMT1_13	24900	1300	2030	270
KMT1_14	31900	1800	2960	320
KMT1_15	8820	250	638	40
KMT1_16	14820	390	3113	66
KMT1_17	17330	390	1642	56
KMT1_18	39800	2400	4290	310
KMT1_19	27900	1000	2860	150
KMT1_20	12650	670	650	120
KMT1_21	34800	1100	4440	150
KMT1_22	11050	320	3105	94
KMT1_23	15750	640	3603	78
KMT1_24	8490	150	785	63
KMT1_25	42600	2000	1970	130
KMT1_26	15510	640	2402	63
KMT1_27	14330	600	3090	260
KMT1_28	31500	2000	4000	120
KMT1_29	13200	1700	950	180
KMT1_30	13760	440	2460	140
KMT1_31	14820	540	2600	110
KMT1_32	11700	1500	640	110
KMT1_33	23330	890	7470	320

KMT1_34	27600	3900	4770	240
KMT1_35	70500	2300	3490	180
KMT1_36	30300	1500	4760	130
KMT1_37	37500	1700	2400	100
KMT1_38	24380	730	4160	210
KMT1_39	26740	690	1760	110
KMT1_40	34310	860	3400	130
KMT1_41	66500	4100	4640	260
KMT1_42	46300	3100	6650	360
KMT1_43	25500	2100	1170	280
KMT1_44	24870	820	3690	120

APPENDIX K: APATITE TRACE ELEMENTS RESULTS

	Mn (ppm)	**2σ**	**Sr (ppm)**	**2σ**	**^{206}Pb (ppm)**	**2σ**	**^{207}Pb (ppm)**	**2σ**	**^{208}Pb (ppm)**	**2σ**	**Th (ppm)**	**2σ**	**U (ppm)**	**2σ**
Standard:														
NIST610_1	450.1	6.3	516.2	7.6	422.3	6.3	423.5	5.6	421.4	6.4	452.6	6	457.9	6.5
NIST610_2	449	6.3	519.2	7.8	429.4	5.8	428.2	5.8	428.6	6.1	461.2	6.1	464.6	6.3
NIST610_3	435.5	6.1	509.8	8.2	422.2	5.9	422	5.9	420.8	6.8	453.7	6.7	456.7	6.7
NIST610_4	440	5.8	515	7.8	428.6	5.5	430.5	5.2	431.5	5.9	460.8	5.7	466.2	5.7
NIST610_5	440.9	6.9	519.8	7.1	422.1	6.2	422.9	5.7	424.4	6.4	453.6	6.7	457.5	7.3
NIST610_6	442.7	7.1	513.6	7.3	426.9	5.3	425.1	4.9	425.4	5.4	457.3	5.9	460.8	5.6
NIST610_7	442.3	6.5	515.2	6.5	427.3	5.1	427.9	5.9	427.5	6.1	458.9	5.7	462.6	5.7
NIST610_8	446.6	6.2	516.2	7.6	429.1	6.2	428.9	6.1	428.7	5.6	461.2	6.4	465.4	7.2
NIST610_9	443.9	7.4	512.6	7.8	426.6	6.8	424.3	6.5	421.1	7.1	455.5	6.7	458.2	6.9
NIST610_10	440	6.9	513.8	7.5	427.1	5.5	427.2	5.3	430.7	5.8	457.9	6.1	463.1	6.3
NIST610_11	450.4	7.3	514.2	8.5	427.7	6.4	426.7	6	428.3	6.5	457.5	6	463.3	6.9
NIST610_12	439.2	6	516.5	6.3	426.2	5.5	427.4	4.7	425.1	6	458.2	6	462.5	5.7
NIST610_13	448.5	6.7	515.4	6.1	421.6	5.1	424.1	5.3	420.5	4.9	453.5	5.6	458.4	5.8
NIST610_14	440.6	6.7	508.3	7.4	417.8	6.1	417.7	6	417.8	6.4	447.9	6.8	455	7
NIST610_15	451.9	5.8	521.9	8	431.1	6.5	429.7	6.2	431.4	6	462.8	6.3	465.8	7.2
NIST610_16	441.1	7.6	517.6	8.3	429.7	7	430.5	6.9	431	7.7	461	7.4	466.2	7.5
NIST610_17	446.2	7.3	511	7.7	419.6	6.5	419.4	6.4	419.4	7.1	449.3	7.3	453.5	7.6
NIST610_18	449	6.7	521.3	6.5	429.4	5.8	426.8	5.9	430.8	6.8	460	6.4	465	7

NIST610_19	449.1	7	520	6.9	431.3	5.6	431.2	4.9	430.7	6.7	463.1	6	467.1	6.4
NIST610_20	436.7	7.7	511.2	9	426.5	7.3	424.3	7.2	428.4	7.9	455.8	7.8	460	7.9
NIST610_21	445.1	7.6	517.6	8.8	429.1	7.3	428.6	7.2	429.6	7.8	458.8	7.9	462.4	7.3
NIST610_22	435.1	7	507.8	8.2	425.5	6.4	424.9	6.3	423.7	6.2	455.7	7.2	457.9	7.1
NIST610_23	448.4	7.8	515.6	8.8	421.7	7	420.8	7.1	423.8	7.5	453.2	7.4	457.4	7.8
NIST610_24	447.4	7.6	516.6	7.8	426.7	6	426.2	5.7	427.6	6.1	459.8	5.7	463.1	6.6
NIST610_25	447.8	7.1	514.4	7.8	423.7	6.2	423	6.3	423.3	6.6	454	6.5	456.2	6.9
NIST610_26	449.2	7.8	522.8	7.3	430.5	5.7	430.5	5.8	430	6.9	461	6.2	466.4	6.5
NIST610_27	442.2	8	516.5	7.6	423.6	5.9	425.4	6.2	424.1	6.3	457.1	6.8	464.1	7.3
NIST610_28	445.5	6.5	513.5	7.7	428.2	5.7	428.3	5.8	430.1	6.1	458.9	6.5	463.8	6.4
NIST610_29	442.3	6.6	514.2	7.7	425.5	5.7	427.1	5.8	423.1	5.9	456.3	6.5	461.9	7
NIST610_30	439.2	7.3	509.7	8.6	420.6	6.3	421.3	6	421.3	7.2	451.2	6.8	457.1	6.8
NIST610_31	439.9	6.8	514.3	8.5	423.8	6.6	427.1	6.7	423.5	6.7	456.8	7.2	461	8
NIST610_32	435.6	7.4	511.4	8.3	421.6	6.4	420	6.2	421.7	7.1	453.2	6.2	458.6	6.5
NIST610_33	439.2	6.3	511.1	7	421.9	5.4	420.9	5.4	419.9	5.9	451.6	6	456.1	6
NIST610_34	453.2	6.1	526	7.9	437.8	6	437.4	6.1	439.4	6.3	469.3	6.3	472.4	7

	Mn (ppm)	**2σ**	**Sr (ppm)**	**2σ**	**^{206}Pb (ppm)**	**2σ**	**^{207}Pb (ppm)**	**2σ**	**^{208}Pb (ppm)**	**2σ**	**Th (ppm)**	**2σ**	**U (ppm)**	**2σ**
Unknowns:														
BKBDG2_1	100.76	0.83	51.77	0.53	2.57	0.05	2.41	0.05	2.43	0.05	0	0	0.25	0.01
BKBDG2_2	100.25	0.92	39.27	0.37	2.08	0.05	1.91	0.05	1.95	0.06	0	0	0.3	0
BKBDG2_3	100.5	1.1	48.64	0.69	2.1	0.04	1.93	0.04	1.95	0.05	0	0	0.29	0.01
BKBDG2_4	96.92	0.89	41.22	0.44	1.81	0.02	1.65	0.02	1.68	0.03	0	0	0.31	0
BKBDG2_5	98.2	1.2	53.2	0.8	2.69	0.05	2.47	0.04	2.5	0.05	0	0	0.21	0.01
BKBDG2_6	100.15	0.93	52.46	0.46	2.62	0.04	2.45	0.04	2.49	0.05	0	0	0.24	0
BKBDG2_7	104.24	0.78	52.08	0.41	2.45	0.02	2.27	0.02	2.29	0.03	0	0	0.29	0
BKBDG2_8	101.86	0.94	50.98	0.49	2.52	0.05	2.32	0.05	2.36	0.05	0	0	0.29	0.01
BKBDG2_9	105.3	1	52.69	0.48	2.5	0.04	2.35	0.03	2.35	0.04	0	0	0.25	0
BKBDG2_10	103.6	1.2	52.47	0.39	2.57	0.03	2.39	0.03	2.41	0.03	0	0	0.28	0
BKBDG2_11	99.57	0.89	52.52	0.48	2.6	0.04	2.42	0.04	2.46	0.05	0	0	0.26	0.01
BKBDG2_12	101	1	52.13	0.41	2.38	0.02	2.21	0.02	2.22	0.03	0	0	0.29	0.01
BKBDG2_13	104.07	0.96	53.3	0.5	2.58	0.05	2.4	0.05	2.48	0.05	0	0	0.24	0
BKBDG2_14	102.8	1.2	54.82	0.5	2.57	0.03	2.41	0.03	2.47	0.03	0	0	0.22	0
BKBDG2_15	101.11	0.87	53.45	0.45	2.55	0.02	2.38	0.02	2.42	0.03	0	0	0.27	0
BKBDG2_16	108.6	1.5	55.56	0.8	3.17	0.06	2.96	0.05	2.98	0.07	0	0	0.25	0.01

BKBDG2_17	100.2	1.2	53.32	0.57	2.99	0.12	2.78	0.11	2.86	0.12	0	0	0.23	0
BKBDG2_18	102.2	1.2	51.78	0.68	2.31	0.03	2.15	0.03	2.18	0.04	0	0	0.23	0.01
BKBDG2_19	101.4	1.2	54.75	0.51	2.64	0.04	2.47	0.03	2.52	0.04	0	0	0.23	0
BKBDG2_20	49.24	0.37	7.46	0.07	0.72	0.01	0.59	0.01	0.6	0.01	0.12	0	0.38	0.01
BKBDG2_21	65.99	0.65	8.02	0.1	0.93	0.01	0.77	0.01	0.78	0.02	0.07	0	0.36	0
BKBDG2_22	97.6	0.96	31.12	0.3	1.8	0.02	1.64	0.02	1.65	0.03	0.01	0	0.34	0
BKBDG2_23	95.7	1	43.64	0.53	2.41	0.02	2.24	0.02	2.29	0.03	0	0	0.25	0
BKBDG2_24	53.61	0.64	9.83	0.11	0.84	0.02	0.73	0.02	0.75	0.02	0.07	0	0.3	0.01
BKBDG2_25	57.28	0.89	12.08	0.17	1.18	0.02	1	0.02	1	0.02	0.1	0	0.48	0.01
BKBDG2_26	52.15	0.5	8.88	0.09	0.92	0.02	0.73	0.01	0.76	0.02	0.31	0.03	0.55	0.03
BKBDG2_27	47.44	0.44	7.4	0.08	0.67	0.01	0.57	0.01	0.58	0.01	0.1	0	0.31	0.01
BKBDG2_28	47.61	0.65	9.79	0.13	0.91	0.03	0.77	0.03	0.78	0.04	0.1	0	0.39	0.01
BKBDG2_29	113	25	10.84	0.21	1.17	0.02	1	0.01	1.02	0.02	0.05	0	0.36	0.01
BKBDG2_30	104.8	1.2	73.41	0.66	2.74	0.05	2.46	0.05	2.5	0.05	0.02	0	0.61	0.01
BKBDG2_31	102.5	3	69.33	0.62	2.5	0.04	2.26	0.04	2.3	0.04	0.02	0	0.55	0.01
BKBDG2_32	54.43	0.58	11.23	0.11	0.95	0.02	0.8	0.01	0.81	0.02	0.11	0	0.4	0.01
BKBDG2_33	53.27	0.58	10.16	0.12	0.95	0.02	0.79	0.01	0.81	0.01	0.2	0	0.45	0.01
BKBDG2_34	52.04	0.61	10.29	0.1	0.9	0.02	0.77	0.02	0.79	0.02	0.26	0	0.4	0.01
BKBDG2_35	54.31	0.55	9.76	0.09	0.79	0.02	0.65	0.01	0.66	0.01	0.09	0	0.37	0.01
BKBDG2_36	101.86	0.96	59.26	0.47	2.79	0.03	2.6	0.03	2.65	0.04	0	0	0.32	0
BKBDG2_37	94.9	1.1	74.19	0.62	2.43	0.05	2.18	0.04	2.22	0.05	0.01	0	0.55	0.01
BKBDG2_38	98.3	1	65.63	0.53	1.66	0.03	1.51	0.02	1.51	0.02	0.01	0	0.34	0
BKBDG2_39	107.74	0.94	81.34	0.61	3.05	0.04	2.81	0.03	2.91	0.04	0.01	0	0.31	0
BKBDG2_40	100.06	0.88	76.52	0.63	2.95	0.03	2.67	0.03	2.72	0.03	0.01	0	0.62	0.01
BKBDG2_41	107.9	1.1	75.39	0.63	2.9	0.05	2.62	0.04	2.64	0.05	0	0	0.59	0.01
BKBDG2_42	110.4	1.2	73.76	0.74	2.83	0.03	2.55	0.03	2.62	0.03	0.01	0	0.63	0.01
BKBDG2_43	91.56	0.95	70.6	0.6	2.58	0.04	2.32	0.04	2.35	0.04	0.02	0	0.56	0.01
BKBDG2_44	71.98	0.78	22.09	0.19	1.19	0.03	1.04	0.02	1.06	0.03	0.07	0	0.4	0.01
BKBDG2_45	99.8	1	71.05	0.66	1.7	0.02	1.55	0.02	1.59	0.03	0	0	0.31	0
BKBDG2_46	94.43	0.87	44.03	0.52	2.19	0.03	2.05	0.02	2.04	0.03	0	0	0.23	0
BKBDG2_47	95.36	0.7	68.4	0.53	1.43	0.02	1.29	0.02	1.32	0.02	0	0	0.33	0
BKBDG2_48	106	1.1	82.7	1.2	3.14	0.08	2.94	0.08	2.95	0.08	0.01	0	0.29	0.01
BKBDG2_49	99.2	1.3	75.97	0.85	2.78	0.06	2.52	0.05	2.55	0.05	0.01	0	0.59	0.01
BKBDG2_50	97.3	1.1	75.16	0.59	2.68	0.05	2.4	0.04	2.45	0.05	0.01	0	0.62	0.01
BKBDG2_51	90.24	0.83	51.04	0.5	1.33	0.01	1.22	0.01	1.23	0.02	0	0	0.27	0
BKBDG2_52	95.4	2	50.6	1.4	1.9	0.06	1.74	0.05	1.76	0.06	0.01	0	0.22	0.01

BK11_1	66.94	0.98	52.54	0.58	2.14	0.05	2	0.04	2.05	0.05	0.05	0.02	0.14	0
BK11_2	73.48	0.71	55.64	0.46	2.19	0.05	1.92	0.04	1.97	0.04	0.56	0.02	0.68	0.03
BK11_3	28.2	1.9	22.7	1.4	0.84	0.06	0.79	0.07	0.8	0.07	0.01	0	0.06	0
BK11_4	49.1	3.8	39.5	3	1.4	0.1	1.31	0.09	1.34	0.09	0.01	0	0.1	0.01
BK11_5	7.12	0.31	6.75	0.08	0.06	0.02	0.01	0	0	0	0.04	0.01	0.15	0.06
BK11_6	31.9	1.8	27.1	1.1	0.94	0.05	0.88	0.05	0.9	0.05	0	0	0.07	0.01
BK11_7	35.2	5.8	29.2	4.3	0.95	0.16	0.89	0.15	0.91	0.16	0	0	0.06	0.01
BK11_8	31.8	3.6	27.2	2.7	1.13	0.14	0.92	0.11	0.94	0.12	0.55	0.14	0.6	0.11
BK11_9	65.7	2.9	51.1	1.8	2.04	0.09	1.95	0.08	1.99	0.09	0	0	0.1	0
BK11_10	35.7	3.7	29.8	2.7	1.05	0.12	0.99	0.11	1.01	0.11	0.01	0	0.06	0.01
BK11_11	43.5	1.3	35.21	0.87	1.31	0.04	1.23	0.04	1.24	0.05	0.02	0	0.08	0
BK11_12	59.4	1.6	47.9	1	1.8	0.06	1.69	0.05	1.71	0.06	0.04	0	0.11	0
BK11_13	55.7	1.5	45.82	0.84	1.64	0.04	1.54	0.04	1.57	0.04	0.01	0	0.1	0
BK11_14	38.8	2	32.7	1.4	1.17	0.07	1.11	0.06	1.12	0.07	0.05	0	0.1	0
BK11_15	54.2	4.6	42.7	3.7	1.76	0.09	1.62	0.09	1.64	0.1	0.07	0.01	0.18	0.01
BK11_16	54.8	3.7	44.1	2.3	1.7	0.12	1.6	0.11	1.63	0.12	0	0	0.09	0.01
BK11_17	38.7	1.9	31.5	1.3	1.11	0.06	1.05	0.06	1.08	0.06	0	0	0.07	0
BK11_18	74	0.9	57	0.53	2.07	0.04	1.95	0.04	1.98	0.04	0.01	0	0.14	0
BK11_19	53.31	0.89	41.95	0.94	1.68	0.02	1.56	0.02	1.56	0.03	0.02	0.01	0.11	0.01
BK11_20	59.9	1.8	48.2	1.5	2.17	0.1	1.91	0.08	1.99	0.09	0.03	0	0.14	0.01
BK11_21	41.8	2.3	34.4	1.7	1.18	0.07	1.13	0.07	1.14	0.07	0	0	0.07	0.01
BK11_22	35.3	2.6	28.4	2.1	0.96	0.07	0.91	0.07	0.91	0.08	0.01	0	0.06	0.01
BK11_23	23.7	1.8	6.96	0.12	0.43	0.05	0.36	0.05	0.39	0.06	0.13	0.02	0.16	0.02
BK11_24	23.1	4.6	21.5	3.5	0.98	0.13	0.89	0.12	0.95	0.12	0.1	0.03	0.07	0.01
BK11_25	20.6	1.8	18.5	1.4	0.76	0.03	0.67	0.03	0.68	0.03	0.08	0.01	0.18	0.02
BK11_26	20.4	4	37	13	2.77	0.79	2.46	0.67	2.4	0.67	0.18	0.03	0.21	0.06
BK11_27	48.8	3	38.6	2.3	1.61	0.12	1.52	0.11	1.55	0.11	0.05	0.01	0.09	0.01
BK11_28	35.2	4.9	31.5	4	0.98	0.15	0.91	0.14	0.92	0.15	0.01	0	0.07	0.01
BK11_29	60.3	1.4	48.34	0.76	2.04	0.07	1.92	0.07	1.96	0.08	0	0	0.1	0
BK11_30	34.1	4.5	28.4	3.1	1.25	0.14	1.19	0.14	1.22	0.14	0.06	0	0.09	0.01
BK11_31	89	25	15.4	2.5	2.85	0.76	2.34	0.63	2.29	0.62	0.07	0.02	0.21	0.04
BK11_32	38.4	4.6	32	3.5	1.2	0.16	1.12	0.15	1.12	0.15	0	0	0.07	0.01
BK11_33	7.77	0.1	7.39	0.08	0.01	0	0	0	0.01	0	0	0	0.01	0
BK11_34	22.8	1.3	20.4	1.1	0.78	0.04	0.72	0.04	0.73	0.05	0.06	0	0.11	0.01
BK11_35	68.32	0.95	53.92	0.81	1.82	0.02	1.71	0.02	1.7	0.03	0	0	0.14	0

BK11_36	21.8	3.8	20.5	3.1	0.65	0.12	0.58	0.11	0.57	0.11	0.04	0	0.07	0.01
BK11_37	9.59	0.24	6.6	0.06	0.13	0.01	0.11	0.01	0.11	0.01	0.09	0.01	0.03	0
BK11_38	8.73	0.13	7.31	0.15	0.01	0	0	0	0	0	0	0	0.02	0
BK11_39	9.49	0.18	6.67	0.08	0.02	0	0.01	0	0.01	0	0.01	0	0.02	0
BK11_40	72	28	7.73	0.37	0.08	0.02	0.07	0.02	0.05	0.02	0.05	0.01	0.12	0.01
BK11_41	5.82	0.18	7.33	0.1	0.01	0	0	0	0	0	0	0	0.01	0
BK11_42	7.66	0.7	14	3.7	0.35	0.1	0.28	0.08	0.32	0.1	0.26	0.07	0.14	0.03
BK11_43	23.8	4.4	22.1	3.5	0.72	0.15	0.68	0.14	0.69	0.15	0.01	0	0.04	0.01
BK11_44	49.2	1	46.64	0.8	1.73	0.07	1.58	0.06	1.6	0.07	0.23	0.03	0.12	0.01
BK11_45	60	2.5	48.8	1.7	2.19	0.08	1.94	0.07	2.01	0.08	0.18	0.01	0.43	0.03
BK11_46	41.7	2.5	40.2	1.9	8.3	1.4	2.86	0.31	11.2	2.2	211	54	24.7	6.2
BK11_47	9.14	0.6	12.1	1.2	0.32	0.04	0.23	0.02	0.27	0.03	1.19	0.22	0.8	0.15
BK11_48	8.67	0.72	9.66	0.58	0.17	0.03	0.16	0.03	0.16	0.03	0.01	0	0.02	0
BK11_49	5.69	0.06	7.19	0.07	0.02	0	0.02	0	0.02	0	0.01	0	0.01	0
BK11_50	3.99	0.06	6.79	0.07	0.01	0	0	0	0.01	0.01	0.11	0.13	0.01	0
BK11_51	18.27	0.62	16.63	0.34	0.31	0.01	0.28	0.01	0.29	0.02	0.01	0	0.07	0
BK11_52	7.43	0.35	7.11	0.09	0.01	0	0.01	0	0.01	0	0.01	0	0.02	0
BK11_53	8.19	0.32	6.95	0.1	0.01	0	0.01	0	0.01	0	0.01	0	0.02	0
BK11_54	25.2	1.8	21.1	1.4	0.66	0.06	0.63	0.06	0.63	0.07	0	0	0.05	0
BK11_55	32.1	3.4	27.4	2.9	0.92	0.12	0.87	0.11	0.86	0.11	0	0	0.06	0.01
BK11_56	70.05	0.88	54.53	0.76	2.2	0.04	2.08	0.04	2.11	0.04	0	0	0.12	0
BK11_57	no value	NAN	no value	NAN	no value	NAN	no value	NAN	no value	NAN	no value	NAN	no value	NAN
BK11_58	71.09	0.64	56.59	0.54	2.37	0.07	2.22	0.07	2.28	0.07	0.09	0.01	0.19	0
BK11_59	73.65	0.62	56.31	0.57	2.28	0.03	2.15	0.03	2.19	0.04	0	0	0.14	0
BK11_60	74.74	0.92	57.87	0.71	2.06	0.03	1.96	0.03	2.01	0.05	0.02	0	0.16	0
BK11_61	72.99	0.83	57.41	0.59	1.91	0.03	1.8	0.03	1.83	0.04	0	0	0.15	0
BK11_62	66.8	1.2	54.5	1	2.28	0.06	2.12	0.05	2.16	0.06	0.07	0.01	0.15	0
BK11_63	58.7	5.5	38.5	5.9	2.06	0.16	1.98	0.17	1.94	0.15	0.11	0.04	0.11	0.02
BK11_64	67.1	1.3	51.8	1.2	2	0.03	1.91	0.03	1.91	0.04	0.03	0	0.13	0
BK14_1	37.64	0.95	15.21	0.22	2.03	0.1	1.9	0.09	1.9	0.09	0.04	0.01	0.17	0
BK14_2	37.53	0.68	16.57	0.25	1.9	0.05	1.78	0.05	1.84	0.05	0	0	0.16	0.01
BK14_3	no value	NAN	no value	NAN	no value	NAN	no value	NAN	no value	NAN	no value	NAN	no value	NAN
BK14_4	40.94	0.61	36.08	0.41	2.43	0.05	2.28	0.04	2.33	0.05	0	0	0.2	0
BK14_5	47.3	2.4	25.28	0.67	6.26	0.77	2.73	0.12	3.09	0.25	12.8	3.8	9	1.6
BK14_6	32.59	0.38	30.15	0.29	1.85	0.03	1.74	0.03	1.75	0.03	0	0	0.17	0

BK14_7	36.29	0.42	35.63	0.32	2.21	0.03	2.09	0.03	2.12	0.04	0	0	0.19	0
BK14_8	64.8	3.9	35.84	0.58	2.07	0.03	1.95	0.03	2	0.03	0.09	0	0.19	0
BK14_9	35.36	0.32	35.33	0.4	2.17	0.02	2.02	0.02	2.06	0.03	0	0	0.23	0
BK14_10	30.68	0.41	23.33	0.25	1.75	0.03	1.62	0.03	1.66	0.03	0.03	0	0.2	0
BK14_11	30.77	0.38	26.42	0.27	1.8	0.03	1.68	0.02	1.7	0.03	0	0	0.22	0
BK14_12	41.32	0.49	42.89	0.42	2.96	0.05	2.79	0.05	2.84	0.06	0	0	0.2	0
BK14_13	30.63	0.4	28.83	0.34	1.78	0.03	1.66	0.03	1.68	0.04	0	0	0.18	0
BK14_14	28.53	0.32	25.43	0.25	1.51	0.02	1.39	0.02	1.39	0.03	0	0	0.25	0
BK14_15	40.92	0.42	16.16	0.4	2.14	0.02	2	0.02	2.02	0.03	0	0	0.24	0
BK14_16	34.5	0.48	31.69	0.33	2.06	0.03	1.94	0.03	1.96	0.03	0	0	0.18	0
BK14_17	40.7	0.42	33.56	0.62	2.89	0.05	2.23	0.03	2.37	0.05	3.88	0.43	2.21	0.16
BK14_18	41.69	0.41	42.83	0.4	2.94	0.03	2.74	0.03	2.79	0.03	0	0	0.23	0
BK14_19	33.05	0.35	24.09	0.26	1.93	0.03	1.78	0.03	1.83	0.03	0	0	0.25	0
BK14_20	38.79	0.39	38.97	0.33	2.48	0.04	2.34	0.03	2.38	0.04	0.06	0	0.19	0
BK14_21	40.97	0.58	39.41	0.48	2.5	0.04	2.34	0.04	2.38	0.05	0	0	0.22	0
BK14_22	39.61	0.52	43.71	0.46	3.17	0.07	2.83	0.05	2.88	0.05	0.27	0.01	0.86	0.04
BK14_23	33.01	0.49	30.09	0.32	1.89	0.04	1.77	0.03	1.8	0.04	0	0	0.18	0
BK14_24	38.88	0.44	43.98	0.42	2.87	0.02	2.7	0.02	2.72	0.03	0.03	0	0.32	0.01
BK14_25	32.59	0.36	29.08	0.27	1.87	0.03	1.74	0.02	1.8	0.03	0	0	0.24	0.01
BK14_26	31.63	0.35	25.09	0.25	1.82	0.03	1.69	0.03	1.73	0.03	0	0	0.17	0
BK14_27	33.51	0.46	24.36	0.24	1.8	0.03	1.7	0.03	1.73	0.03	0	0	0.16	0
BK14_28	35.49	0.81	22.61	0.3	1.76	0.05	1.66	0.04	1.71	0.05	0.04	0.01	0.16	0
BK14_29	33.76	0.57	24.94	0.26	1.79	0.03	1.69	0.02	1.73	0.03	0	0	0.18	0
BK14_30	34.57	0.79	24.37	0.34	1.83	0.04	1.72	0.04	1.74	0.05	0.01	0	0.18	0
BK14_31	39.6	0.47	38.74	0.35	2.39	0.03	2.26	0.02	2.29	0.03	0.01	0	0.19	0
BK14_32	759	84	29.8	1.9	39	6.3	5.42	0.44	33.1	5.7	700	150	119	23
BK14_33	734	81	18.72	0.43	8.2	1.3	2.85	0.11	2.58	0.09	5.03	0.87	16	3.7
BK14_34	41.1	0.38	40.82	0.35	2.83	0.04	2.68	0.04	2.75	0.05	0	0	0.23	0
BK14_35	38.81	0.35	39.89	0.37	2.63	0.03	2.48	0.03	2.53	0.04	0	0	0.2	0
BK14_36	38.55	0.63	31.9	1	2.24	0.05	2.11	0.05	2.12	0.05	0	0	0.18	0
BK14_37	38.52	0.44	40.06	0.42	2.47	0.05	2.3	0.04	2.34	0.04	0	0	0.19	0
BK14_38	42.23	0.54	36.37	0.68	2.37	0.02	2.21	0.02	2.26	0.03	0.01	0	0.27	0.01
BK14_39	35.93	0.44	29.96	0.43	1.99	0.02	1.88	0.02	1.92	0.03	0	0	0.18	0
BK14_40	40.88	0.48	22.51	0.24	2.06	0.03	1.96	0.03	1.99	0.03	0.02	0	0.16	0
BK14_41	41	0.41	17.73	0.16	2.04	0.02	1.91	0.02	1.96	0.03	0	0	0.18	0
BK14_42	39.14	0.36	18.94	0.22	1.93	0.02	1.82	0.02	1.85	0.03	0	0	0.17	0

BK14_43	31.01	0.37	31.07	0.3	1.76	0.03	1.66	0.03	1.7	0.03	0	0	0.18	0
BK14_44	47.3	2.4	23.02	0.2	1.68	0.03	1.58	0.03	1.6	0.03	0.01	0	0.2	0.01
BK14_45	31.82	0.33	30.8	0.29	1.76	0.02	1.65	0.02	1.69	0.03	0	0	0.18	0
BK14_46	42.98	0.44	42.76	0.42	2.85	0.03	2.69	0.03	2.78	0.04	0	0	0.23	0
BK14_47	31.04	0.26	30.75	0.31	1.79	0.02	1.67	0.02	1.7	0.03	0	0	0.19	0
BK14_48	33.67	0.34	22.72	0.21	1.84	0.03	1.71	0.03	1.72	0.03	0	0	0.28	0
BK14_49	31.42	0.32	25.37	0.21	1.77	0.02	1.64	0.02	1.67	0.03	0	0	0.23	0
BK14_50	37.18	0.44	17.83	0.16	1.9	0.03	1.77	0.02	1.81	0.03	0	0	0.26	0
BK14_51	34.14	0.36	18.13	0.14	1.77	0.02	1.65	0.02	1.68	0.03	0	0	0.18	0
BK14_52	34.58	0.29	18.98	0.19	1.8	0.02	1.67	0.02	1.68	0.03	0	0	0.26	0
BK14_53	33.56	0.39	19.38	0.18	1.76	0.02	1.63	0.02	1.67	0.03	0	0	0.19	0
BK14_54	35.77	0.32	17.78	0.18	1.85	0.02	1.74	0.02	1.78	0.03	0.02	0	0.18	0
BK14_55	37.35	0.45	19.82	0.18	1.89	0.03	1.77	0.03	1.79	0.03	0	0	0.26	0
BK14_56	32.76	0.38	21.2	0.25	1.75	0.02	1.62	0.02	1.64	0.03	0	0	0.26	0
BK14_57	33.59	0.44	20.66	0.17	1.75	0.03	1.62	0.02	1.65	0.03	0	0	0.21	0
BK14_58	34.37	0.38	33.2	0.35	1.96	0.04	1.84	0.04	1.89	0.04	0	0	0.18	0
BK14_59	34.74	0.35	28.06	0.25	1.8	0.02	1.67	0.02	1.71	0.03	0.06	0	0.22	0
BK14_60	37.04	0.53	36.12	0.34	2.22	0.04	2.09	0.04	2.11	0.05	0	0	0.18	0
BK14_61	42.53	0.4	41.1	0.34	2.74	0.04	2.61	0.04	2.65	0.04	0	0	0.18	0
BK14_62	40.68	0.45	40.6	0.42	2.57	0.04	2.44	0.03	2.47	0.04	0	0	0.19	0
BK14_63	37.55	0.36	36.47	0.35	2.31	0.03	2.17	0.03	2.19	0.03	0	0	0.23	0
BK14_64	32.46	0.29	22.38	0.21	1.76	0.02	1.65	0.02	1.68	0.03	0	0	0.19	0
BK14_65	38.57	0.36	17.57	0.16	1.9	0.02	1.8	0.02	1.83	0.03	0	0	0.16	0
BK18_1	14.66	0.15	11.82	0.12	0.05	0	0.03	0	0.03	0	0.01	0	0.06	0
BK18_2	8.82	0.11	6.57	0.1	0.11	0.01	0.05	0.01	0.32	0.05	7.1	1.3	0.31	0.06
BK18_3	11.3	0.18	7.28	0.09	0.01	0	0.01	0	0.01	0	0	0	0.02	0
BK18_4	27.74	0.36	52.47	0.7	7.02	0.12	6.74	0.11	6.84	0.1	0.04	0	0.27	0.01
BK18_5	17.82	0.99	23.2	1.5	1.79	0.16	1.64	0.16	1.65	0.16	0.02	0	0.19	0.02
BK18_6	27.8	1.3	42.7	3.5	6.05	0.56	5.88	0.53	5.93	0.55	0.03	0	0.13	0.02
BK18_7	19.05	0.22	28.5	1.3	2.39	0.14	2.26	0.13	2.29	0.15	0.01	0	0.13	0.01
BK18_8	15.43	0.17	13.51	0.13	0.05	0	0.03	0	0.04	0	0.02	0	0.07	0
BK18_9	21.65	0.25	12.28	0.14	0.12	0	0.08	0	0.08	0	0.01	0	0.14	0
BK18_10	19.01	0.31	12.13	0.15	0.08	0	0.05	0	0.05	0.01	0.02	0.01	0.09	0.01
BK18_11	19.9	0.2	24.4	0.53	1.86	0.1	1.77	0.09	1.81	0.1	0.01	0	0.13	0
BK18_12	25.16	0.93	34.2	3.4	3.82	0.46	3.63	0.45	3.72	0.47	0.01	0	0.17	0.01

BK18_13	19.38	0.42	12.45	0.16	0.12	0.01	0.08	0.01	0.08	0.01	0.02	0	0.12	0
BK18_14	22.36	0.32	10.62	0.11	0.06	0	0.03	0	0.03	0	0	0	0.09	0
BK18_15	25.21	0.32	38.1	2.5	3.5	0.35	3.27	0.34	3.3	0.36	0.16	0.04	0.36	0.02
BK18_16	20.86	0.25	13.96	0.48	0.7	0.07	0.62	0.06	0.68	0.07	0.01	0	0.13	0
					2.57	0.05	2.41	0.05	2.43	0.05	0	0	0.25	0.01
BK25B_1	22	1.6	16.52	0.94	2.08	0.05	1.91	0.05	1.95	0.06	0	0	0.3	0
BK25B_2	43.3	1.1	30.46	0.51	2.1	0.04	1.93	0.04	1.95	0.05	0	0	0.29	0.01
BK25B_3	35.7	2.4	24.6	1.7	1.81	0.02	1.65	0.02	1.68	0.03	0	0	0.31	0
BK25B_4	4.95	0.11	7.27	0.11	2.69	0.05	2.47	0.04	2.5	0.05	0	0	0.21	0.01
BK25B_5	6.92	0.67	8.17	0.4	2.62	0.04	2.45	0.04	2.49	0.05	0	0	0.24	0
BK25B_6	1.22	0.31	6.34	0.24	2.45	0.02	2.27	0.02	2.29	0.03	0	0	0.29	0
BK25B_7	7.46	0.43	8.63	0.19	2.52	0.05	2.32	0.05	2.36	0.05	0	0	0.29	0.01
BK25B_8	30.6	3.3	20.2	1.8	2.5	0.04	2.35	0.03	2.35	0.04	0	0	0.25	0
BK25B_9	4.57	0.26	7.25	0.12	2.57	0.03	2.39	0.03	2.41	0.03	0	0	0.28	0
BK25B_10	0.85	0.12	7.16	0.49	2.6	0.04	2.42	0.04	2.46	0.05	0	0	0.26	0.01
BK25B_11	7.07	0.75	8.23	0.35	2.38	0.02	2.21	0.02	2.22	0.03	0	0	0.29	0.01
BK25B_12	6.8	0.63	7.69	0.46	2.58	0.05	2.4	0.05	2.48	0.05	0	0	0.24	0
BK25B_13	5.4	0.11	7.11	0.11	2.57	0.03	2.41	0.03	2.47	0.03	0	0	0.22	0
BK25B_14	5.96	0.08	8.21	0.1	2.55	0.02	2.38	0.02	2.42	0.03	0	0	0.27	0
BK25B_15	4.67	0.15	6.52	0.11	3.17	0.06	2.96	0.05	2.98	0.07	0	0	0.25	0.01
BK25B_16	0.93	0.15	10.8	1.3	2.99	0.12	2.78	0.11	2.86	0.12	0	0	0.23	0
BK25B_17	8.44	0.6	7.22	0.21	2.31	0.03	2.15	0.03	2.18	0.04	0	0	0.23	0.01
BK25B_18	9.07	0.55	7.44	0.33	2.64	0.04	2.47	0.03	2.52	0.04	0	0	0.23	0
BK25B_19	6.13	0.27	7.09	0.14	0.72	0.01	0.59	0.01	0.6	0.01	0.12	0	0.38	0.01
BK25B_20	3.72	0.46	7.1	0.21	0.93	0.01	0.77	0.01	0.78	0.02	0.07	0	0.36	0
BK25B_21	5.76	0.2	7.32	0.11	1.8	0.02	1.64	0.02	1.65	0.03	0.01	0	0.34	0
BK25B_22	4.33	0.18	6.93	0.08	2.41	0.02	2.24	0.02	2.29	0.03	0	0	0.25	0
BK25B_23	6.76	0.21	11.23	0.42	0.84	0.02	0.73	0.02	0.75	0.02	0.07	0	0.3	0.01
BK25B_24	19.7	2	21.1	1.9	1.18	0.02	1	0.02	1	0.02	0.1	0	0.48	0.01
BK25B_25	6.58	0.72	8.55	0.35	0.92	0.02	0.73	0.01	0.76	0.02	0.31	0.03	0.55	0.03
BK25B_26	3.44	0.28	11.64	0.9	0.67	0.01	0.57	0.01	0.58	0.01	0.1	0	0.31	0.01
BK25B_27	5.4	0.1	7.56	0.11	0.91	0.03	0.77	0.03	0.78	0.04	0.1	0	0.39	0.01
BK25B_28	4.3	0.15	13.78	0.57	1.17	0.02	1	0.01	1.02	0.02	0.05	0	0.36	0.01
BK25B_29	3.7	0.07	8.5	0.1	2.74	0.05	2.46	0.05	2.5	0.05	0.02	0	0.61	0.01
BK25B_30	48	5.5	25.9	2.7	2.5	0.04	2.26	0.04	2.3	0.04	0.02	0	0.55	0.01
BK25B_31	5.86	0.48	7.27	0.28	0.95	0.02	0.8	0.01	0.81	0.02	0.11	0	0.4	0.01

BK25B_32	39.8	5.9	7.95	0.18	0.95	0.02	0.79	0.01	0.81	0.01	0.2	0	0.45	0.01
BK25B_33	7.22	0.12	7.8	0.17	0.9	0.02	0.77	0.02	0.79	0.02	0.26	0	0.4	0.01
BK25B_34	5.55	0.08	6.75	0.06	0.79	0.02	0.65	0.01	0.66	0.01	0.09	0	0.37	0.01
BK25B_35	0.73	0.09	6.62	0.18	2.79	0.03	2.6	0.03	2.65	0.04	0	0	0.32	0
BK25B_36	0.69	0.09	6.9	0.38	2.43	0.05	2.18	0.04	2.22	0.05	0.01	0	0.55	0.01
BK25B_37	0.69	0.11	8.8	1	1.66	0.03	1.51	0.02	1.51	0.02	0.01	0	0.34	0
BK25B_38	5.93	0.11	9.09	0.19	3.05	0.04	2.81	0.03	2.91	0.04	0.01	0	0.31	0
BK25B_39	0.67	0.09	6.3	0.18	2.95	0.03	2.67	0.03	2.72	0.03	0.01	0	0.62	0.01
BK25B_40	0.71	0.09	6.23	0.2	2.9	0.05	2.62	0.04	2.64	0.05	0	0	0.59	0.01
KTDD089_1	4.37	0.06	11.08	0.14	0.12	0.01	0.1	0.01	0.09	0.01	0.02	0	0.08	0.01
KTDD089_2	3.43	0.13	9.06	0.74	0.12	0.03	0.11	0.03	0.11	0.03	0.02	0	0.03	0.01
KTDD089_3	22.32	0.47	47.38	0.75	4.28	0.09	3.76	0.09	3.79	0.1	0.05	0	1.19	0.03
KTDD089_4	19.6	1.5	46.4	2.7	3.66	0.23	3.3	0.2	3.31	0.23	0.03	0	0.73	0.06
KTDD089_5	110.9	2.3	53.3	0.99	4.54	0.08	3.93	0.07	3.98	0.1	0.06	0	1.35	0.03
KTDD089_6	39.82	0.35	56.86	0.49	4.27	0.03	3.74	0.03	3.78	0.04	0.02	0	1.38	0.01
KTDD089_7	30.95	0.51	56.96	0.57	4.34	0.09	3.87	0.08	3.95	0.08	0.02	0	1.12	0.01
KTDD089_8	31.49	0.98	57.62	0.85	4.59	0.1	4.06	0.08	4.16	0.09	0.02	0	1.2	0.03
KTDD089_9	4.48	0.11	12.77	0.3	0.26	0.03	0.23	0.03	0.24	0.03	0.01	0	0.06	0.01
KTDD089_10	174	29	28.2	2.8	4.03	0.77	3.56	0.63	3.53	0.6	0.3	0.05	0.37	0.05
KTDD089_11	20.29	0.59	44.3	1.1	3.57	0.07	3.23	0.06	3.26	0.08	0.09	0.01	0.73	0.03
KTDD089_12	21.15	0.26	46.01	0.54	3.73	0.05	3.34	0.04	3.38	0.05	0.01	0	0.82	0.02
KTDD089_13	21.73	0.52	48.46	0.69	3.77	0.06	3.34	0.04	3.44	0.06	0.17	0.03	0.84	0.02
KTDD089_14	26.29	0.57	51.77	0.66	4.08	0.07	3.71	0.06	3.77	0.07	0.03	0	0.92	0.02
KTDD089_15	24.06	0.49	44.1	1	3.66	0.06	3.34	0.05	3.43	0.06	0.03	0	0.56	0.02
KTDD089_16	24	1.4	50.7	2.6	3.91	0.21	3.52	0.19	3.61	0.18	0.03	0	0.82	0.06
KTDD089_17	8.11	0.69	21.2	1.7	0.99	0.14	0.87	0.12	0.89	0.13	0.03	0	0.3	0.04
KTDD089_18	51.3	1.1	74.8	1.3	7.99	0.19	7.16	0.17	7.26	0.17	0.14	0.01	1.72	0.06
KTDD089_19	35.04	0.94	57.33	0.69	4.88	0.09	4.36	0.08	4.45	0.1	0.1	0	1.11	0.03
KTDD089_20	18.94	0.78	37.6	1.5	2.86	0.12	2.53	0.11	2.55	0.11	0.11	0.01	0.78	0.06
KTDD089_21	3.45	0.07	11.49	0.14	0.02	0	0.01	0	0.01	0	0.2	0.01	0.04	0
KTDD089_22	38.31	0.57	61.88	0.59	5.84	0.08	5.3	0.07	5.43	0.07	0.02	0	1.15	0.01
KTDD089_23	23.06	0.45	47.53	0.42	3.61	0.06	3.25	0.06	3.27	0.07	0.01	0	0.79	0.01
KTDD089_24	25.32	0.44	57.08	0.67	4.42	0.07	3.92	0.07	3.99	0.08	0.01	0	1.06	0.01
KTDD089_25	14.84	0.78	35	1.4	2.75	0.12	2.2	0.11	2.19	0.12	0.09	0	1.59	0.06
KTDD089_26	14.62	0.87	28.8	2.5	2.07	0.21	1.84	0.19	1.9	0.19	0.09	0.01	0.41	0.05

KTDD089_27	34.99	0.36	61.71	0.56	5.37	0.05	4.83	0.05	4.93	0.06	0.02	0	1.2	0.02
KTDD089_28	16.8	1.4	27.1	1.8	2.9	0.25	2.38	0.22	2.42	0.23	0.28	0.03	1.35	0.15
KTDD089_29	15.49	0.66	31.43	0.97	2.19	0.1	1.95	0.09	1.99	0.1	0.18	0.02	0.68	0.04
KTDD089_30	4.11	0.06	14.19	0.14	0.03	0	0.01	0	0.02	0	0.15	0.02	0.07	0
KTDD089_31	14.41	0.24	13.92	0.22	0.12	0.01	0.08	0.01	0.08	0.01	0.16	0.01	0.13	0.01
KTDD089_32	23.8	0.66	47.26	0.85	3.72	0.13	3.34	0.12	3.42	0.13	0.02	0	0.87	0.02
KTDD089_33	3.27	0.06	11.7	0.12	0.01	0	0	0	0.01	0	0.03	0.01	0.03	0
KTDD089_34	29.41	0.65	61.62	0.54	5.29	0.09	4.49	0.1	4.58	0.11	0.36	0.06	1.93	0.09
KTDD089_35	27.41	0.72	55.3	1	4.59	0.09	4.16	0.08	4.22	0.08	0.02	0	1	0.03
KTDD089_36	35.92	0.37	62.75	0.59	5.85	0.09	5.28	0.08	5.43	0.1	0.02	0	1.24	0.01
KTDD089_37	6.8	1.1	17.3	2	0.61	0.2	0.52	0.17	0.56	0.19	0.09	0.01	0.17	0.05
KTDD089_38	20	1.4	27	1.7	1.96	0.17	1.79	0.15	1.79	0.15	0.16	0.03	0.41	0.04
KTDD089_39	13.44	0.56	23.01	0.97	1.06	0.05	0.91	0.05	0.93	0.05	0.11	0.03	0.36	0.03
KTDD089_40	20.54	0.68	39.1	1.4	3.23	0.14	2.85	0.15	2.93	0.16	0.17	0.02	0.5	0.04
KTDD089_41	13.2	1.5	28.2	3	1.81	0.26	1.61	0.23	1.63	0.24	0.04	0.01	0.39	0.08
KTDD089_42	21.6	1.2	46.9	2.3	3.73	0.18	3.35	0.16	3.43	0.16	0.19	0.03	0.82	0.05
KTDD089_43	33.38	0.52	53.52	0.69	4.19	0.07	3.7	0.06	3.76	0.07	0.06	0	1.26	0.01
KTDD089_44	32.02	0.46	48.9	0.53	3.89	0.08	3.42	0.07	3.46	0.07	0.02	0	1.17	0.02
KTDD089_45	23.76	0.48	44.5	1.2	3.41	0.1	2.91	0.09	2.93	0.1	0.07	0.01	1.41	0.07
KTDD089_46	27.1	1.9	49.4	2.6	4.04	0.25	3.63	0.23	3.62	0.24	0.13	0.02	1	0.08
KTDD089_47	11.7	1.9	24.2	3.5	0.94	0.24	0.83	0.22	0.79	0.22	0.31	0.09	0.26	0.08
KTDD089_48	11.9	1.8	27.4	3.9	1.73	0.36	1.55	0.33	1.57	0.34	0.02	0	0.32	0.08
KTDD089_49	31.74	0.54	60.4	1	5.76	0.12	4.79	0.08	4.82	0.08	0.14	0.02	3	0.2
KTDD089_50	9.5	1.2	22.4	2.6	1.19	0.25	1.06	0.23	1.05	0.22	0.19	0.01	0.25	0.05
KTDD089_51	21	1.5	40.5	3.2	3.15	0.31	2.76	0.29	2.85	0.31	0.34	0.04	0.55	0.08
KTDD089_52	23.92	0.96	47.6	1.4	3.67	0.15	3.25	0.13	3.26	0.14	0.26	0.02	0.92	0.05
KTDD089_53	14.1	1.1	33.3	2.2	2.4	0.24	2.16	0.21	2.22	0.22	0.05	0	0.5	0.05
KTDD089_54	19.34	0.41	40.4	1.1	3.41	0.15	2.94	0.11	2.94	0.12	0.07	0.01	1.31	0.1
KTDD089_55	7.04	0.77	18.7	1.4	0.86	0.15	0.79	0.13	0.83	0.15	0.03	0.01	0.2	0.03
KTDD089_56	32.82	0.55	53.57	0.81	4.48	0.07	4.02	0.06	4.05	0.06	0.2	0.03	1.08	0.03
KTDD089_57	7.92	0.47	18.7	1.1	1.1	0.11	0.98	0.1	0.97	0.11	0.03	0.01	0.22	0.03
KTDD089_58	3.27	0.06	8.28	0.19	0.07	0.01	0.06	0.01	0.06	0.01	0.06	0.01	0.02	0